The 1st Space Science School Payload Design - An Example of Advanced Ionospheric Probe

Chi-Kuang Chao

Graduate Institute of Space Science, National Central University

Space Krenovation Park, Sri Racha, Chonburi, Thailand

October 24, 2016

Outline - the 1st hour

- Requirements
- Science objectives
- Principles of measurement
- Designs
- Verifications
- Future works

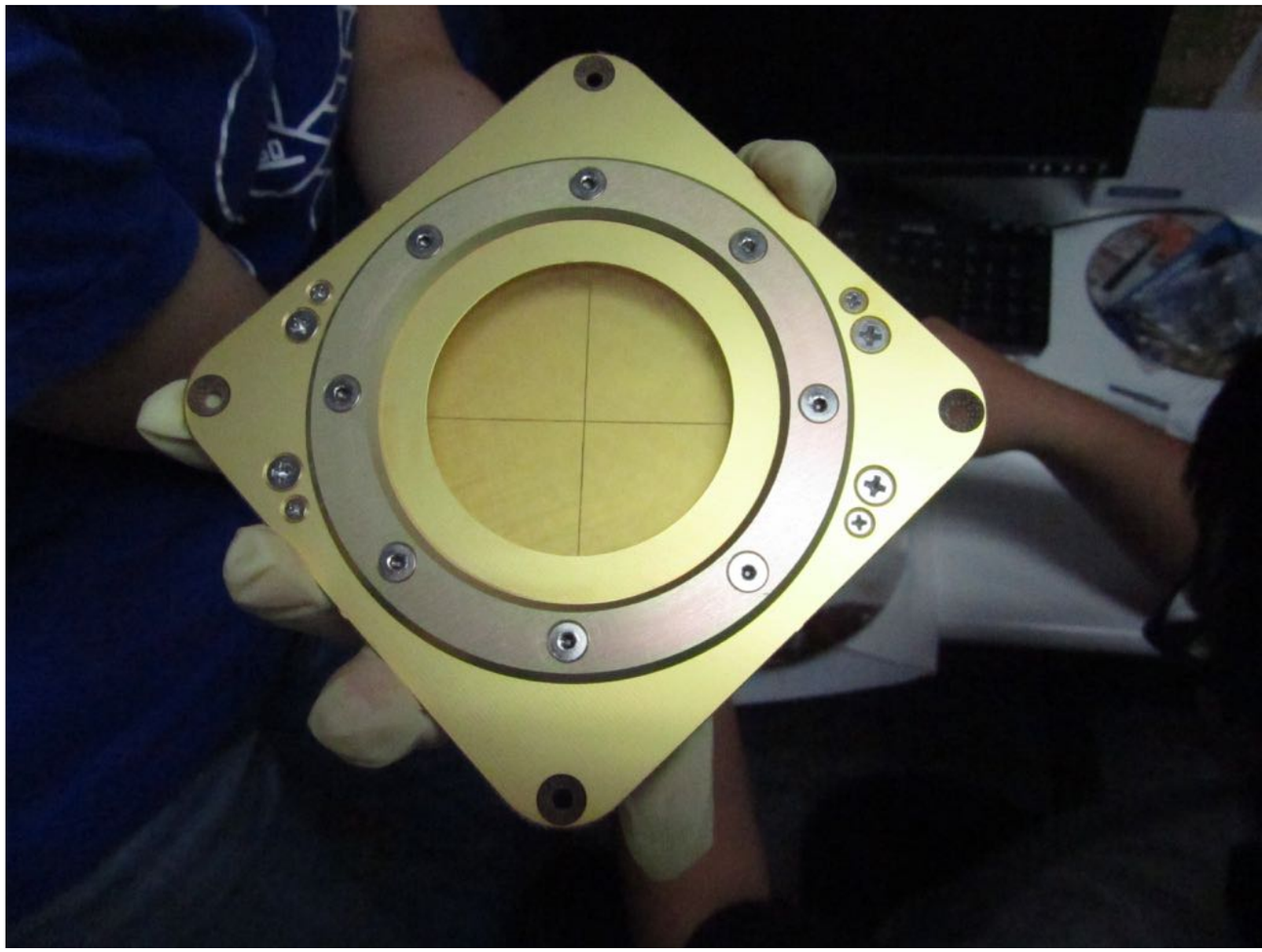

FS-5 to P/L interface requirements

- System
- Mechanical interface requirements
- Electrical interface requirements
- Environmental test requirements

FORMOSAT-5 satellite

The **FORMOSAT-5** (FS-5) is a remote sensing satellite and currently scheduled to be launched by SpaceX in October 2016. The FS-5 is anticipated to fly in a 98.28° inclination sun-synchronous circular orbit at 720 km altitude in the 1030/2230 LT sectors. The primary payload is Remote Sensing Instrument (RSI) organized by NSPO. In addition, a scientific instrument, Advanced Ionospheric Probe (AIP) developed by National Central University, has been chosen as the secondary payload.

Configuration of AIP

The AIP consists of a sensor unit (a sensor cube mounted on a stand to enlarge its field of view) located on a top panel of the FORMOSAT-5 satellite, a Science Payload Electronics Unit (**SPEU**) housed on a side panel, and an interconnection cable between the two units.

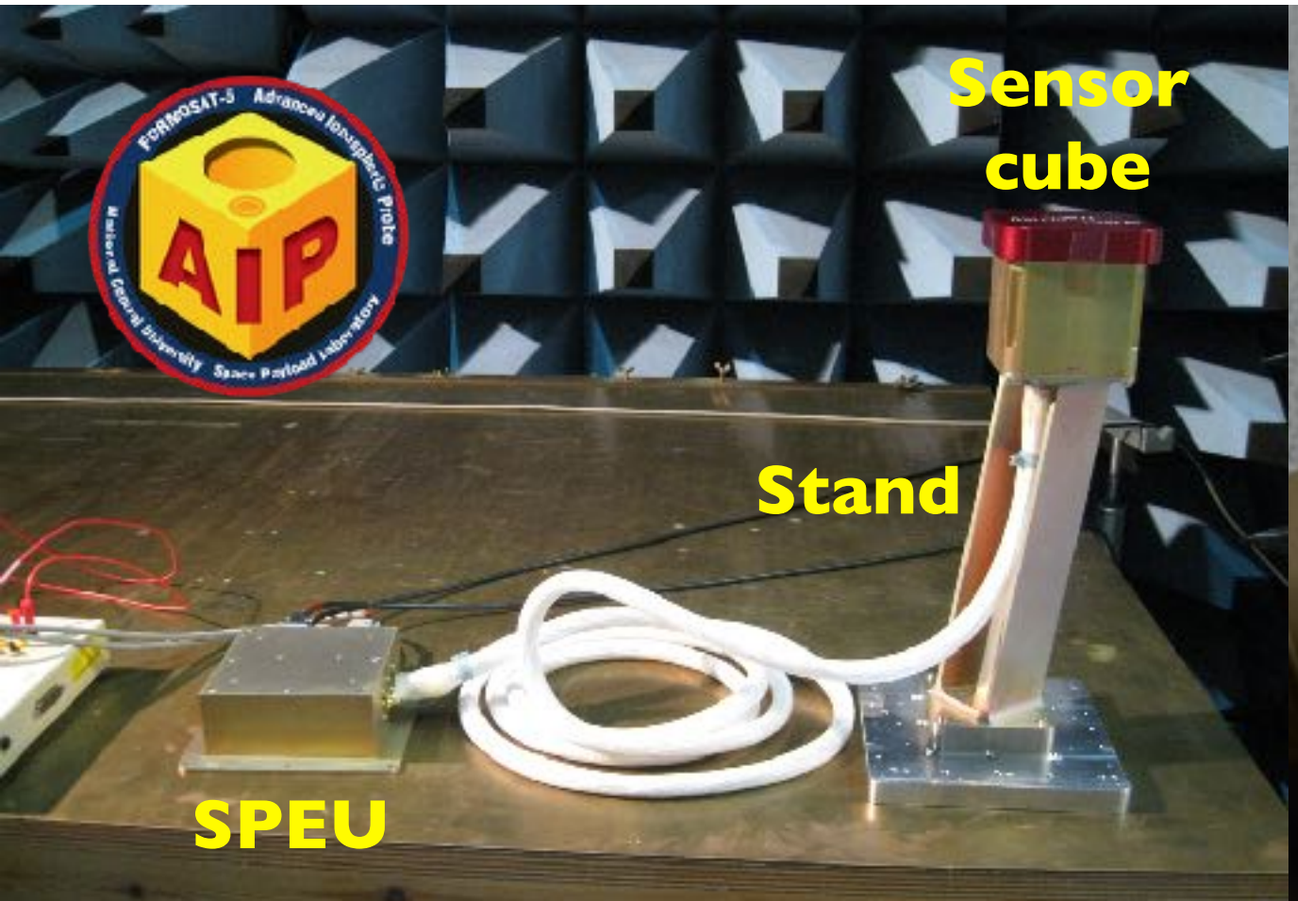

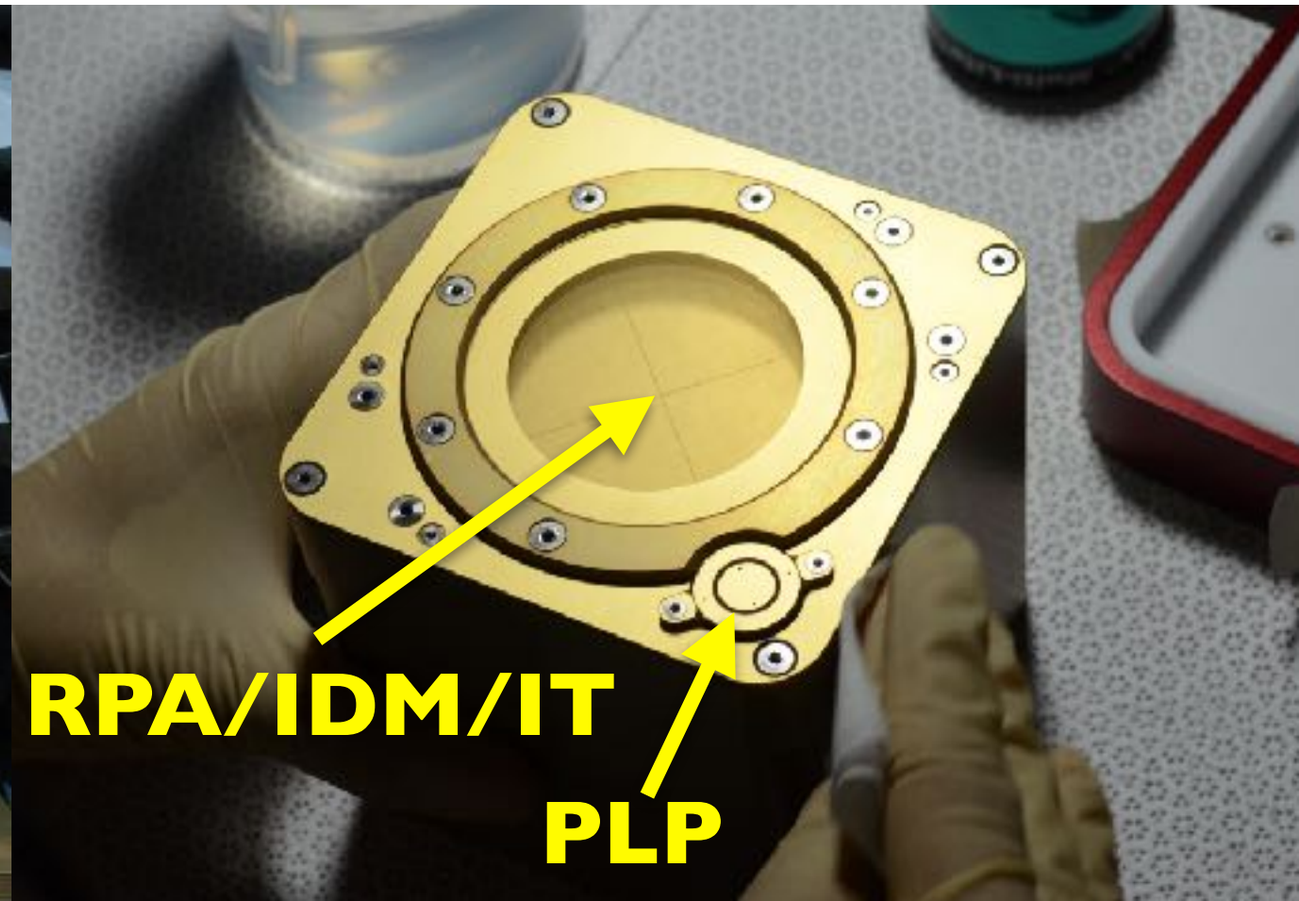

Functional diagram

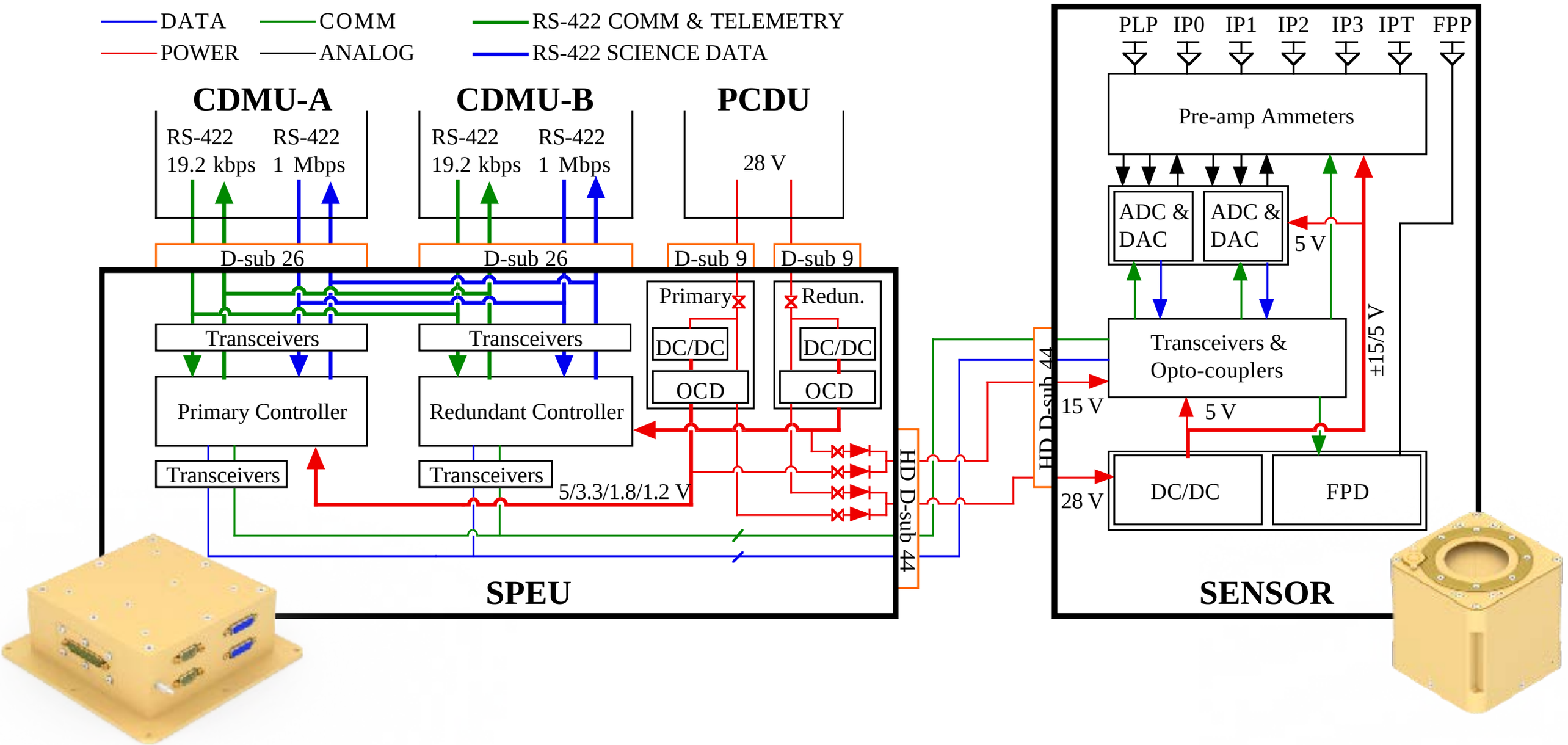

Redundant design on controllers, transceivers, powers, ADC/DAC, ammeters, etc.

Mechanical interface requirements

- Mass: sensor ≤ 1 kg, SPEU ≤ 4 kg, and total mass ≤ 5 kg.
- Natural frequency of the sensor: >120 Hz.
- Load factors
  - Out of plane: >20 G.
  - In-plane: >20 G.
- Margin of safety (MS)
  - Ultimate: > 0.
  - Yield: > 0.
- Buckling safety margin (MS_B): > 0.
- Sinusoidal vibration (no collision during vibration)
  - 9G in-plane.
  - 10-300 Hz.

SPEU

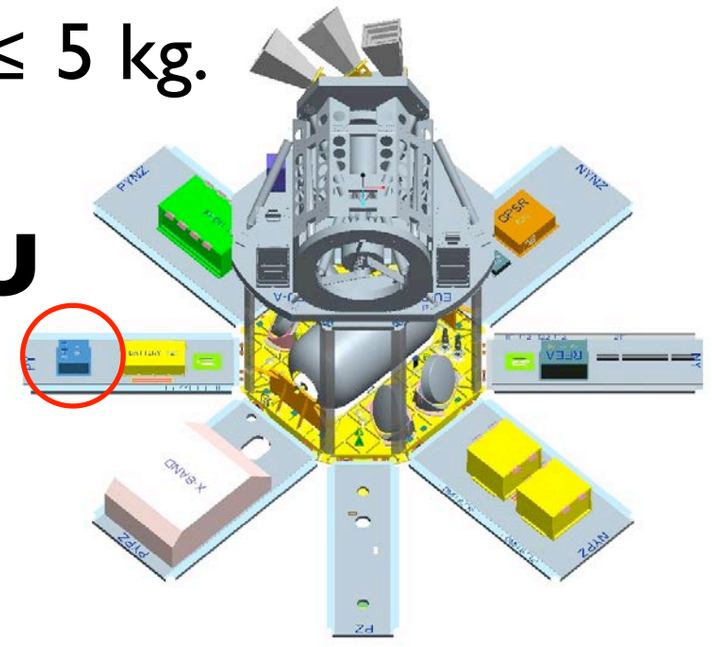

Sensor

Electrical interface requirements

- Power: ≤ 5W average power per orbit, ≤ 2 A with 26V to 34 V input voltage, and over-current-protection is required (1.75x max op. current with time duration > 1ms) to prevent from SEL.
- Command and telemetry interface (RS-422, 19.2 kbps, ASYN, bi-directional).
- Science data interface (RS-422, 1 Mbps, SYNC, only from SPEU to CDMU in a 1,024-byte science data packet).

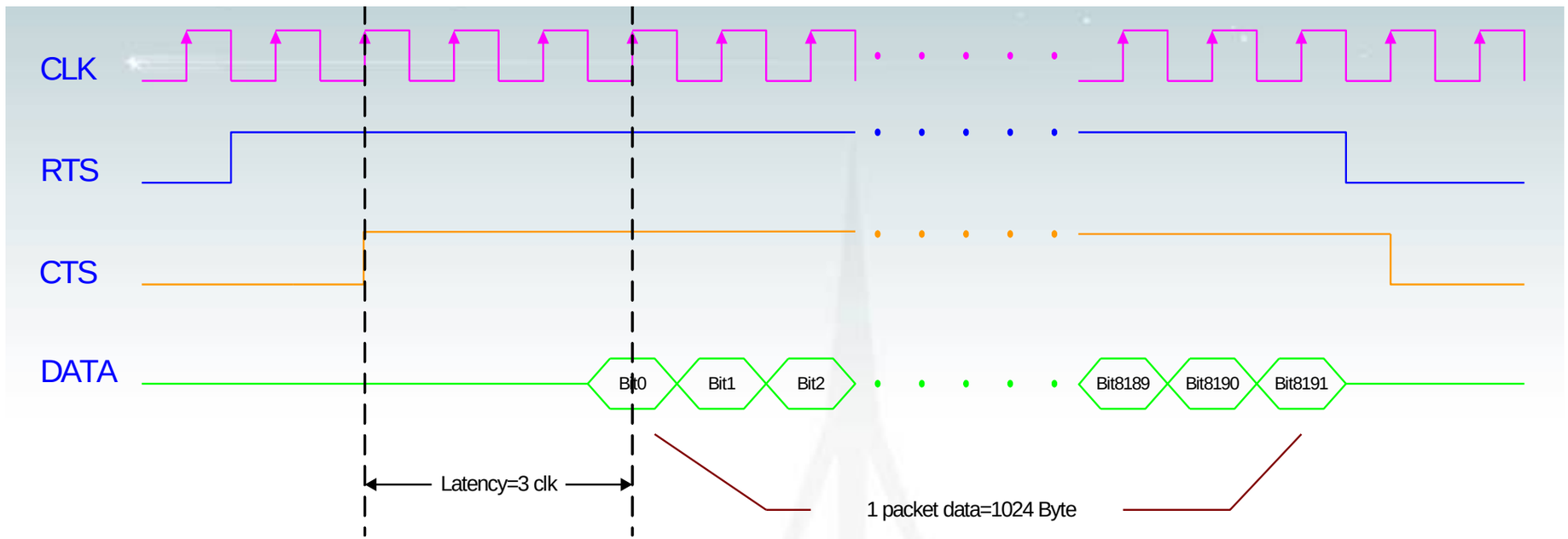

Environmental test requirements

- Sine vibration
- Random vibration
- Shock
- Thermal vacuum
- EMC

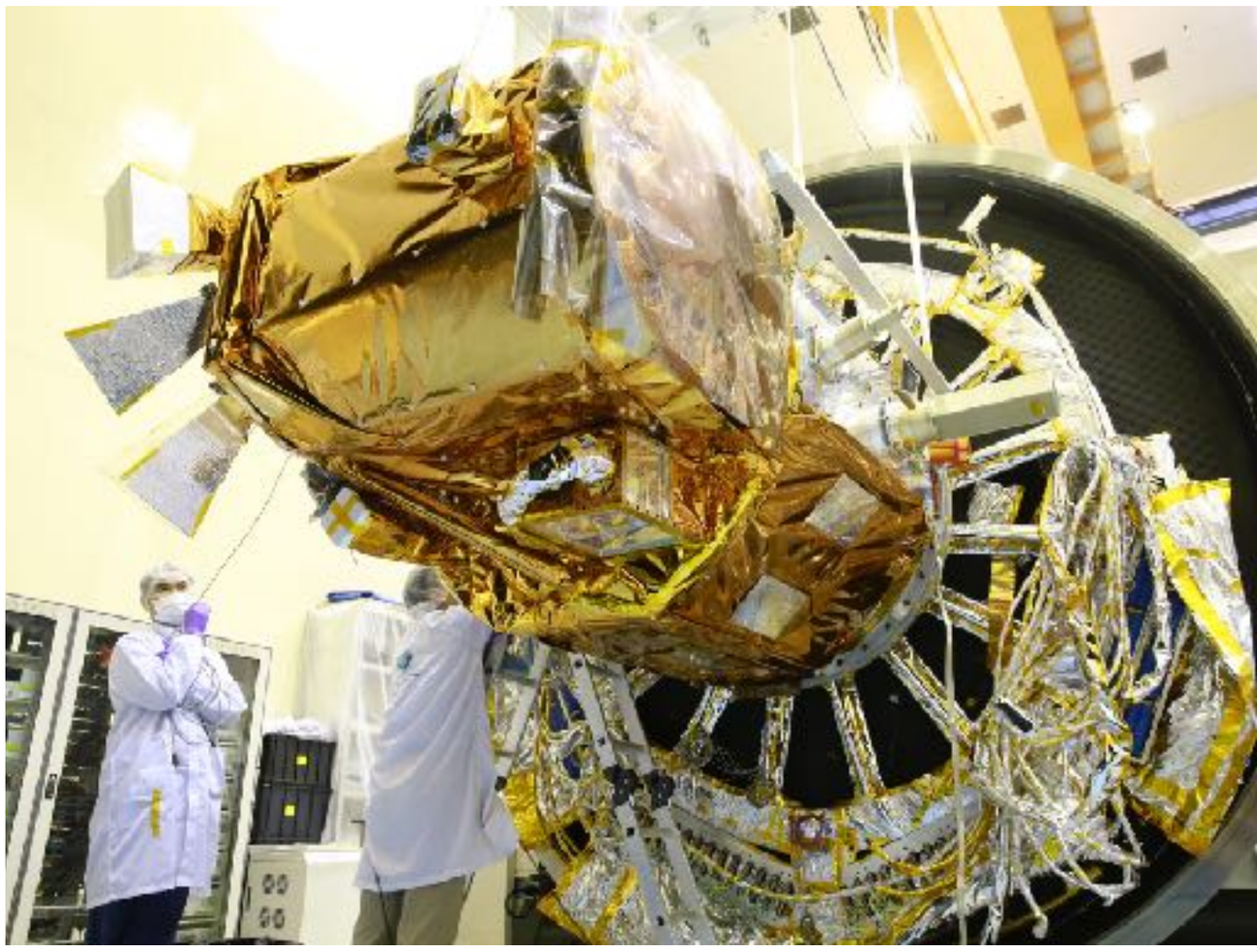

Scientific objectives

- Space weather and climate
- Earthquake precursor

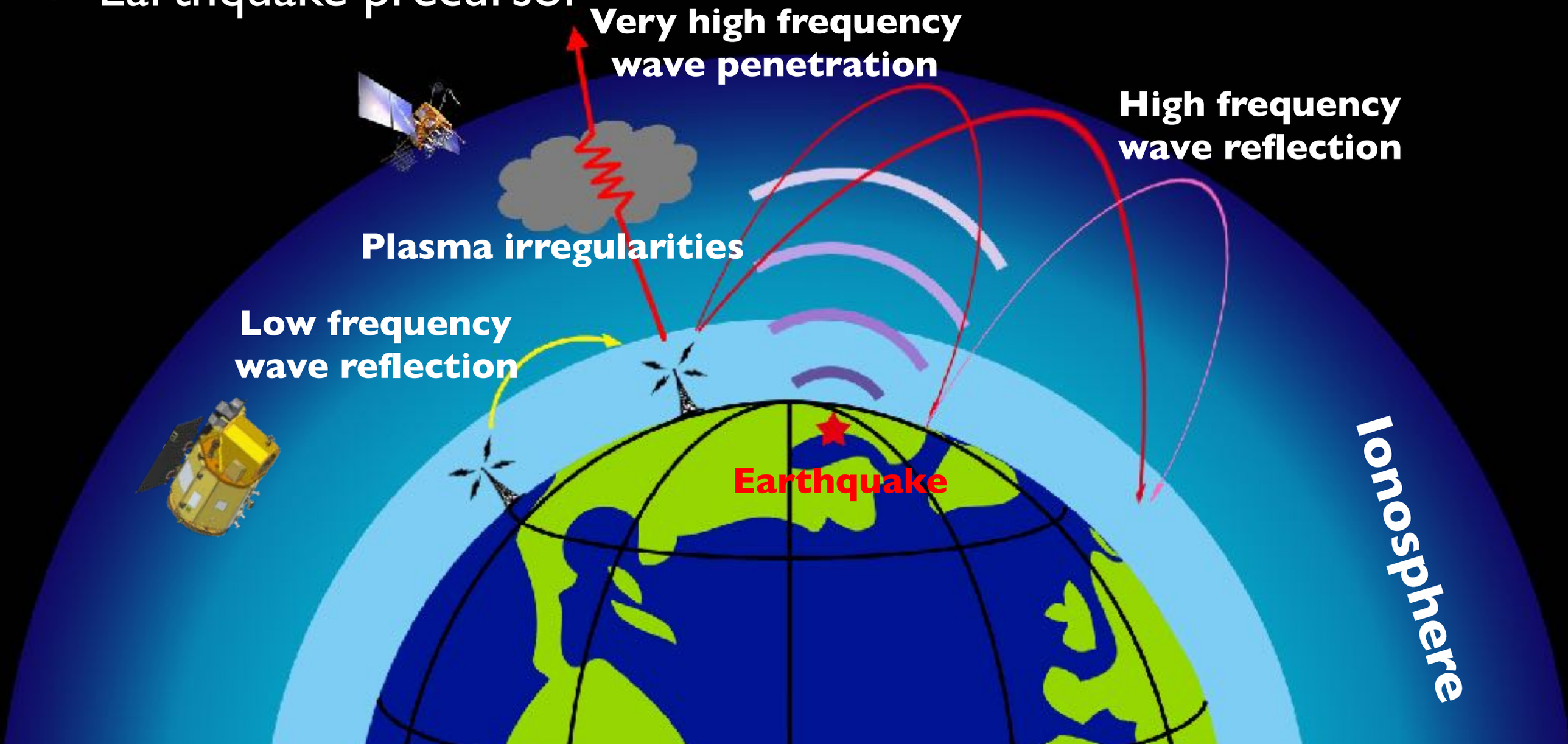

Ionosphere

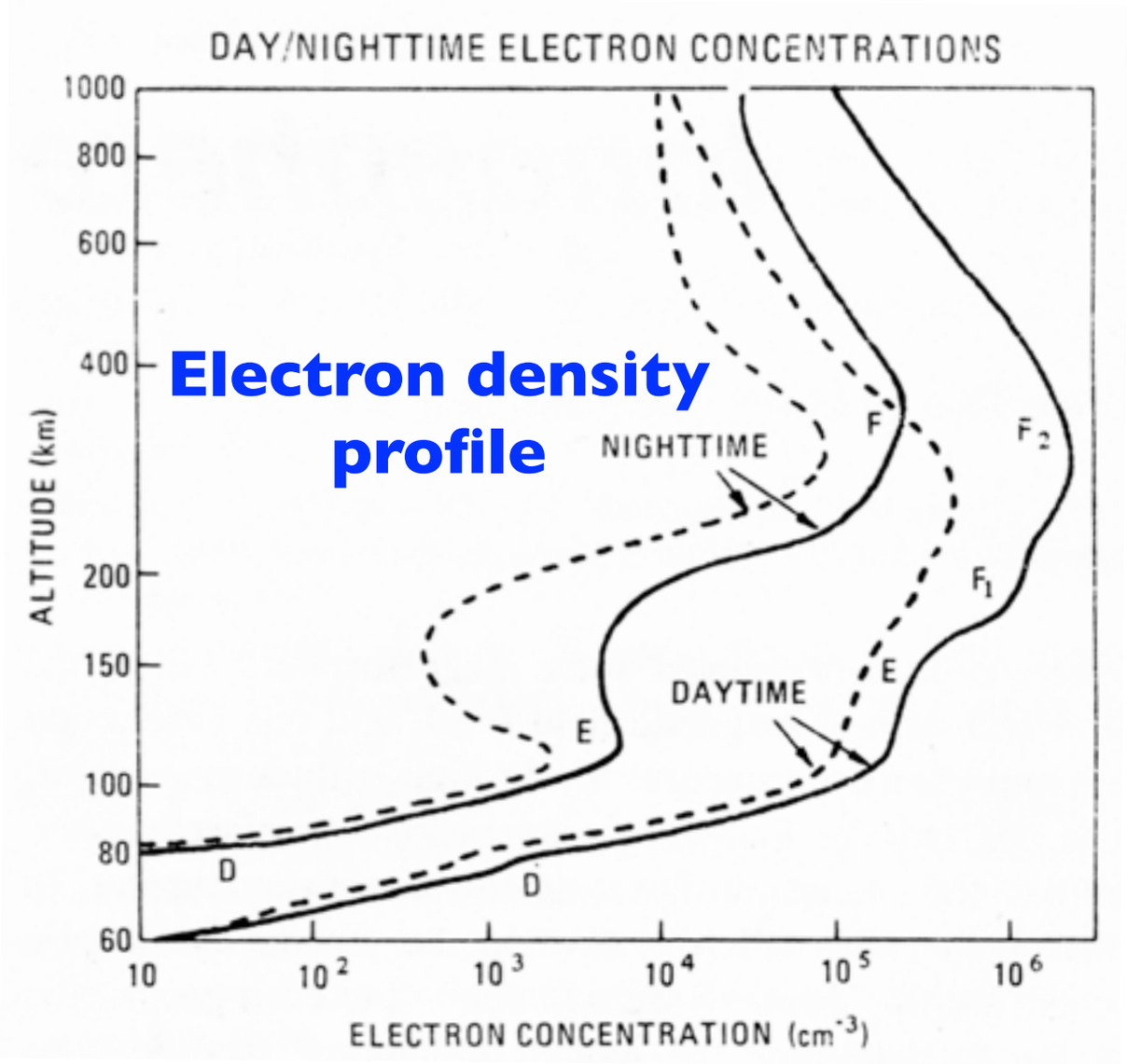

Electron density profile

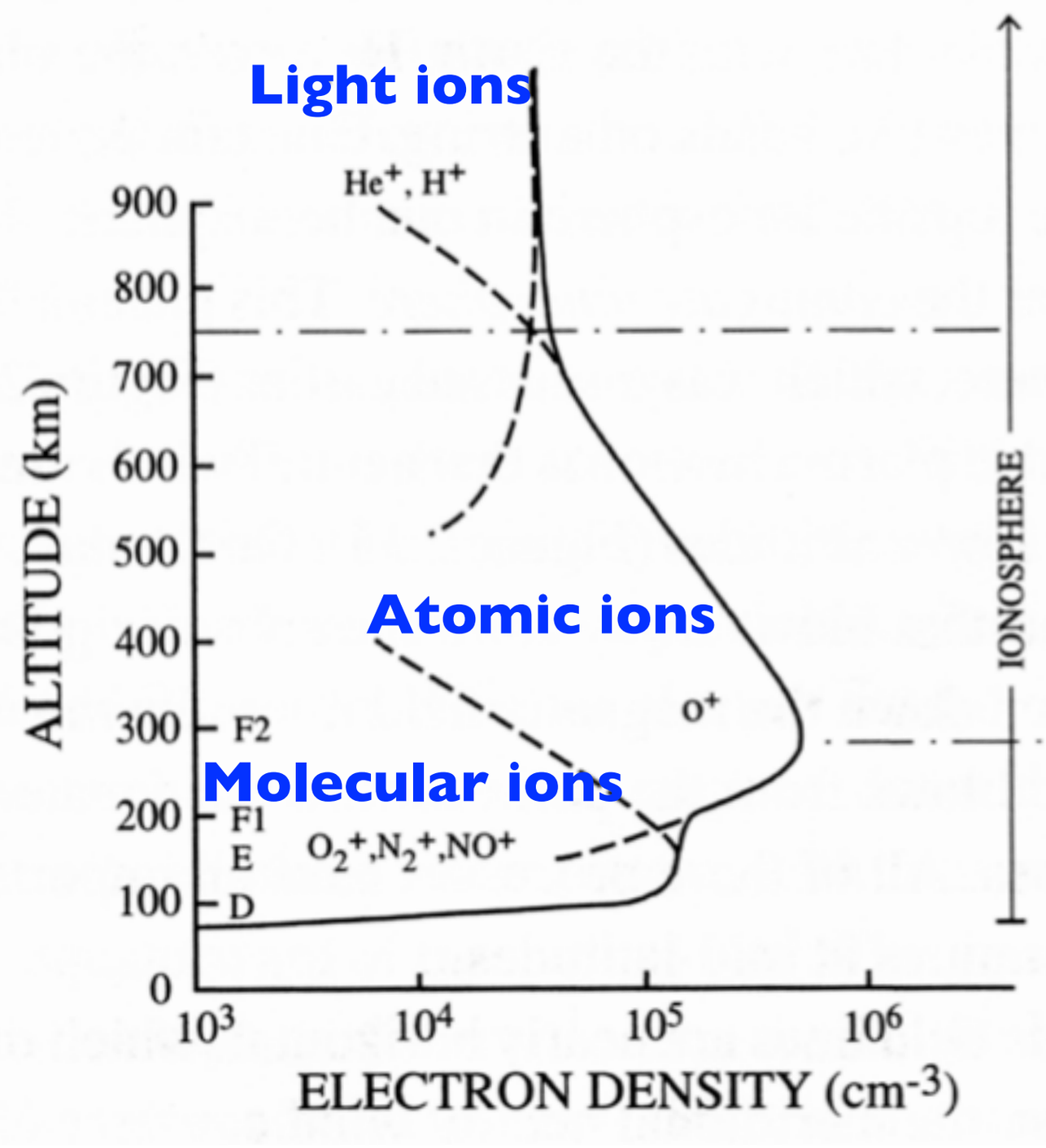

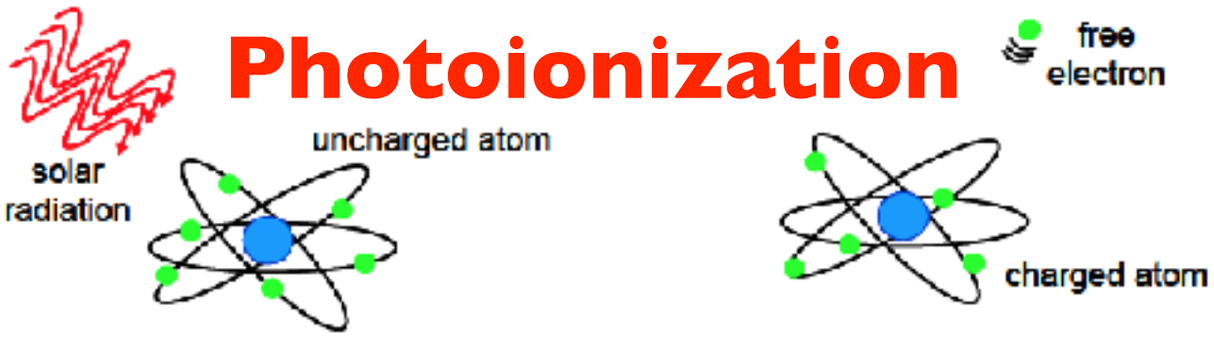

Ionosonde

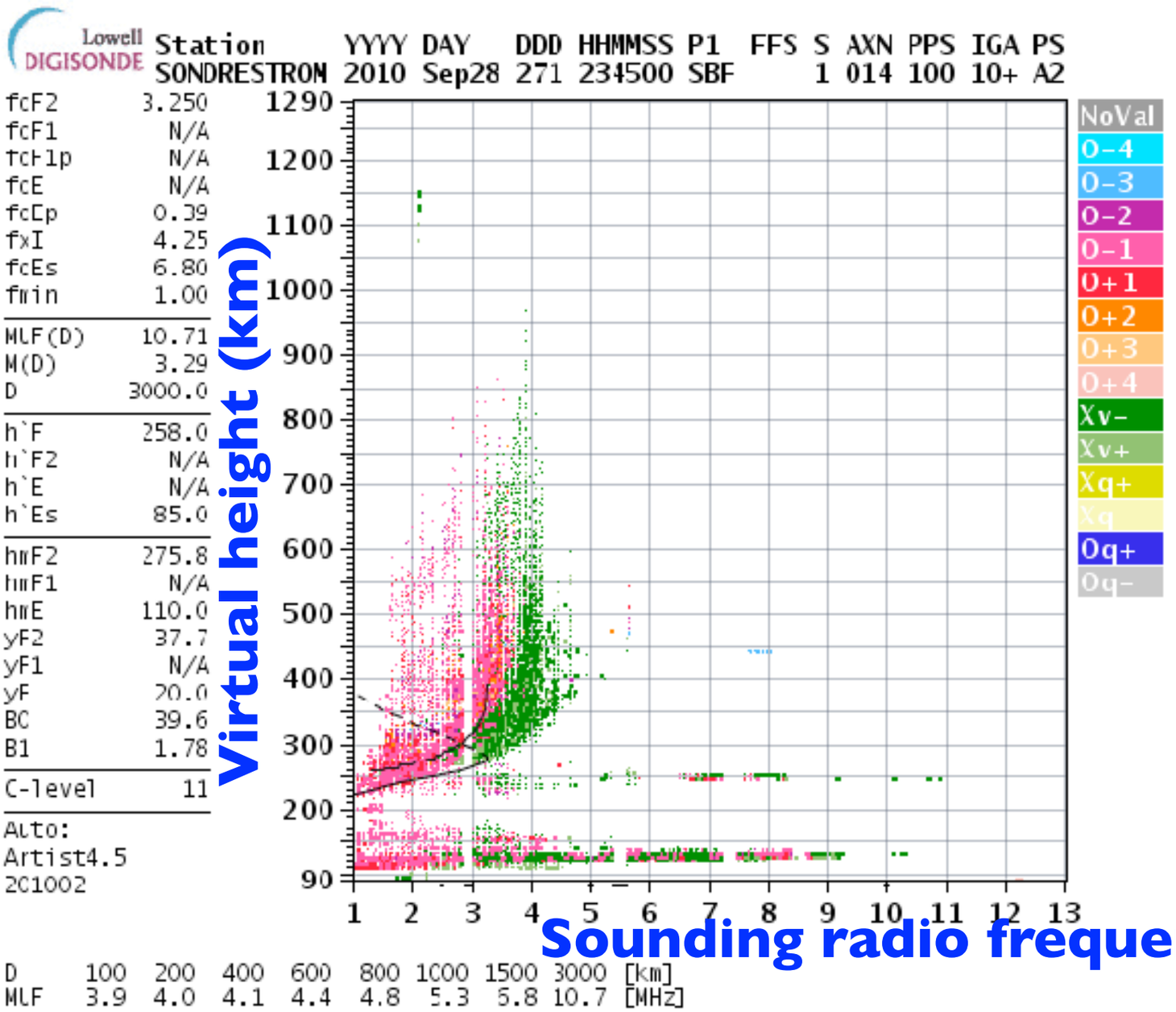

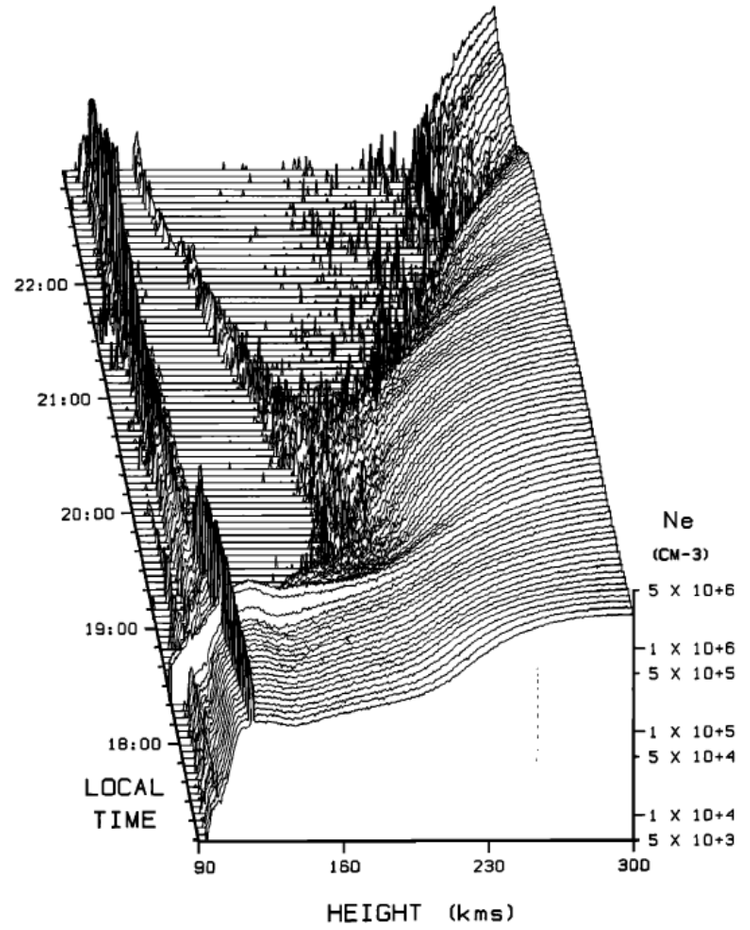

Incoherent scatter radar

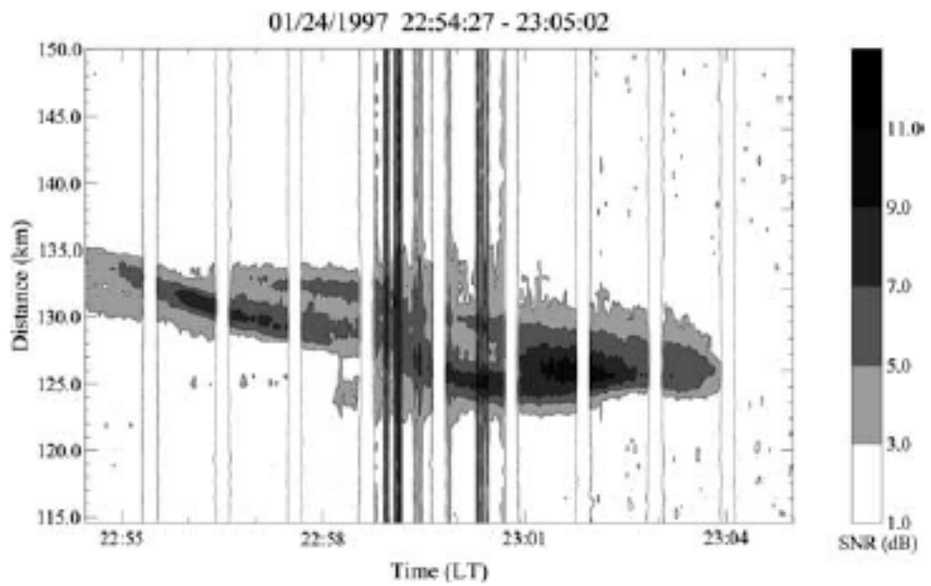

Coherent scatter radar

Space communication anomaly

Equatorial Spread F

Receiving signals disturbance

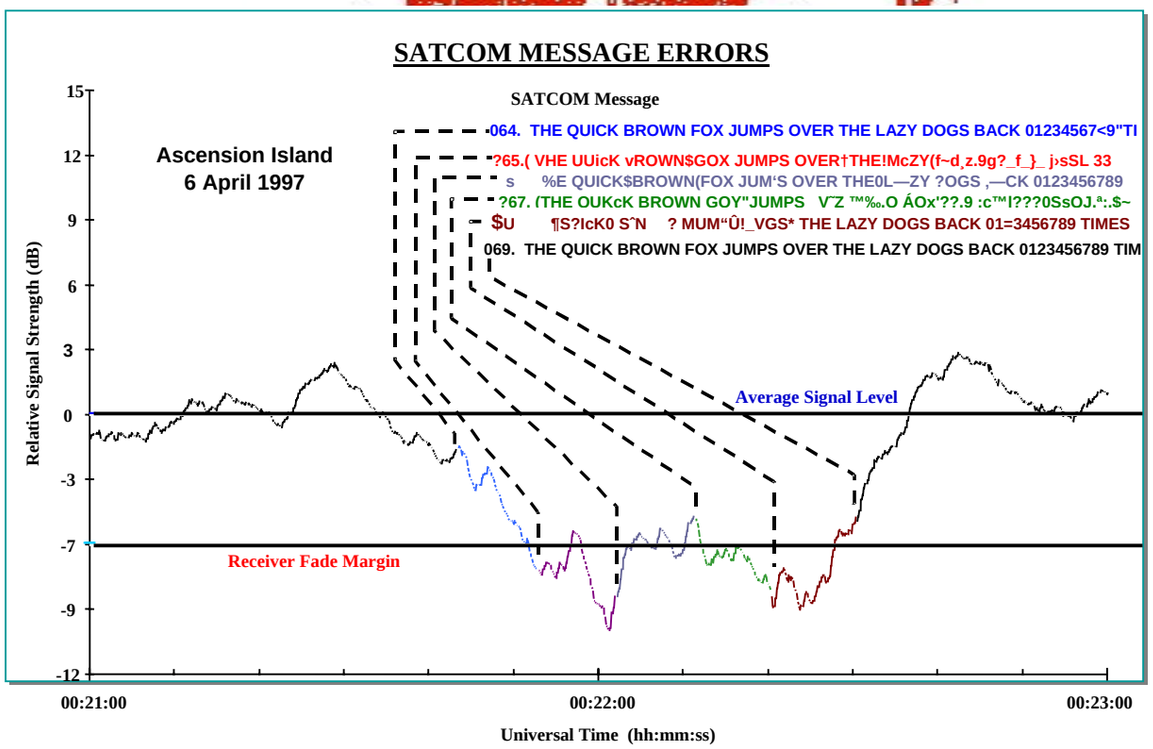

Plasma irregularities

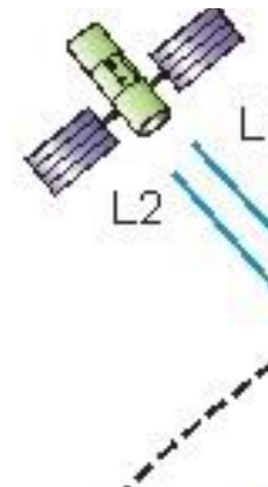

Signals slightly affected

Irregularities disturb signals strongly

FORMOSAT-5

Fine structures of the equatorial plasma irregularities

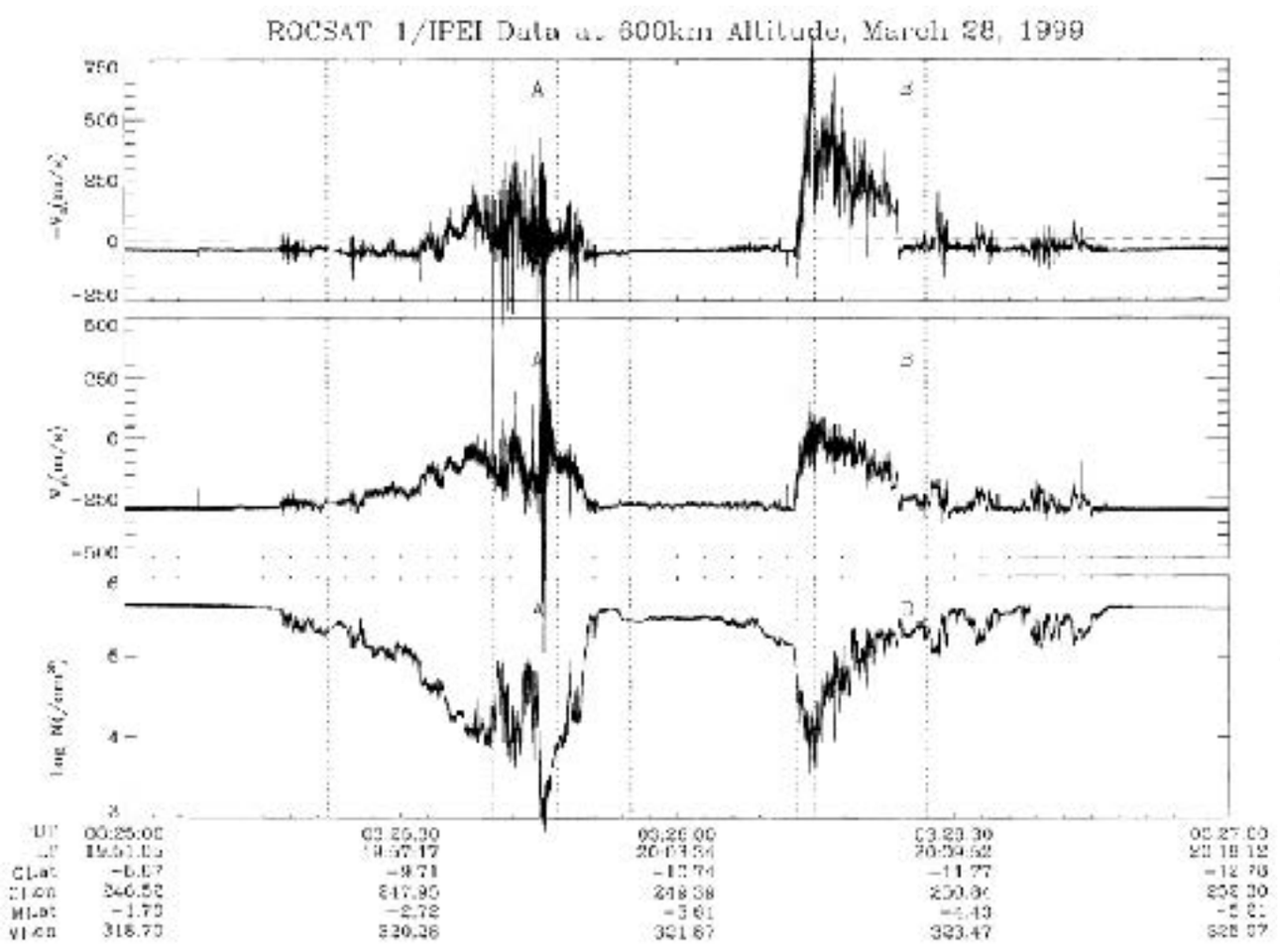

Figure 2. The expanded plot of Figure 1 for the time period 0325-0327 UT for bubble A and bubble B near the magnetic equator. The corotation component in V_y has been removed. Vertical dotted lines indicate the locations of sampled 1-s power spectra plotted in Figure 3.

Su et al., 2001, *JGR*

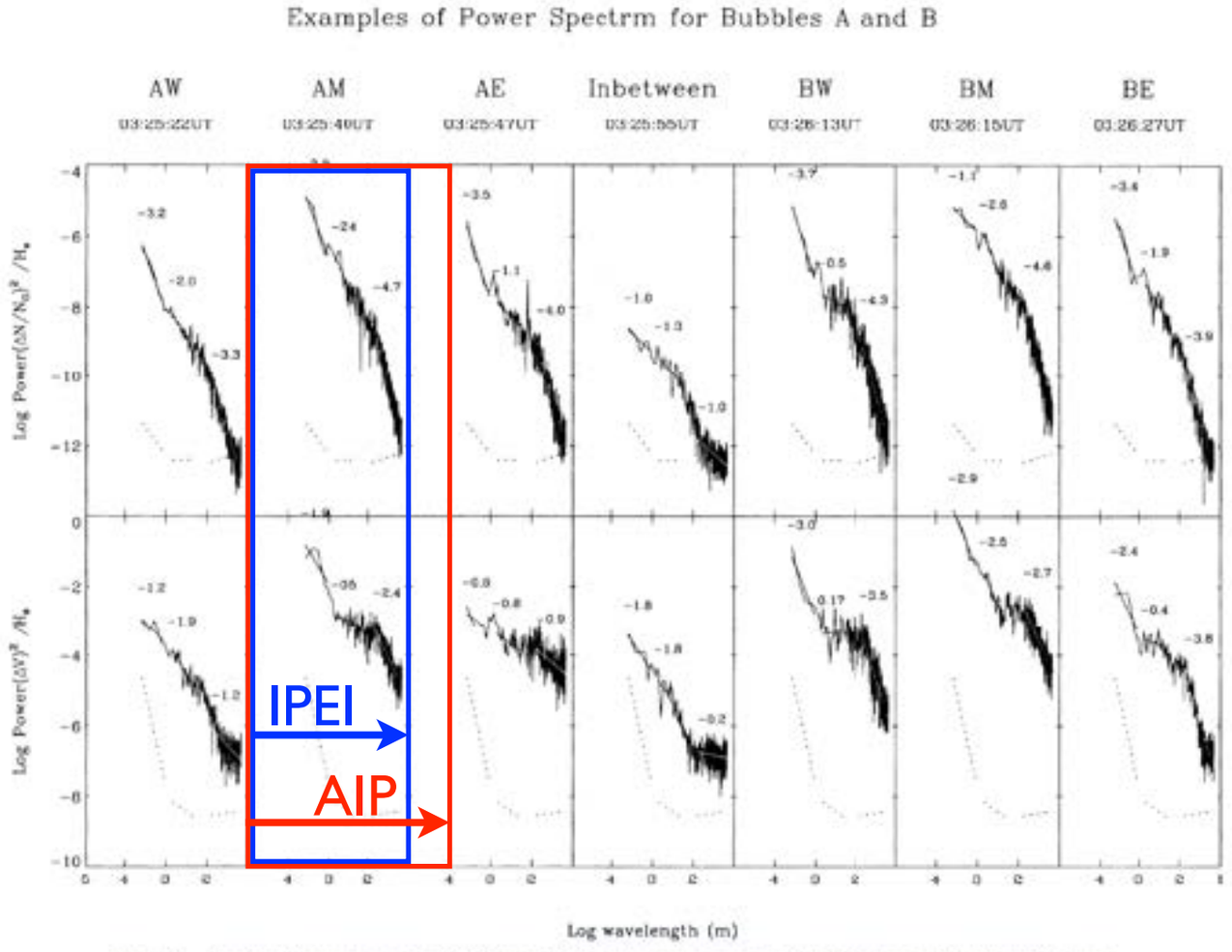

Figure 3. Examples of power spectra for $(\Delta N/N_0)$ and ΔV_z fluctuations at various parts of the bubbles as indicated by vertical lines in bubbles A and B in Figure 2.

The AIP can explore 8 x finer scale fluctuations than those measured by ROCSAT-1/IPEI.

Propagation simulation

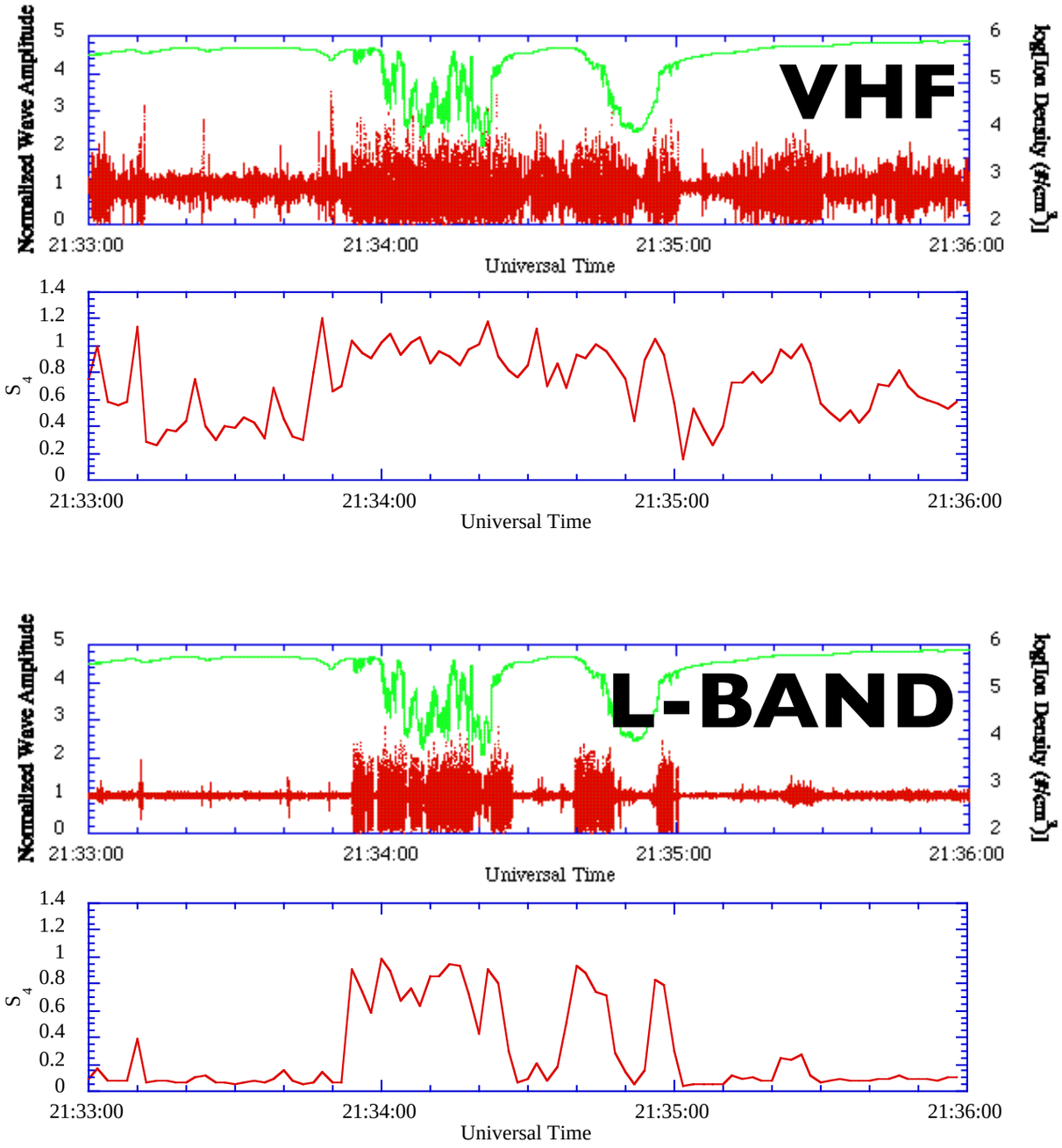

Liu et al., 2012, *Radio Sci.*

Simulation vs. ground data

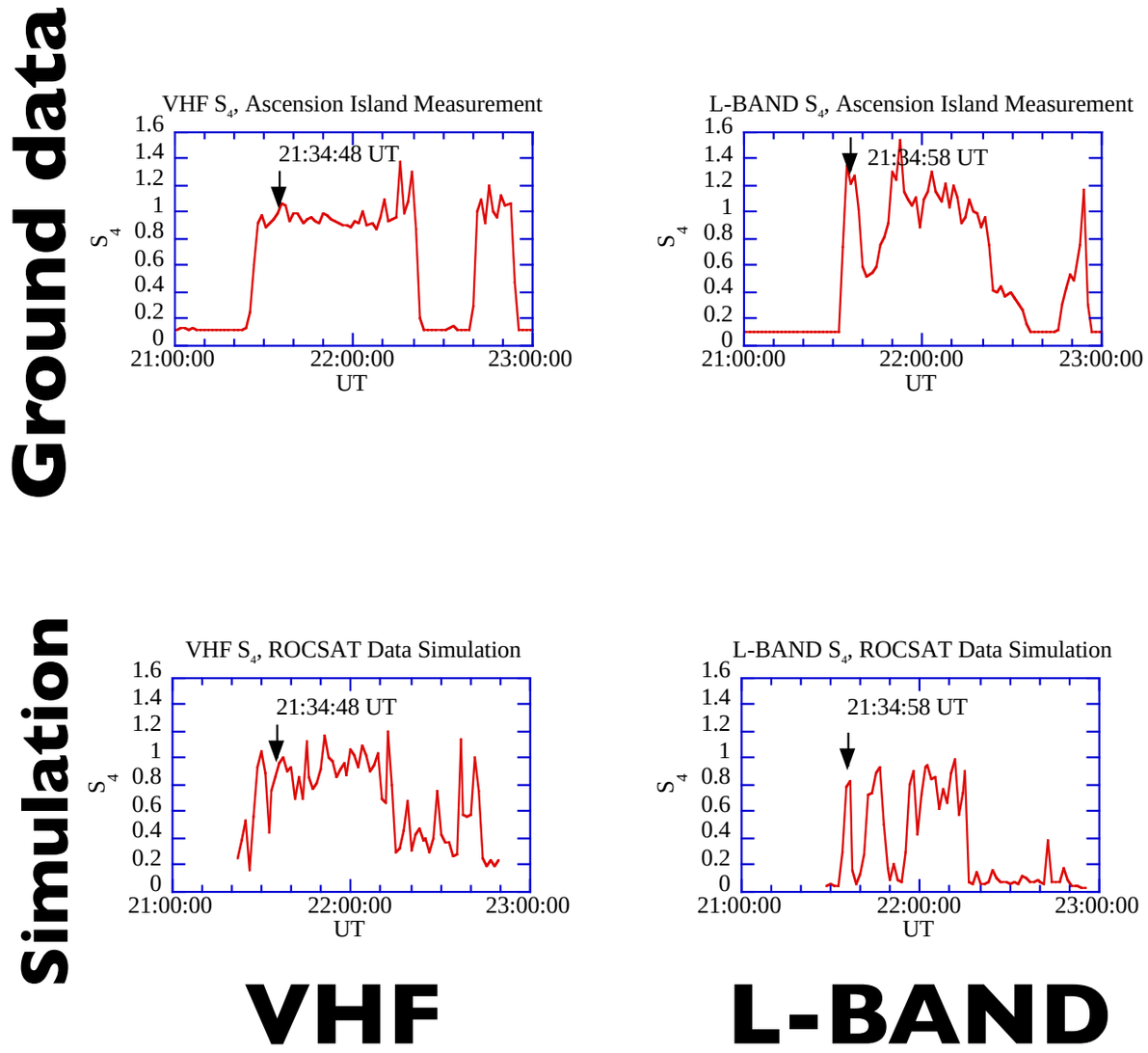

AIP can measure N_i structures to compare to RF signals at ground equivalent to 100 Hz samples for ionospheric scintillation study if eastward drift of the equatorial plasma irregularities is ~100 ms^{-1}.

Ionospheric earthquake precursor

6-10 days before the EQ | **1-5 days before the EQ** | **1-5 days after the EQ** | **6-510 days after the EQ**

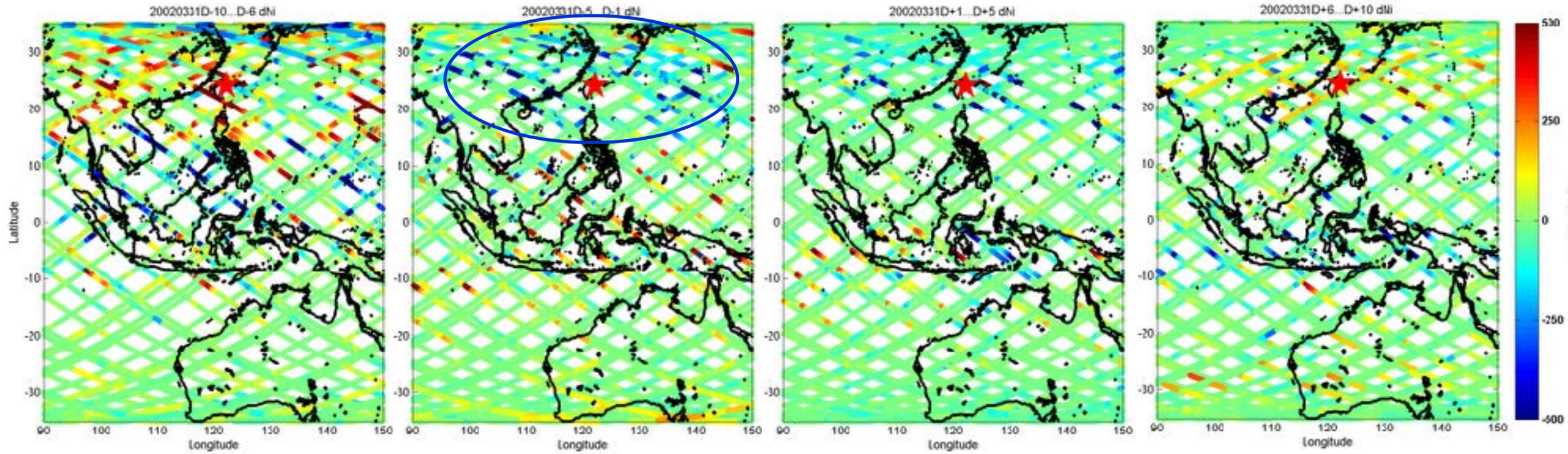

Total ion concentration detected by ROCSAT-1 satellite is abnormally reduced 1-5 days before the Yilan earthquake, M6.8, on 3/31/2002.

Total Electron Content (TEC) by GPS are greatly reduced 2 days before the earthquake.

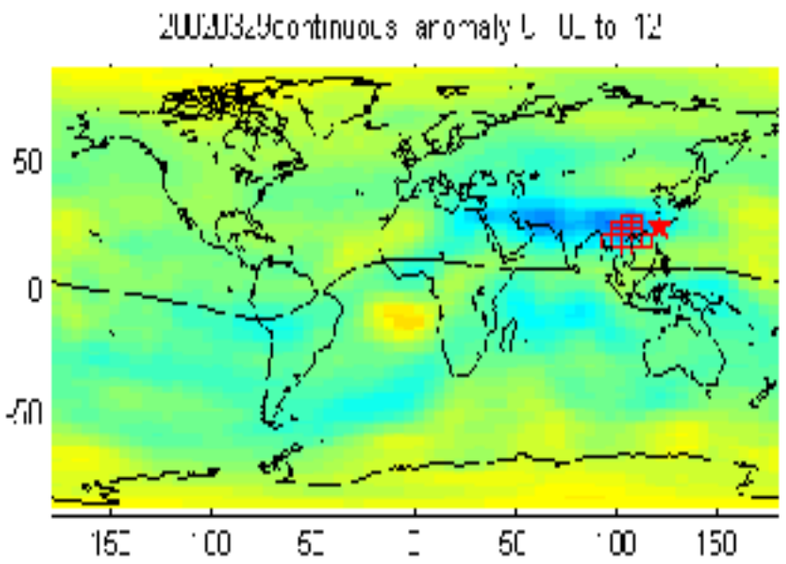

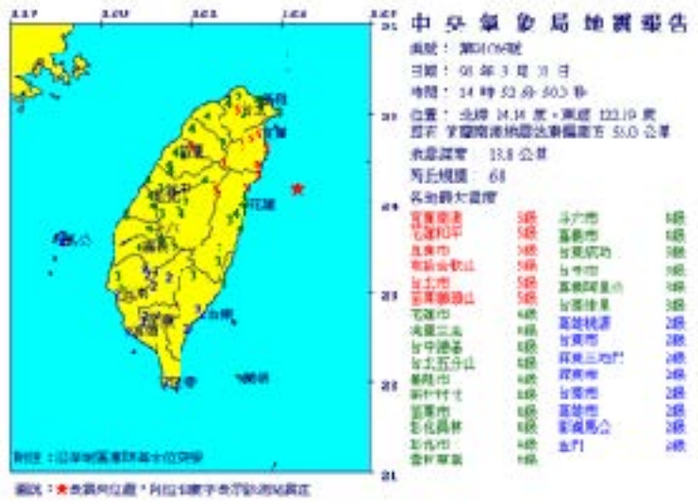

Requirements for geophysical parameters

- The FORMOSAT-5 mission orbit is at 720 km altitude with inclination 98.28° as a sun-synchronous orbit at 1030/2230 LT sector.
- Derived from International Reference Ionosphere - 2001.
- Parameter ranges (according to day & night, seasons, and solar fluxes):
  - N_e (or N_i): 5.13×10^3 to 2.61×10^5 # cm^{-3}.
  - T_e: 910 to 3,100 K.
  - T_i: 770 to 2,370 K.

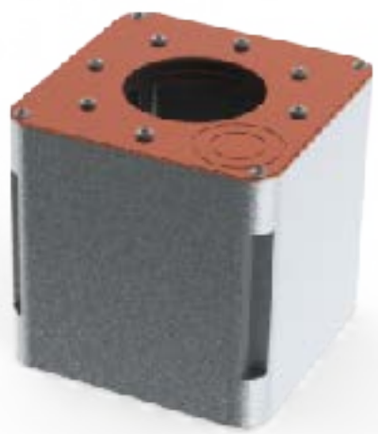

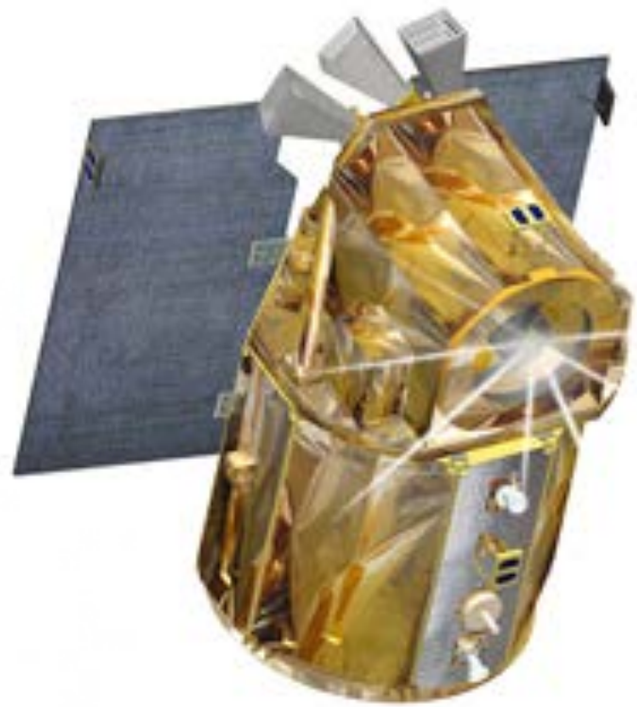

Requirements

Parameters	Range	Accuracy
C_i	5% to 100%	10%
N_i	10^3 to $5x10^6$ cm^{-3}	10%
$\mathbf{v}_i$ (w.r.t ground)	±2 km s^{-1} (cross track) ±2 km s^{-1} (ram)	± 50 m s^{-1} ± 200 m s^{-1}
T_i	750 to 5,000 K	±200 K
T_e	750 to 5,000 K	±200 K

Data availabilities

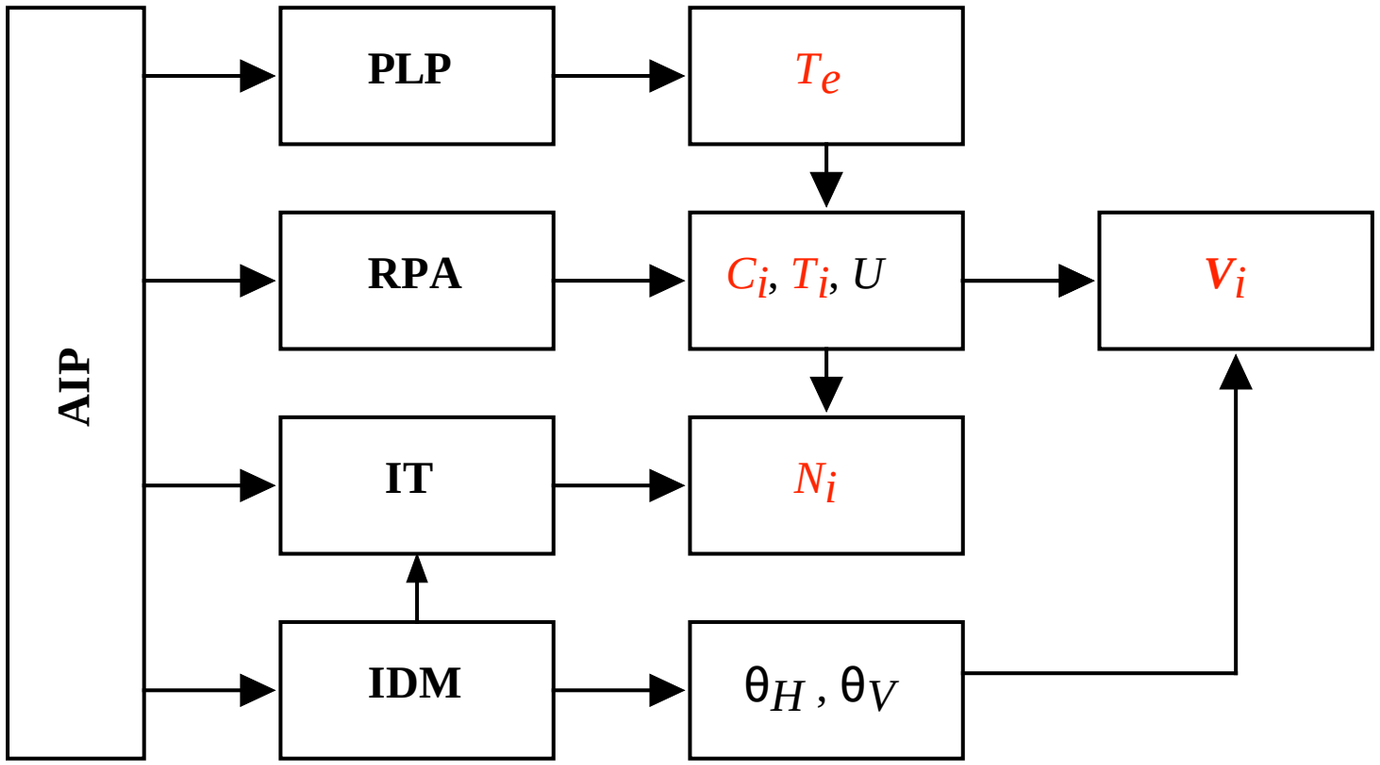

Mode	N_i	Transverse components of the ion velocity	Others
NORMAL	128 Hz	32 Hz	1 Hz
FAST	1,024 Hz	256 Hz	1 Hz
BURST	8,192 Hz	2,048 Hz	1 Hz

Parameters	Range	Sensitivity	Accuracy
C_i	3% to 100%	1%	10%
N_i	10^3 to 10^6 cm^{-3}	1%	10%
$\boldsymbol{V}_i$ (w.r.t satellite)	±2.5 km s^{-1} 7.5±1 km s^{-1} (ram)	± 10 m s^{-1} ± 100 m s^{-1}	± 50 m s^{-1} ± 200 m s^{-1}
T_i	500 to 5,000 K	±50 K	±200 K
T_e	500 to 5,000 K	±50 K	±200 K

Principles of measurement

- Distribution function for a steady state condition
- Langmuir probe
- Retarding potential analyzer
- Ion drift meter

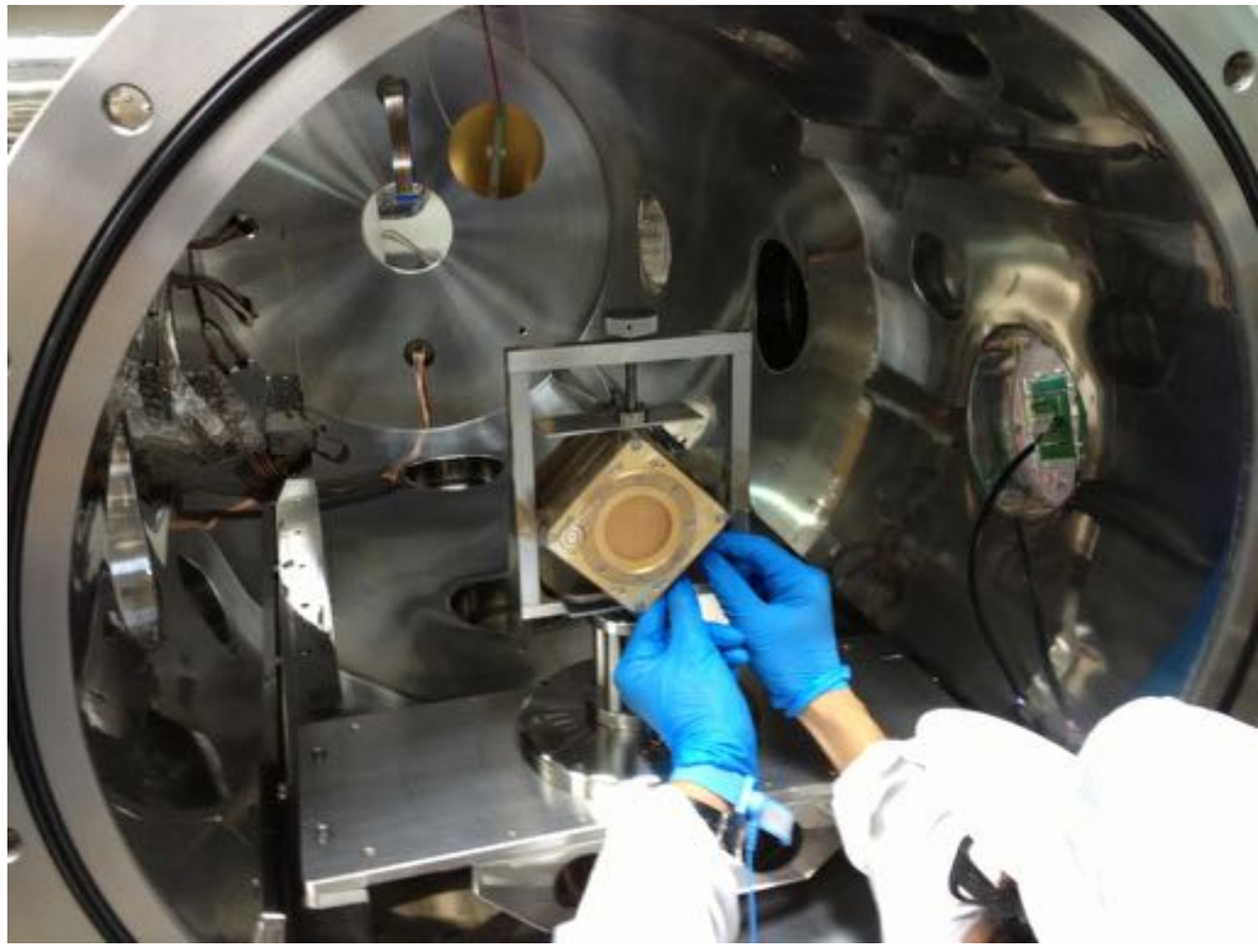

Integration of constant

Assuming a collision-less, electrostatic and no external magnetic field condition, the Vlasov equation can be rewritten as

$$\frac{\partial f_j}{\partial t} + \mathbf{v} \cdot \frac{\partial f_j}{\partial \mathbf{x}} + \frac{q_j}{m_j}\left(\mathbf{E} + \frac{\mathbf{v} \times \mathbf{B}}{c} \right) \cdot \frac{\partial f_j}{\partial \mathbf{v}} = 0$$

The phase space distribution function will be conserved if follows a dynamical trajectory described as

$$\frac{dx}{\upsilon_x} = \frac{dy}{\upsilon_y} = \frac{dz}{\upsilon_z} = \frac{d\upsilon_x}{-\frac{q_j}{m_j}\frac{\partial V}{\partial x}} = \frac{d\upsilon_y}{-\frac{q_j}{m_j}\frac{\partial V}{\partial y}} = \frac{d\upsilon_z}{-\frac{q_j}{m_j}\frac{\partial V}{\partial z}}$$

An integration of constant (conservation law of total energy) can be obtained as

$$\frac{m_j \upsilon^2}{2} + q_j V = const$$

Maxwell-Boltzmann distribution function

Any function with the energy conservation form will be accepted as a solution of the Vlasov equation, so the distribution function can be described as

$$f(\mathbf{x},\mathbf{v}) = f\left(\frac{m\upsilon^2}{2} + qV(\mathbf{x})\right)$$

In our application, a satellite flows through the ionosphere horizontally with a supersonic speed, a three-dimensional Maxwell-Boltzmann distribution function with drift velocity *U* is applied to obtain the steady flux collected within the retarding potential analyzer as

$$f(\mathbf{x},\mathbf{v}) = n_o\left(\frac{m}{2\pi\kappa T}\right)^{\frac{3}{2}} \exp\left[-\left(\sqrt{\frac{m\upsilon^2}{2\kappa T} + \frac{qV(\mathbf{x})}{\kappa T}} - \sqrt{\frac{mU^2}{2\kappa T}}\right)^2\right]$$

~~$$f(\mathbf{x},\mathbf{v}) = n_o\left(\frac{m}{2\pi\kappa T}\right)^{\frac{3}{2}} \exp\left[-\left(\frac{m(\upsilon-U)^2}{2\kappa T} + \frac{qV(\mathbf{x})}{\kappa T}\right)\right]$$~~

The moment equations

The particle number density *n* and flux Φ are defined by integrating the phase space distribution function over velocity space as

$$n(\mathbf{x}) \equiv \int f(\mathbf{x},\mathbf{v})\, d\mathbf{v}$$

$$\Phi(\mathbf{x}) \equiv n(\mathbf{x})\mathbf{u}(\mathbf{x}) \equiv \int f(\mathbf{x},\mathbf{v})\,\mathbf{v}\, d\mathbf{v}$$

where **u**(**x**) is the average velocity of incoming plasma at position **x**. It is noted that lower and upper velocity limits become important in deriving these macroscopic density and flux for different boundary conditions.

Planar Langmuir Probe (PLP)

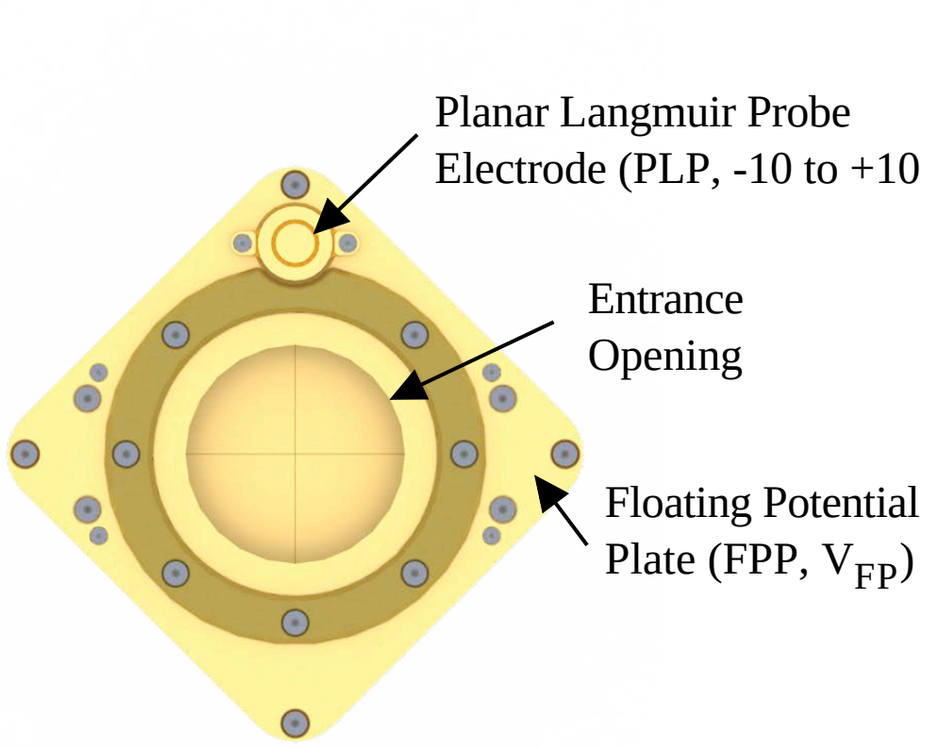

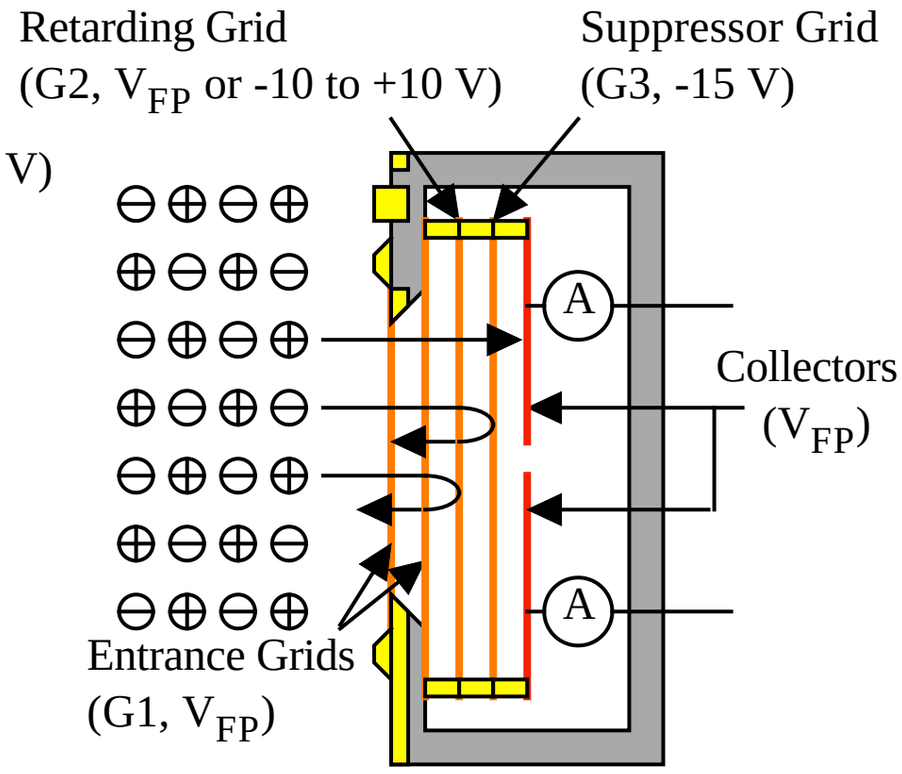

$$\frac{\kappa T_e}{e} = \frac{1}{\frac{d}{dV}\left[\ln(I)\right]}$$

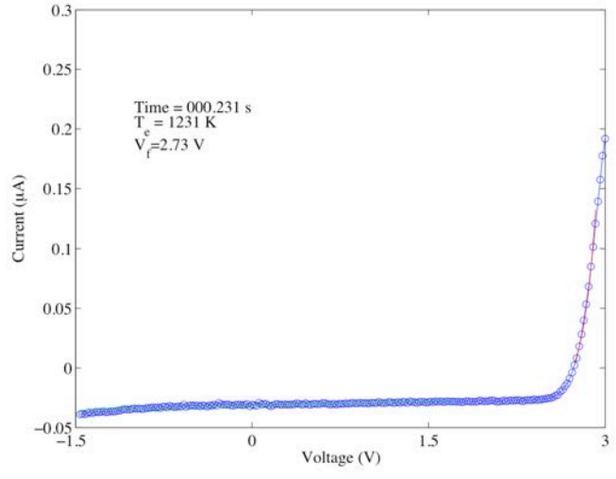

I-V curve

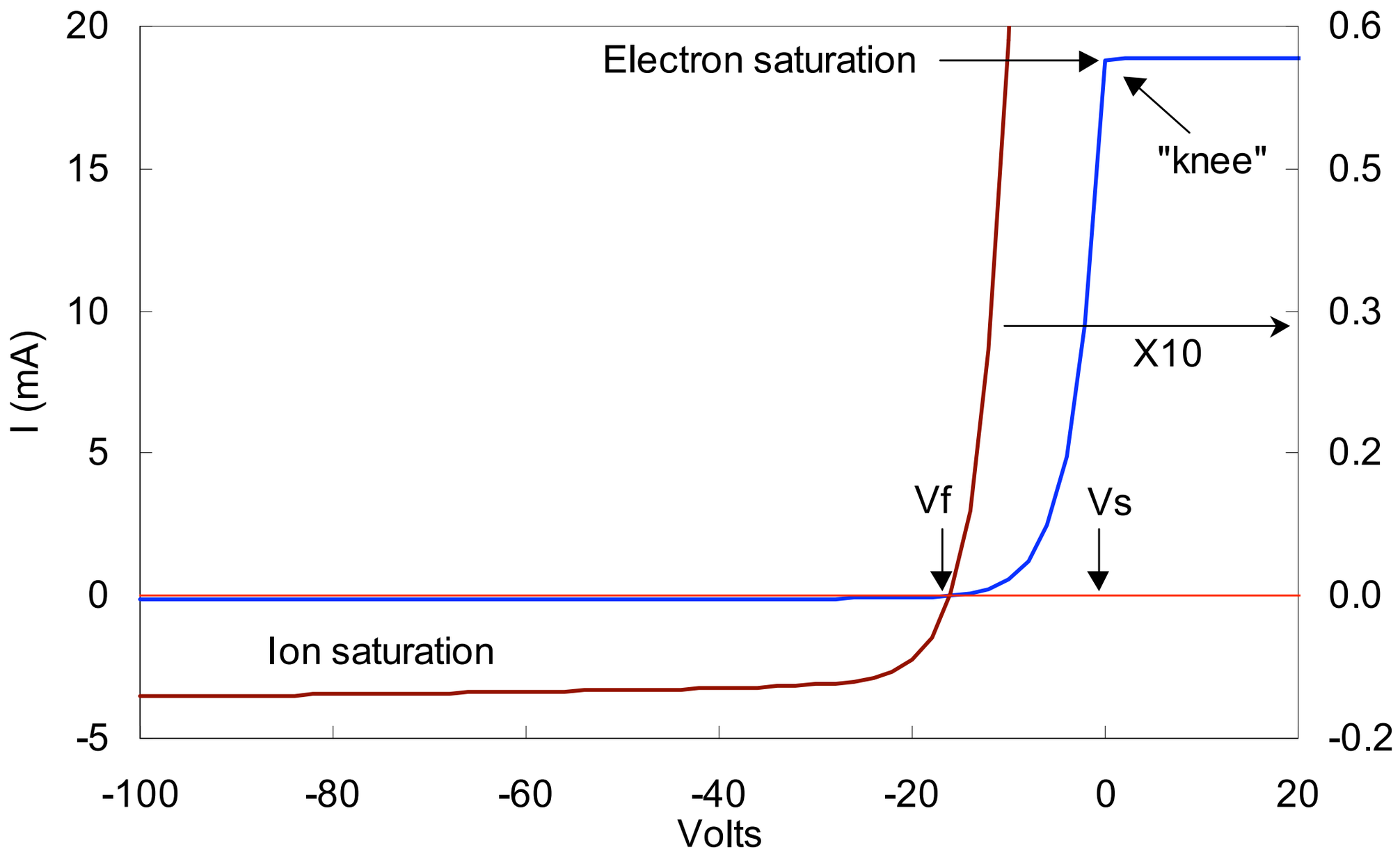

$$I = I_e - I_i$$

Transition region

If the probe voltage is made negative relative to plasma potential, the probe begins to repel electrons and accelerate ions.

Because the fraction of electrons with velocities sufficient for overcoming the decelerating field diminished, the electron current falls as probe voltage decreases, which we shall call the transition region or retarding-field region of the characteristic.

If the electron distribution were Maxwellian, the shape of the curve, after the contribution of ions is subtracted, would be exponential.

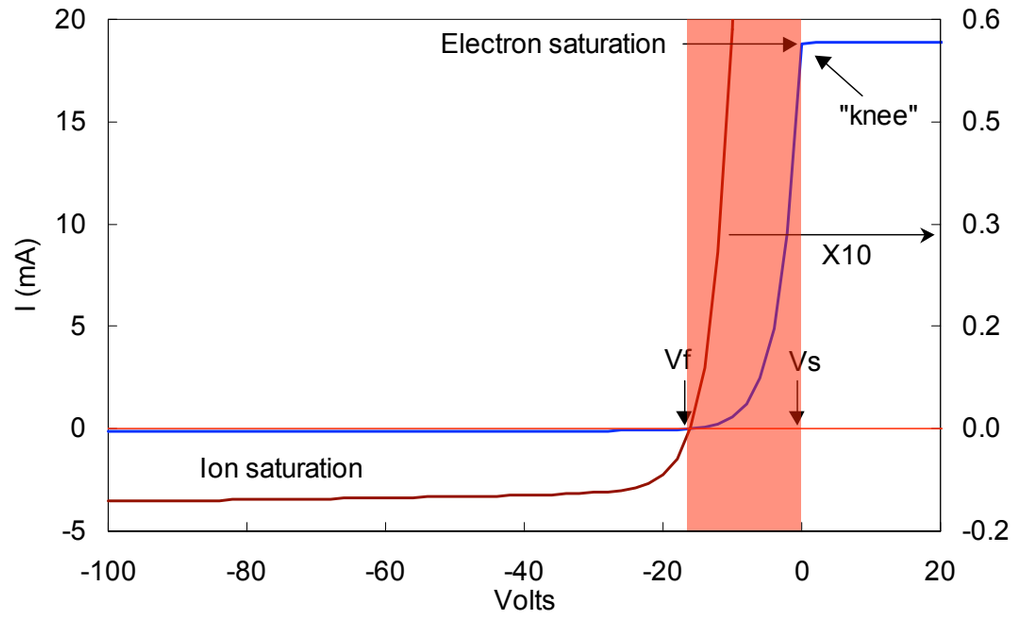

For $V < 0$, the lowest limit for a free electron to hit on probe surface is zero.

$$\int_{\omega}^{\infty} \upsilon \exp\left(-\alpha\upsilon^2\right)d\upsilon = \frac{\exp\left(-\alpha\omega^2\right)}{2\alpha}$$

$$\Phi(V) = \int_{-\infty}^{\infty}\int_{-\infty}^{\infty}\int_{0}^{\infty} n_o \sqrt{\left(\frac{m_e}{2\pi\kappa T_e}\right)^3} \exp\left[-\left(\frac{m_e\left(\upsilon_x^2+\upsilon_y^2+\upsilon_z^2\right)-2eV}{2\kappa T_e}\right)\right]\upsilon_x\, d\upsilon_x d\upsilon_y d\upsilon_z$$

$$= n_o \exp\left(\frac{eV}{\kappa T}\right)\left[\int_{-\infty}^{\infty}\sqrt{\frac{m_e}{2\pi\kappa T_e}}\exp\left(-\frac{m_e\upsilon_y^2}{2\kappa T_e}\right)d\upsilon_y\right]\left[\int_{-\infty}^{\infty}\sqrt{\frac{m_e}{2\pi\kappa T_e}}\exp\left(-\frac{m_e\upsilon_z^2}{2\kappa T_e}\right)d\upsilon_z\right]$$

$$\left[\int_{0}^{\infty}\sqrt{\frac{m_e}{2\pi\kappa T_e}}\upsilon_x \exp\left(-\frac{m_e\upsilon_x^2}{2\kappa T_e}\right)d\upsilon_x\right] = n_o \exp\left(\frac{eV}{\kappa T_e}\right)\frac{\sqrt{\frac{m_e}{2\pi\kappa T_e}}}{2\frac{m_e}{2\kappa T_e}} = \frac{1}{4}n_o\sqrt{\frac{8\kappa T_e}{\pi m_e}}\exp\left(\frac{eV}{\kappa T_e}\right)$$

$$I(V) = qA\Phi(V) = I_e = A(-e)n_o \exp\left(\frac{eV}{\kappa T_e}\right)\sqrt{\frac{\kappa T_e}{2\pi m_e}}$$

$$\rightarrow \ln(I) = \ln\left[A(-e)n_o \exp\left(\frac{eV}{\kappa T_e}\right)\sqrt{\frac{\kappa T_e}{2\pi m_e}}\right] = \ln\left[A(-e)n_o\sqrt{\frac{\kappa T_e}{2\pi m_e}}\right] + \frac{eV}{\kappa T_e}$$

$$\rightarrow \frac{d}{dV}\left[\ln(I)\right] = \frac{e}{\kappa T_e} \rightarrow \boxed{T_e = \frac{e}{\kappa}\frac{1}{\frac{d}{dV}\left[\ln(I)\right]}}$$

Retarding Potential Analyzer (RPA)

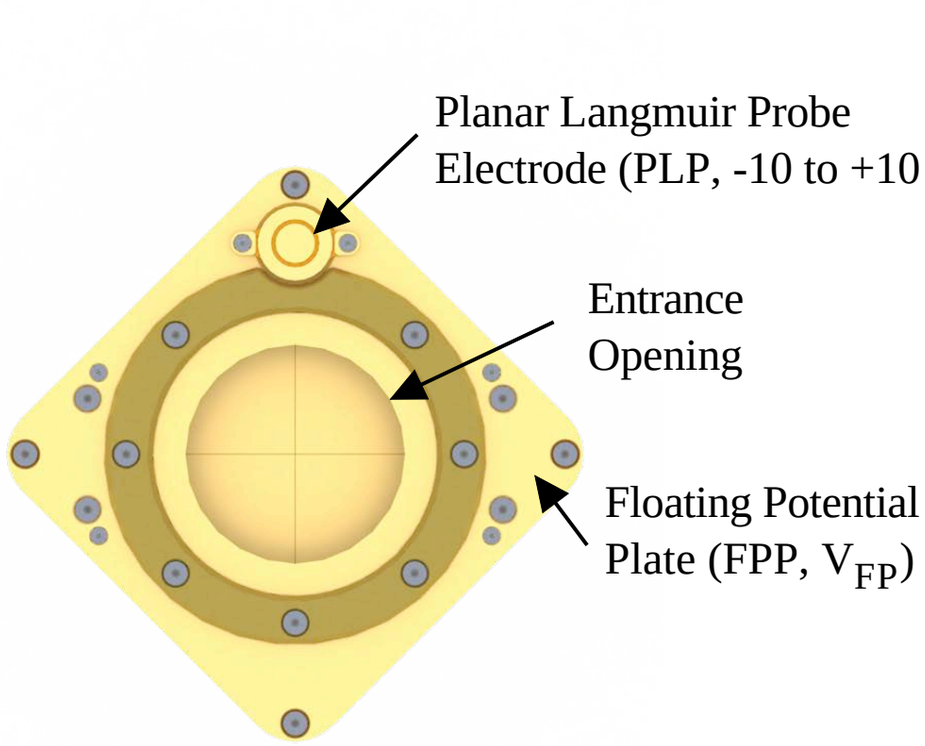

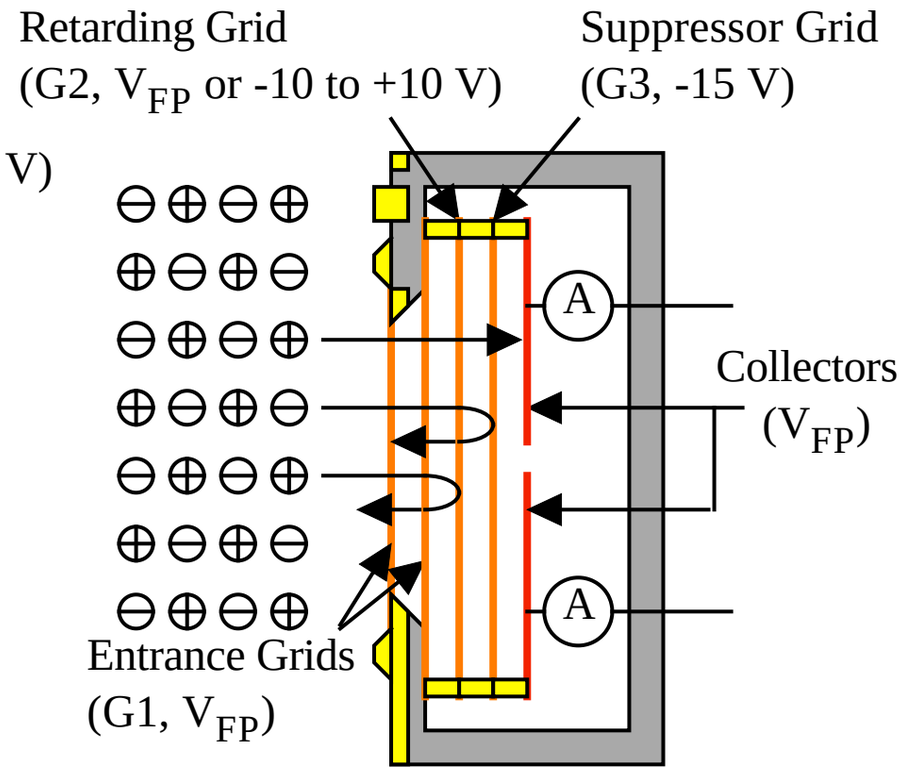

$$I = CA\sum_s q_s n_{so} U_s \left\{ \frac{1}{2}\left[1 + erf\left(\beta_s F_s\right) + \frac{\exp\left(-\beta_s^2 F_s^2\right)}{\sqrt{\pi}\beta_s U_s} \right] \right\}$$

$$\beta_s = \sqrt{\frac{m_s}{2\kappa T_s}},\ \beta_s F_s = U_s / \sqrt{\frac{2\kappa T_s}{m_s}} - \sqrt{\frac{q_s V_{G2}}{\kappa T_s}}\ .$$

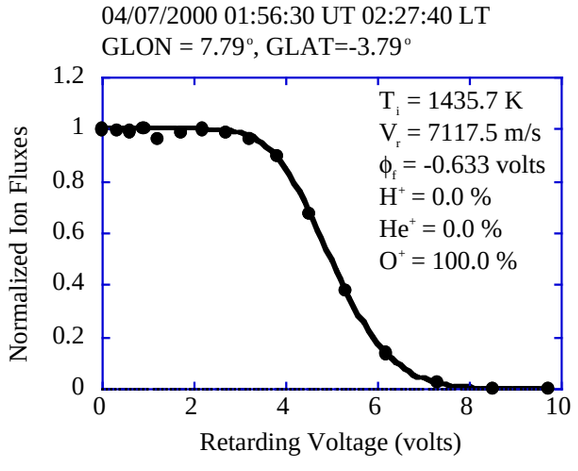

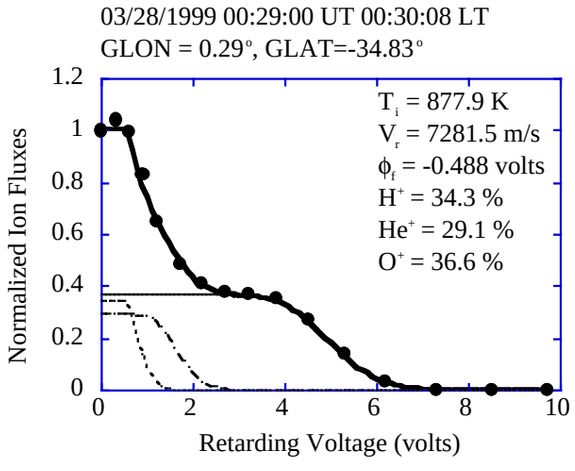

The lower velocity limit

To derive the ion flux within the RPA, several assumptions are made here. We set electric potential to zero for plasma far away from collector. In a fixed frame of a satellite rigid body, positive ions can stream with about satellite velocity from outside the RPA into the collector. Based on the conservation of energy, the retarding potential structure inside the RPA will prevent the low energy positive ions from reaching the collector. The lower velocity limit v_L for integration is depended on the maximum potential V_M along the streaming path and its location

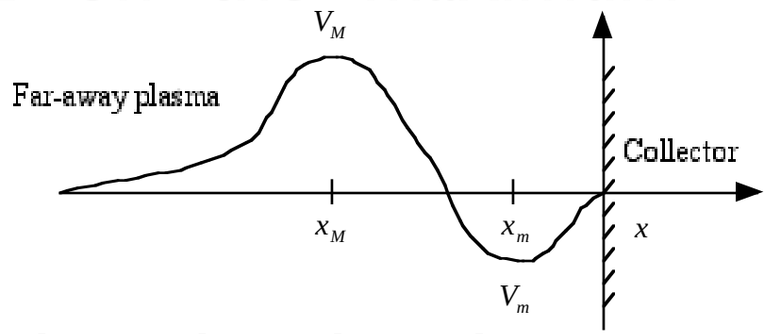

$$v_L = \pm\sqrt{\frac{2q\left[V_M - V(x)\right]}{M}}$$

where M is the ion mass. The positive sign indicates that the distribution has overcome the maximum potential barrier (between the retarding grid and the collector, i.e., $x > x_M$) and the negative sign indicates that the distribution has return particles (between the far away space and retarding grid, i.e., $x < x_M$).

The ion flux equation

The flux for a single species can be integrated as

$$\Phi(x) = \int_{\upsilon_L}^{\infty} f\upsilon\, d\upsilon = \int_{\pm\sqrt{\frac{2q[V_M - V(x)]}{M}}}^{\infty} n_o \sqrt{\frac{M}{2\pi\kappa T}} \exp\left[-\left(\sqrt{\frac{M\upsilon^2}{2\kappa T} + \frac{qV}{\kappa T}} - \sqrt{\frac{MU^2}{2\kappa T}} \right)^2 \right] \upsilon\, d\upsilon$$

Let's define the variable α and substitute it into the flux equation

$$\alpha = \sqrt{\frac{M\upsilon^2}{2\kappa T} + \frac{qV}{\kappa T}} - \sqrt{\frac{MU^2}{2\kappa T}} \rightarrow \upsilon d\upsilon = \frac{\alpha + \sqrt{\frac{MU^2}{2\kappa T}}}{\left(\frac{M}{2\kappa T}\right)} d\alpha$$

The lower limit of the integration is not a function of position any more and can be changed to

$$\alpha_L = \sqrt{\frac{qV_M}{\kappa T}} - \sqrt{\frac{MU^2}{2\kappa T}}$$

The ion flux equation (cont.)

The flux can be modified as

$$\Phi = \int_{\sqrt{\frac{qV_M}{\kappa T}}-\sqrt{\frac{MU^2}{2\kappa T}}}^{\infty} n_o \sqrt{\frac{M}{2\pi\kappa T}} \exp\left[-\alpha^2\right]\left(\alpha + \sqrt{\frac{MU^2}{2\kappa T}}\right)\frac{d\alpha}{\left(\frac{M}{2\kappa T}\right)}$$

Using these definite integrals from mathematical handbook

$$\int_x^{\infty} \exp\left[-\alpha^2\right] d\alpha = \frac{\sqrt{\pi}}{2}\left[1 - erf\left(x\right)\right] \qquad \int_x^{\infty} \exp\left[-\alpha^2\right] \alpha\, d\alpha = \frac{\exp\left[-x^2\right]}{2}$$

The flux equation can be derived as

$$\Phi\left(V_M\right) = n_o U\left\{\frac{1}{2}\left[1 + erf\left(\beta F\right) + \frac{\exp\left[-\left(\beta F\right)^2\right]}{\sqrt{\pi}\beta U}\right]\right\}$$

, where

$$\beta = \sqrt{\frac{M}{2\kappa T}} \qquad F = U - \sqrt{\frac{2qV_M}{M}}$$

$$\beta F = \frac{U}{\sqrt{\frac{2\kappa T}{M}}} - \sqrt{\frac{qV_M}{\kappa T}}$$

High ram velocity

From the ion flux equation for multiple species, the ion flux at far away plasma (the electric potential is set to zero) is expressed as

$$\Phi(0) = \sum_i \Phi_i(0) = \sum_i n_{oi} U_i \left\{ \frac{1}{2} \left[1 + erf\left(\beta_i U_i\right) + \frac{\exp\left[-\left(\beta_i U_i\right)^2\right]}{\sqrt{\pi}\beta_i U_i} \right] \right\}$$

For ROCSAT observation, the ion ram velocities U_i (~ satellite velocity) are larger than the ion thermal speeds, i.e.:

$$\beta_i U_i = U_i / \sqrt{\frac{2\kappa T_i}{M_i}} >> 1$$

The error function can be expanded for large $\beta_i U_i$ and the ion flux at zero electric potential can be reduced to

$$\Phi(0) = \sum_i \Phi_i(0) \sim \sum_i n_{oi} U_i \left\{ \frac{1}{2} \left[1 + 1 - \frac{\exp\left[-\left(\beta_i U_i\right)^2\right]}{\sqrt{\pi}\beta_i U_i} \left(1 - \frac{1}{2\beta_i^2 U_i^2} + \ldots \right) + \frac{\exp\left[-\left(\beta_i U_i\right)^2\right]}{\sqrt{\pi}\beta_i U_i} \right] \right\} \sim \sum_i n_{oi} U_i$$

Cut-off potential

We can define a cut-off electric potential V_{ci} for species i to make $\beta_i F_i = 0$. It is similar to zero point of the second derivative of the I-V curve with respect to the potential mentioned by *Greenspan* et al. [1986]. Such the cut-off potential can be written as

$$V_{ci} \equiv \frac{M_i U_i^2}{2q_i}$$

The **cut-off potential** was defined [*Chao and Su*, 1999] as the potential that prevents the mean flow of a specific species from reaching the collector plate. The ion fluxes can be written as

$$\Phi_j\left(V_{ci}\right) \sim \begin{cases} 0, & \text{if } i > j \\ \Phi_i(0)\left\{\frac{1}{2}\left[1+\frac{1}{\sqrt{\pi}\sqrt{\frac{q_i V_{ci}}{\kappa T_i}}}\right]\right\} = \Phi_i(0)\left\{\frac{1}{2}\left[1+\frac{1}{\sqrt{\pi}\sqrt{\frac{M_i U_i^2}{2\kappa T_i}}}\right]\right\}, & \text{if } i = j \\ \Phi_j(0), & \text{if } i < j \end{cases}$$

Half current approximation

Considering the ROCSAT flying speed and the ionospheric environment at 600 km altitude, most of cases that we study indicate $M_i U_i^2/2 > \kappa T_i$.
Therefore the total ion flux $\Phi(V_{ci})$ can be approximated as

Half current at cut-off potential

$$\Phi(V_{ci}) = \sum_j \Phi_j(V_{ci}) \sim \boxed{\frac{\Phi_i(0)}{2}} + \sum_{i<j} \Phi_j(0)$$

Once the $\Phi(V_{ci})$ are estimated, the cut-off potentials V_{ci} can be searched from the I-V data measured by the RPA through interpolation methods and are expressed as

$$V_{ci} \sim V\left(\Phi = \frac{1}{2}\Phi_i(0) + \sum_{i<j}\Phi_j(0)\right)$$

The ram velocity and the ion density for each species can be derived from

$$U_i = \sqrt{\frac{2q_i V_{ci}}{M_i}}$$

$$n_{oi} = \frac{\Phi_i(0)}{U_i\left\{\frac{1}{2}\left[1 + erf(\beta_i U_i) + \frac{\exp\left[-(\beta_i U_i)^2\right]}{\sqrt{\pi}\beta_i U_i}\right]\right\}} \sim \frac{\Phi_i(0)}{U_i}$$

Half current approximation (cont.)

To derive the ion temperature, we can differentiate the ion flux equation for species *i* with electric potential

$$\frac{d\Phi_i}{dV} = \frac{q_i n_{oi}}{\sqrt{2\pi}} \frac{\exp\left[-\left(\beta_i F_i\right)^2\right]}{\sqrt{M_i \kappa T_i}}$$

The slope of *j*-ion flux at V_{ci} can be approximated as

$$\frac{d\Phi_j}{dV}\left(V_{ci}\right) \sim \begin{cases} 0, & \text{if } i \neq j \\ -\dfrac{q_i \Phi_i\left(0\right)}{U_i \sqrt{2\pi M_i \kappa T_i}}, & \text{if } i = j \end{cases}$$

Therefore the slope of the total ion flux at V_{ci} can be estimated as

$$\frac{d\Phi}{dV}\left(V_{ci}\right) = \sum_j \frac{d\Phi_j}{dV}\left(V_{ci}\right) = -\frac{q_i \Phi_i\left(0\right)}{U_i \sqrt{2\pi M_i \kappa T_i}}$$

Half current approximation (cont.)

Once the $d\Phi(V_{ci})/dV$ is known (also available from the interpolation of the I-V data), the ion temperature for species *i* can then be calculated as

$$\kappa T_i = \frac{q_i^2 \Phi_i^2(0)}{2\pi M_i U_i^2 \left[\frac{d\Phi}{dV}(V_{ci})\right]^2} = \frac{q_i \Phi_i^2(0)}{4\pi V_{ci} \left[\frac{d\Phi}{dV}(V_{ci})\right]^2}$$

Hence the half-current approximation can obtain the ion ram velocity, ion density and ion temperature for each species. These results can be served as initial guesses for a more sophisticate regression fit.

Half current method

The half-current method is composed by the half-current approximation and a variety of numerical schemes.

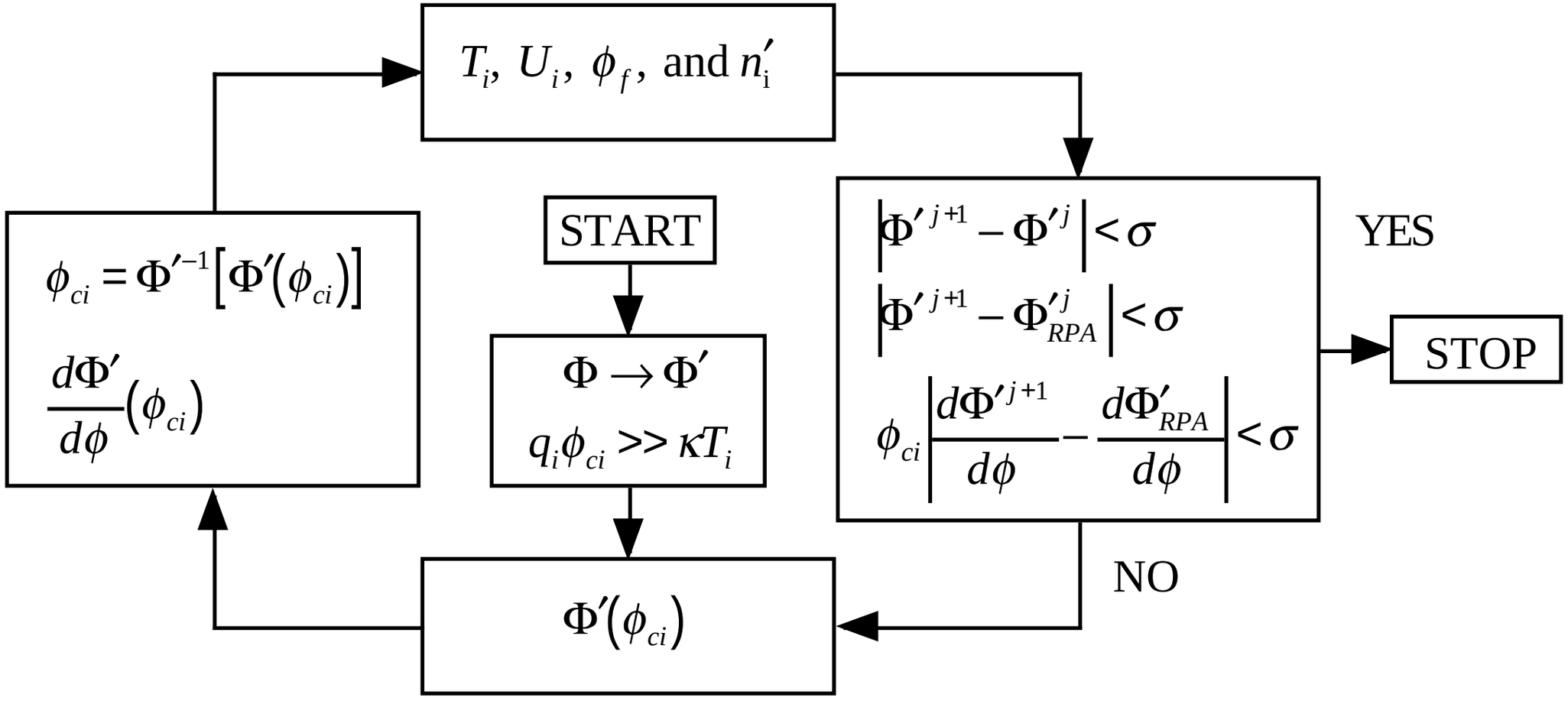

Grid search method

In most statistic textbooks, χ^2 has been recognized as a measure of goodness of fit [*Bevington*, 2002],

$$\chi^2 \equiv \sum_i \left\{ \frac{\left[\Phi'_i - \Phi'(V_i)\right]^2}{\sigma_i^2} \right\}$$

where i is the subscript for different data points and the σ_i are the uncertainties in the normalized data points Φ'_i. The analytical values are the normalized ion fluxes calculated at the potentials V_i from the derived parameters. One of the easiest methods to find out the minimum of the χ^2 is to use a grid search method. The minimum of the χ^2 can be derived from the derivative of the χ^2 with respect to each parameter as

$$\frac{\partial \chi^2}{\partial \alpha_k} = \frac{\partial}{\partial \alpha_k} \sum_i \left\{ \frac{\left[\Phi'_i - \Phi'(V_i)\right]^2}{\sigma_i^2} \right\} = 0$$

Half-current method only single species

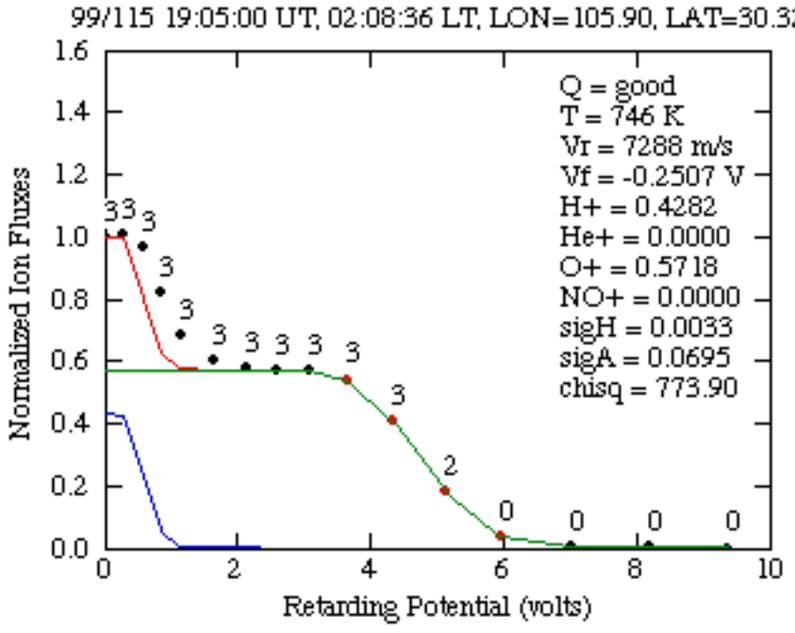

Half-current method only multiple species

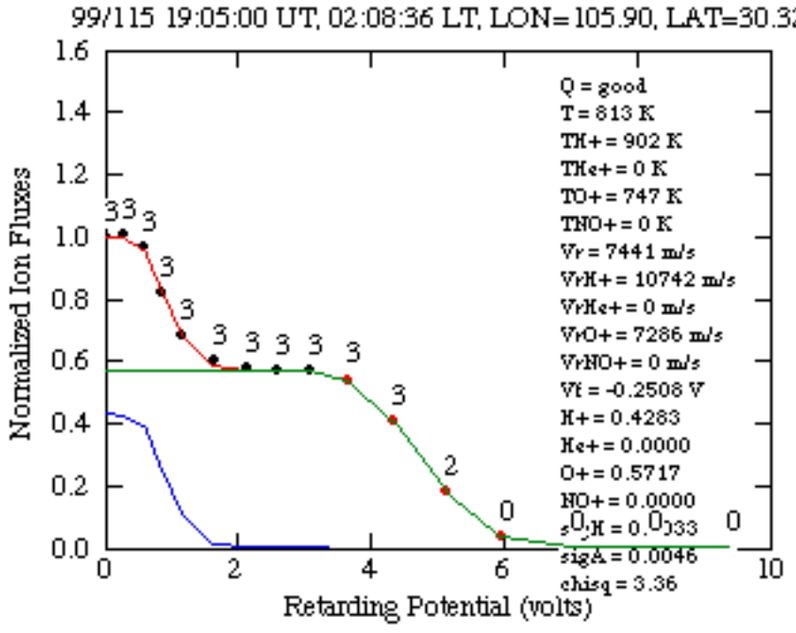

Least-squares fit single species

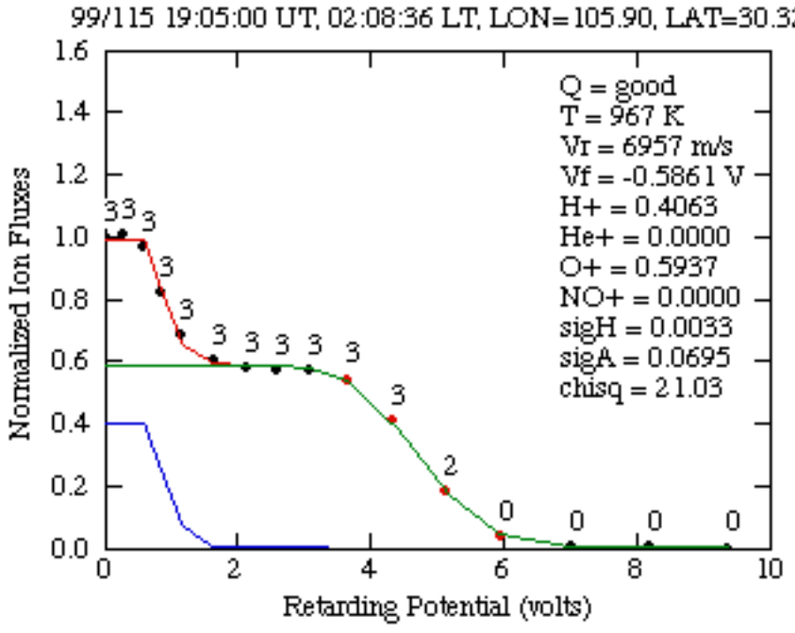

Least-squares fit multiple species

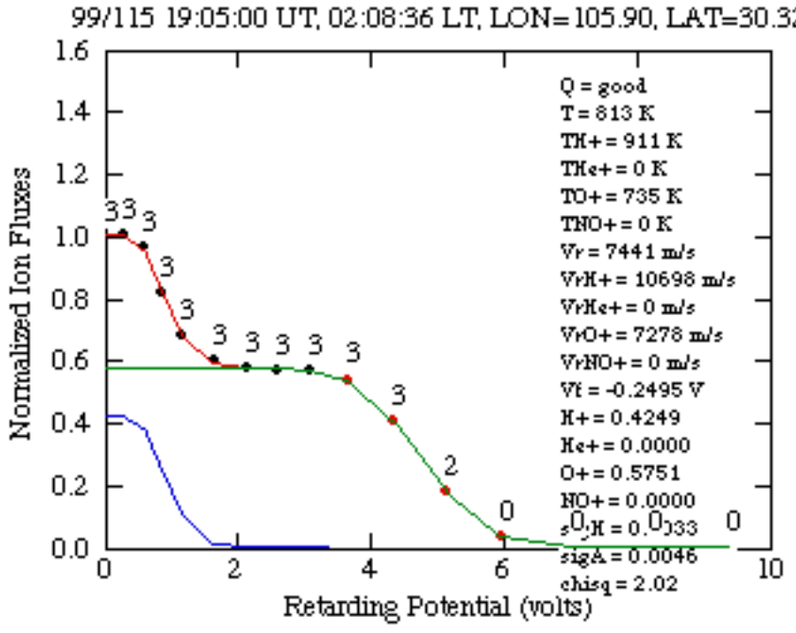

Grid potential depression

Since the retarding grid cannot provide a uniform electric potential perfectly, there is some calibration on the retarding potential. The suppressor and dual aperture grids are both possible to reduce the potential on a saddle point of the retarding grids. Thus particles with energies smaller than the retarding voltage could pass through these potential depressions on the retarding grid planes to reach the collector.

According to the simulation results shown in the figure, the potential depression factor for the IPEI/RPA configuration is about 0.96501 [*Chao et al.*, 2003]. That means the retarding potential will be used by the input retarding voltage multiplied by the depression factor.

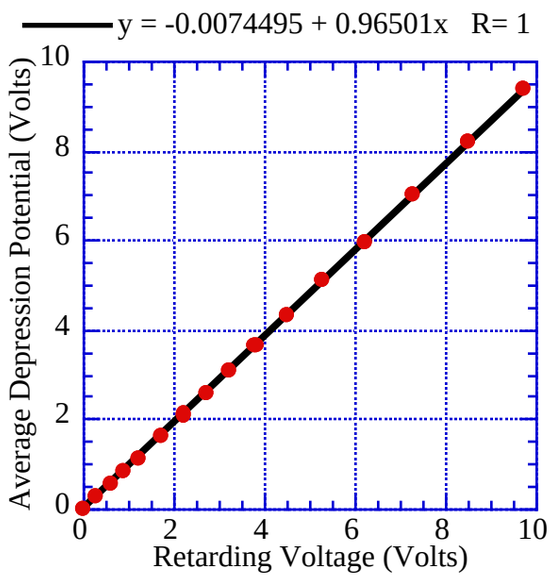

Effects on ion T_i and U_r

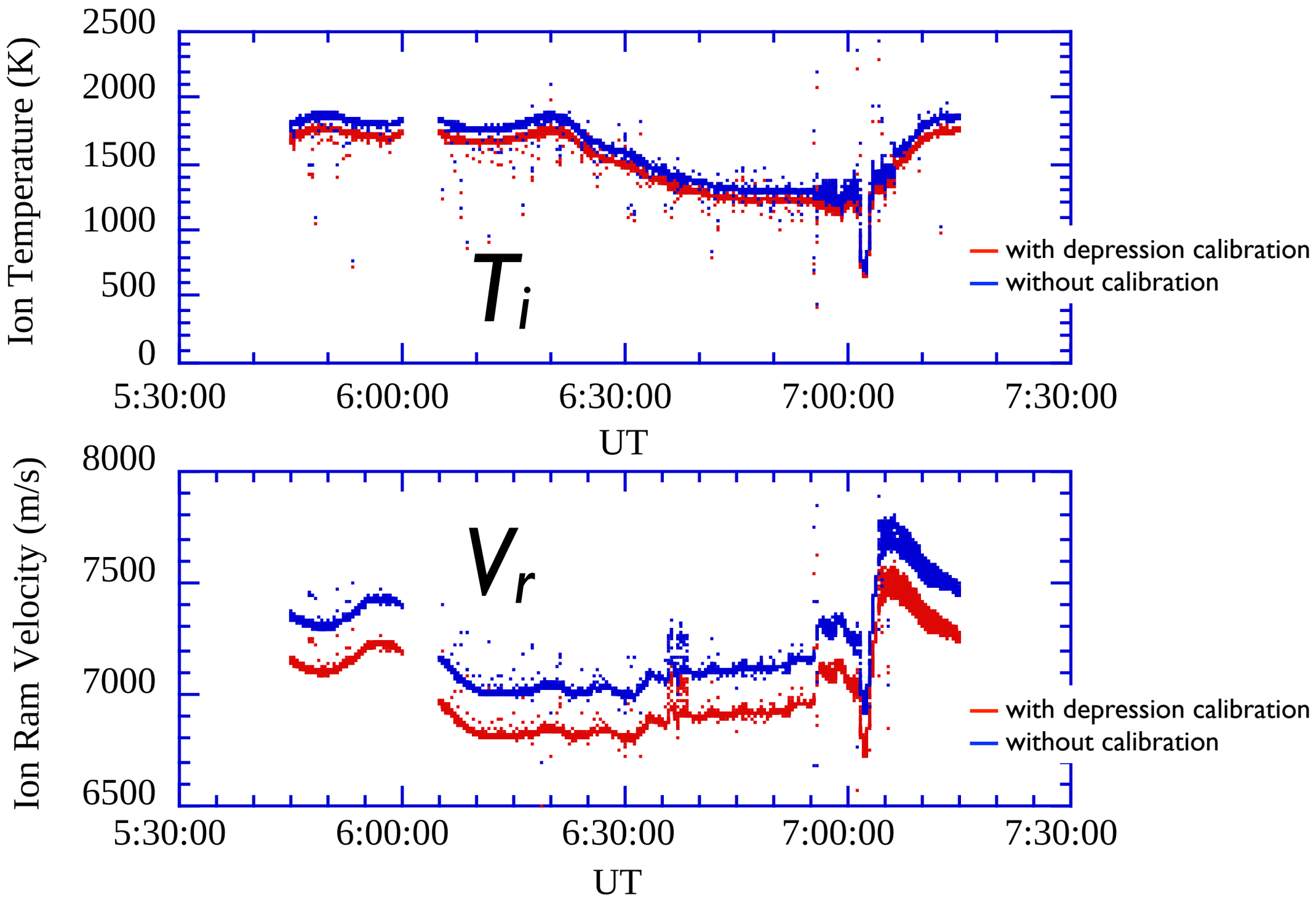

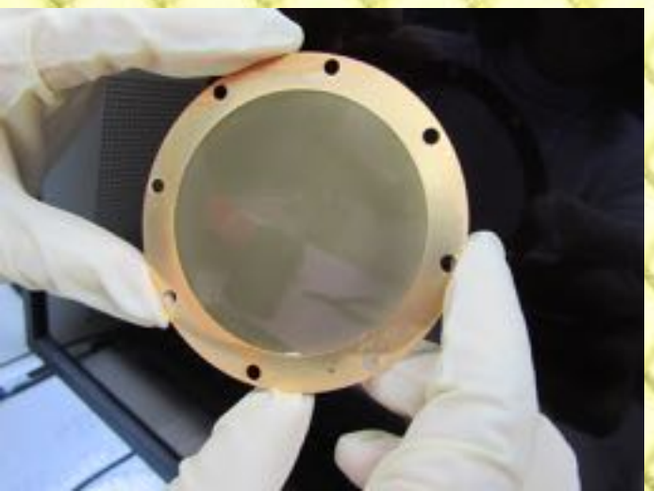

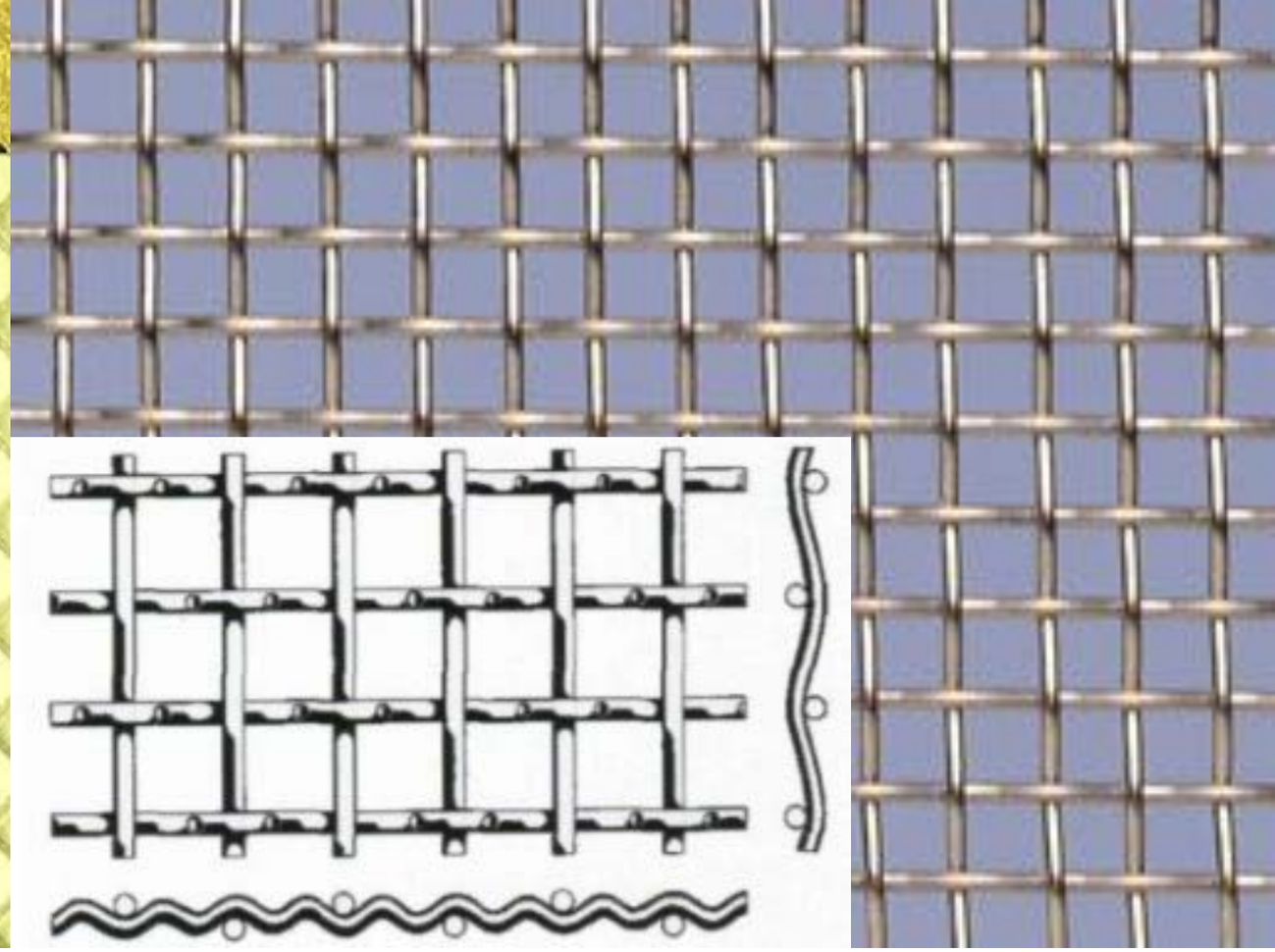

Electro-formed grids (AIP)

99.98% gold grid, good equal potential surface, reduced I-V hysteresis, poor resilience.

Mesh density: 100 LPI.

Grid diameter: 0.5 mil

Transparency: 0.9025 ◦

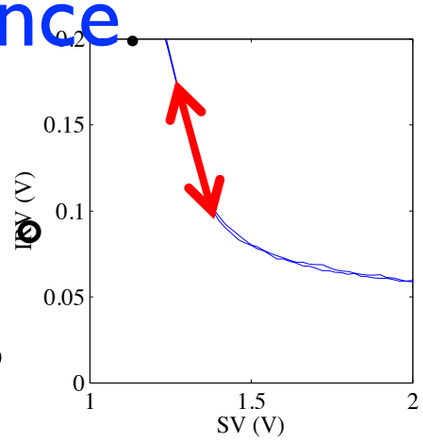

Weaved grids (IPEI)

Stainless steel grid coated in gold, bad equal potential surface, apparent I-V hysteresis, good resilience.

Mesh density: 50/100 LPI.

Grid diameter: 1 mil.

Transparency: 0.9025/0.81.

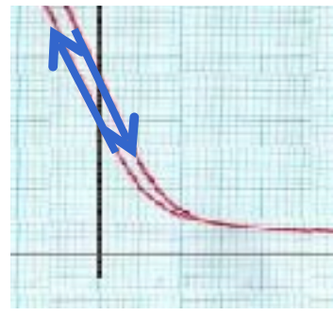

1 mil (10^{-3} inch = 25.4 μm) and diameter of a human hair ~4 mil.

Ion Drift Meter (IDM)

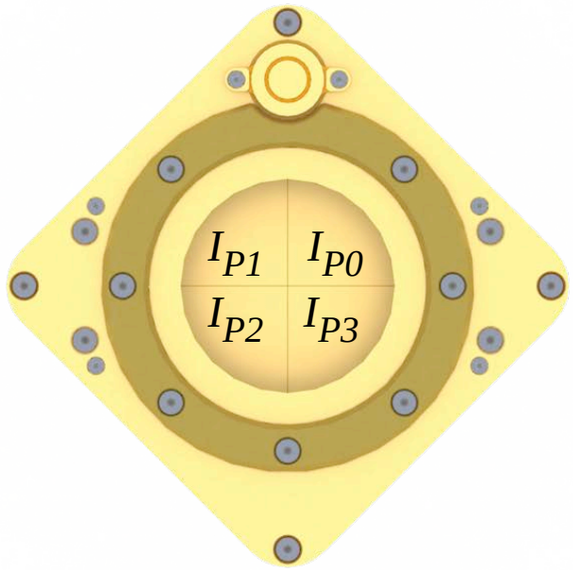

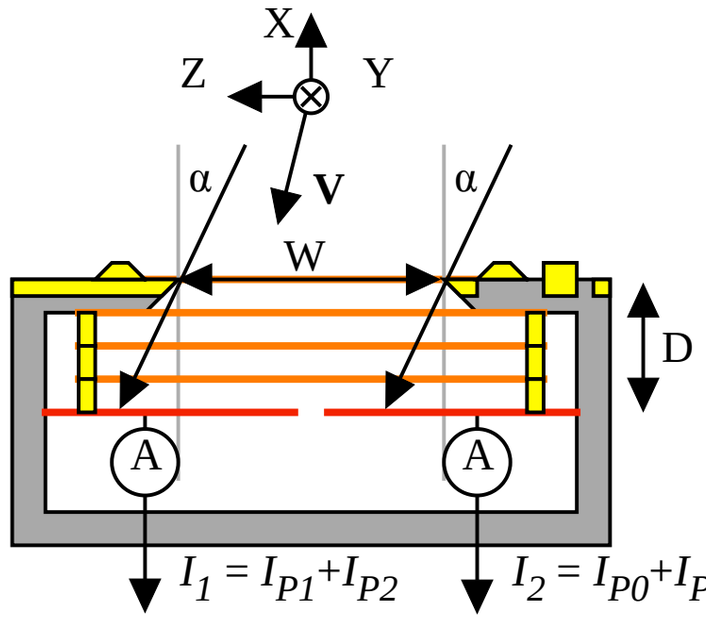

For a circular aperture in AIP

$$\tan\alpha = \frac{W}{2D}\cos\frac{\theta}{2}, \quad \theta = \sin\theta + \left[1 - \left(\frac{I_1 - I_2}{I_1 + I_2}\right)\right]\pi$$

For a square aperture in IPEI

$$\tan\alpha = \frac{W}{2D}\left(\frac{I_1 - I_2}{I_1 + I_2}\right)$$

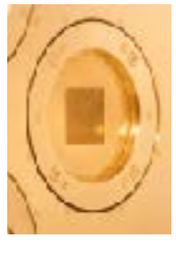

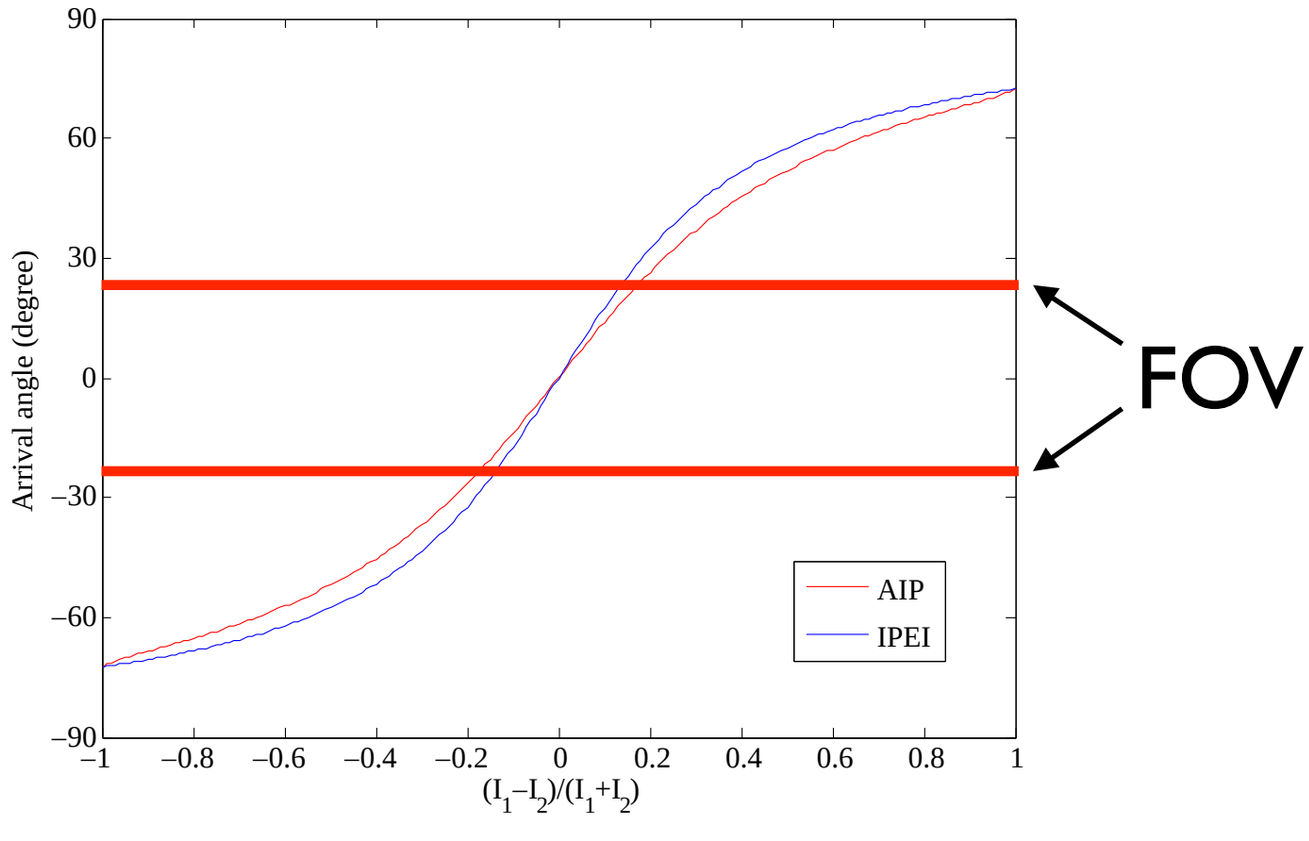

Advanced Ionospheric Probe

Advanced Ionospheric Probe (AIP) is an all-in-one thermal plasma sensor to measure ionospheric plasma concentrations (N_i), velocities ($\boldsymbol{V}_i$), and temperatures (T_i and T_e) in a time sharing way to play Ion Trap (IT), Ion Drift Meter (IDM), Retarding Potential Analyzer (RPA), and Planar Langmuir Probe (PLP).

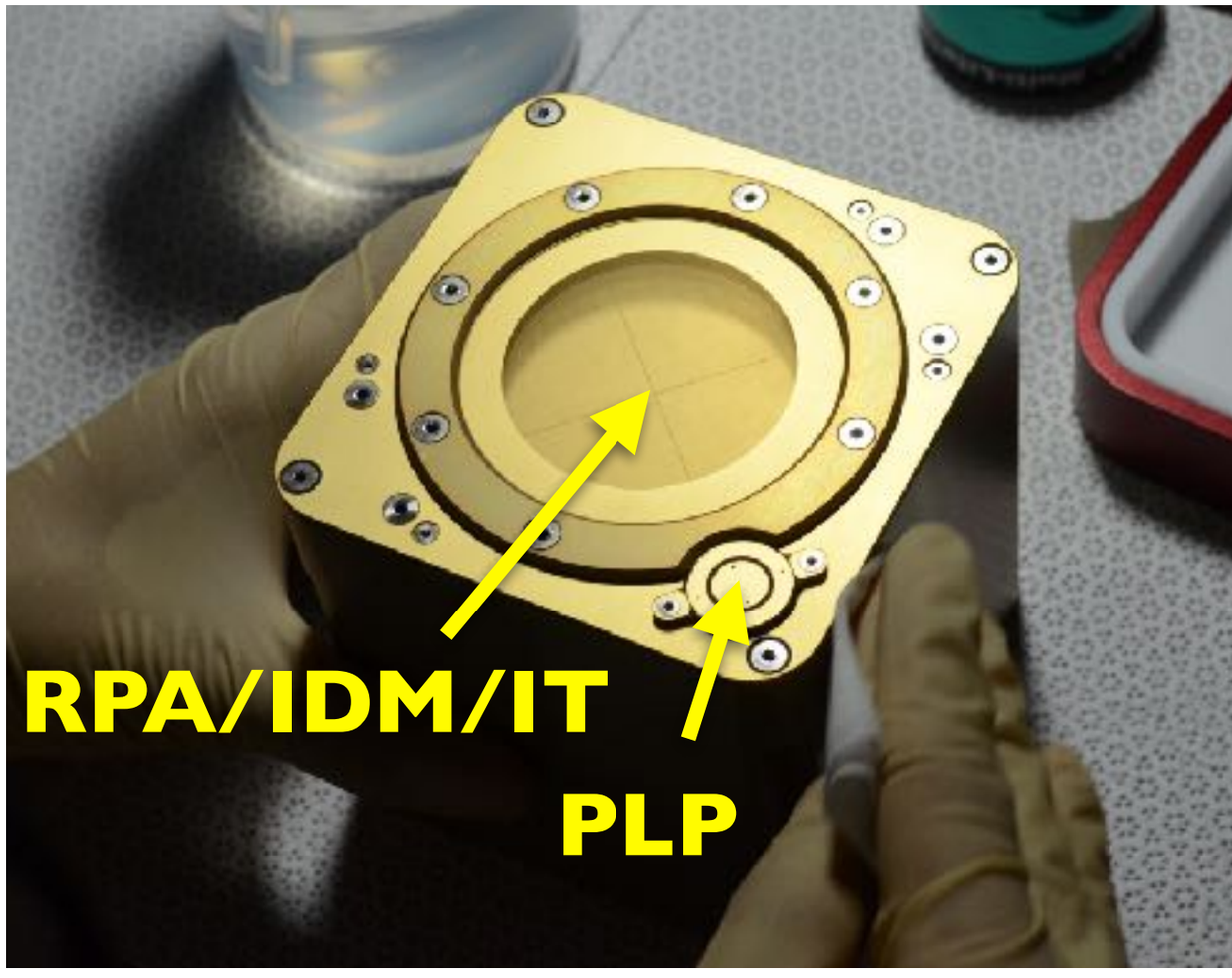

The AIP is capable of measuring ionospheric plasma irregularities with sampling rate up to 8,192 Hz. Electro-formed gold grids used in the AIP can reduce quasi-hysteresis effect on I-V curves and approximate ideal electrical potential surfaces for accurate geophysical parameters.

AIP organization

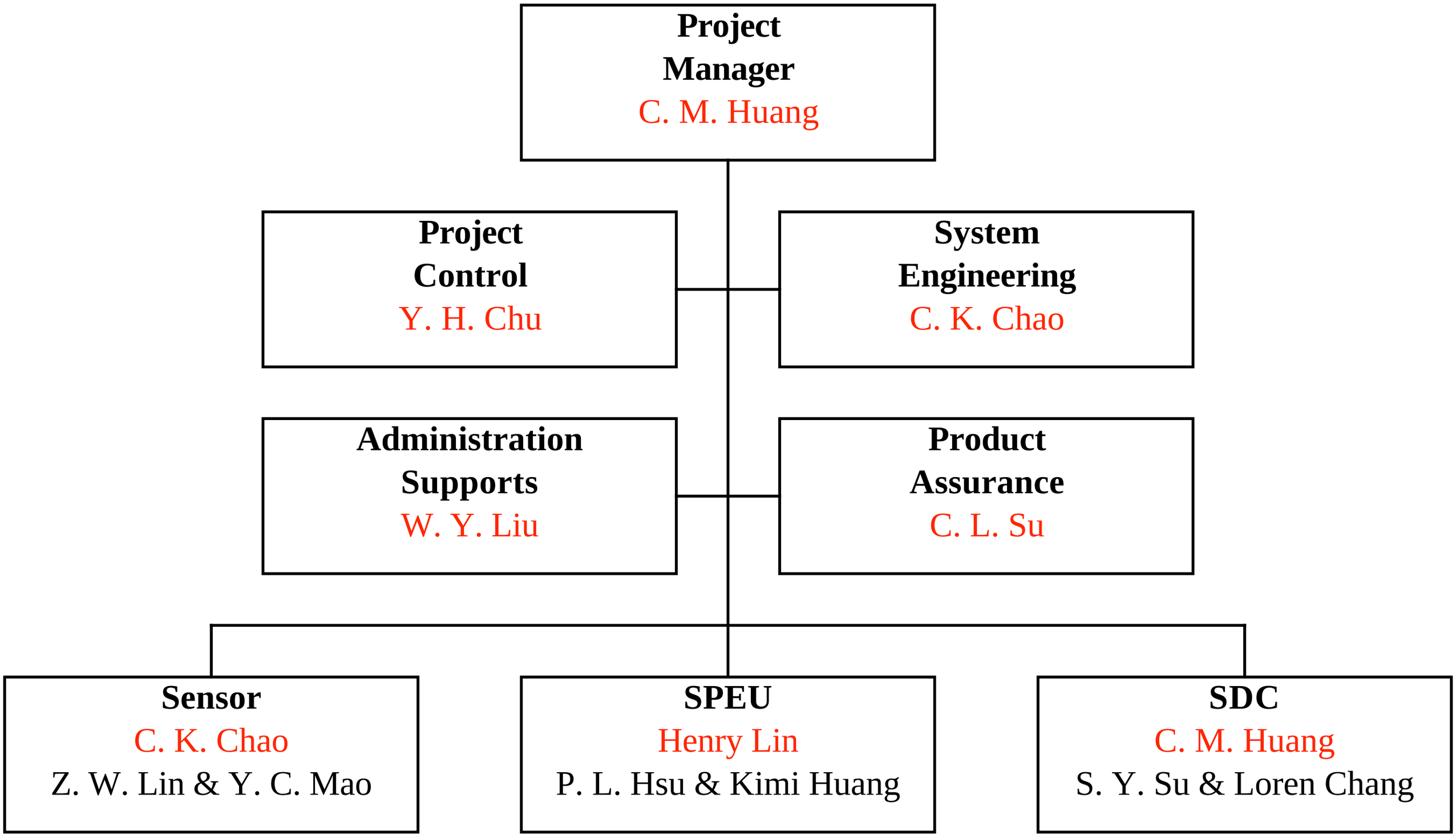

Sensor organization

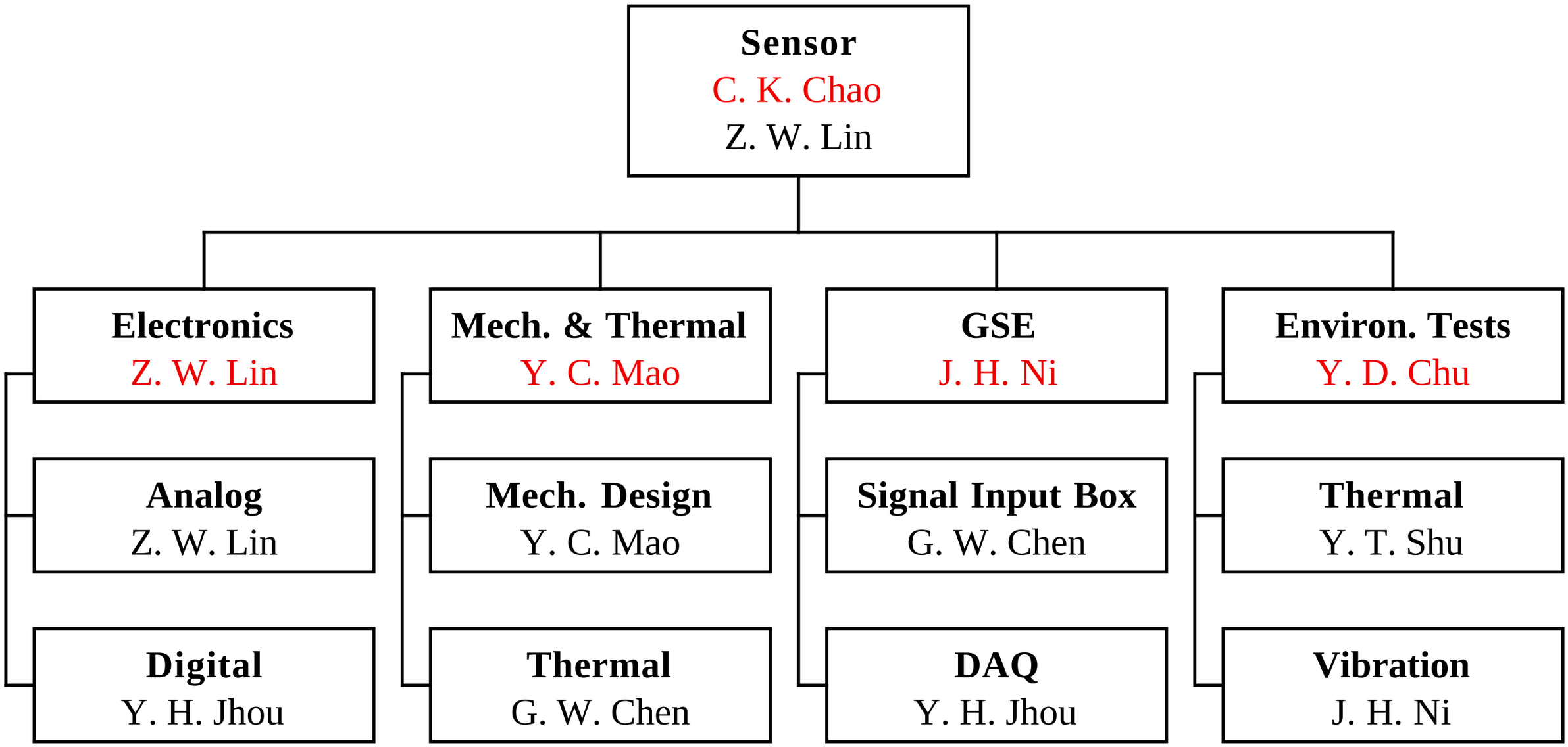



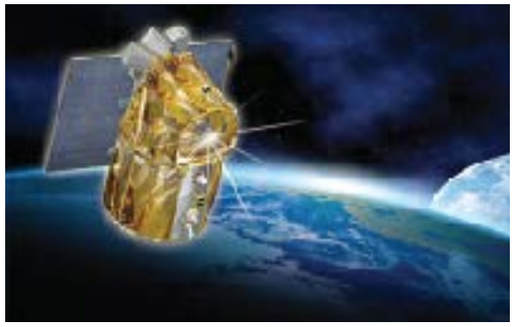

Satellites	**DMSP**	**DEMETER**	**FORMOSAT-5**
Nations	US	France	Taiwan
Sun-synchronous Orbits	840 km	715 km	720 km
Solar activity	All	Low	Low
Thermal plasma sensors	SSI/ES-3: IT + DM + RPA + LP.	RPA + IDM + LP.	AIP: PLP, RPA, or IDM/IT.
Sampling rates	24 S/s (N_i) 2.5 S/s (others)	160 S/s (N_i) 3 S/s (others)	128 - 8,192 S/s (N_i) 32 - 2,048 S/s ($V_{y,z}$) 1 S/s (others)
Sensor functions	Fixed	Fixed	Software programmable

Schedule	WSD
38 months	2012/01/13 to 2015/03/12
Milestone	Due
MDR / SDR	2012/03/12 (WSD + 2m)
PDR	2012/05/12 (WSD + 4m)
ISD	2012/07/12 (WSD + 6m)
CDR	2012/09/12 (WSD + 8m)
DRR	2013/01/12 (WSD + 12m)
PAR	**2013/08/12 (WSD + 19m)**
SMRR	2014/07/12 (WSD + 30m)
ITR	2014/07/12 (WSD + 30m)
PSR	2014/08/12 (WSD + 31m)
IOCR	2015/03/12 (WSD + 38m)
FR	2015/03/12 (WSD + 38m)

Functional diagram

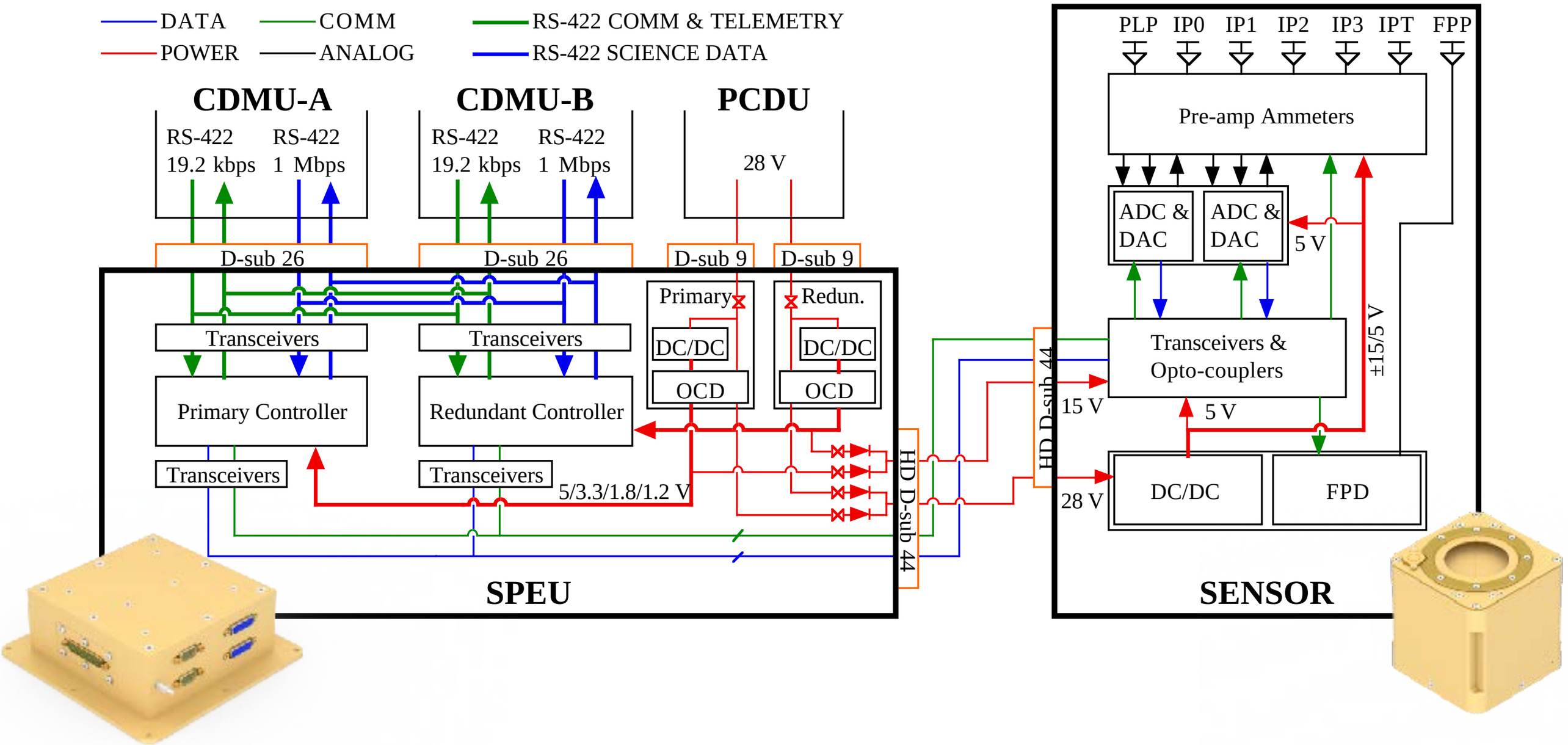

Redundant design on controllers, transceivers, powers, ADC/DAC, ammeters, etc.

Block diagram of the sensor

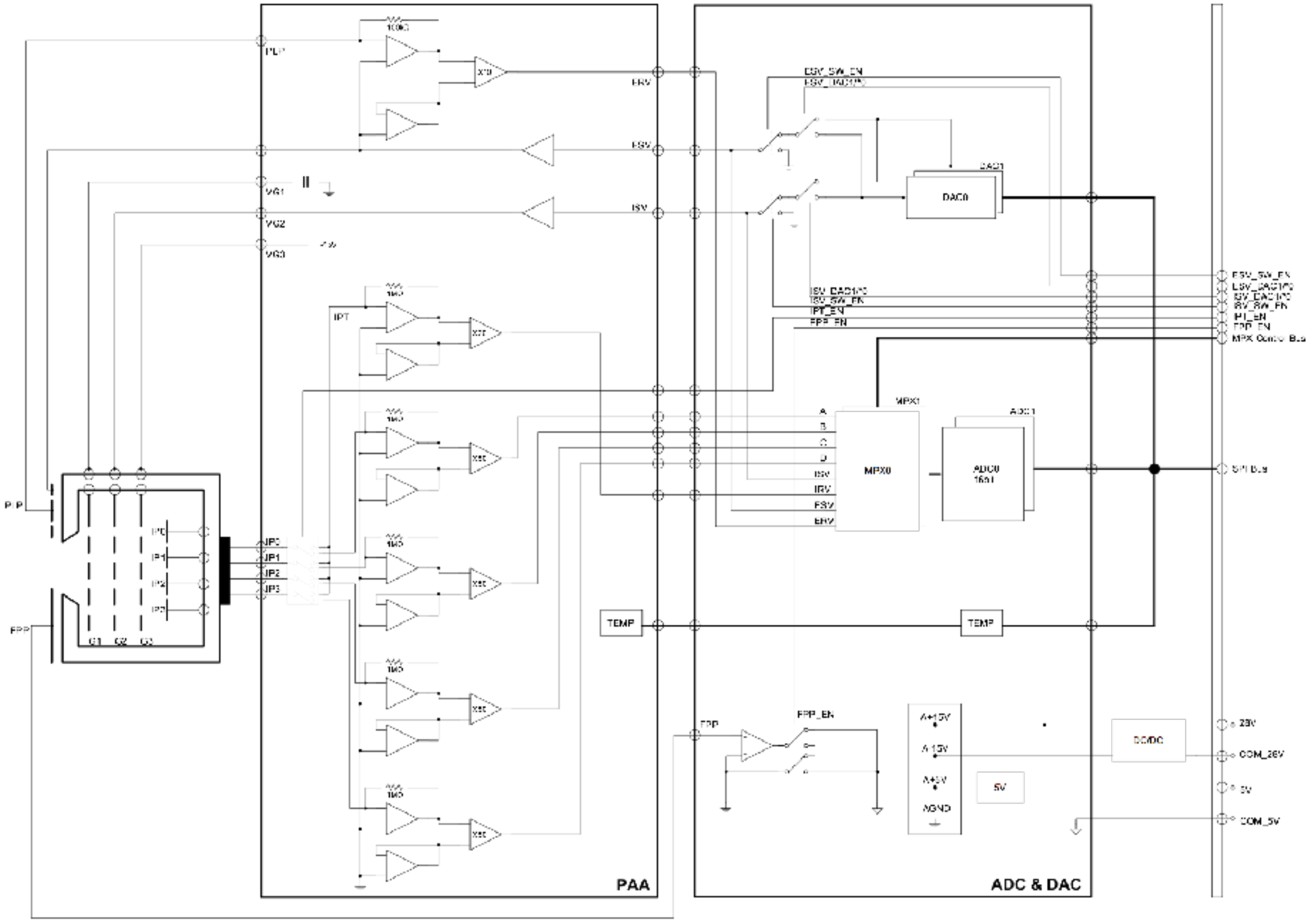

Power consumption - sensor only

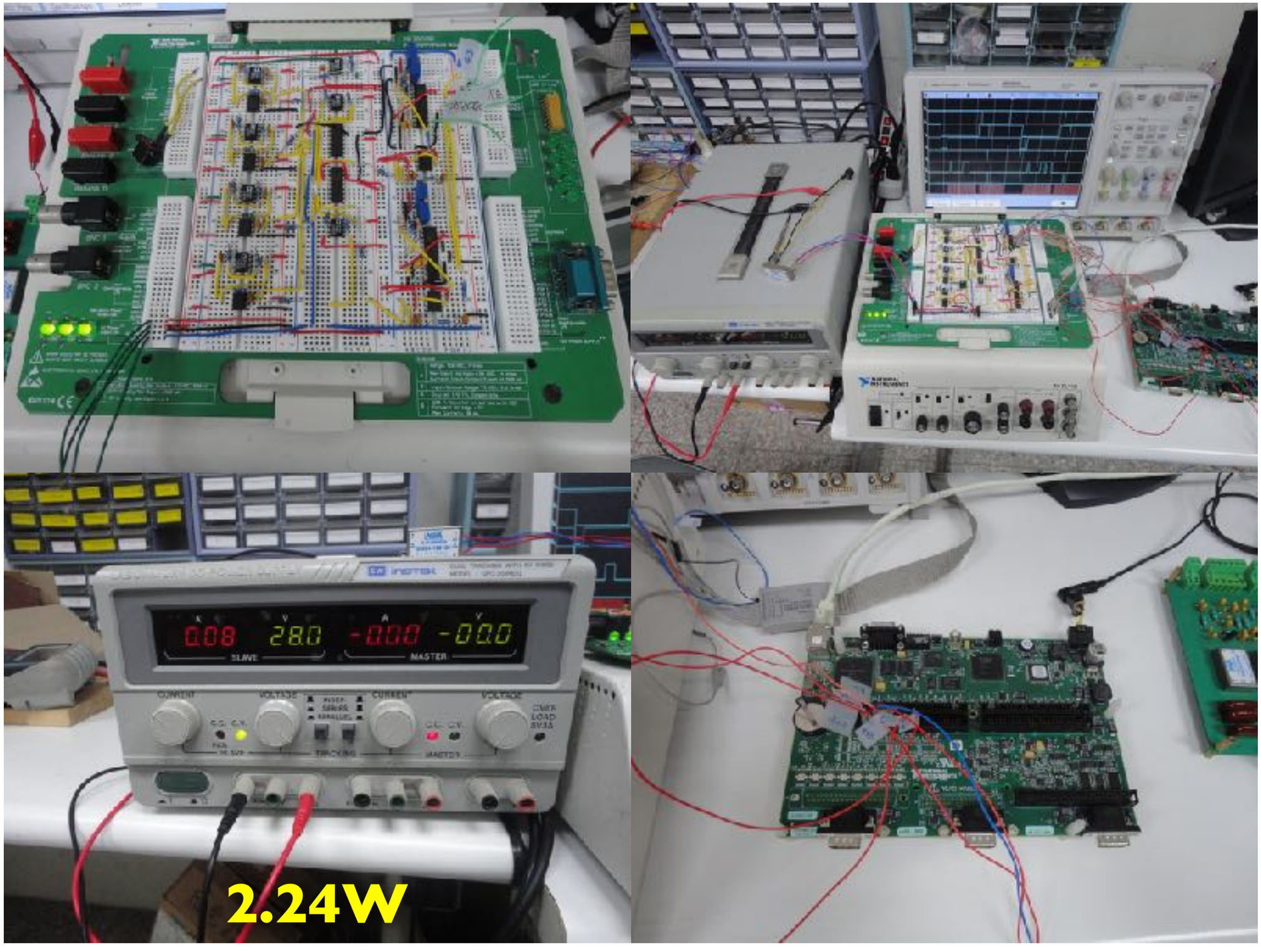

Ammeters

Sensor	Range	Sensitivity	Rate	If noise level is 1 mV
IP0, IP1, IP2, and IP3	**±1.25 μA**	±38.1 pA	0.5 μA/V or 2.0 mV/nA	0.5 nA → 10^3 cm^{-3}
IPT and PLP	**±2.5 μA**	±76.3 pA	1.0 μA/V or 1.0 mV/nA	1 nA → 10^3 cm^{-3}

Geophysical parameters

Parameters	Range	Sensitivity	Accuracy
C_i	3% to 100%	1%	10%
N_i (or N_e)	10^3 to 10^6 cm^{-3}	1%	10%
$\boldsymbol{v}_i$	**±2.5 km s^{-1}** (cross track) **7.5±1 km s^{-1}** (ram)	±10 m s^{-1} ±100 m s^{-1}	±50 m s^{-1} ±200 m s^{-1}
T_i	500 to 5,000 K	±50 K	±200 K
T_e	500 to 5,000 K	±50 K	±200 K

Mechanical specifications

- Sensor: **2.046** kg (shall be less than 1.0 kg) and installed on the top panel with field of view (FOV) **46.4°** (≥ 45°).

  - Head:
    - Material: 6061-T6 with chromate coating.
    - Dimension: 100 (L) x 100 (W) x **100.6** mm (H).
    - Mass: **0.8617** kg (**3 mm thickness**).

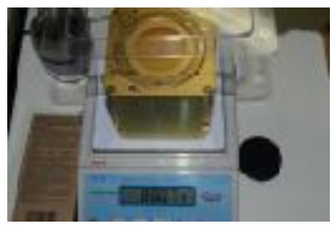

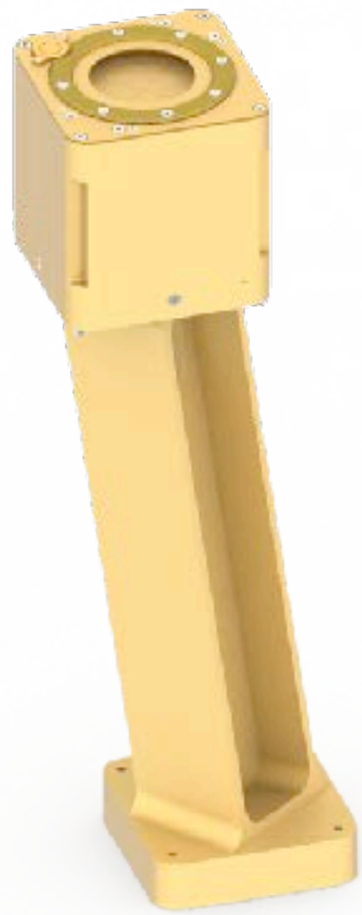

  - Stand:
    - Material: 7075-T6 with chromate coating.
    - Dimension: 140 (L) x 130 (W) x **300** mm (H).
    - Footprint: 100 (L) x 100 mm (W).
    - Mass: **1.184** kg.

Mechanical specifications (cont.)

- SPEU: installed inside S/C.

  - Material: 6061-T6 with chromate coating.
  - Dimension: 180 mm (L) x 180 mm (W) x 60 mm (H).
  - Mass: **1.761** kg.

- Harness between SPEU & sensor: **1.747** kg and **3.8** m.
- Total mass: **5.554** kg (shall be less than 5.0 kg).

Structure analysis for sensor

- Ref. to FS-5 AIP Mechanical Structure Analysis Report, FS5SPL-MECH-ANLYS.
- Natural frequency: **130.4** Hz (>120 Hz).
- Load factors
  - Out of plane: **61.9** G (>20 G).
  - In-plane: **46.4** G (>20 G).
- Margin of safety (MS)
  - Ultimate: **1.27** (> 0).
  - Yield: **1.42** (> 0).
- Buckling safety margin (MS_B): **44.7** (> 0).
- Sinusoidal vibration (no collision during vibration)
  - 9G in-plane.
  - 10-300 Hz.

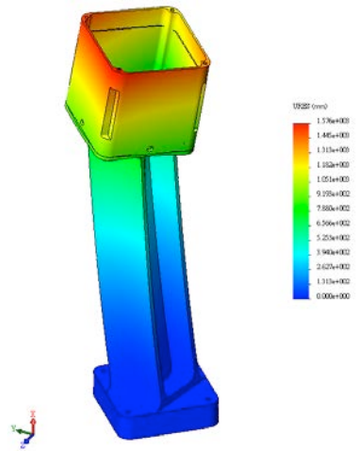

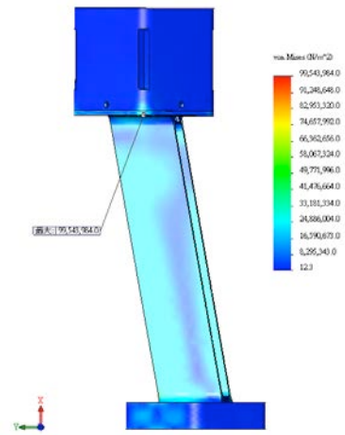

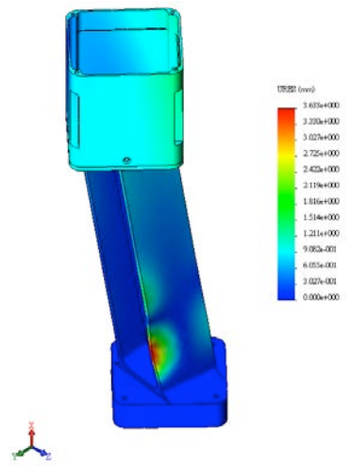

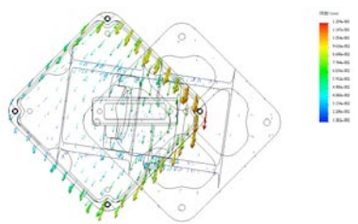

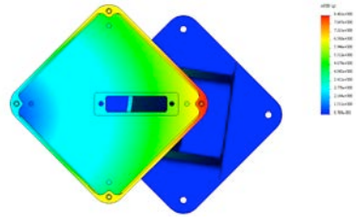

Total ionizing dose

- For a 3 mm thickness of 6061-T6 sensor cube, the requirement of total ionizing dose for a two-year mission life time is **3.6 krad (Si)**.
- It is lower than **5 krad (Si)** for untested COTS EEE parts (ref. IAC-02-IAA.6.3.04, In-orbit Monitoring of "Space Weather" and Its Effects on Commercial-Off-The-Shelf, COTS, Electronics - A Decade of Research Using Micro-Satellites)

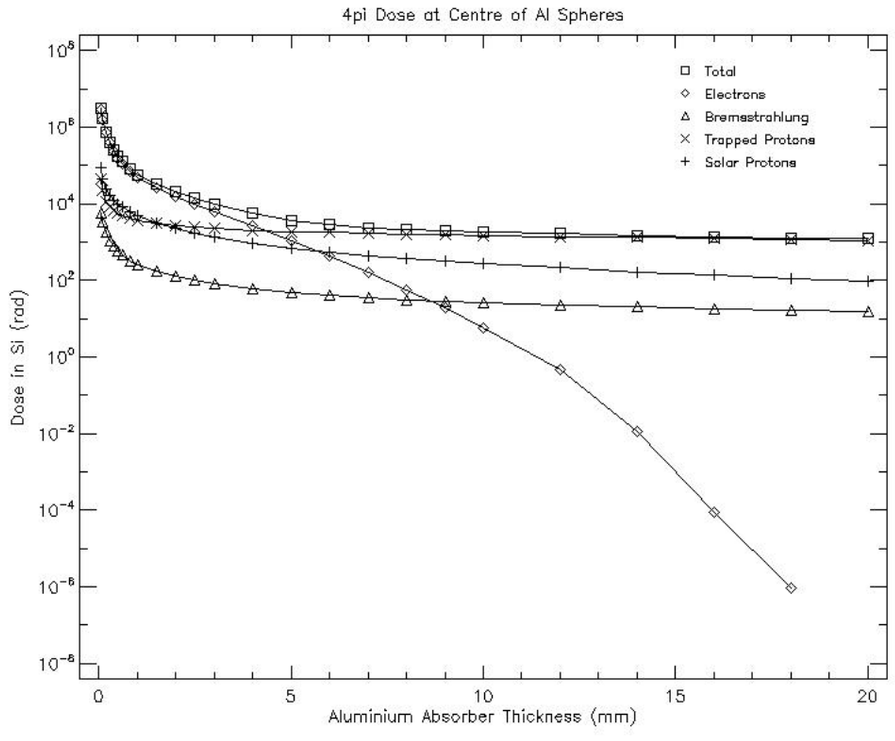

Electrical specifications

- Input voltage: **28±6** VDC (wider than +26 V to +34 V).
- Power on: 23.8 to 26.9 W and 0.85 to **0.96** A (≤ 1.3 A, limited by PCDU) for +28 V.
- Operation: **11.9** W in average.
  - Sensor: **7.11** W (<11.3 W in analysis), 0.12 A for +28 V and 0.25 A for +15 V.
  - SPEU (without sensor load): **4.76** W (< 8.15 W in analysis), 0.17 A for +28 V.
- Average power per orbit: can be reduced to 5 W if the duty cycle of AIP can be reduced to **42 %** (≥ 30 %).
- Single event latch-up (over-current) protection.

Single event latch-up protection

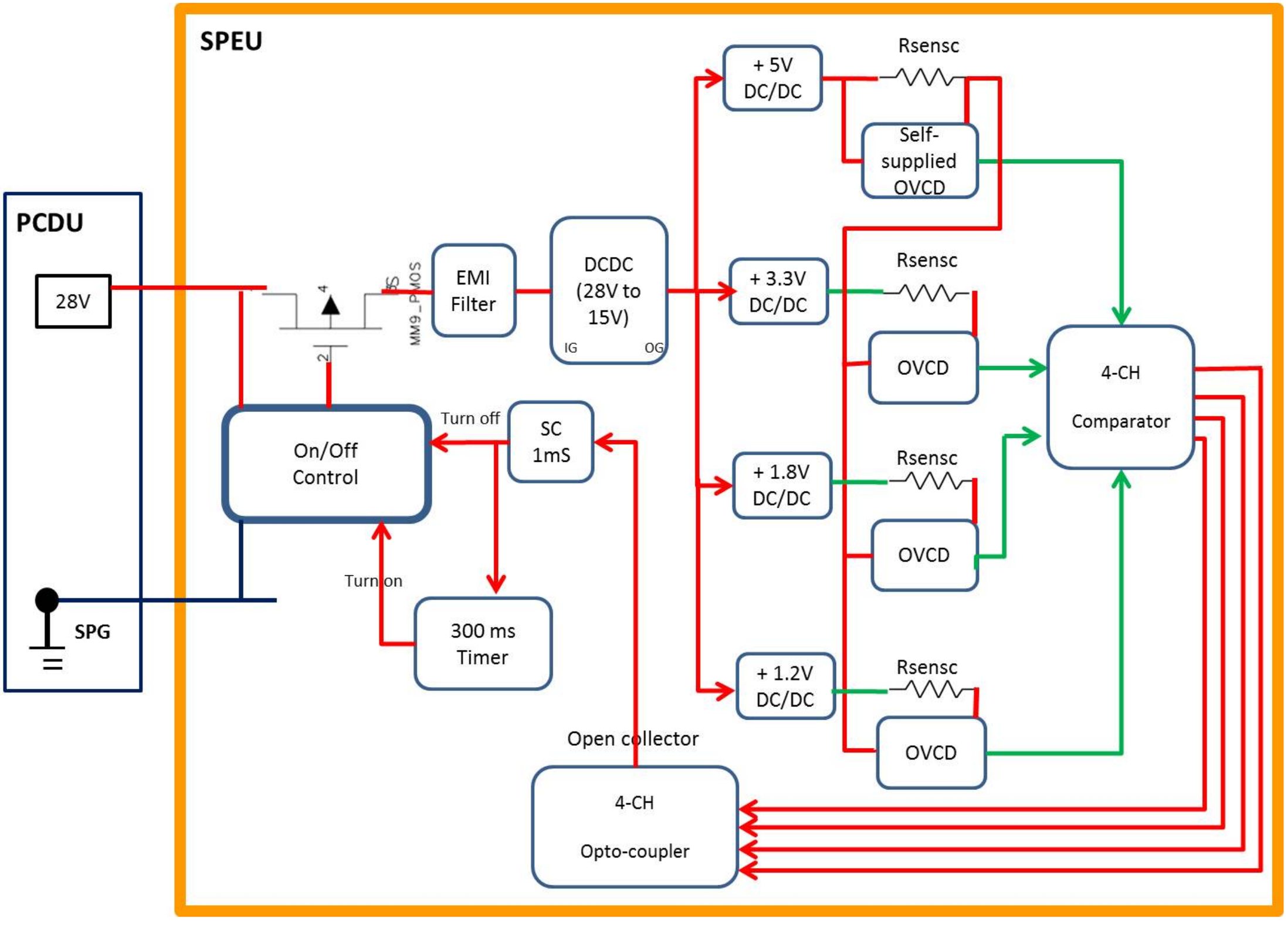

Commands and telemetry

- Command and telemetry interface (RS-422, 19.2 kbps, ASYN)
  - From CDMU to SPEU
    - Command: 1 command (3 bytes) in a 6-byte command packet. The command packet is sent every 1s.
    - Ancillary data: 64-byte ancillary data in a 68-byte ancillary data packet. The ancillary data packet is sent every 1s.
  - From SPEU to CDMU
    - Status of health (SOH): a 19-byte SOH in a 22-byte SOH packet. The SOH packet is sent every 1s.
- Science data interface (RS-422, 1 Mbps, SYNC)
  - Only from SPEU to CDMU: 3 sets of science data in a 1024-byte science data packet.

Mode operation

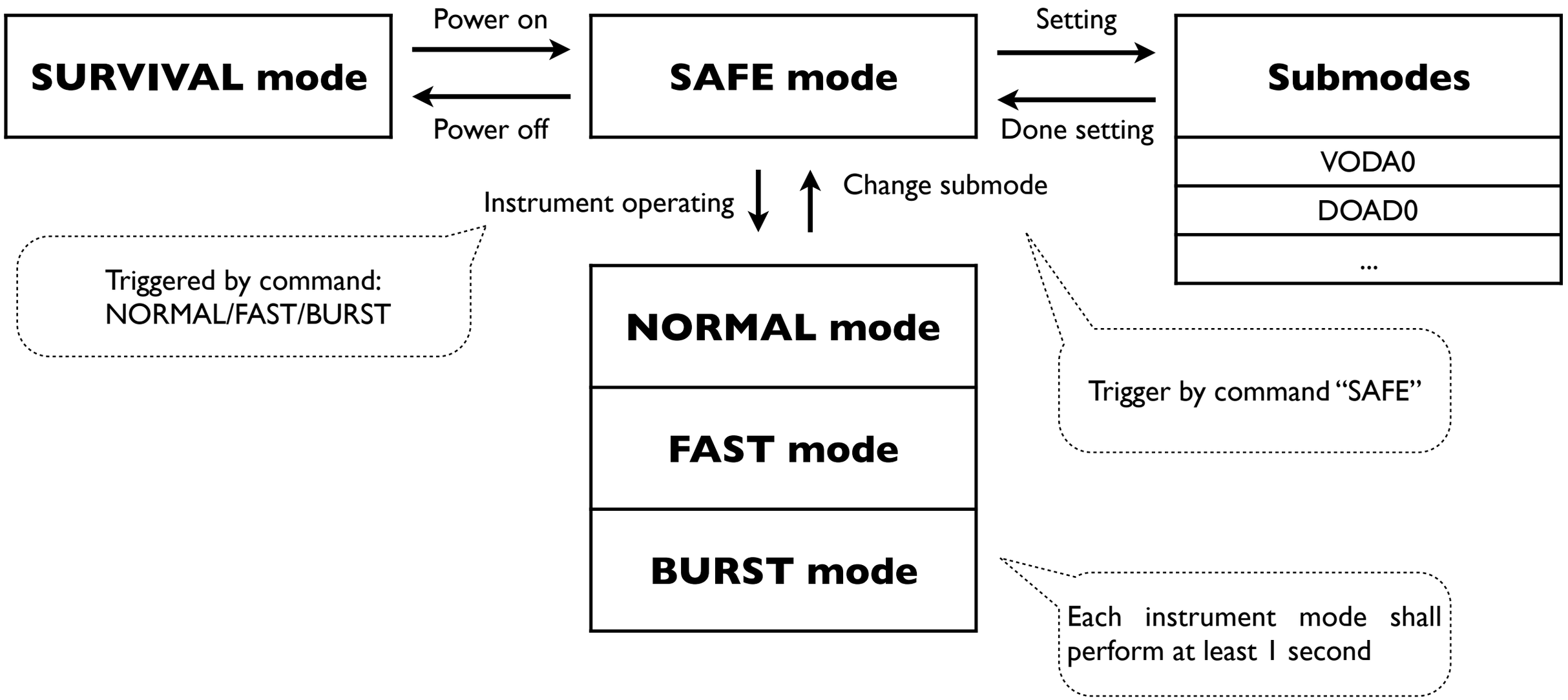

When turning on SPEU (SAFE mode), the submode is setting to default value. To change the submode setting, the instrument shall go to SAFE mode first and then change the submodes according to the commands received from CDMU. After the setting is done, the instrument can start measuring as NORMAL, FAST, or BURST mode.

Fabrications

- Mechanical components
  - Sensor cube and stand.
  - Bonded meshes.
  - PLP electrodes, aperture, insulator rings, collector, etc.
- Electrical components
  - Harness
  - PCB fabrication
  - Components assembly
- Final assembly
  - Sensor by NCU
  - SPEU by T&C

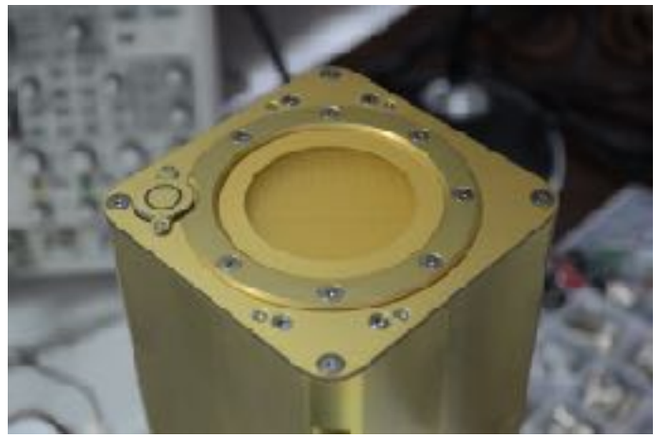

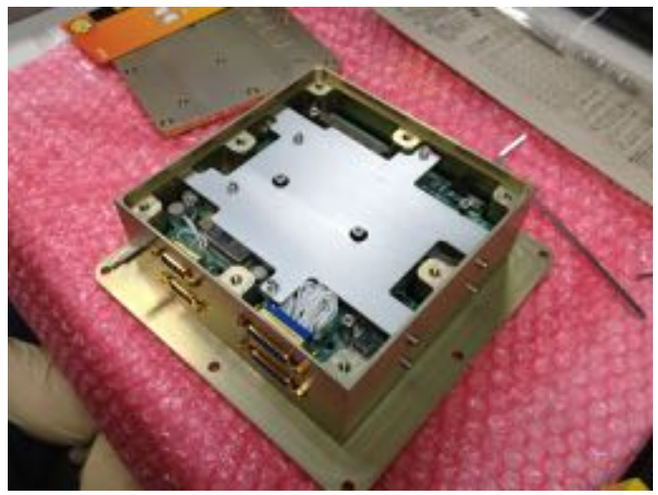

Sub-contractors

- SPEU: T&C Technologies Inc.
- Component acquisition: BUY-A Technology Corp. and Bentech Computer Corp.
- Bonded meshes: Precision Eforming LLC.
- Aperture and collector construction:
- Gold-coating: ATI.
- PCB and coating: BoardTek Electronics Corp.
- Assembly: EMTT Systems Corp.
- ISD: National Instruments Corp.
- Vibration and shock test: CSIST.

Sensor cube and stand

- Manufactured by BCV Tech. and Min-Wang Co.
  - Head:
    - Material: **6061-T6** with chromate coating.
  - Stand:
    - Material: **7075-T6** with chromate coating.
- Bolts and nuts: manufactured by Bulten Stainless.
  - Material: Bumax 88 (S31603) and Bumax A4 (S31600).

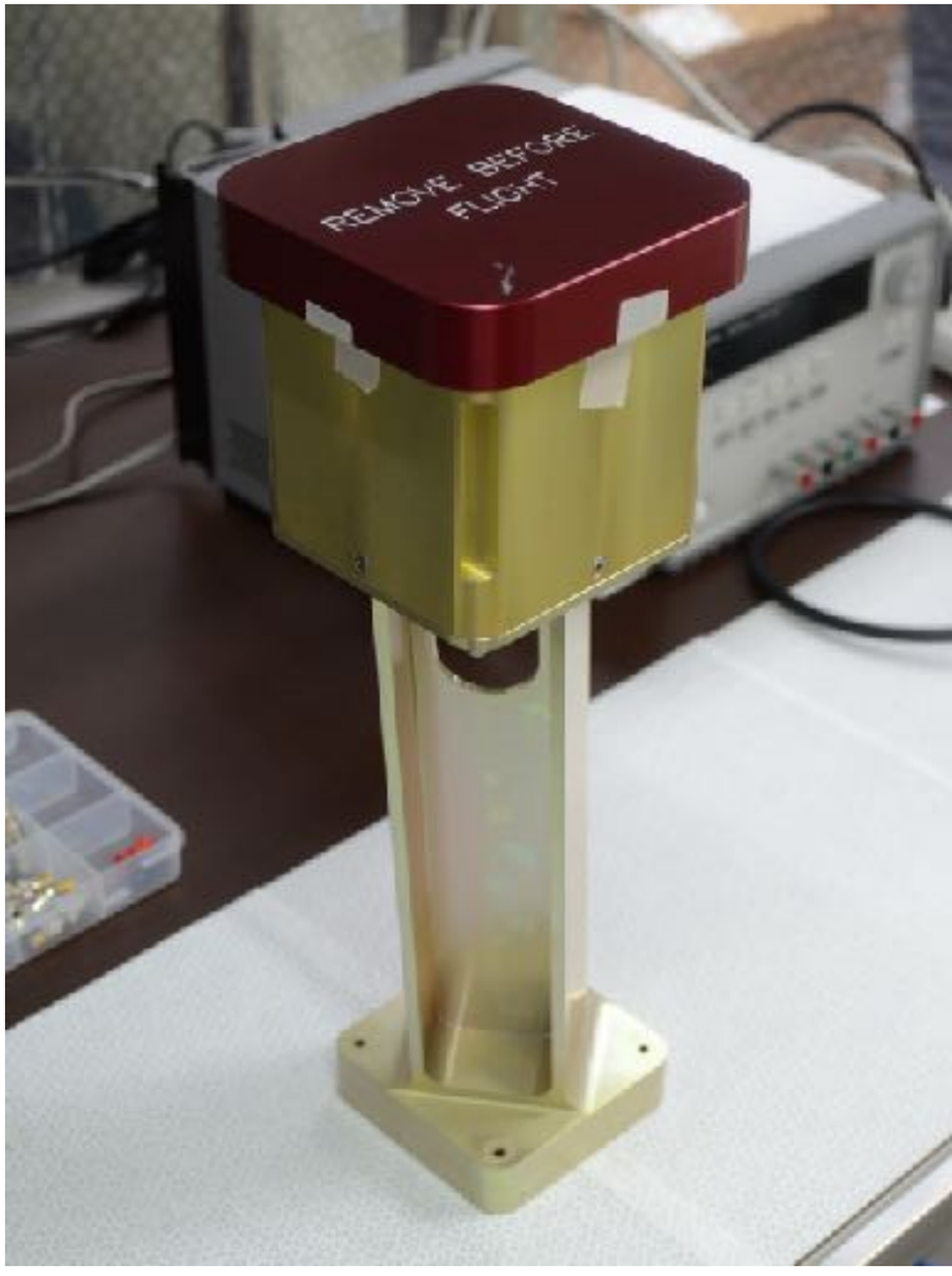

Bonded meshes

- Electroformed bonded gold mesh manufactured by Precision Eforming LLC.
- Material:
  - Stainless steel 304 frame and coated in gold.
  - **99.98% pure gold mesh**.
- Mesh density: 100 LPI.
- Mesh thickness: 0.5 mil.
- Transparency: **0.9025**.

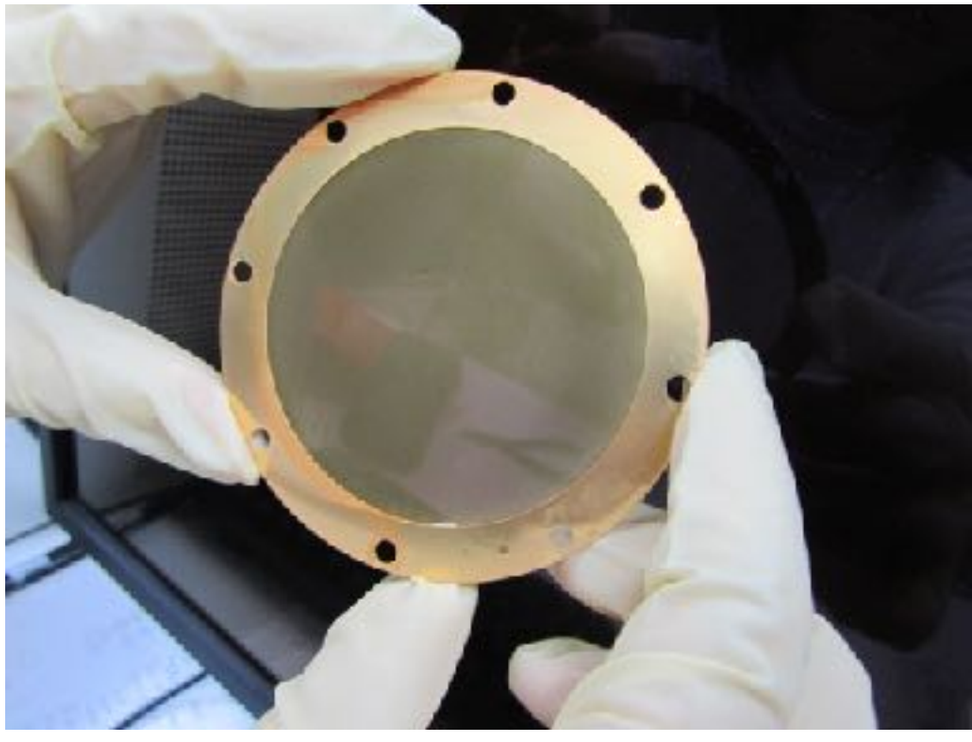

PLP electrodes, aperture, insulator rings, and collector

- Manufactured by Ting Ann Enterprises Co., Ltd. and Advantic Tech. Inc.
- Material: **ARLON 85N PCB** and coated in gold.
  - PCB thickness: 1.6 mm.
  - Copper thickness: 0.5 Oz.
- Structuring and through-hole plating.
- All coppers are coated in gold with **50 µ-inch**.

Harness

- Manufactured by Rosnol RF/ Microwave Technology
- Length: **3.8 m**.
- Connectors: **ITT Cannon** DBMA44PNMBK52 and DBMA44SNMBK52.
- Twist-pair cables: Super-Temp M27500 24 RC 2 S06.
- Kyner heat shrink tubing: AWC M23053/8.
- Expandable sleeving: Techflex Techon PFA.

PCB fabrication

- Manufactured by Speedy Circuits Co. Ltd.
- Material: **ARLON 85N PCB**.
  - Layer count: 2 for sensor and 4 for SPEU.
  - Thickness: 1.6 mm.
  - Copper thickness: 0.5 Oz for sensor and 1.0 Oz for SPEU.
- Solder mask: TAIYO PSR-4000 MP.
- Inkjet legend ink: TAIYO IJR-4000 MW300.
- Surface finish: Hot-Air Solder Leveling (HASL) with tin/lead.

Components assembly

- Soldering by EMMT Systems Corp.





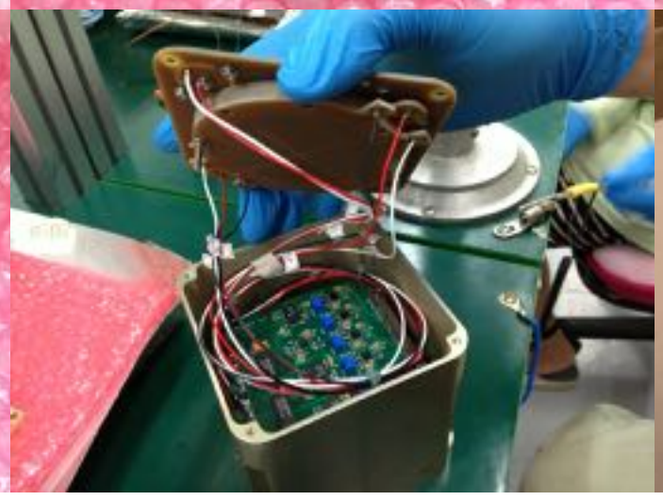

Sensor assembly by students


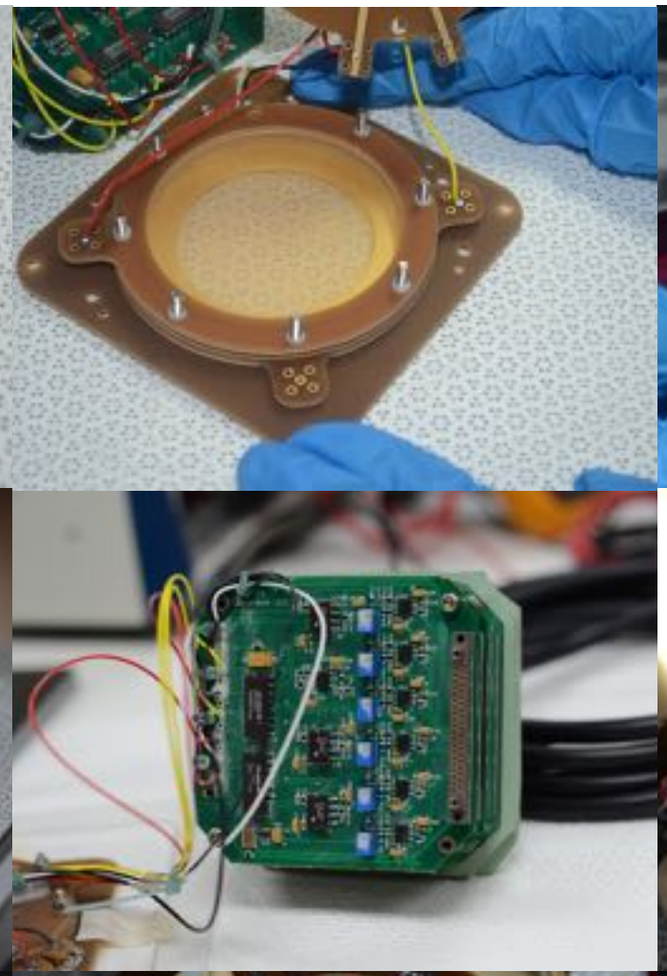
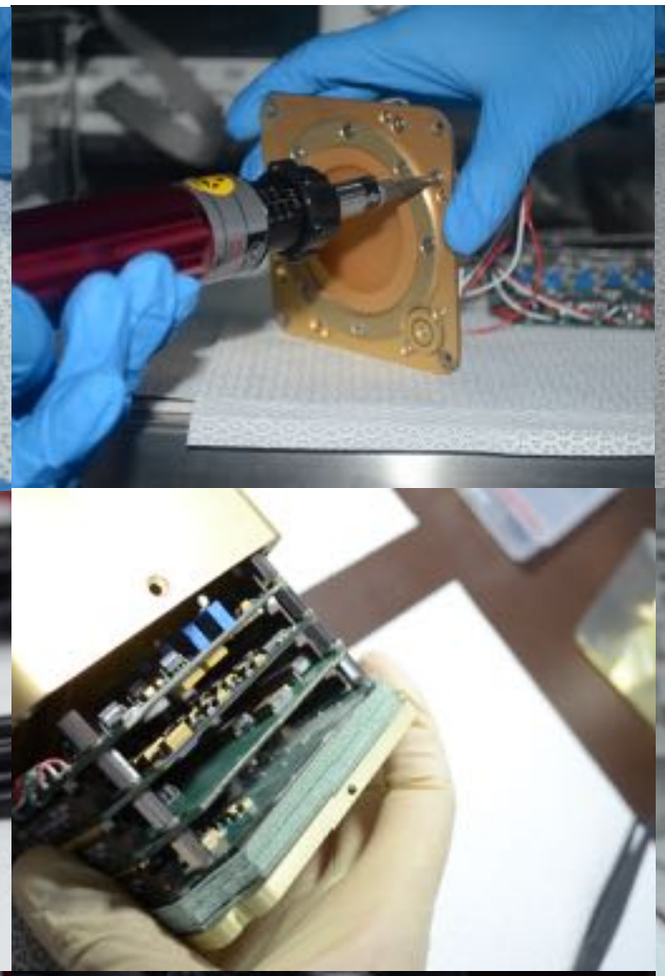
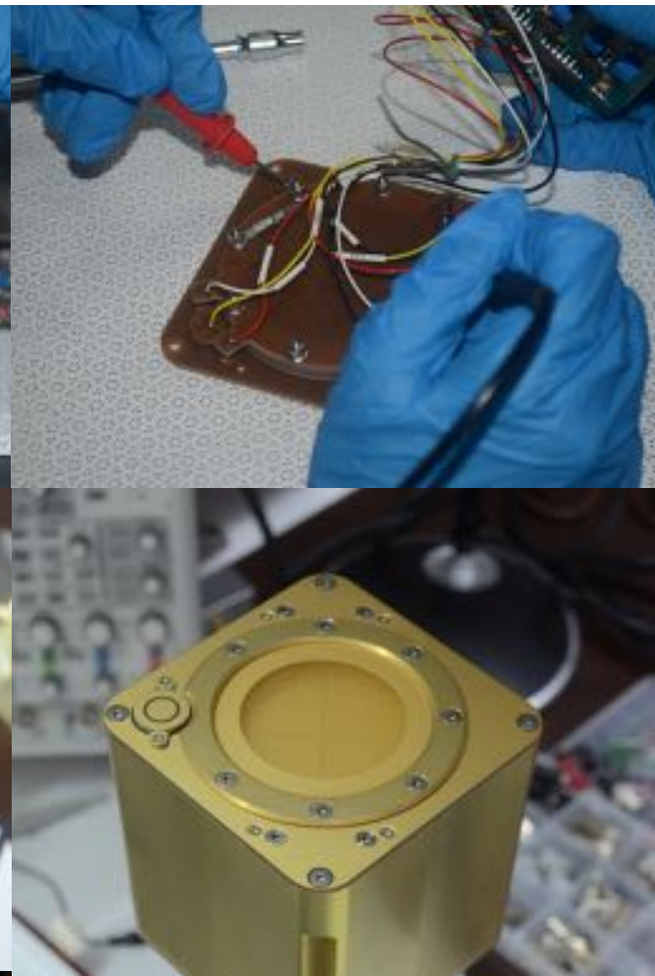


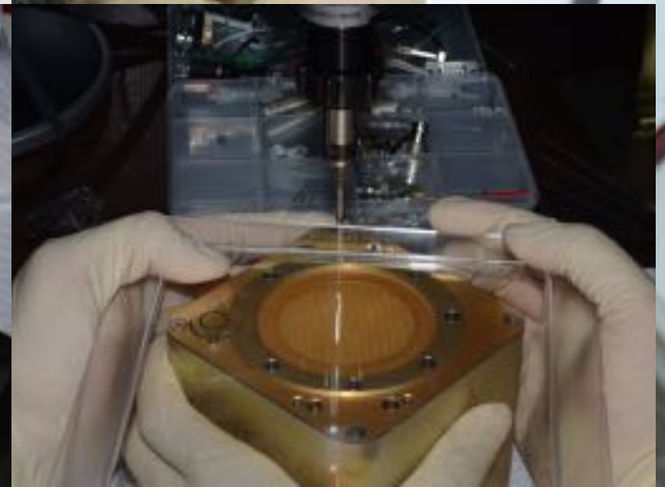
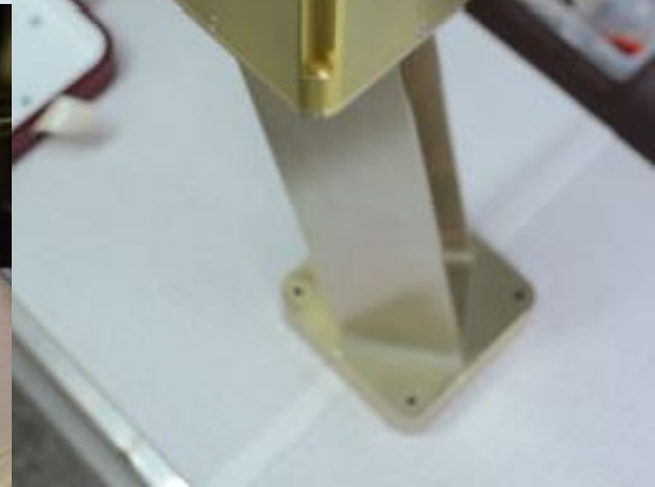

SPEU assembly by T&C




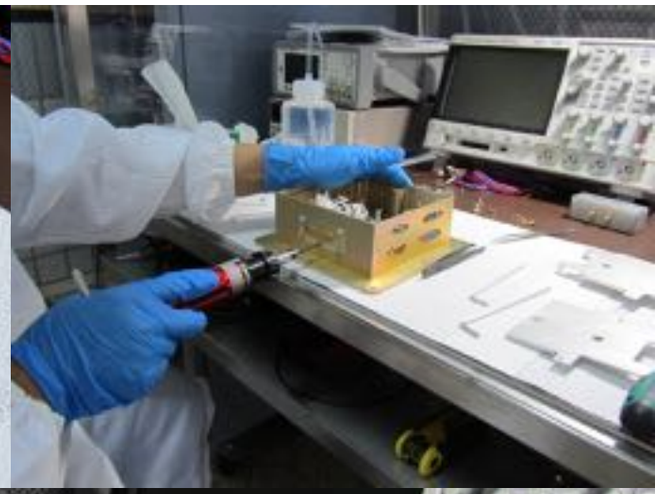
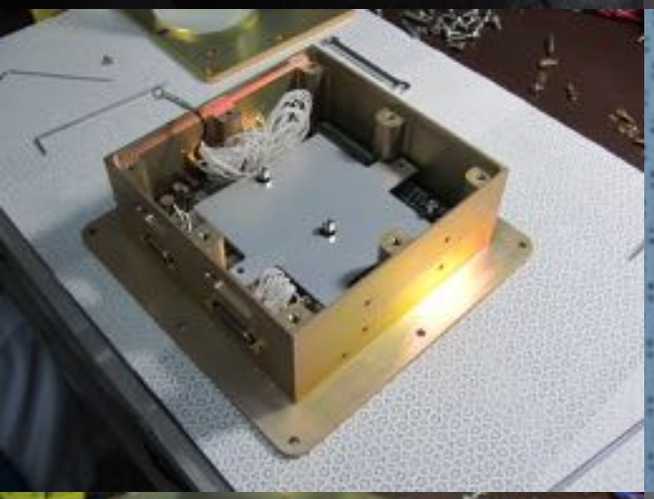
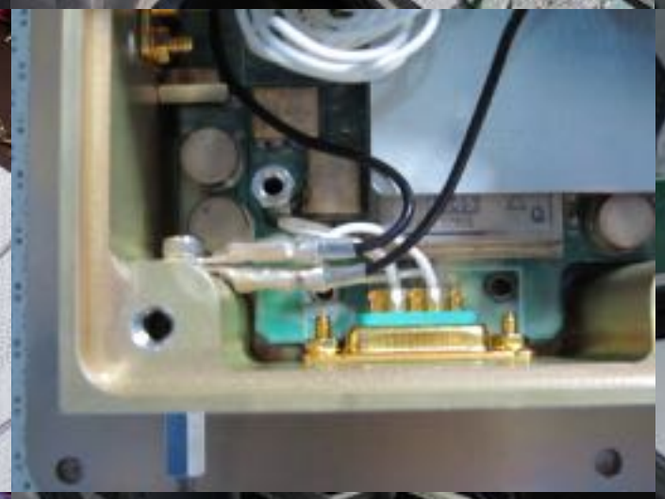
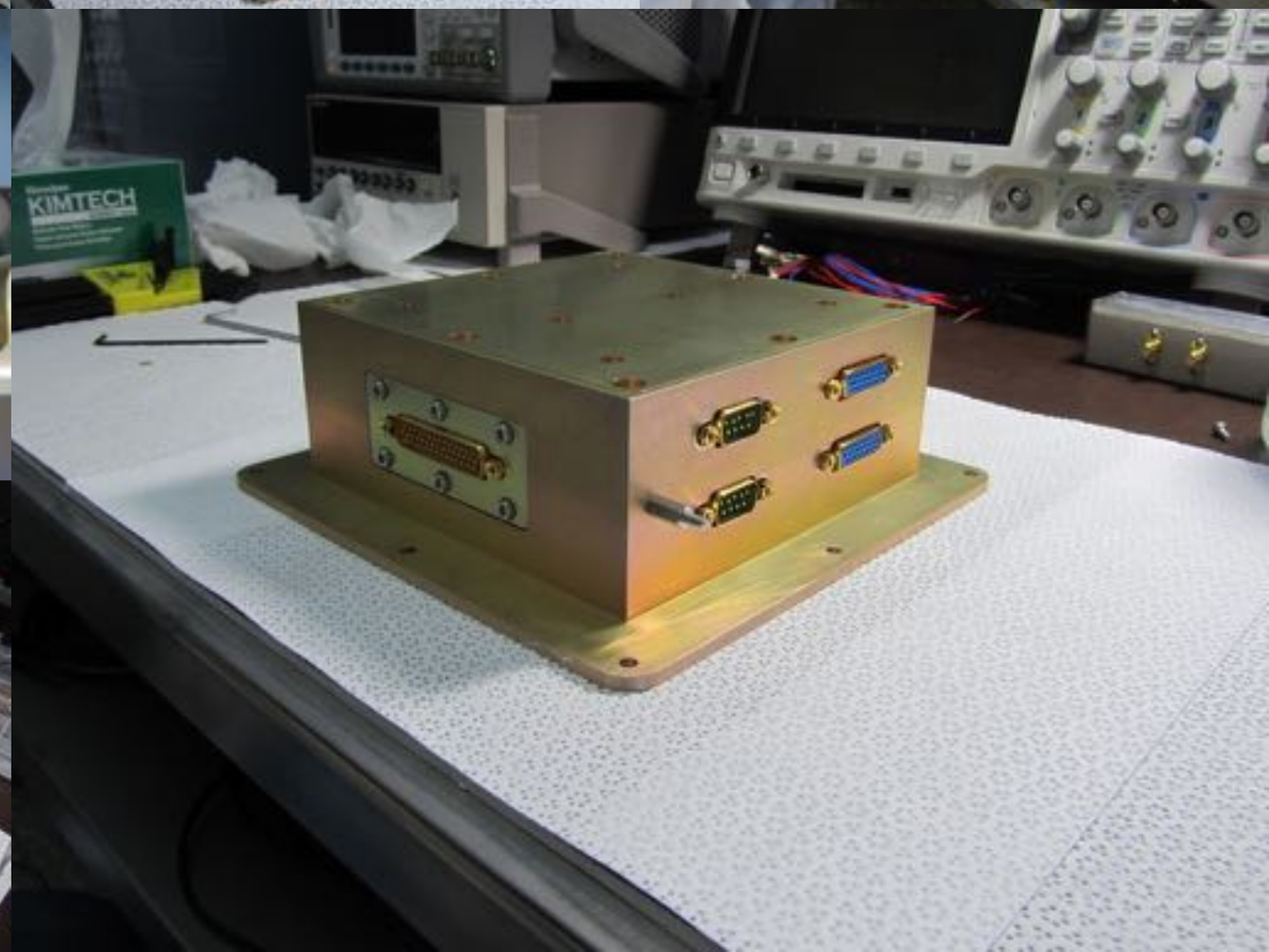

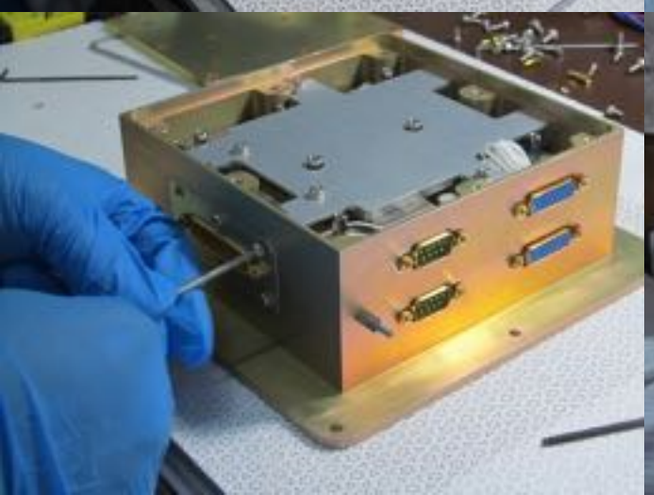
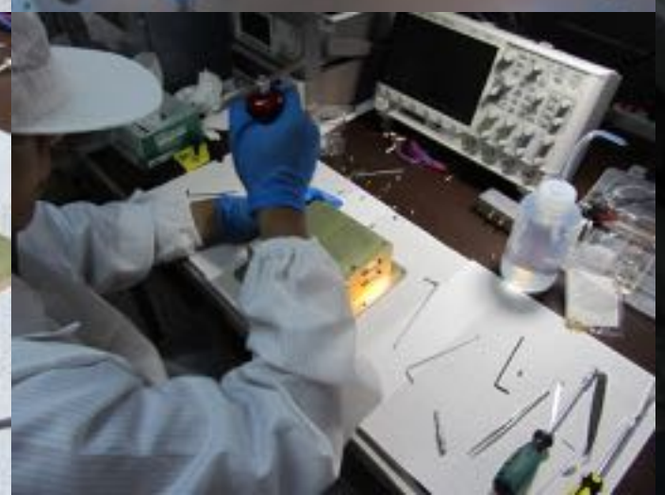

The 1st Space Science School Payload Design - An Example of Advanced Ionospheric Probe

Chi-Kuang Chao

Graduate Institute of Space Science, National Central University

Space Krenovation Park, Sri Racha, Chonburi, Thailand

October 24, 2016

Outline - the 2nd hour

- Requirements
- Science objectives
- Principles of measurement
- Designs
- Verifications
- Future works

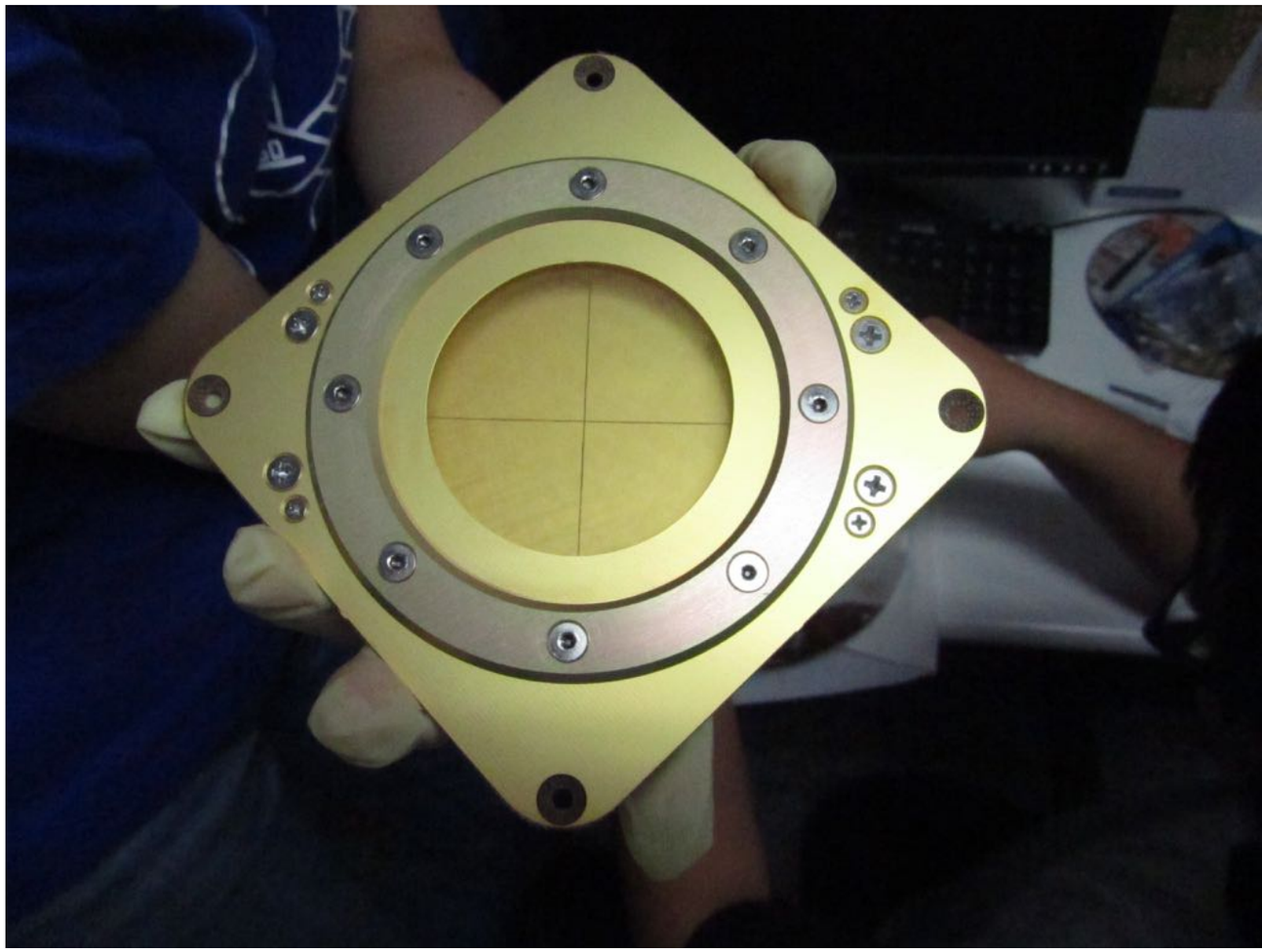

Verifications

- The payload design shall be verified by the following methods:
- **Inspection** is the process of physically measuring, examining or comparing an article to the design drawings, schematics, or other records to assure requirements compliance.
- **Analysis** can be performed through systems engineering analysis, statistics & qualitative analysis, and computer & hardware simulations to be used in reliability assessment, life, storage, failure analysis, safety, interchangeability, and other performance requirements which are difficult or impractical to test.
- **Test** requires the precise measurement of performance parameters relative to functional, electrical, mechanical, and environmental requirements imposed on an article.

19 documents submitted for PAR

- **FS5SPL-CDRL-1014**: PAR presentation.
- **FS5SPL-CDRL-1015**: P/L test report, 1st draft.
  - **FS5SPL-FUNC-PROC/RPT**: functional test procedure/report.
    - ***FS5SPL-CPT-PROC/RPT***: circuit protection test procedure/report.
    - ***FS5SPL-PIT-PROC/RPT***: plasma injection test procedure/report.
    - ***FS5SPL-PMT-PROC/RPT***: power measurement test procedure/ report.
    - ***FS5SPL-CIT-PROC/RPT***: current injection test procedure/report.
    - ***FS5SPL-CT-PROC/RPT***: communication test procedure/ report.
  - **FS5SPL-SINE-PROC/RPT**: sine vibration test procedure/report.
  - **FS5SPL-RAND-PROC/RPT**: random vibration test procedure/ report.
  - **FS5SPL-SHOCK-PROC/RPT**: shock test procedure/report.
  - **FS5SPL-TVT-PROC/RPT**: thermal vacuum test procedure/report.
  - **FS5SPL-CEMC-PROC/RPT**: conduced EMC test procedure/report.
  - **FS5SPL-REMC-PROC/RPT**: radiated EMC test procedure/report.
- **FS5SPL-CDRL-1016**: EIDP (End-item Data Package) for P/L flight module.
  - **FS5SPL-DM-PACK**: Design and manufacturing package.
  - **FS5SPL-VQA-PACK**:Verification and quality assurance package.
- **FS5SPL-CDRL-1017**: P/L system operation handbook, 1st draft.
- **FS5SPL-CDRL-1018**: P/L verification control document, 2nd draft.

Functional tests

- **Circuit protection test** (T&C, 8/13/2013): FS5SPL-CPT-PROC/RPT.
- **Plasma injection test** (NCU, 8/14/2013 to 8/15/2013): FS5SPL-PIT-PROC/RPT.
- **Power measurement** (NCU, 8/22/2013): FS5SPL-PMT-PROC/RPT.
- **Current injection test** (NCU, 8/27/2013): FS5SPL-CIT-PROC/RPT.
- **Communication test** (NCU, 9/11/2013): FS5SPL-CT-PROC/RPT.

Circuit protection test

28 V to sensor (0.98 A)

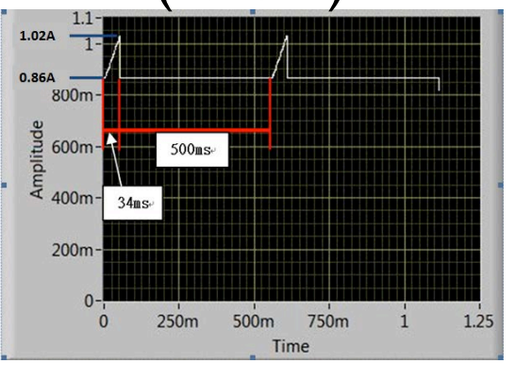

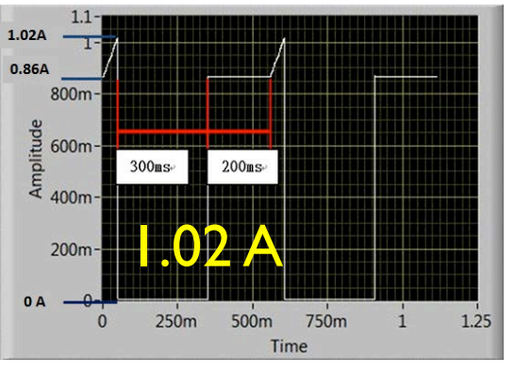

15 V to sensor (0.49 A)

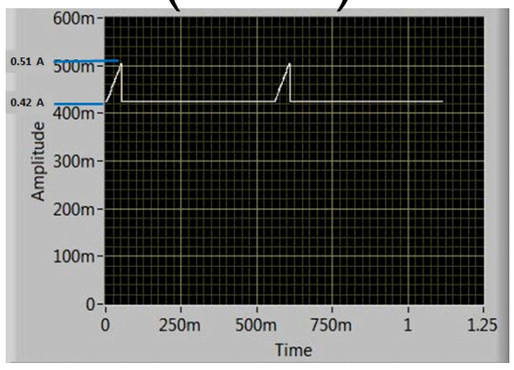

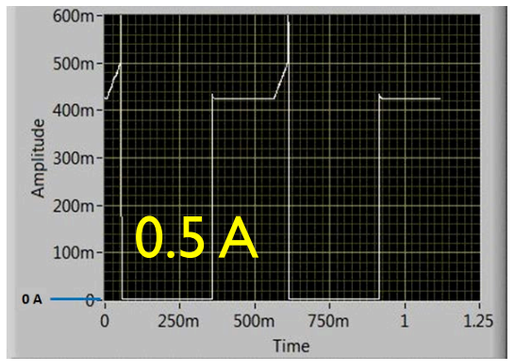

3.3 V to FPGA (0.62 A)

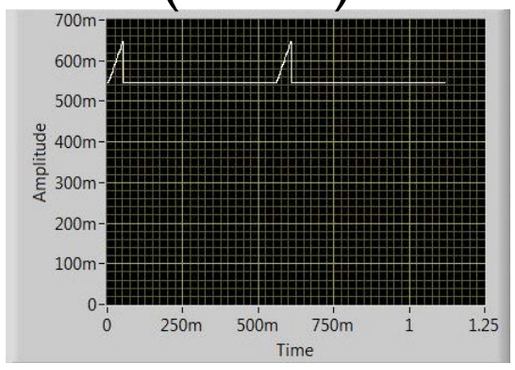

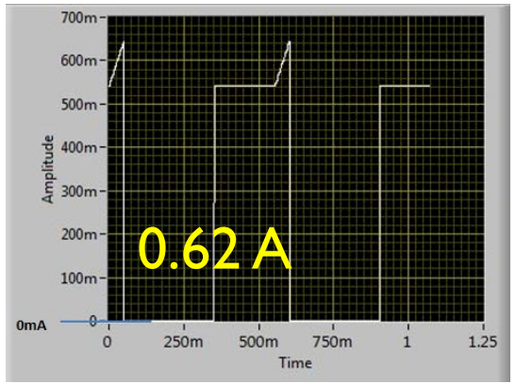

3.3 V to FLASH (0.0175 A)

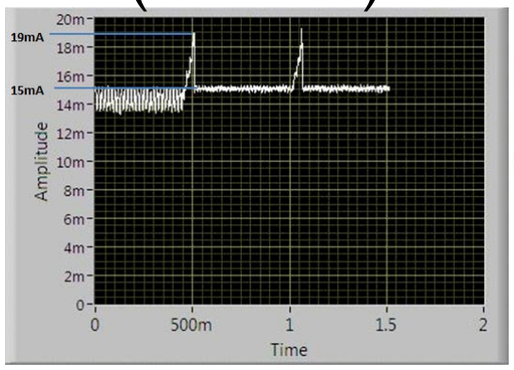

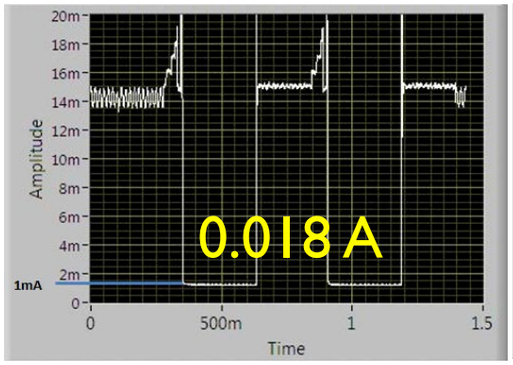

1.2 V to FPGA (0.18 A)

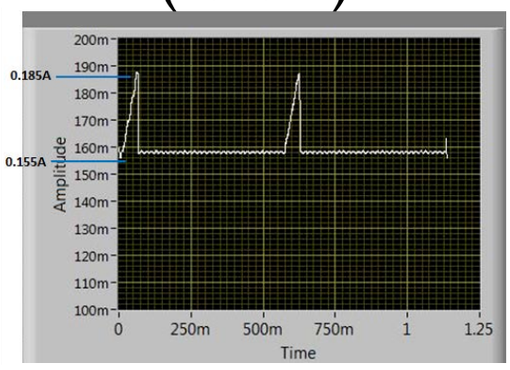

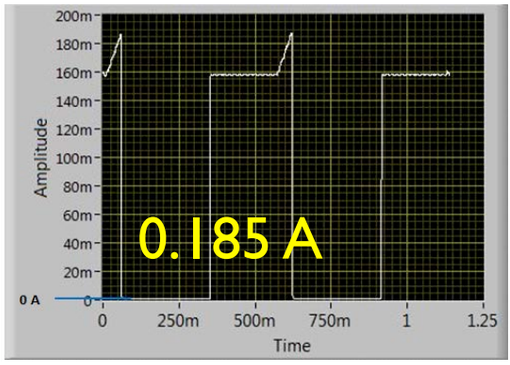

Plasma injection test

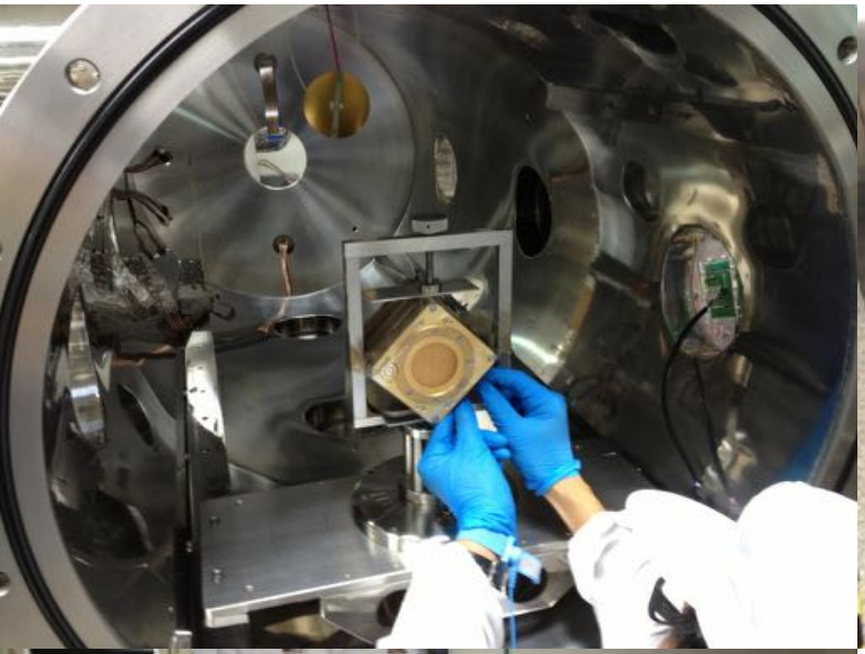

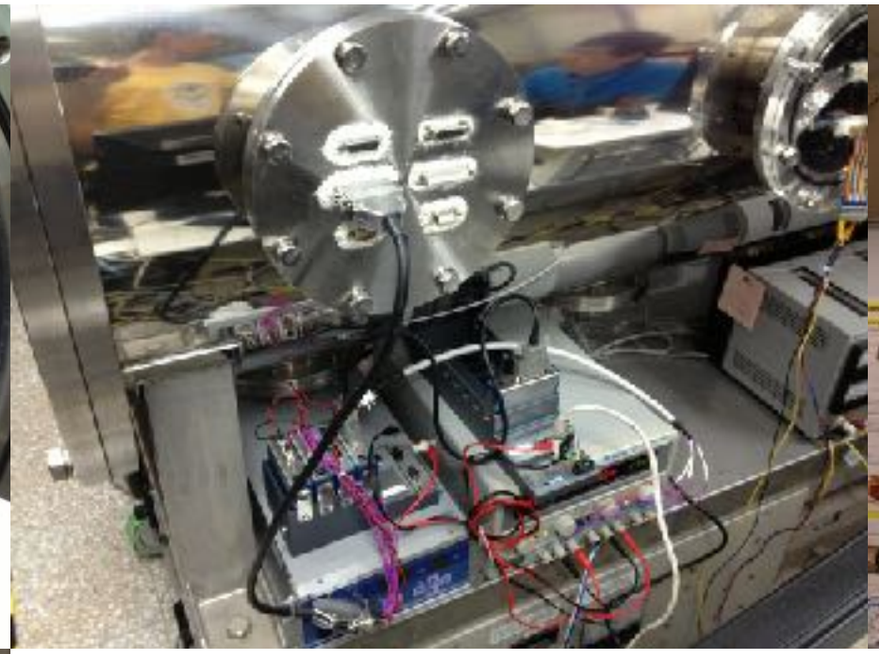

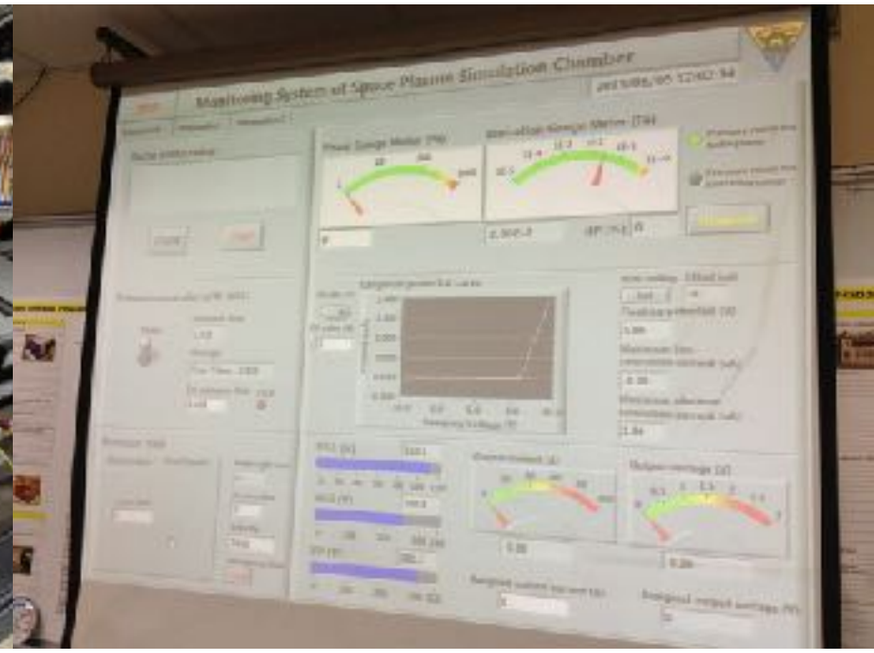

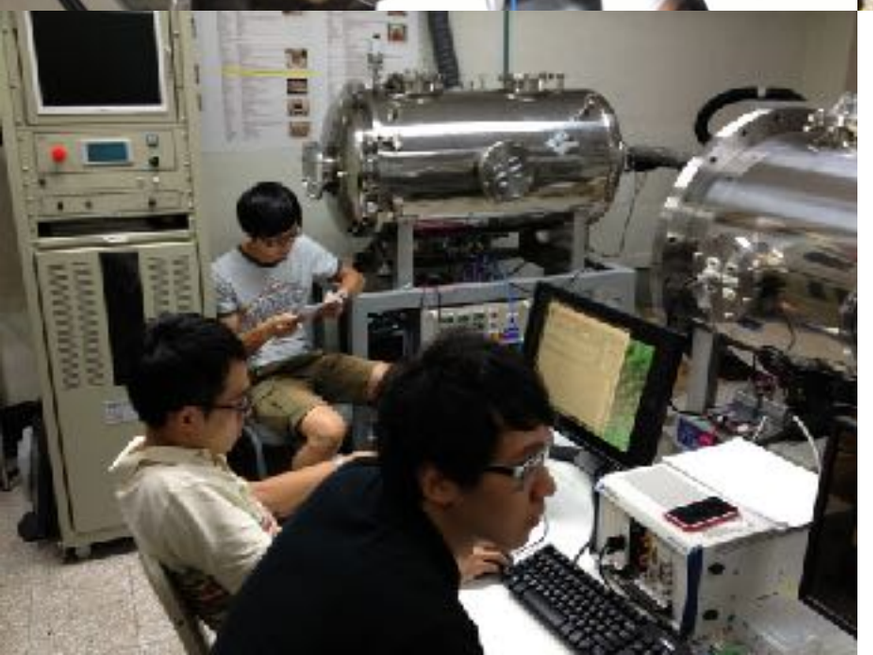

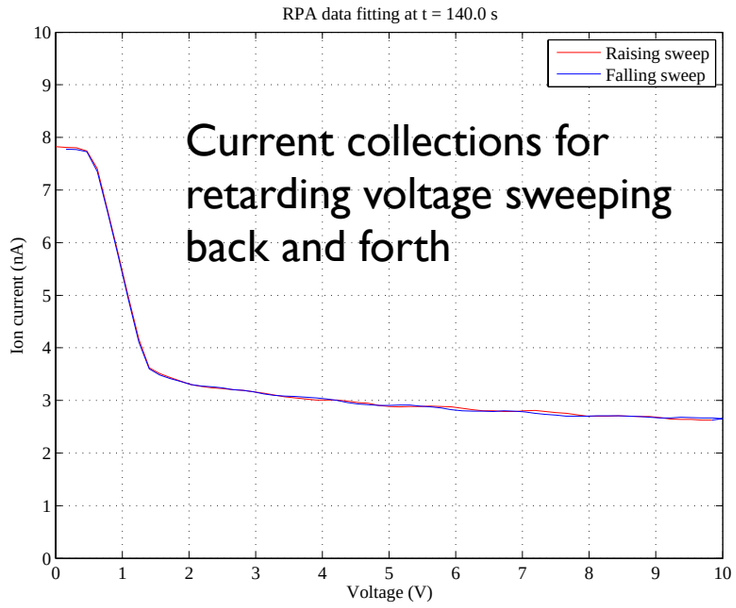

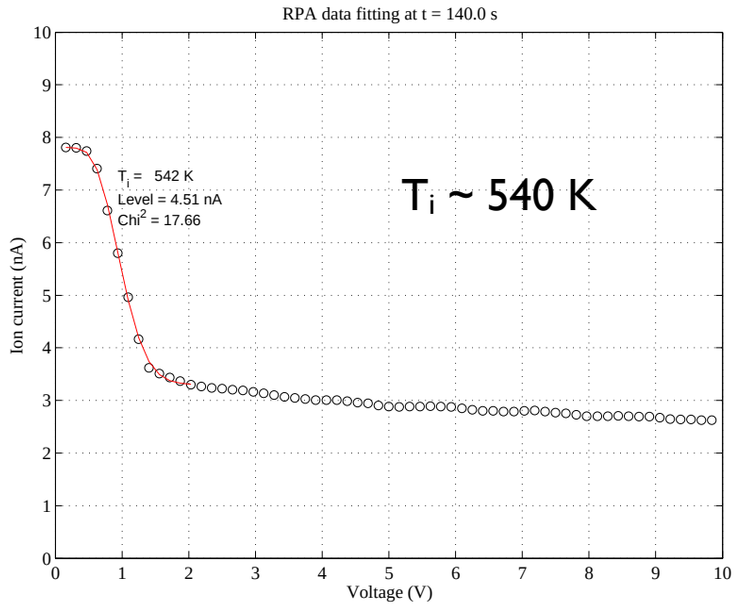

Plasma injection test on Jun. 1, 2016

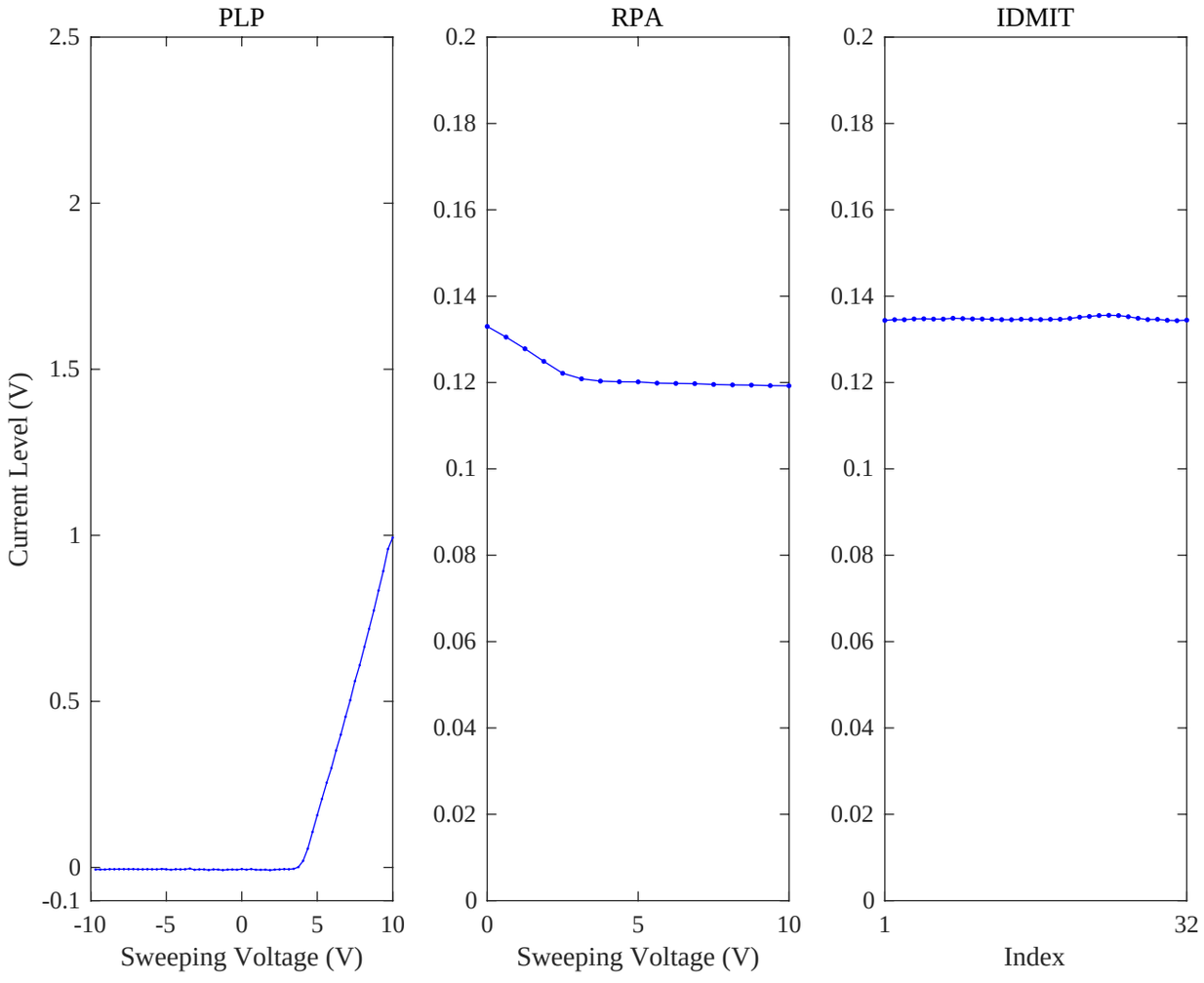

NORMAL mode

sensor is faced to plasma source

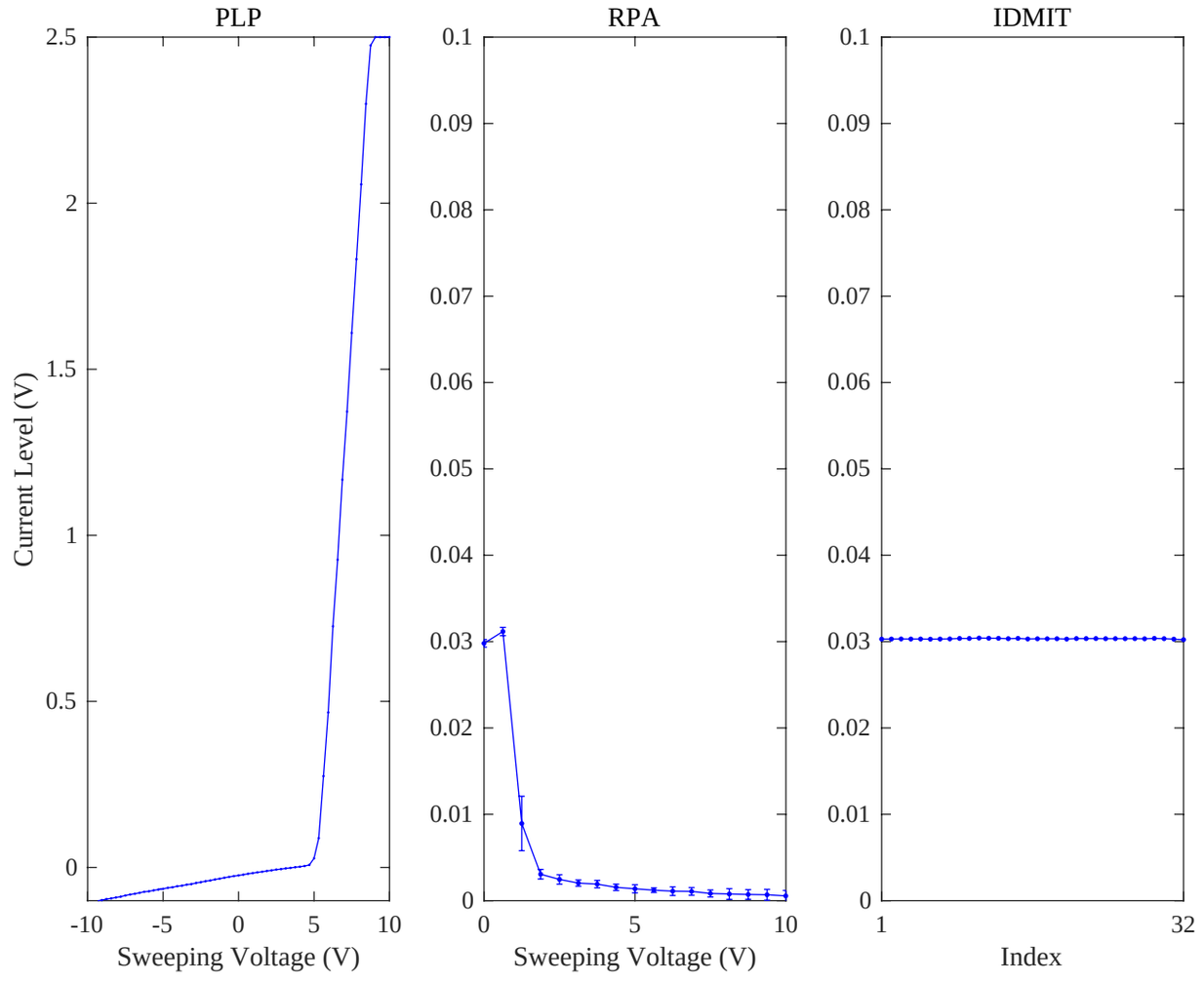

FAST mode

sensor is perpendicular to plasma source

Power measurement

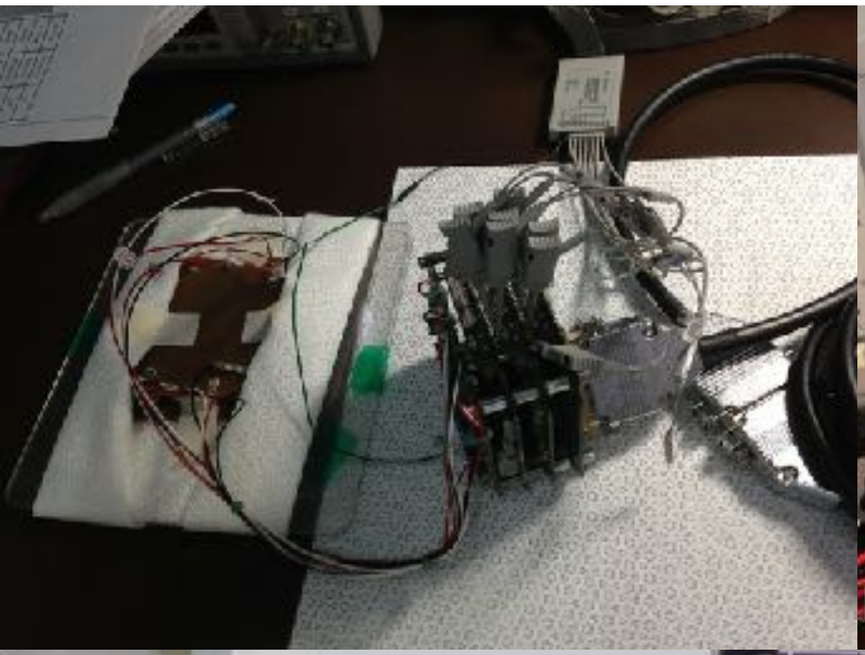

Power measurement (cont.)

The switch-on current shall return to nominal current level within 5 ms.

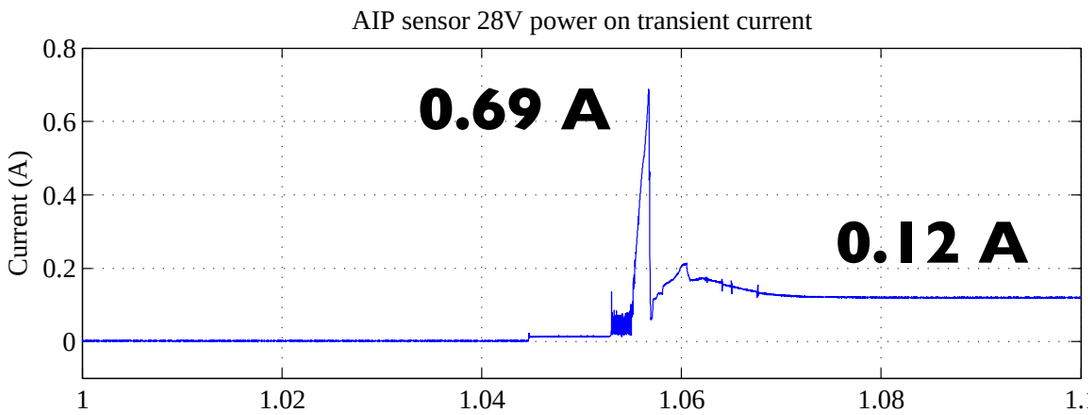

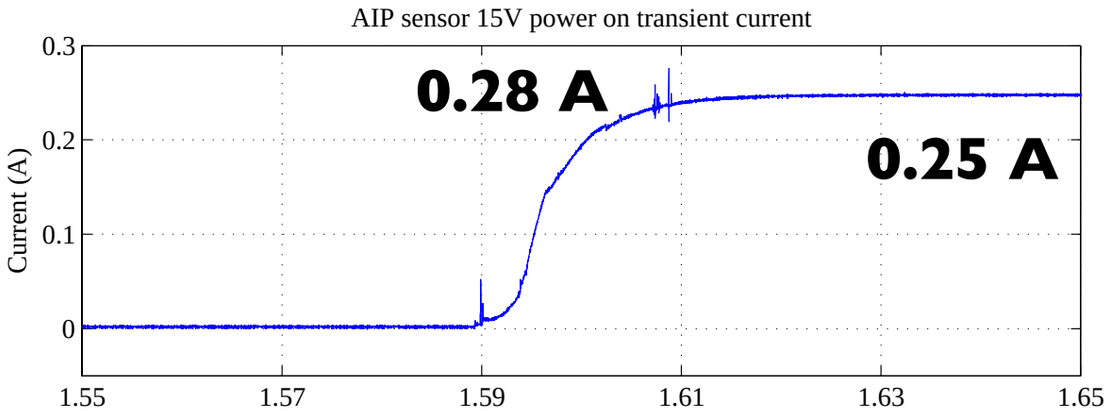

Sensor

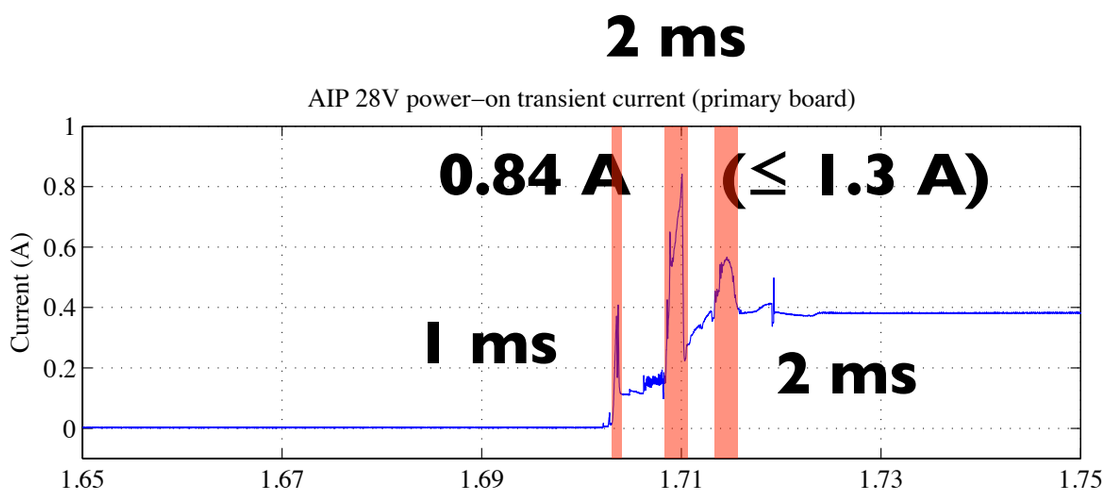

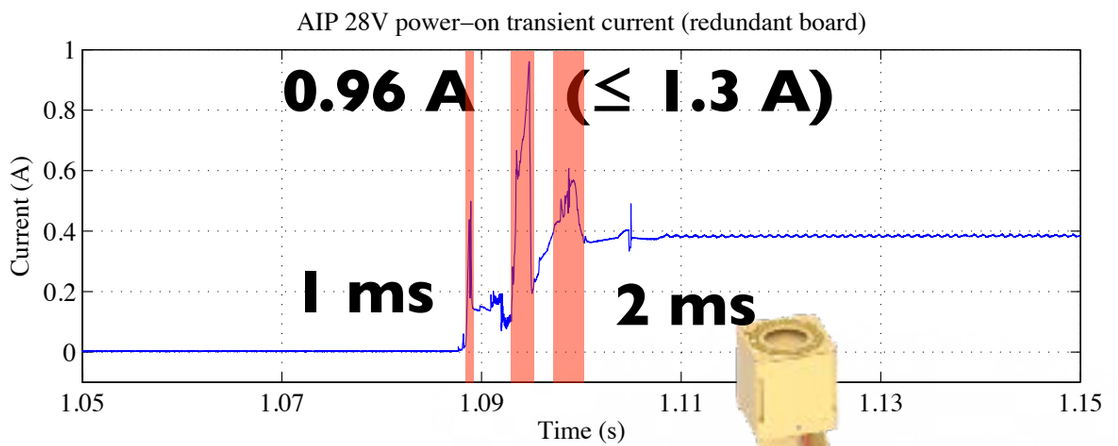

AIP

Current injection test

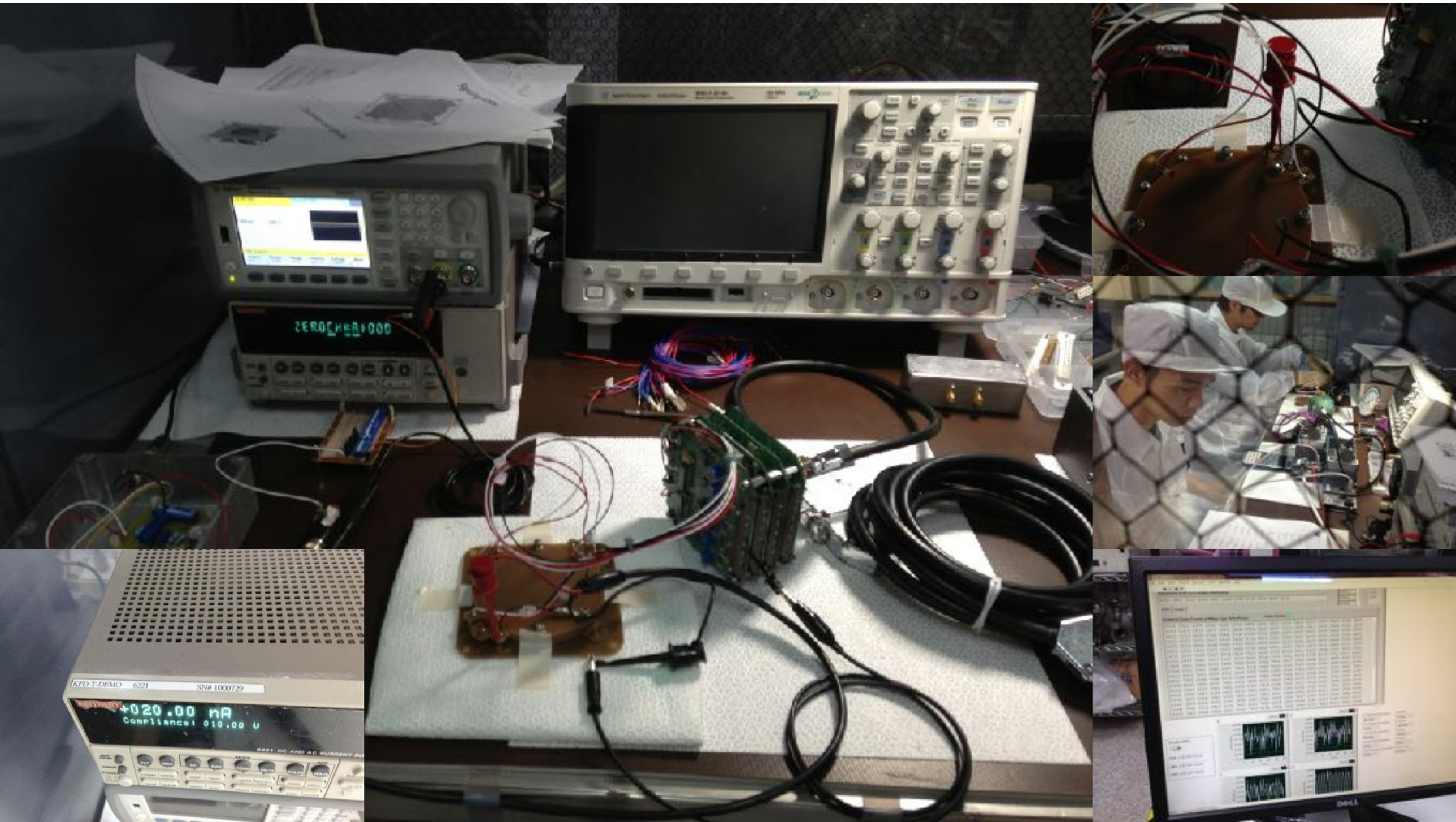

Current injection test (cont.)

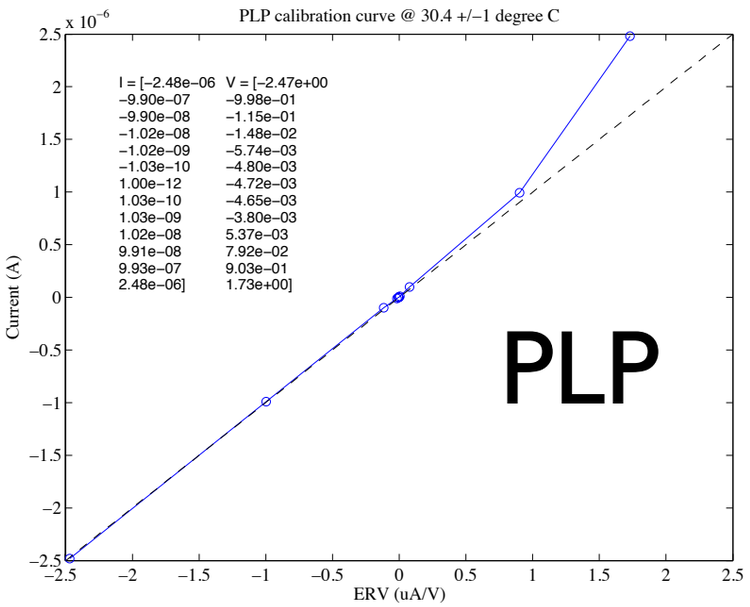

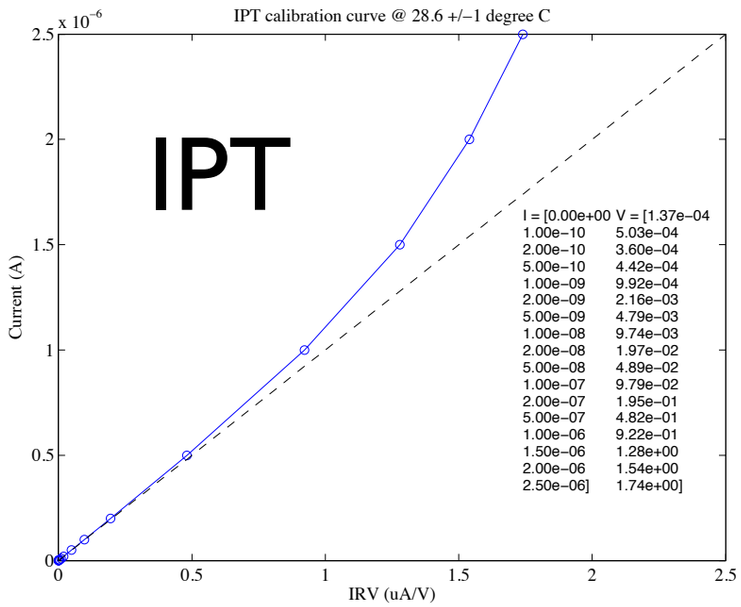

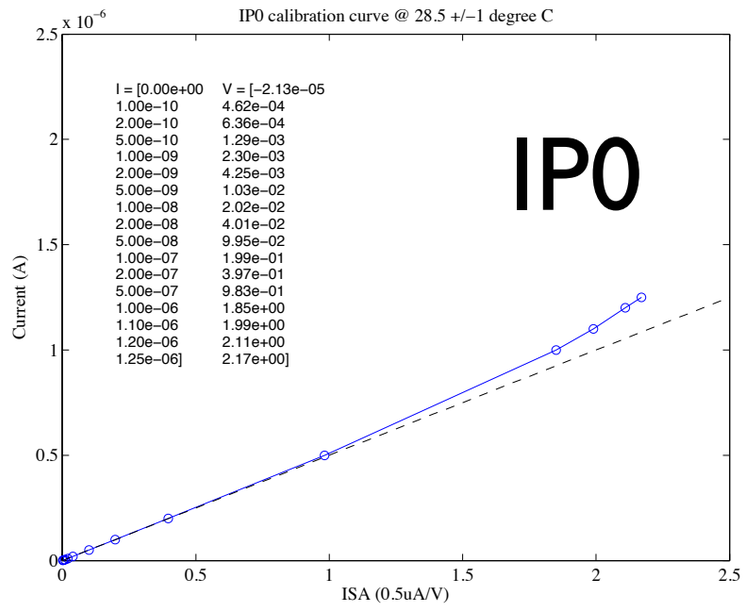

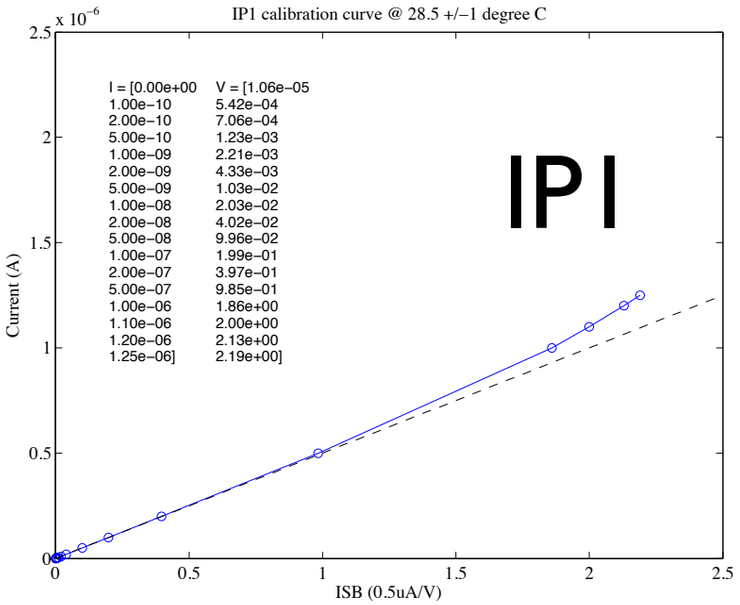

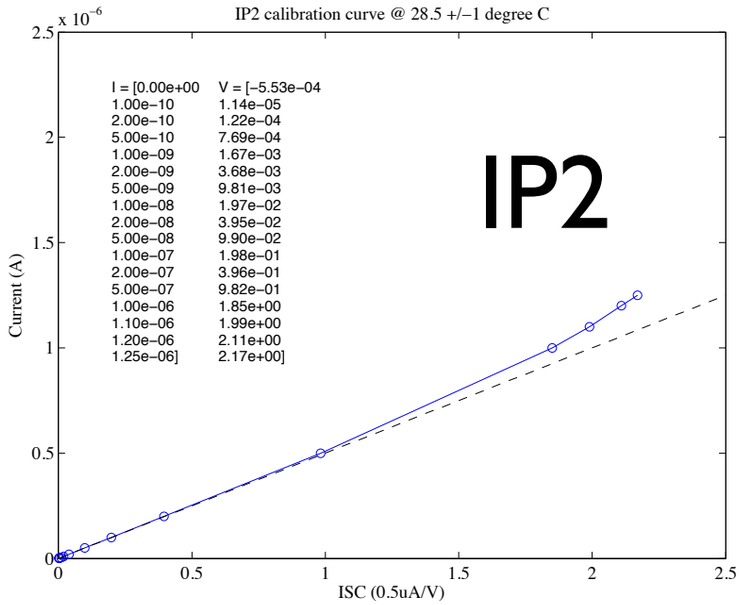

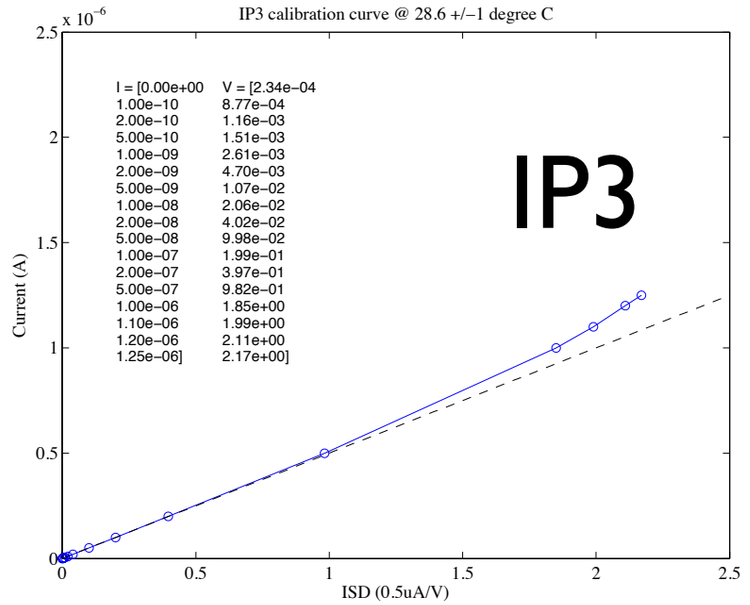

A zener diode is placed in front of an ADC to suppress input voltage smaller than 5 V and can prevent the ADC from damage. It results a non-linear voltage trend (above 1 V) for high current measurement.

Communication test

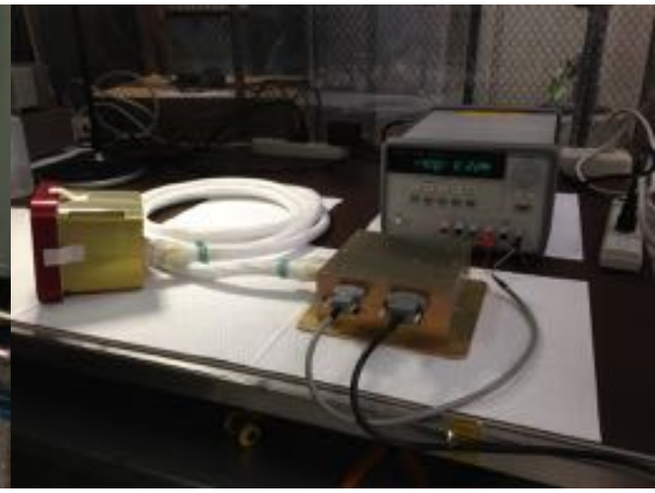

	Sensor only	SPEU only	AIP
EGSE	SPEU & CDMU simulator	CDMU simulator	CDMU simulator
Command	✔	✔	✔
SOH	✔	✔	✔
Ancillary	N/A	✔	✔
Science data	✔ (TESTOFF)	✔ (TESTON)	✔ (TESTOFF)

Environmental tests

- **Sine vibration test** (CSIST, 8/8/2013 & 8/29/2013): FS5SPL-SINE-PROC/RPT.
- **Random vibration test** (CSIST, 8/8/2013 & 8/29/2013): FS5SPL-RAND-PROC/RPT.
- **Shock test** (CSIST, 8/8/2013 & 8/29/2013): FS5SPL-SHOCK-PROC/RPT.
- **Thermal vacuum test** (NCU, 9/4/2013 to 9/11/2013): FS5SPL-TVT-PROC/RPT.
- **EMC test** (NSPO, 9/16/2013 to 9/18/2013 & 9/23/2013 to 9/27/2013): FS5SPL-CEMC-PROC/RPT and FS5SPL-REMC-PROC/RPT.

Structure measurement for sensor

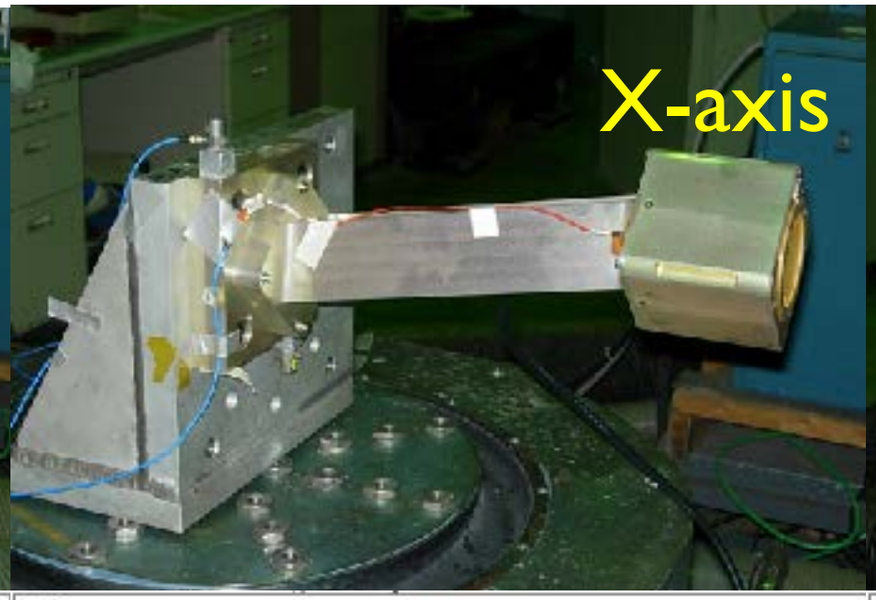

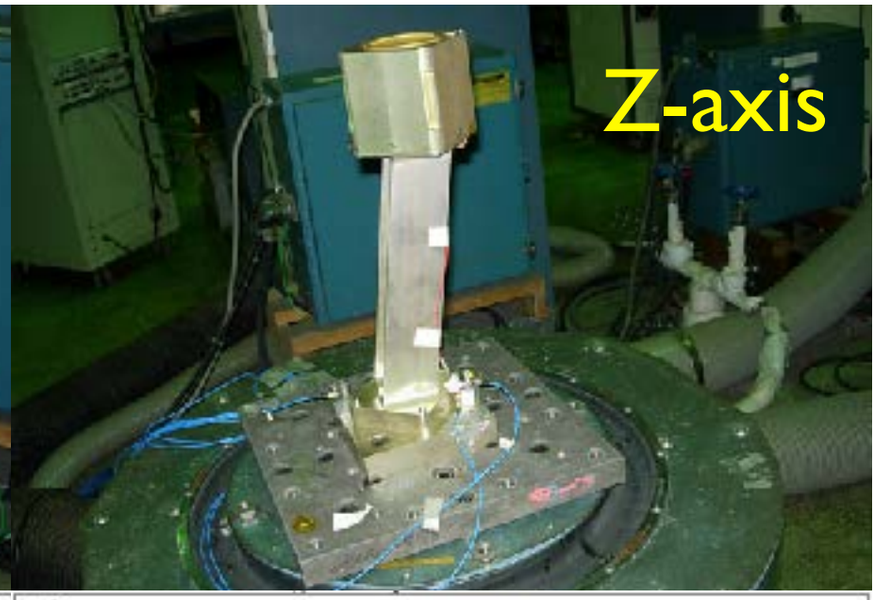

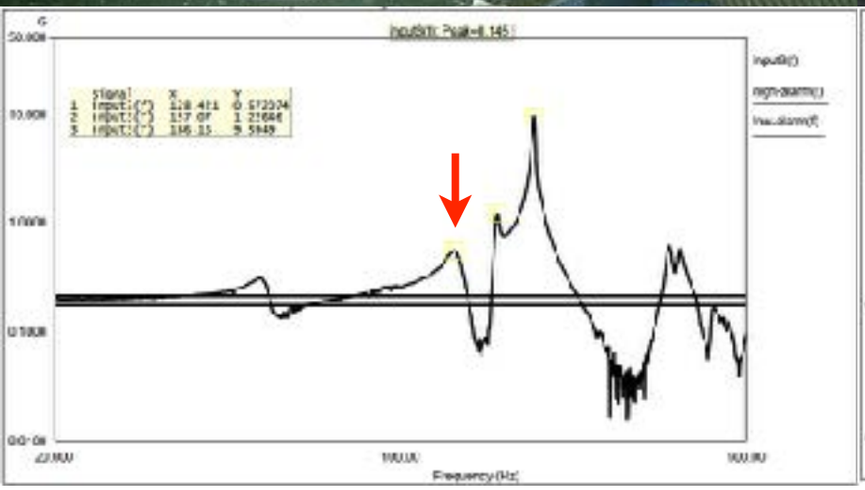

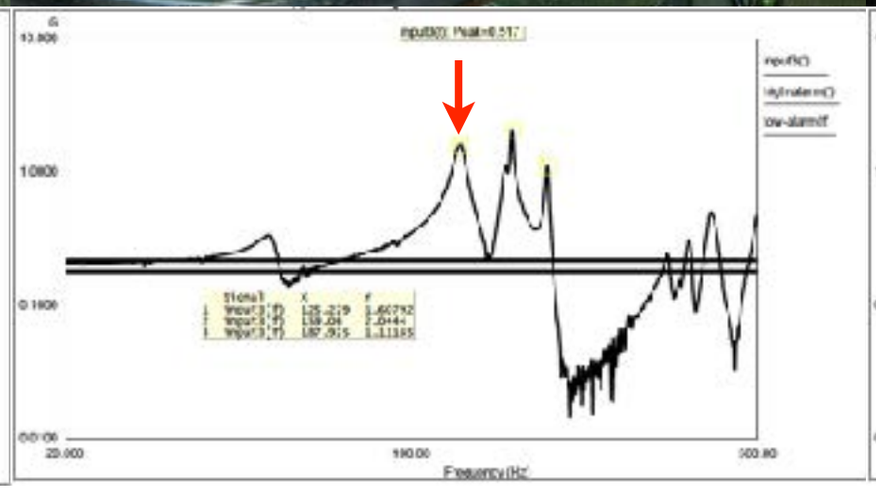

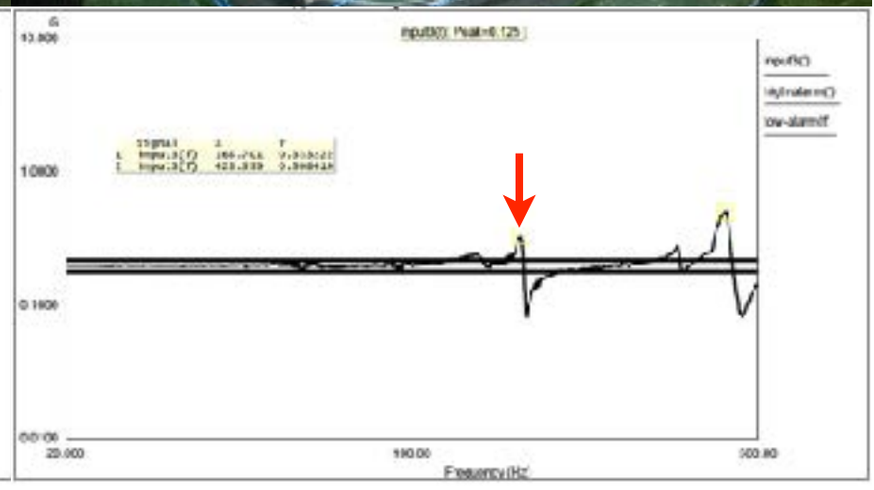

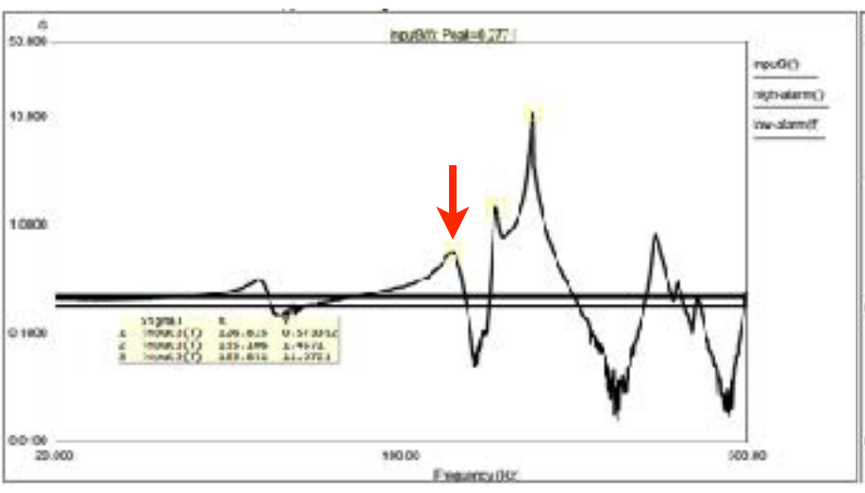

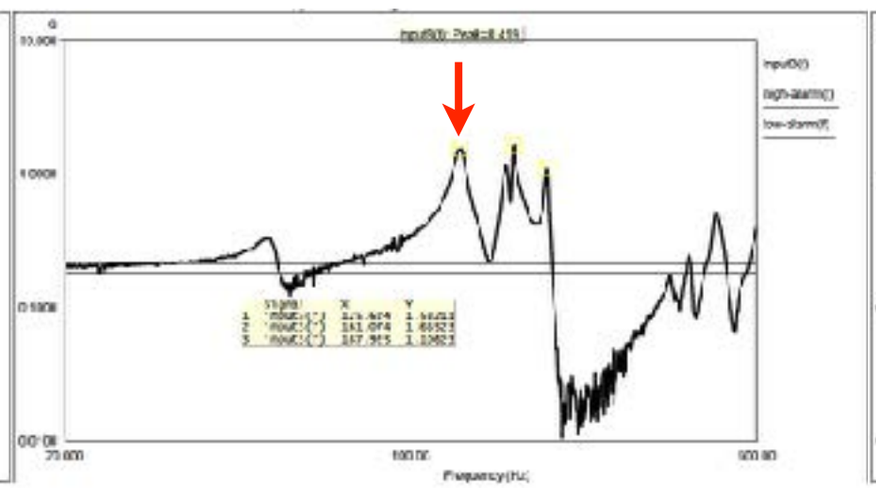

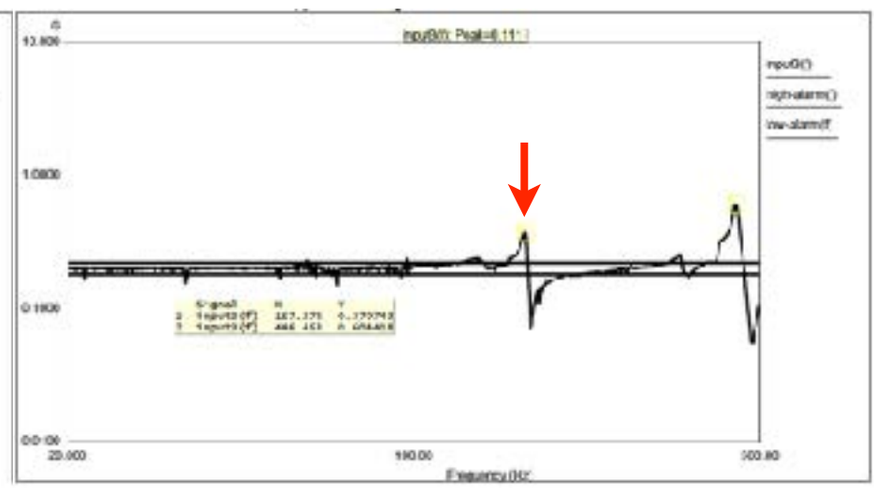

1st mode natural frequency

145.6 Hz estimated by SolidWorks and 136.1 Hz measured by NCU.

CSIST	Y-axis	X-axis	Z-axis
Before	128.4 Hz (x2.71)	125.2 Hz (x8.04)	165.7 Hz (x1.67)
After	126.8 Hz (x2.87)	125.6 Hz (x7.91)	167.3 Hz (x1.85)

All 1st mode natural frequencies measured by NCSIST are higher than 120 Hz.

Structure measurement for SPEU

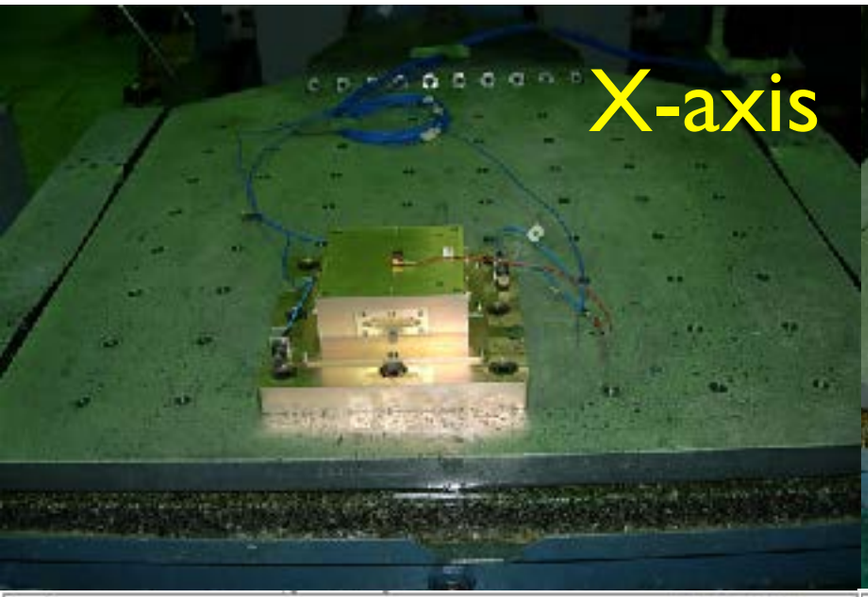

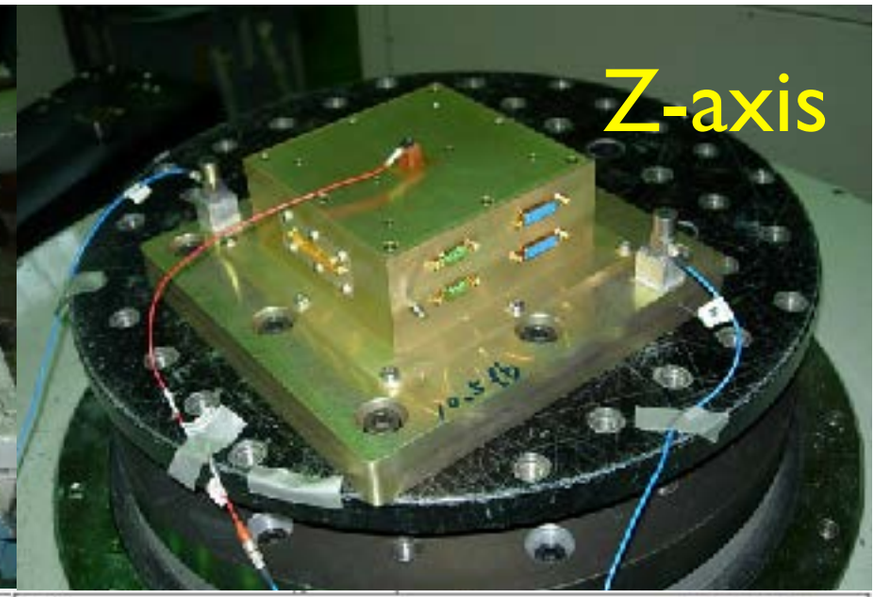

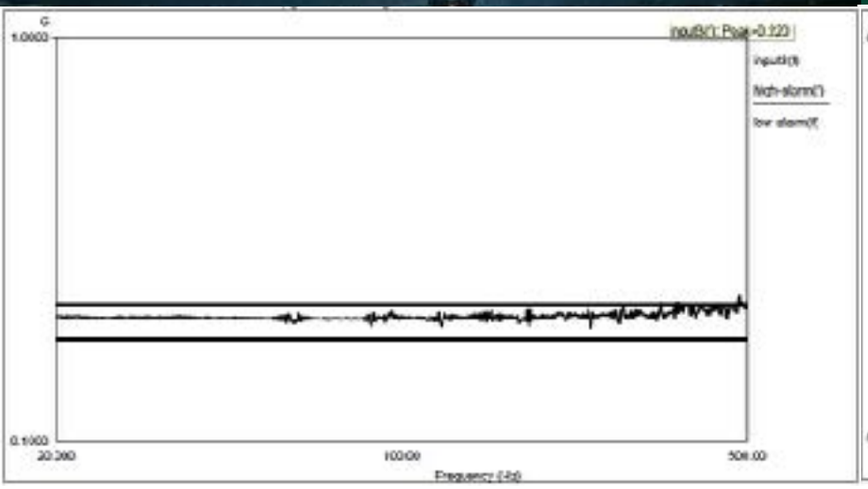

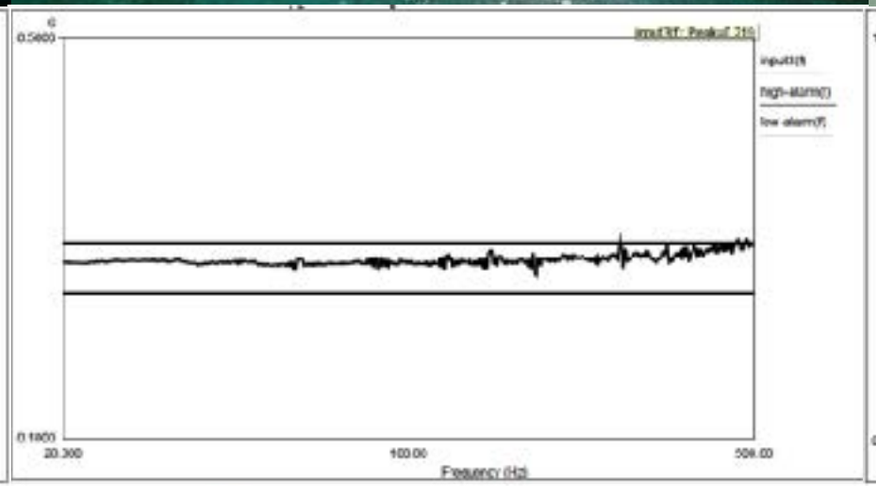

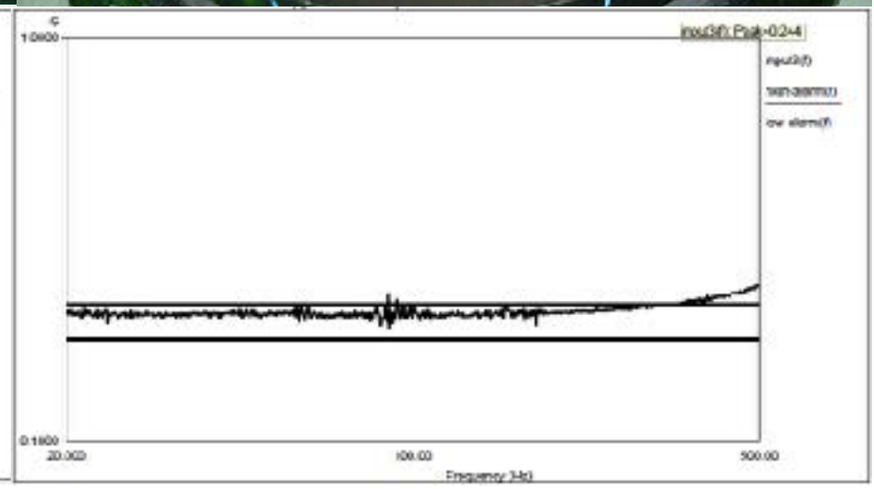

No significant natural frequencies are detected within the measurement range (20 to 500 Hz) in three different orientations.

Vibration test for sensor

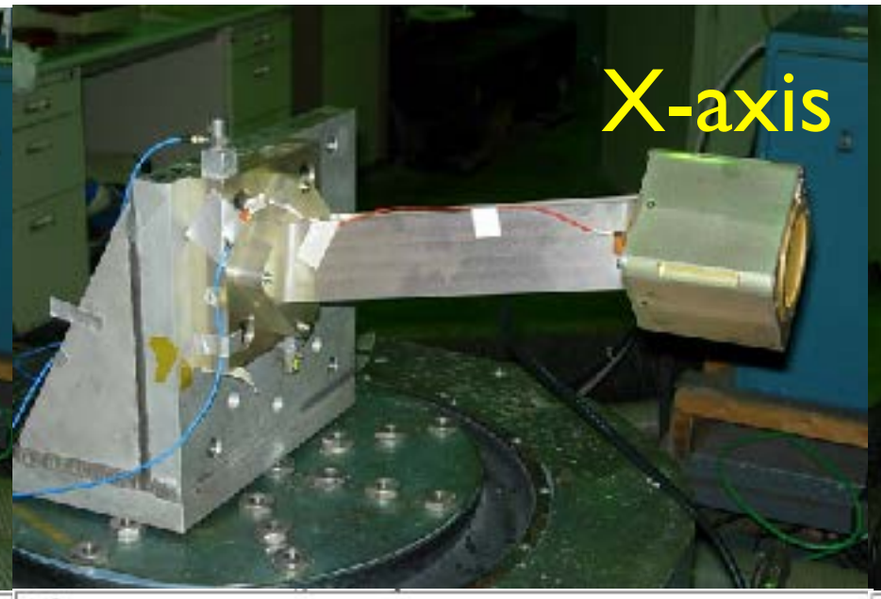

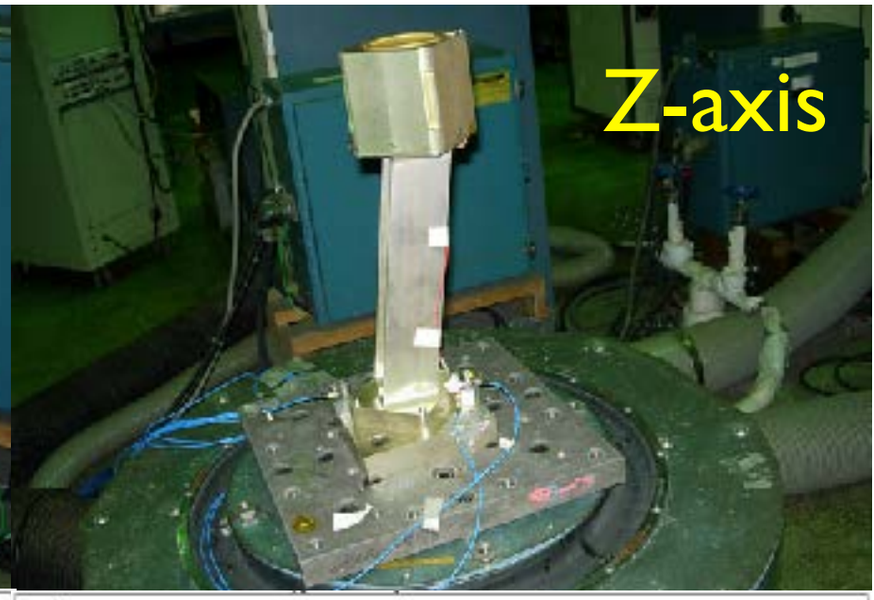

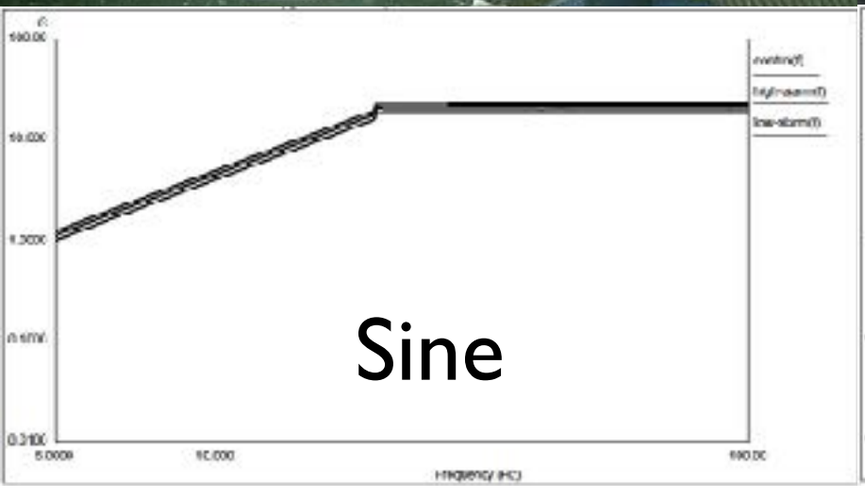

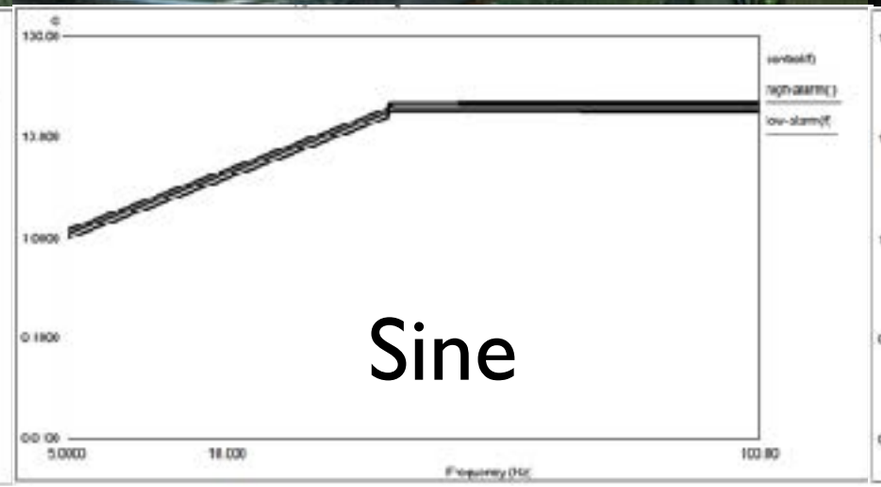

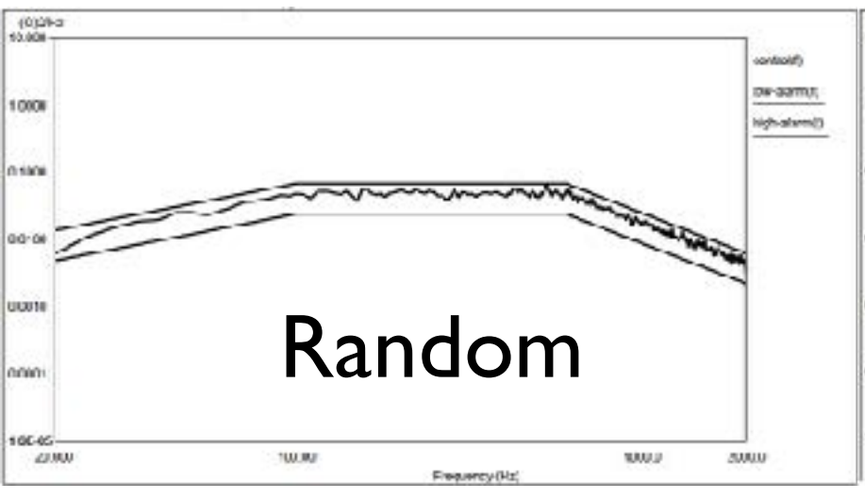

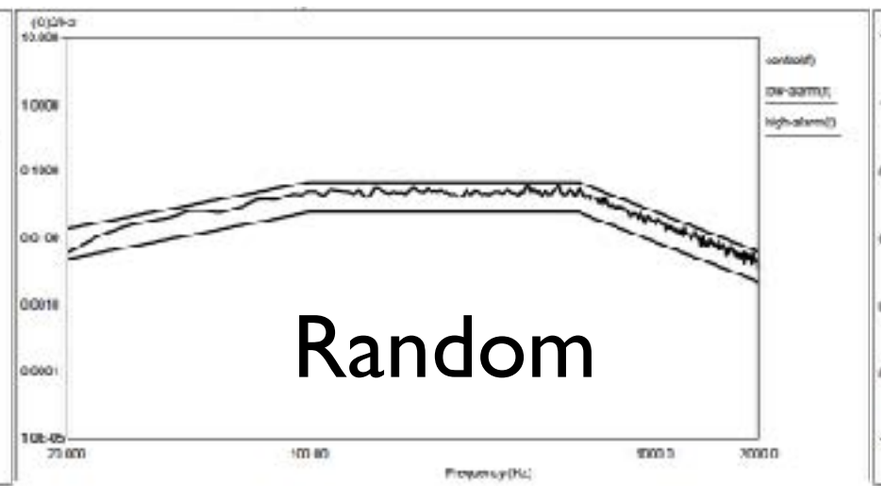

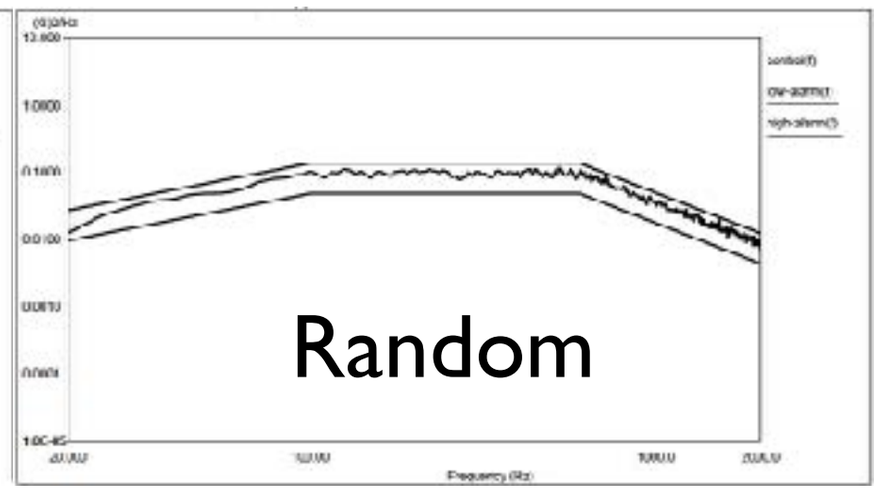

Vibration test for SPEU

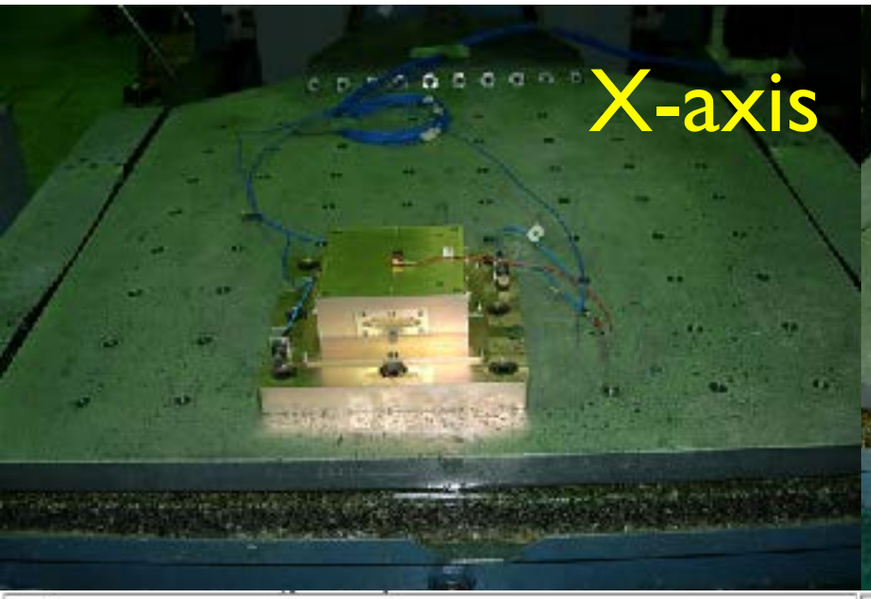

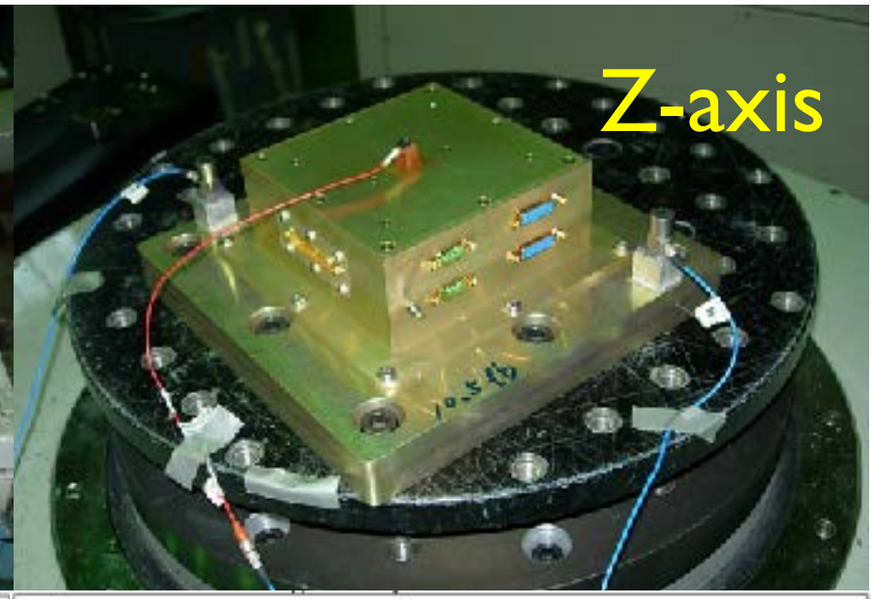

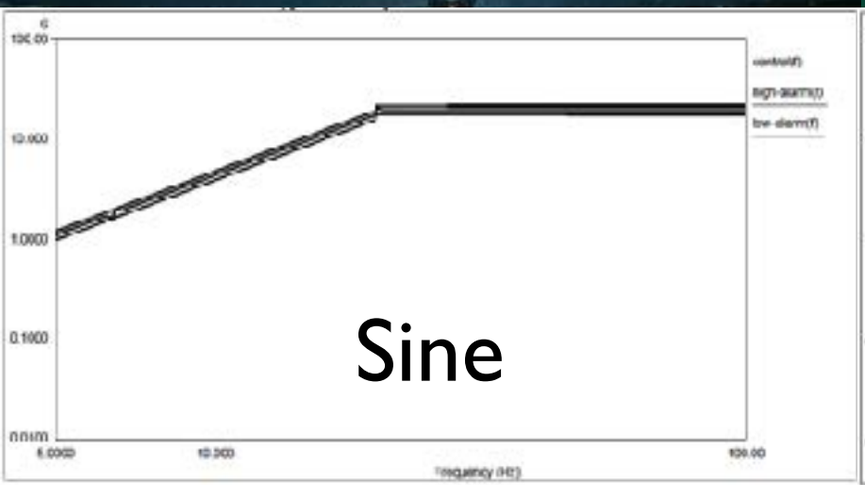

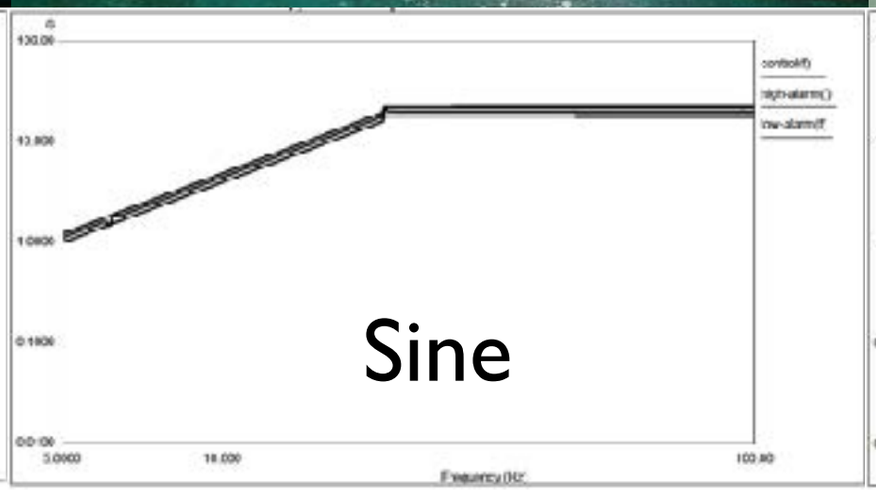

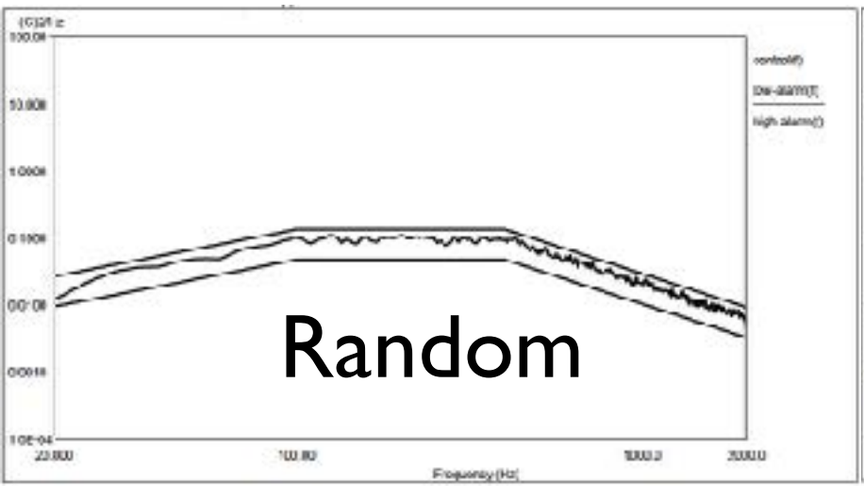

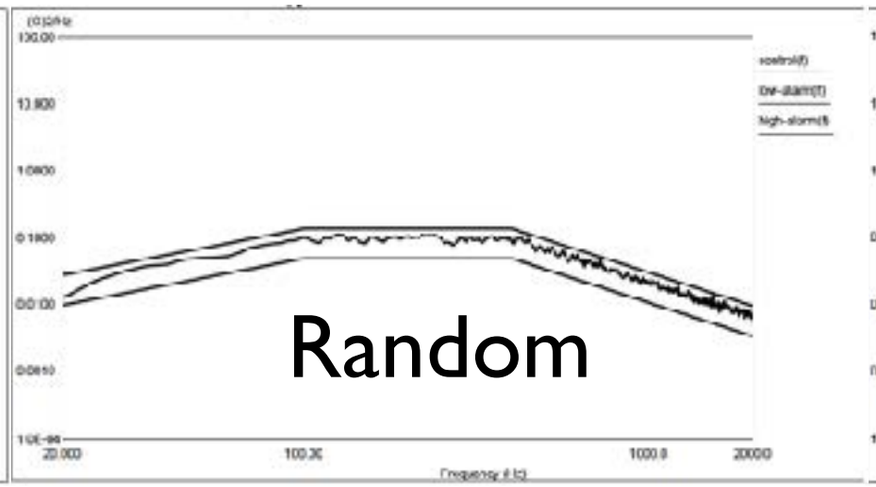

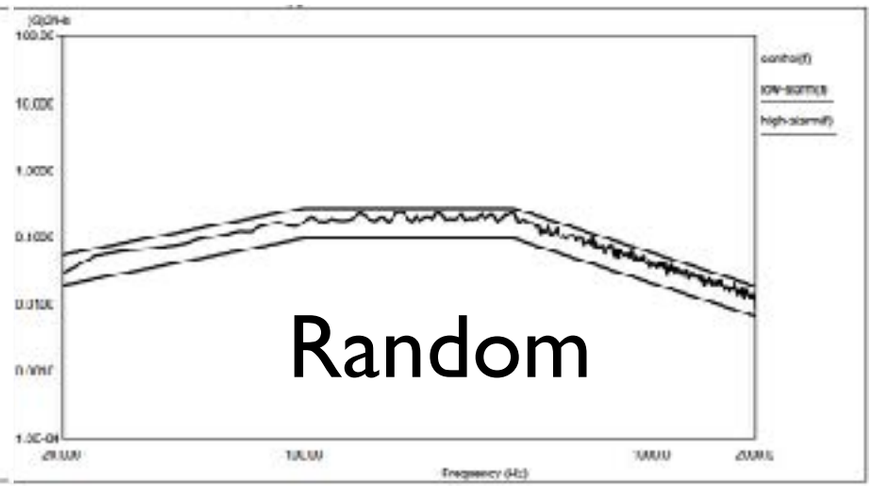

Shock test for sensor

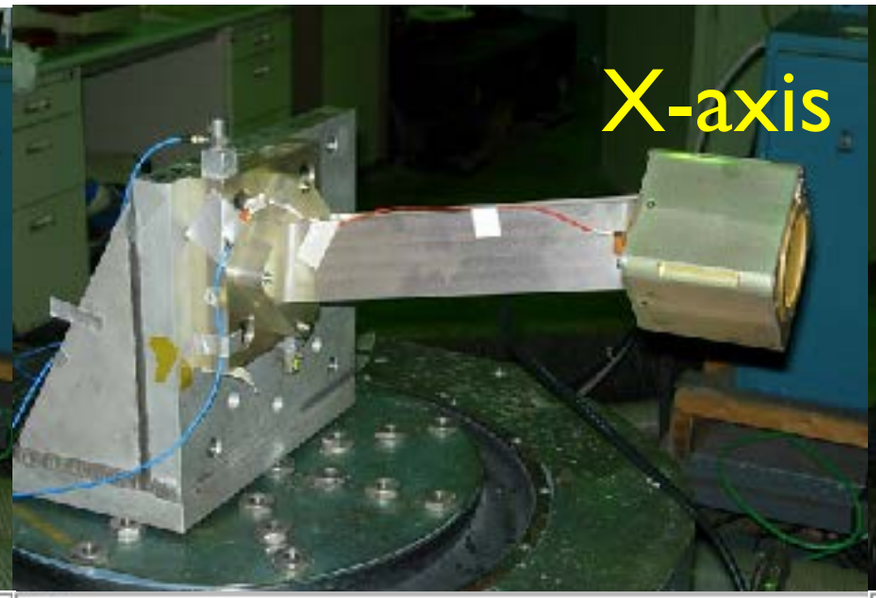

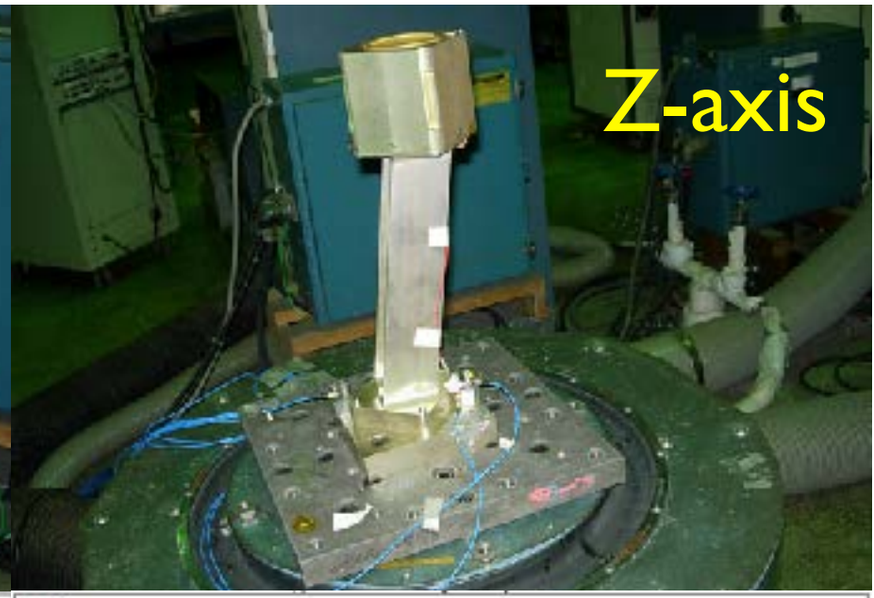

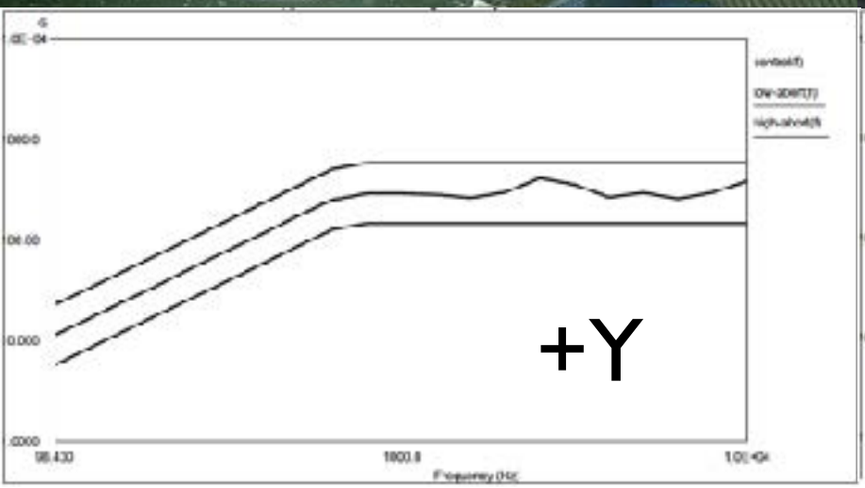

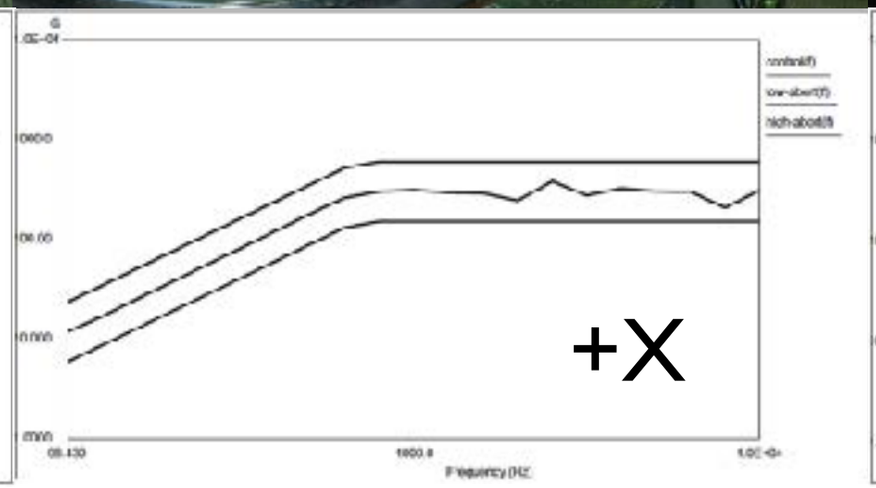

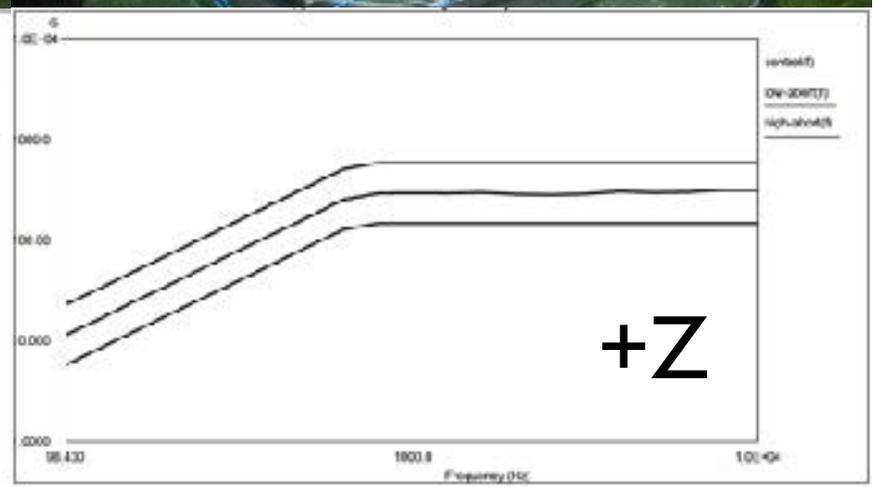

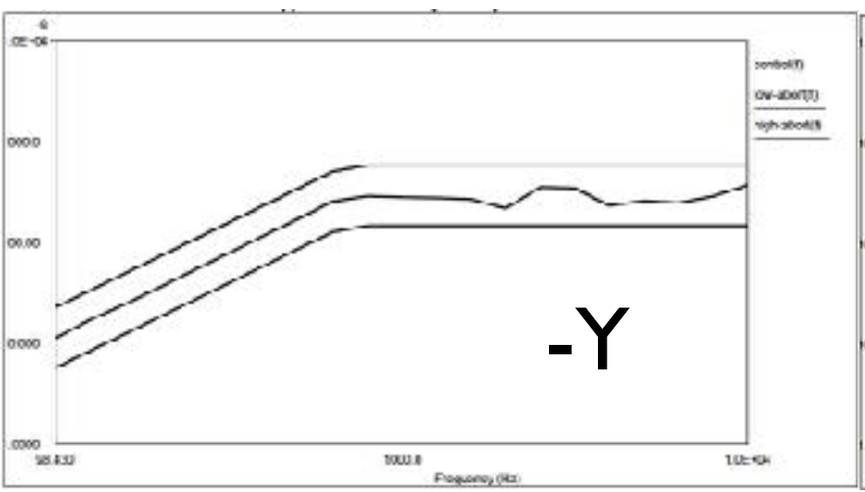

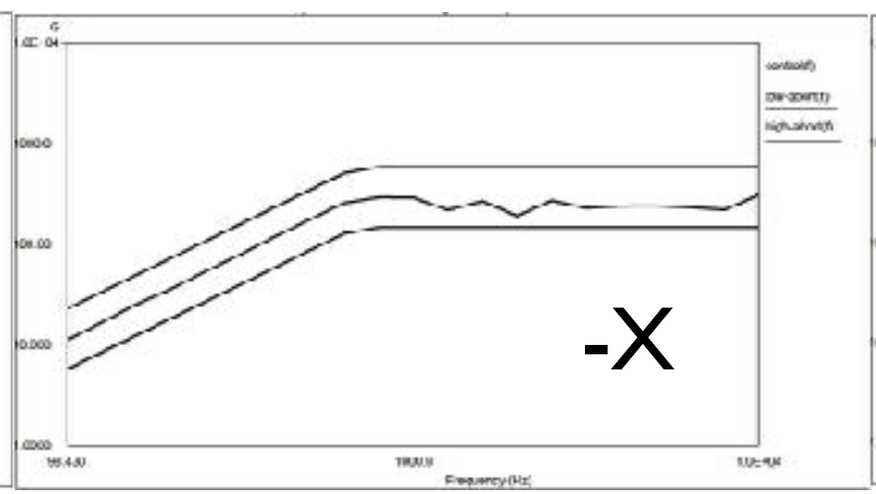

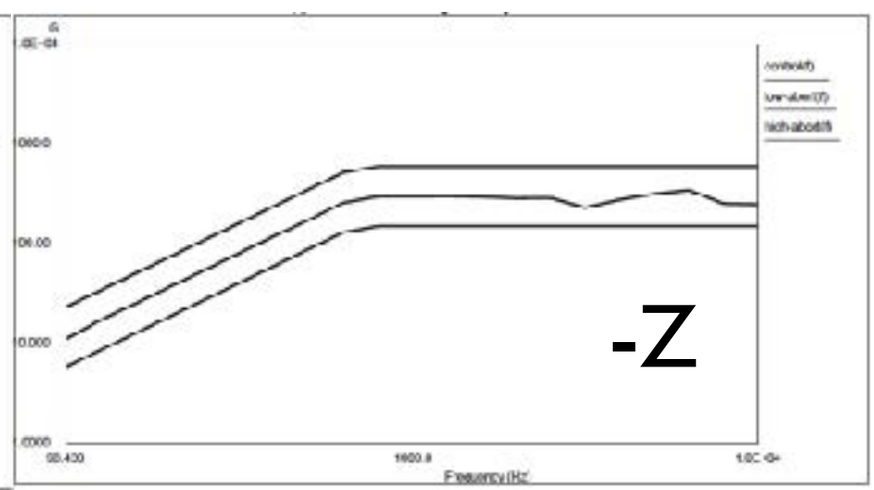

Shock test for SPEU

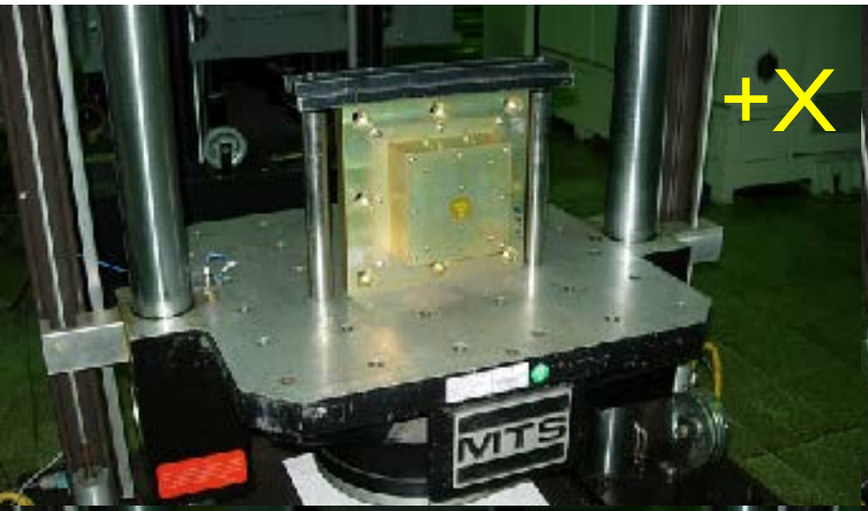

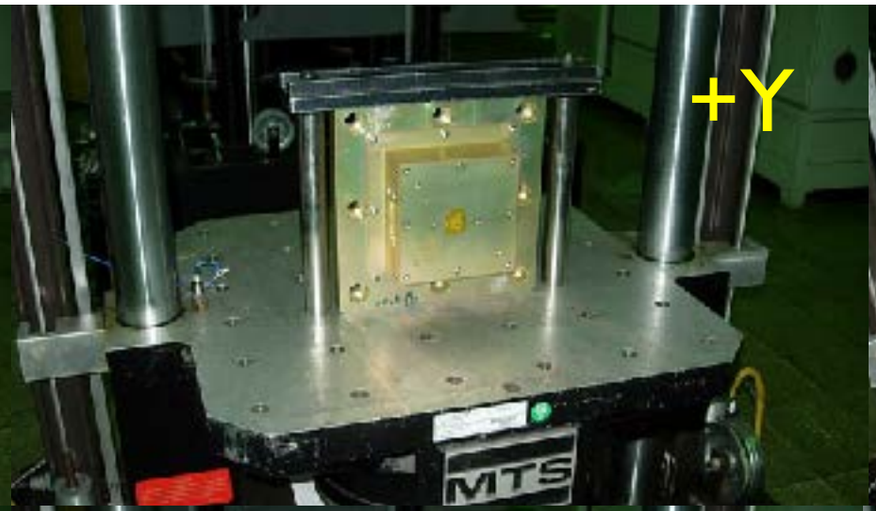

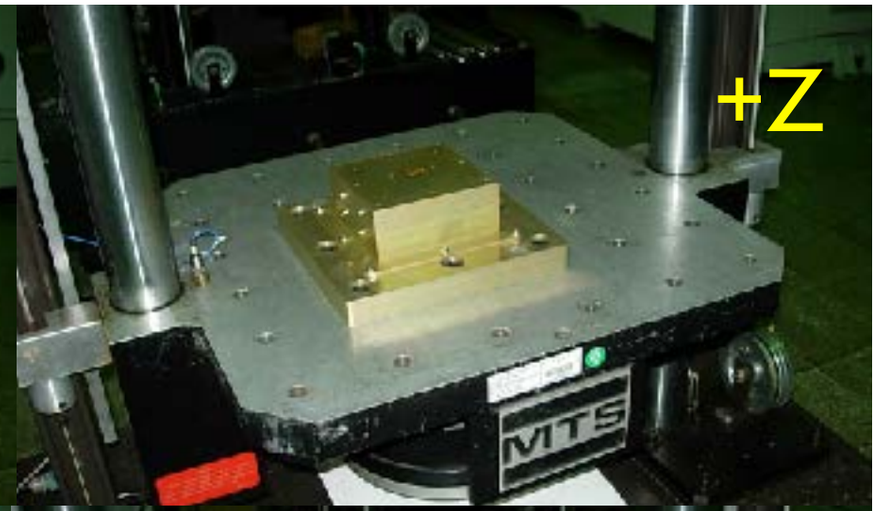

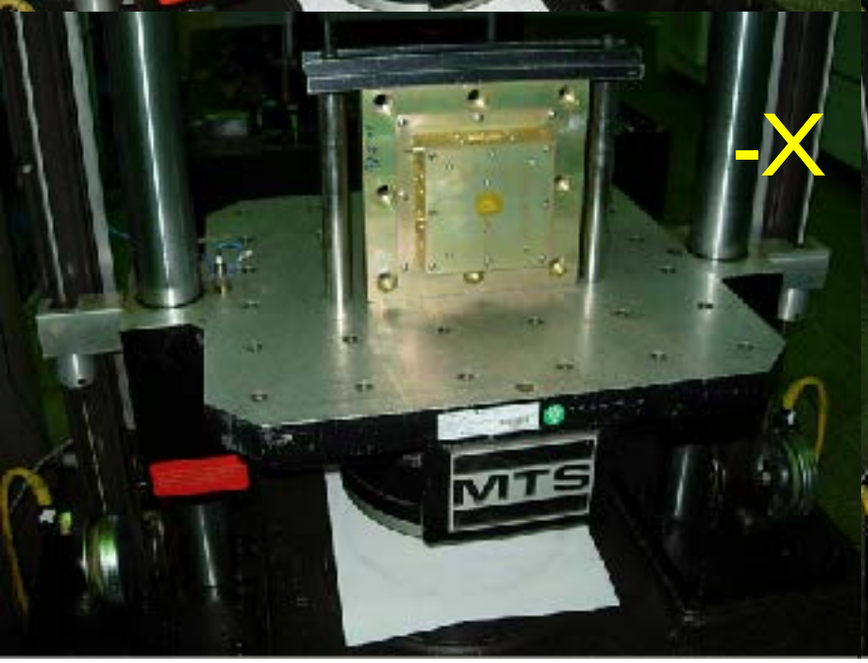

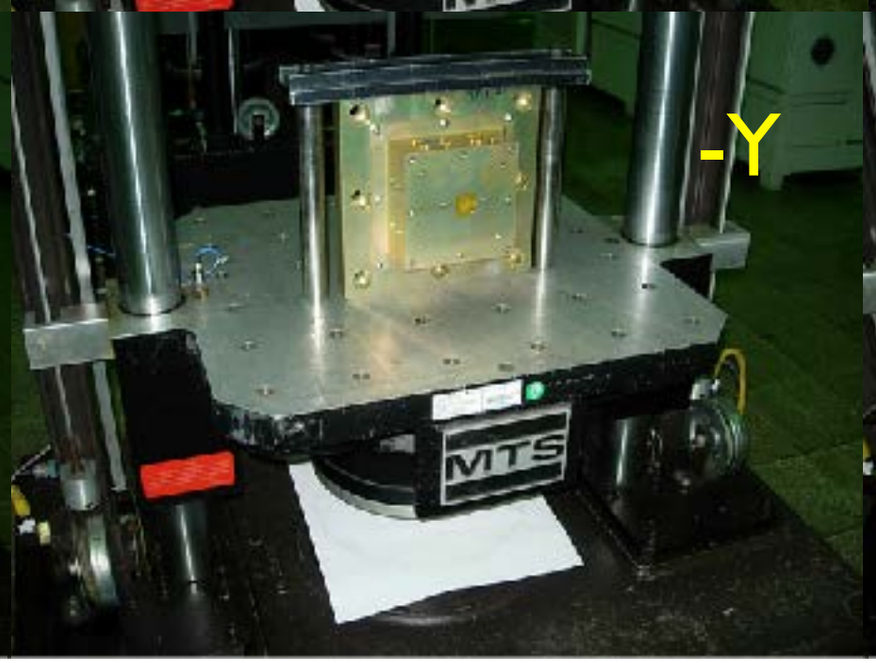

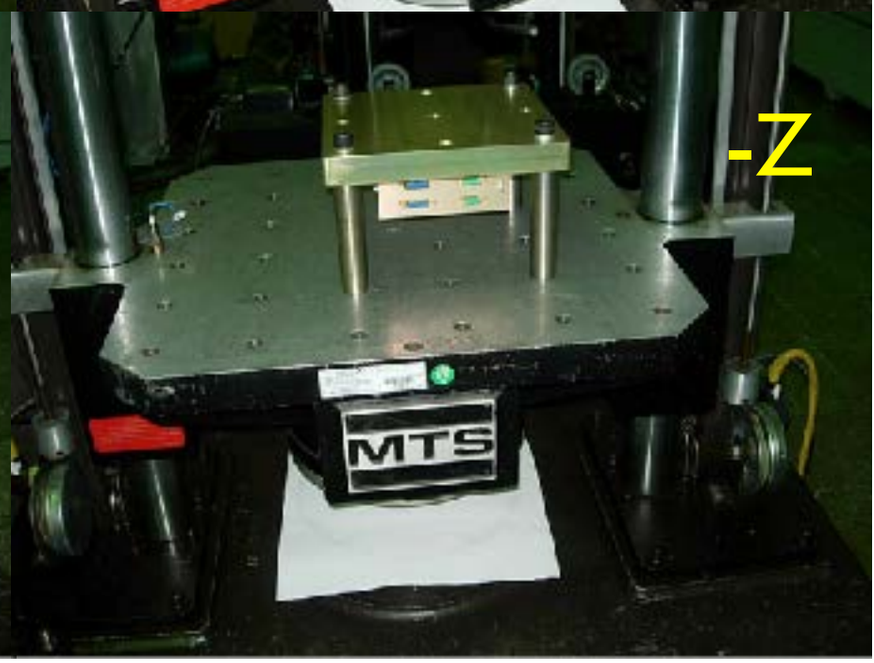

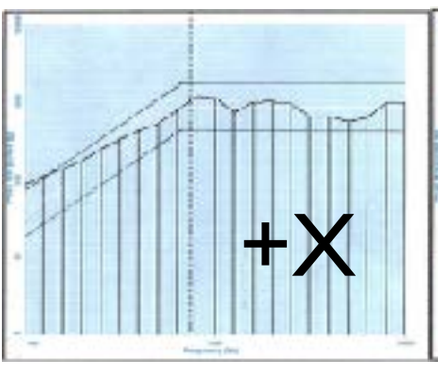

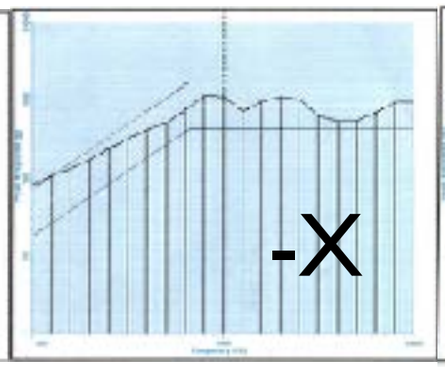

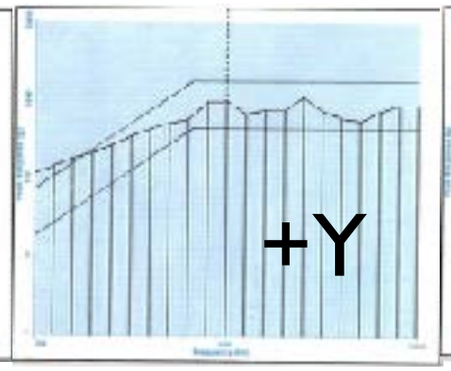

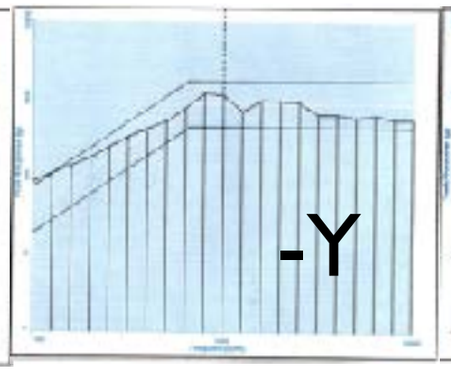

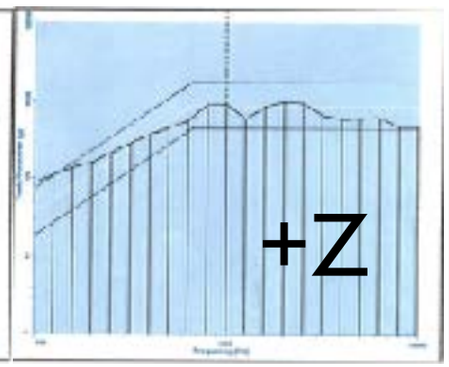

Thermal vacuum test

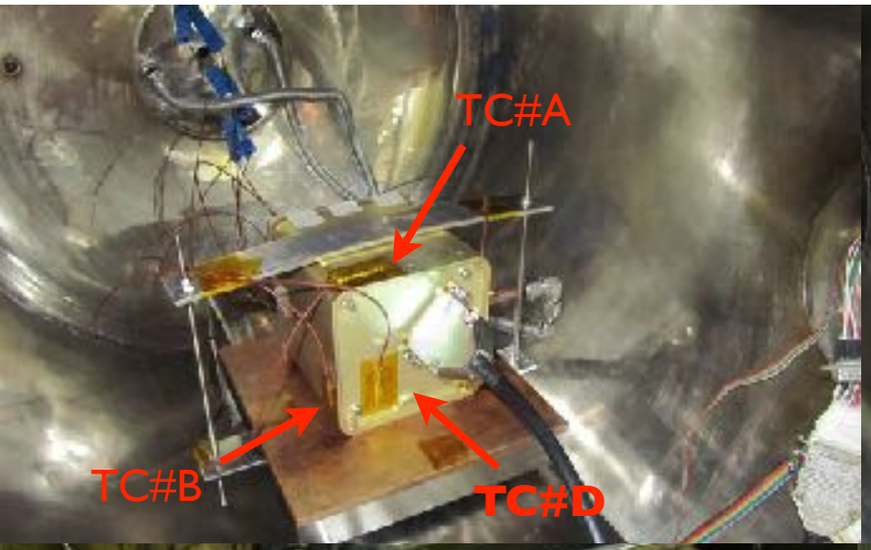

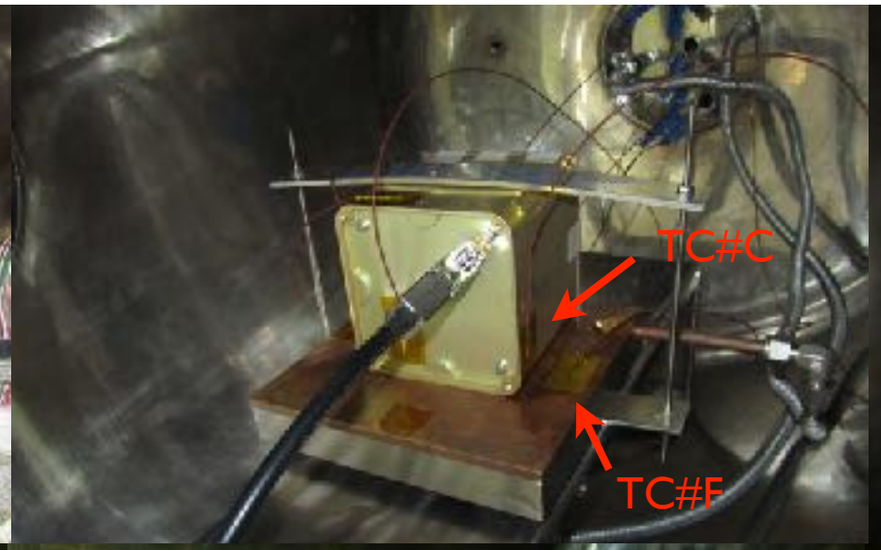

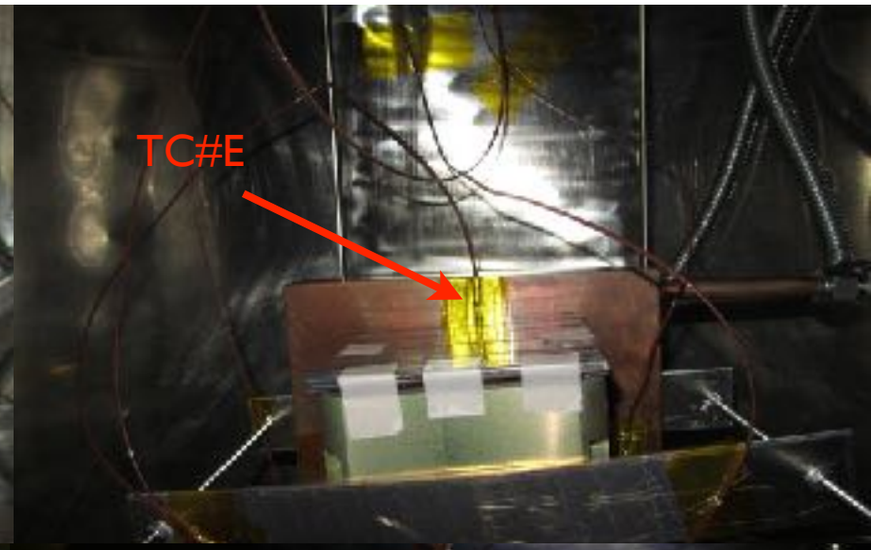

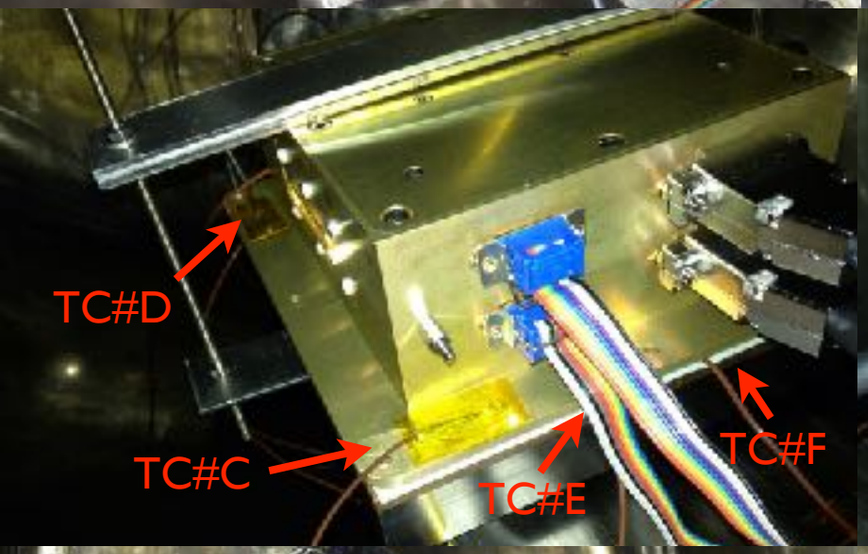

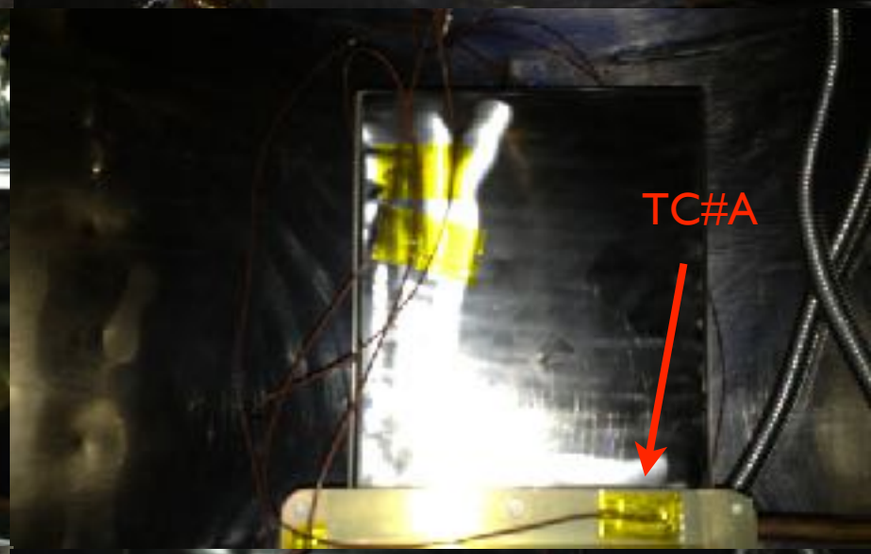

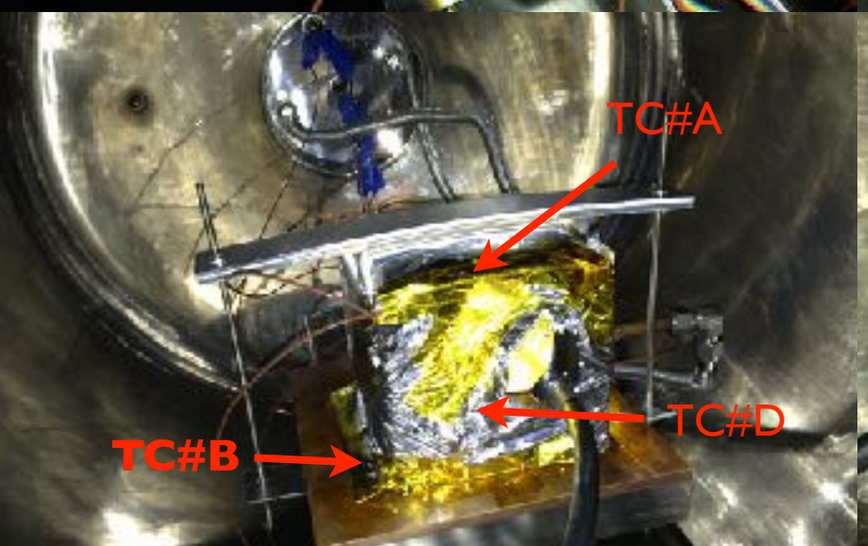

TVT for sensor

Chamber pressure is under 5 x 10^{-3} Pa except for cycle#1 at T_{max}.

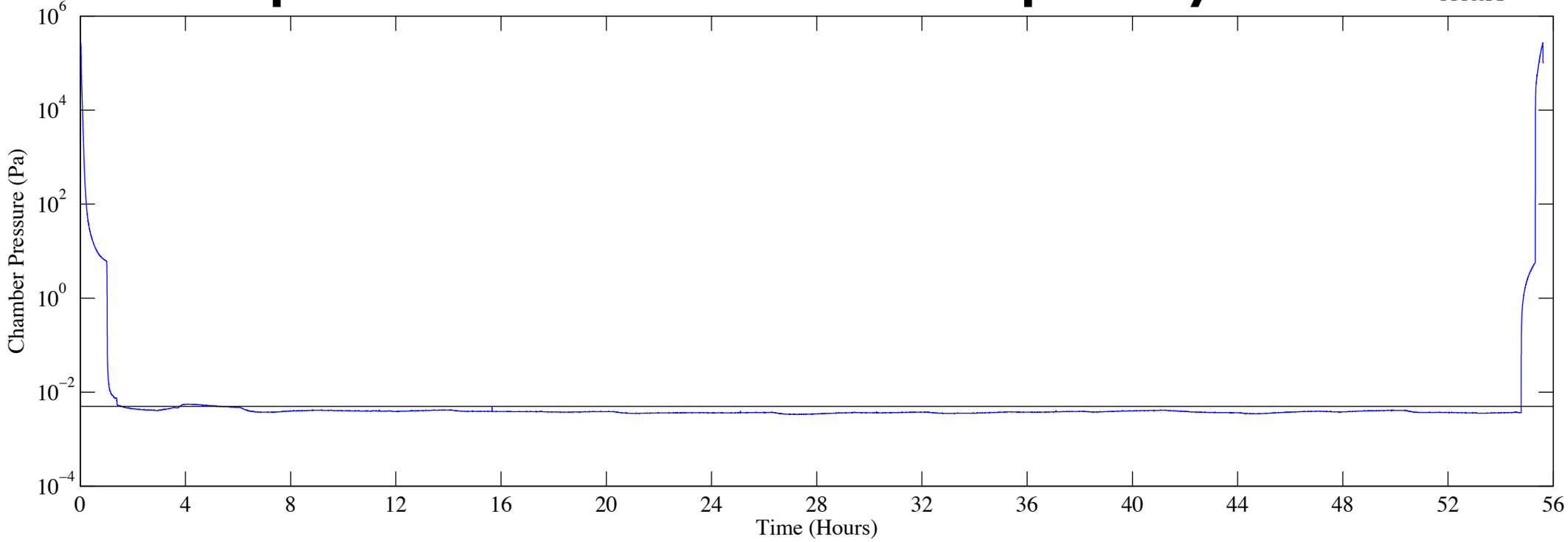

TC#D was used as a control point and located at base plate of the sensor.

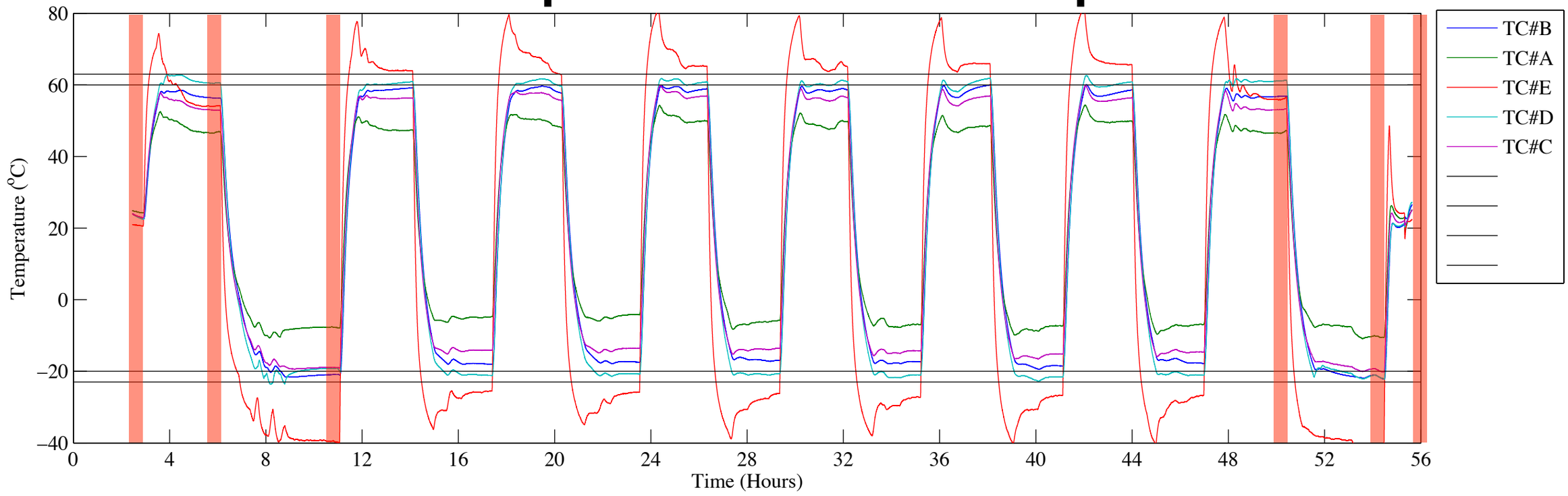

TVT for SPEU

Chamber pressure is under 5 x 10^{-3} Pa during the cycles.

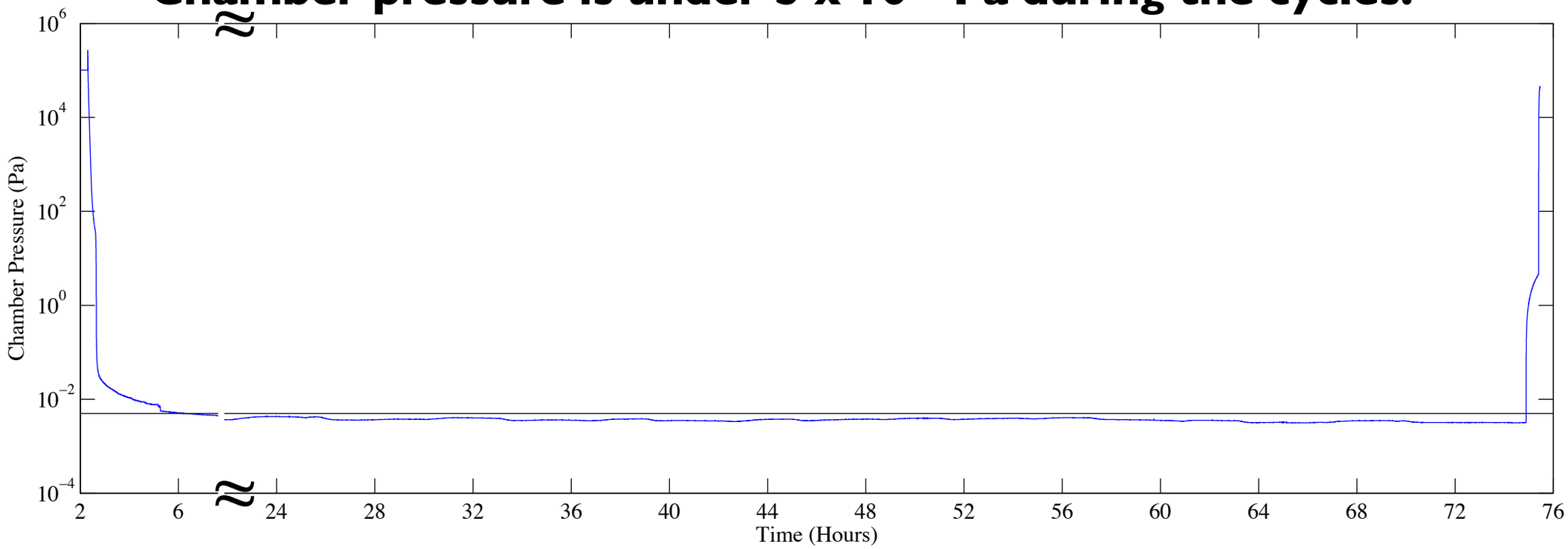

TC#B was used as a control point and located at base plate of the sensor.

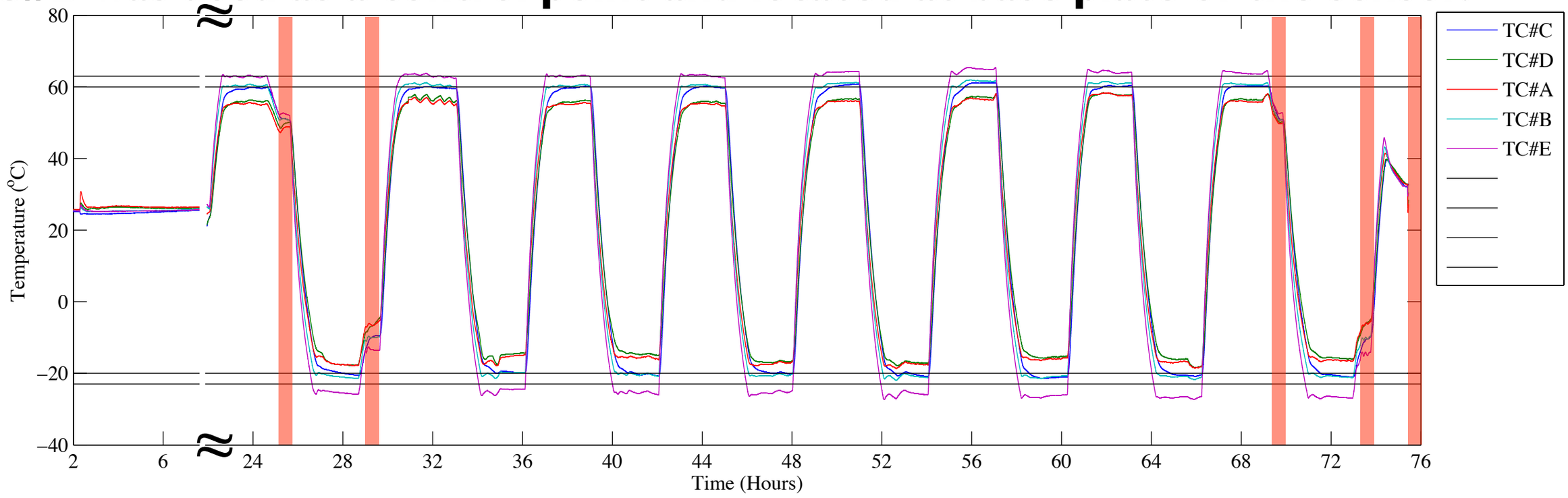

Temperature at SPEU's PCB

CYCLE#1

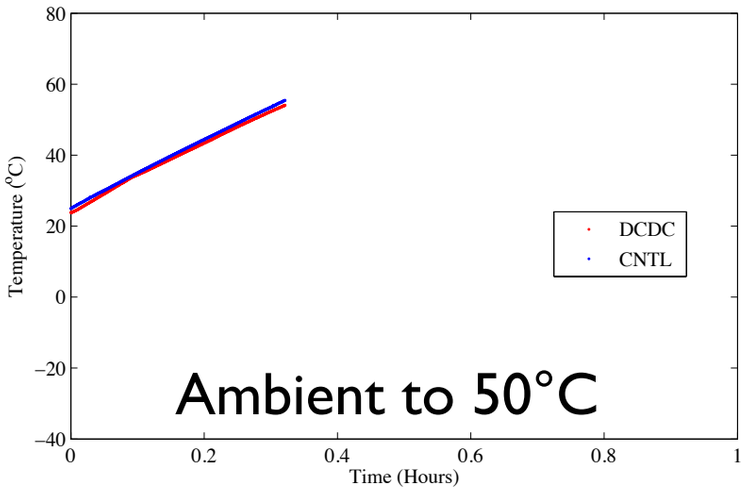

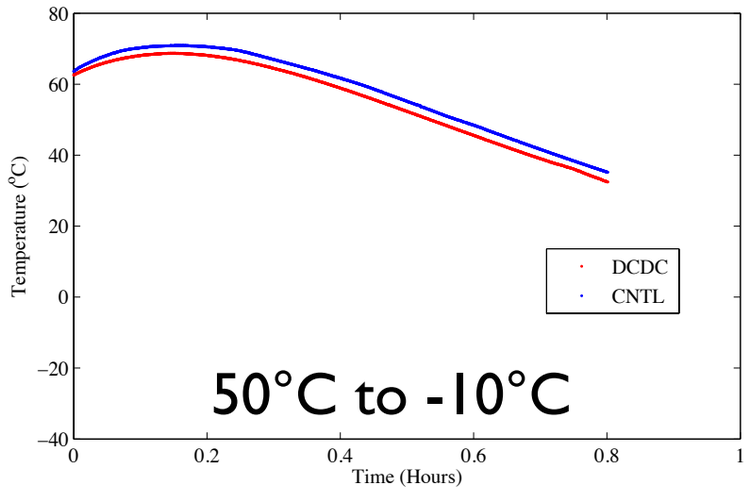

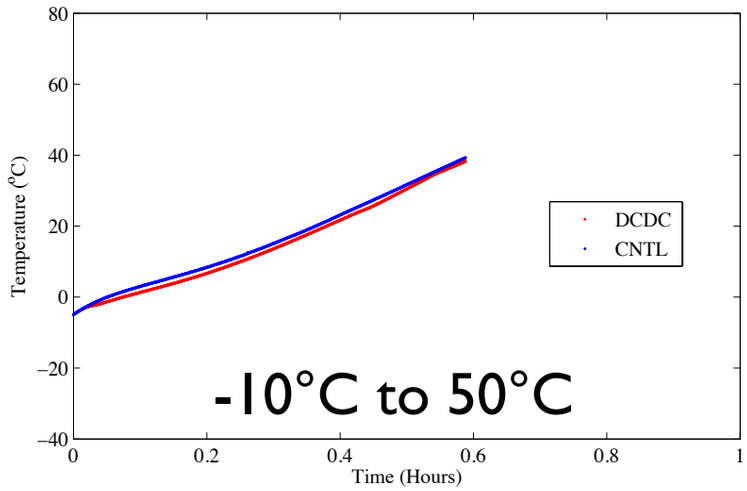

CYCLE#8

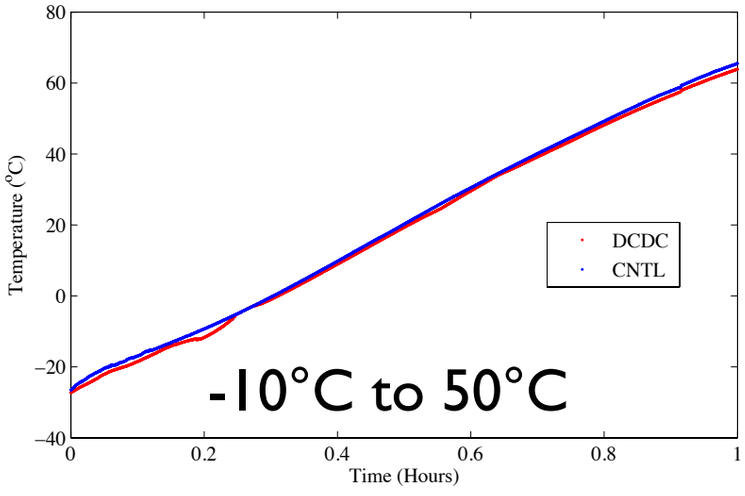

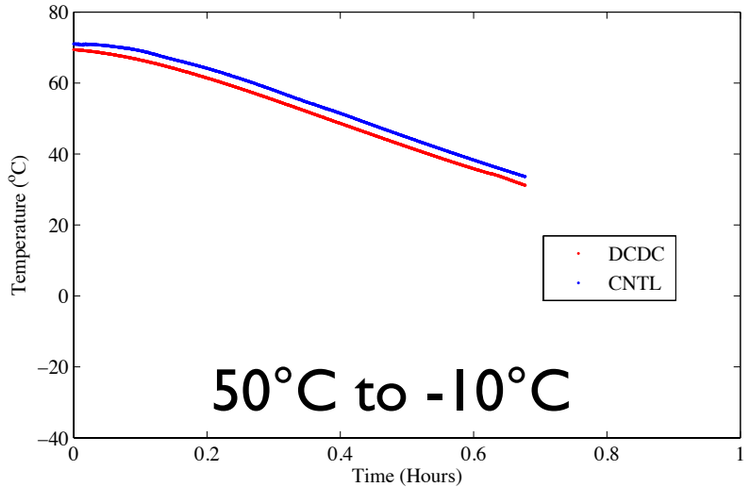

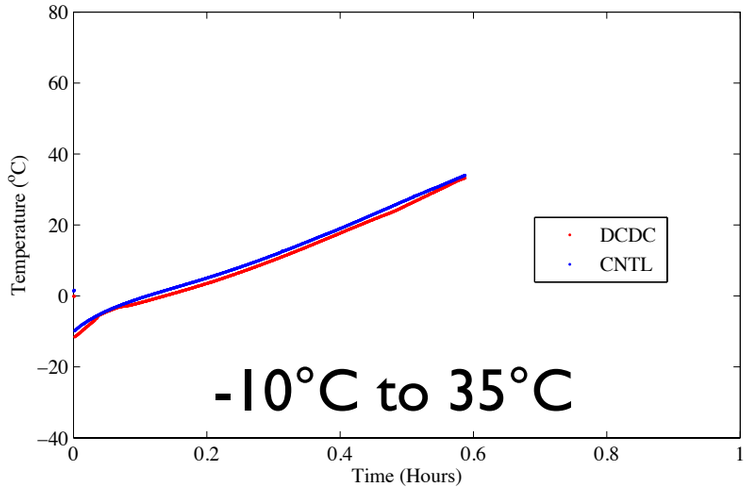

TVT for sensor with MLI

Chamber pressure is under 5 x 10^{-3} Pa except for cycle#1 at T_{max}.

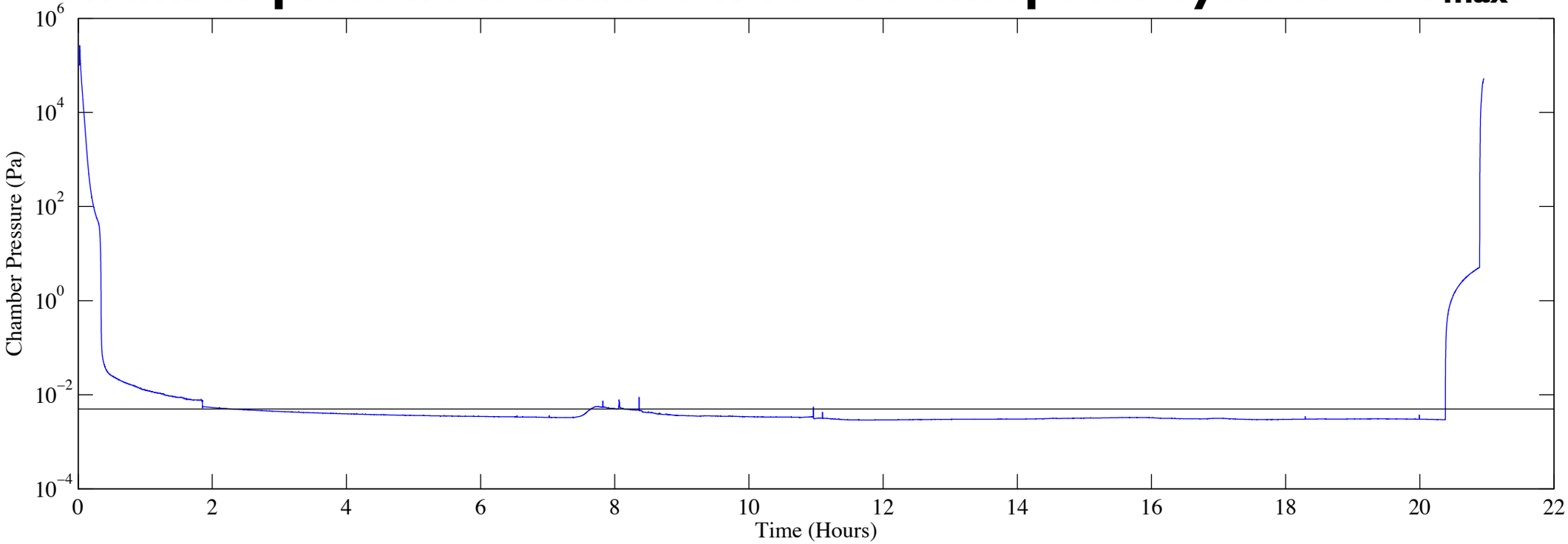

TC#B was used as a control point at T_{max} and TC#C at T_{min}.

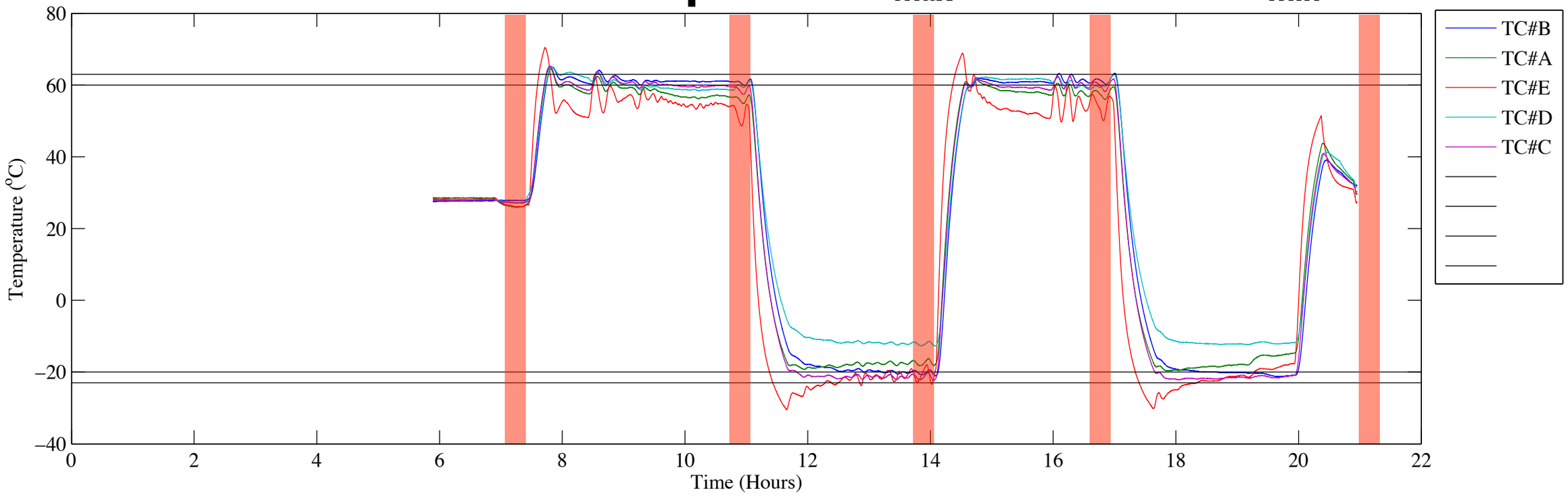

Temperature at sensor's PCB

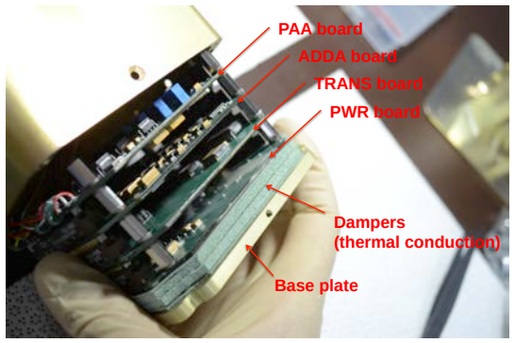

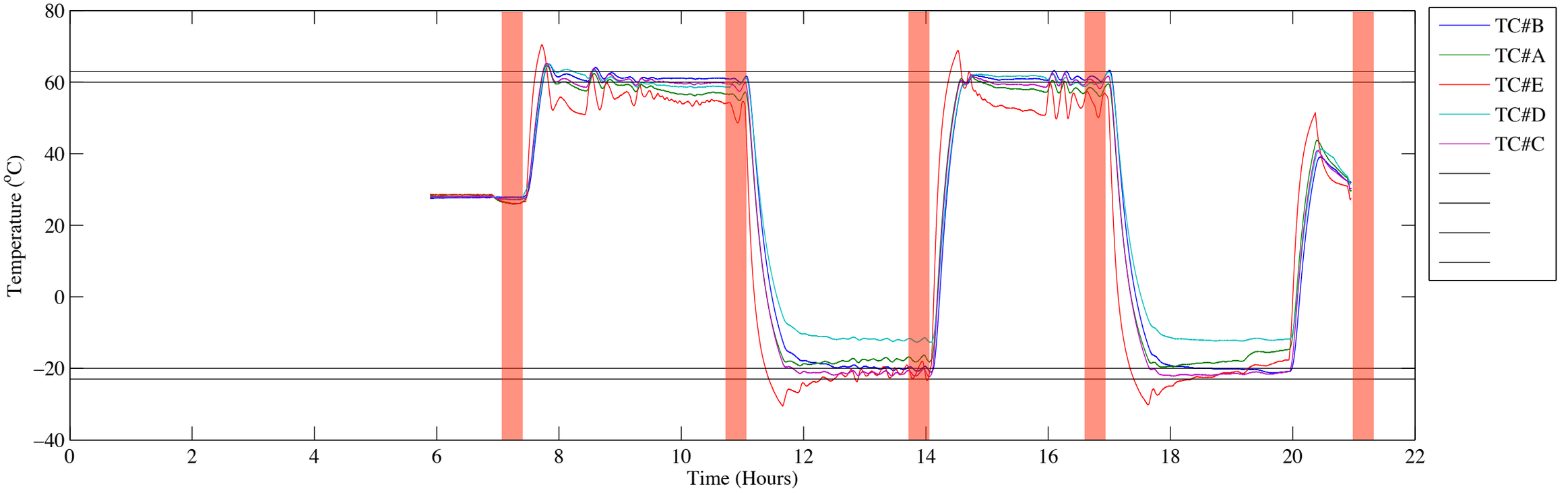

EMC test

- Conducted EMC
  - Grounding and isolation.
  - CE on transient voltage and in-rush current - time domain, on primary power lines - frequency domain, and on signal lines - time domain.
  - CS on primary power lines - sine wave and spike injection.
- Radiated EMC
  - RE - 14 KHz to 10 GHz, GPS receiver, S band receiver, and launcher receiver.
  - RS - 200 MHz to 10 GHz, local E-field by bus antennas, and launcher environment (under a conclusion of TRR meeting on EMC, 14 KHz to 200 MHz could be performed after an amplifier for this radio band returns to NSPO).

Grounding and isolation

Resistance	Requirement	Measurement
Resistance between SPEU chassis and the test bench	< 100 mΩ	6.8 mΩ
Resistance between SPEU chassis and secondary ground	≤ 100 mΩ	ND
Resistance between SPEU chassis and primary power +28 V of primary controller	> 1 MΩ	OL
Resistance between SPEU chassis and primary power +28 V of redundant controller	> 1 MΩ	OL
Resistance between SPEU chassis and primary power ground of primary controller	> 1 MΩ	OL
Resistance between SPEU chassis and primary power ground of redundant controller	> 1 MΩ	OL
Resistance between primary power +28 V of primary controller and the secondary power +15 V	> 1 MΩ	OL
Resistance between primary power +28 V of redundant controller and the secondary power +15 V	> 1 MΩ	OL
Resistance between primary power ground of primary controller and the secondary power +15 V	> 1 MΩ	OL
Resistance between primary power ground of redundant controller and the secondary power +15 V	> 1 MΩ	OL

CE on transient voltage and in-rush current - time domain

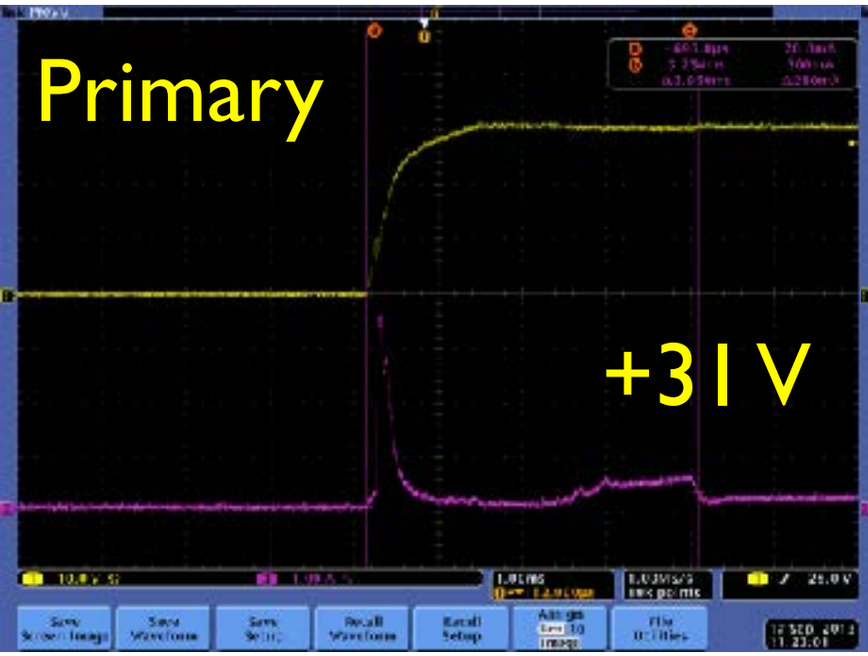

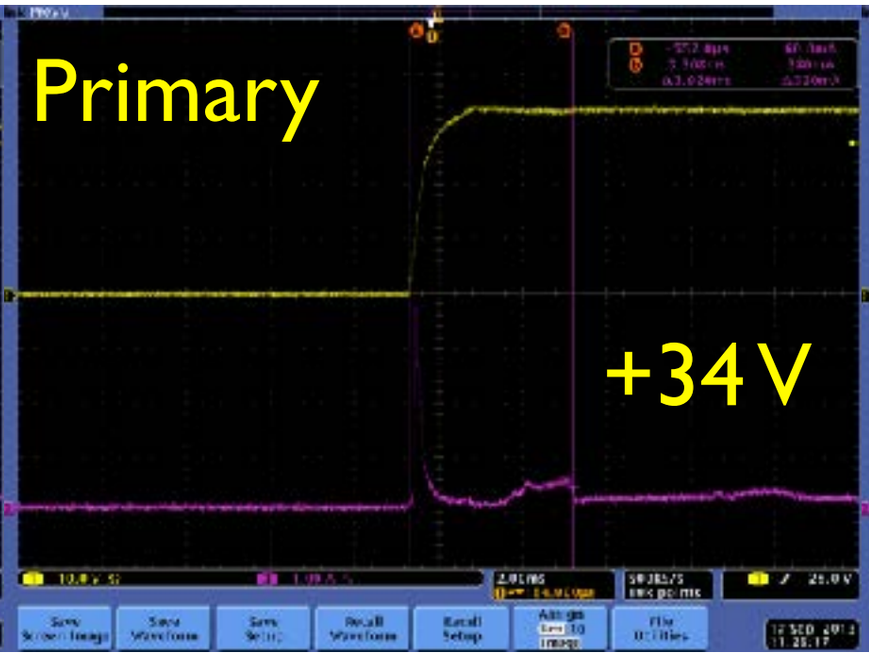

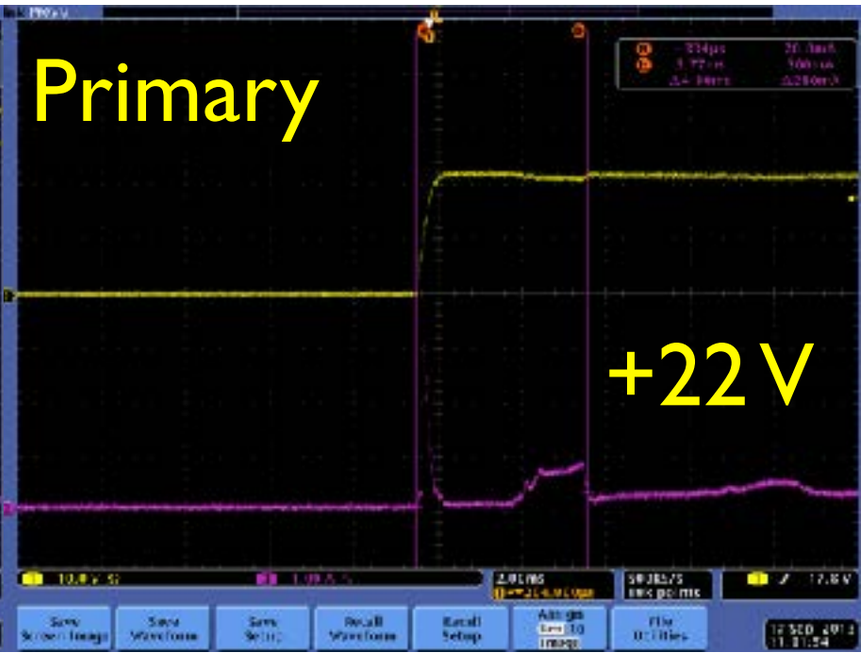

CE on primary power lines - frequency domain

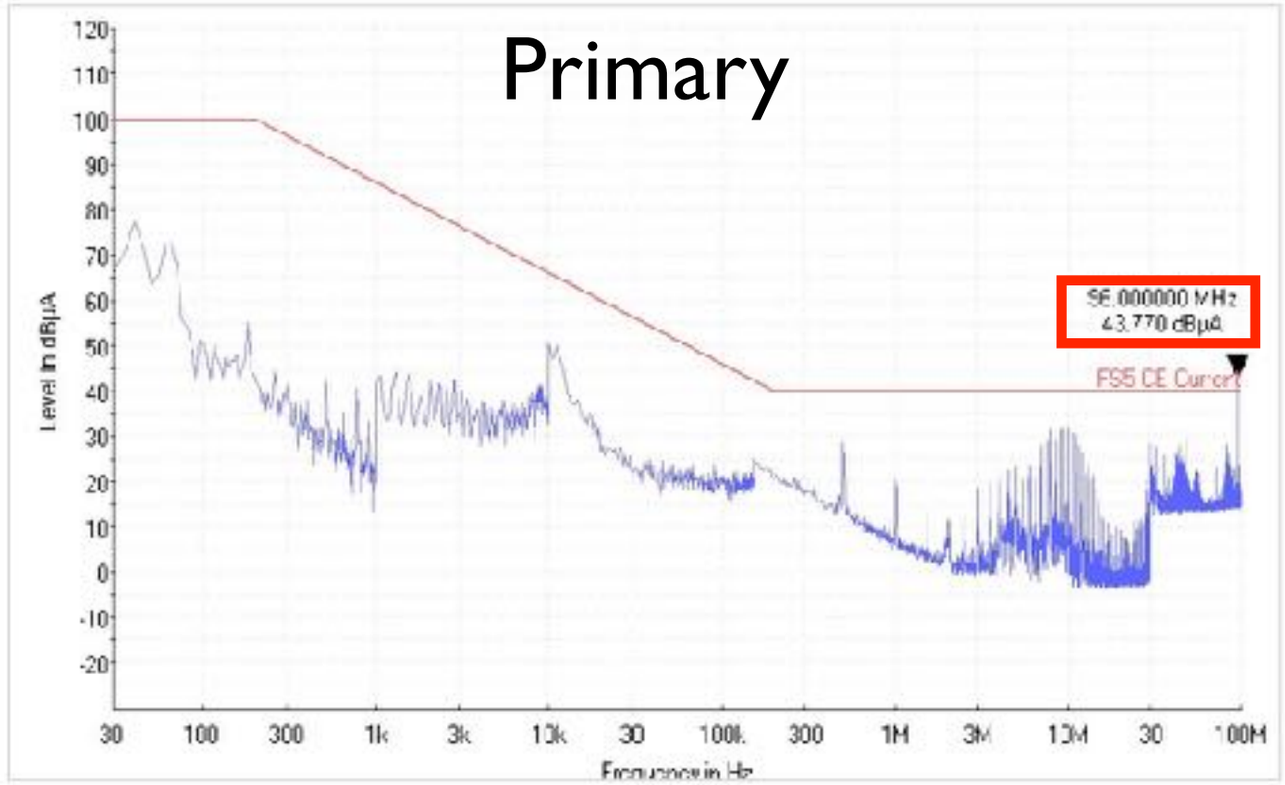

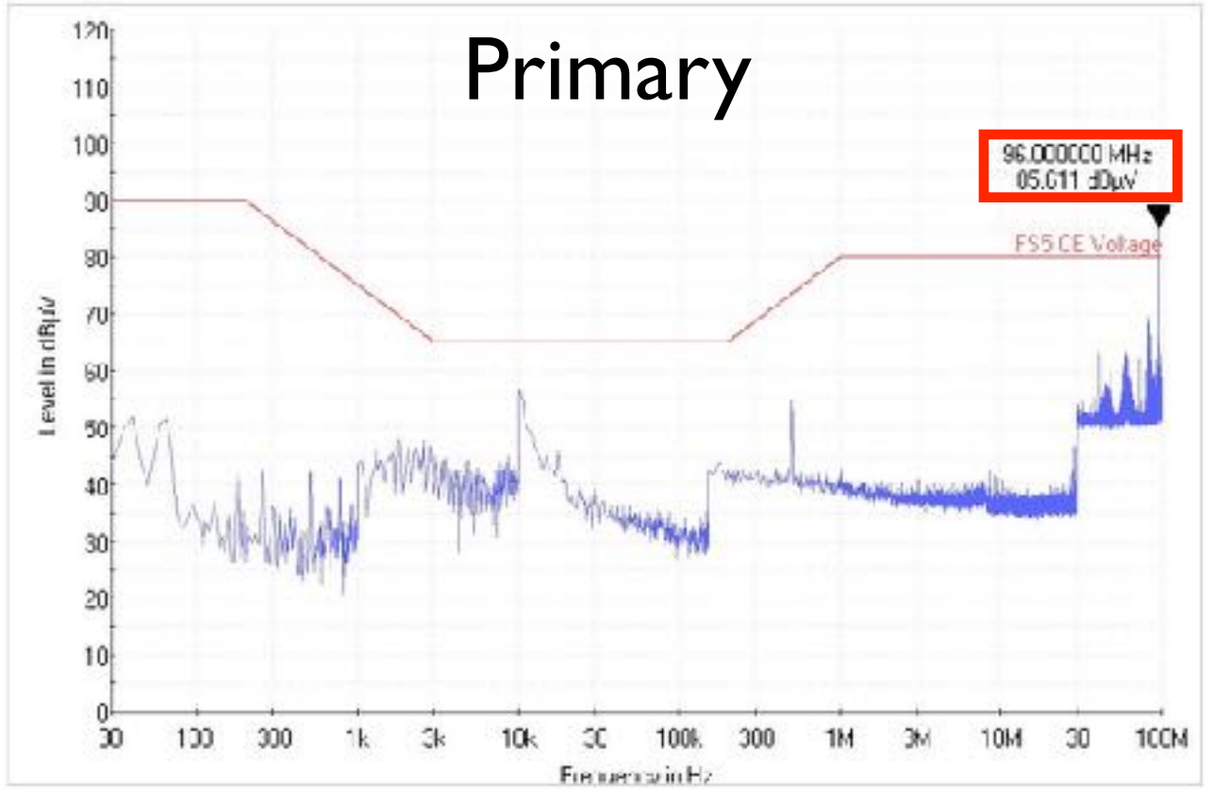

CE on signal lines - time domain

Primary

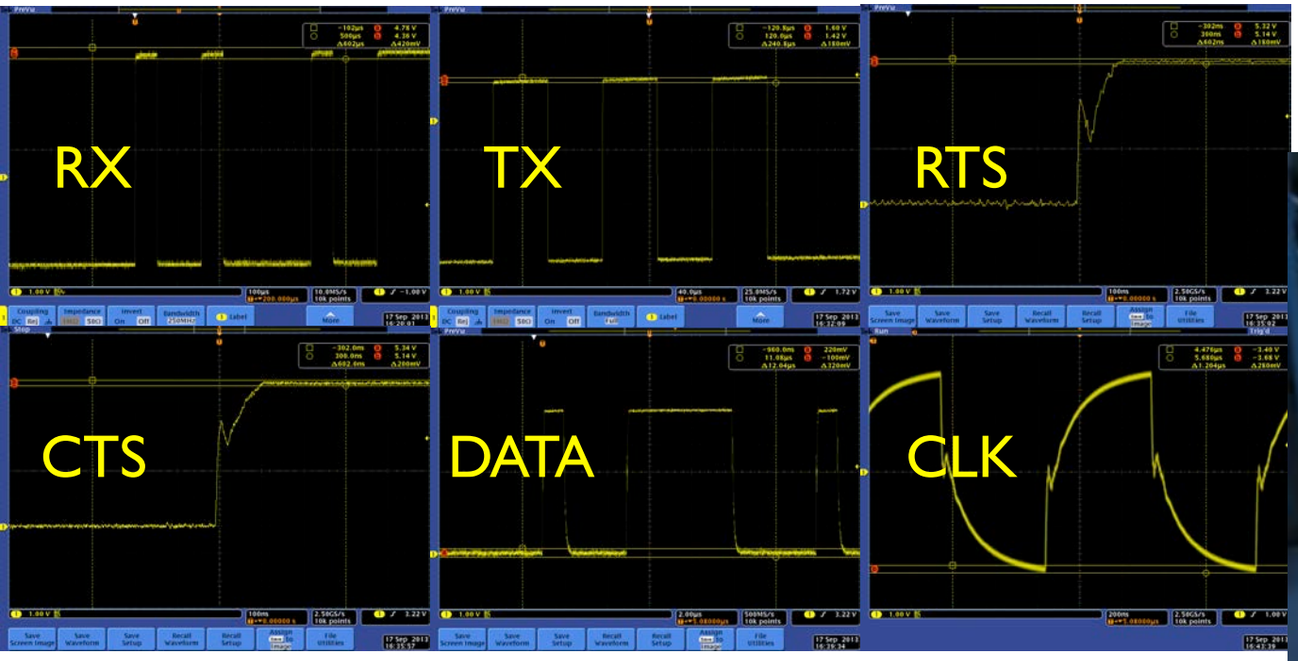

Redundant

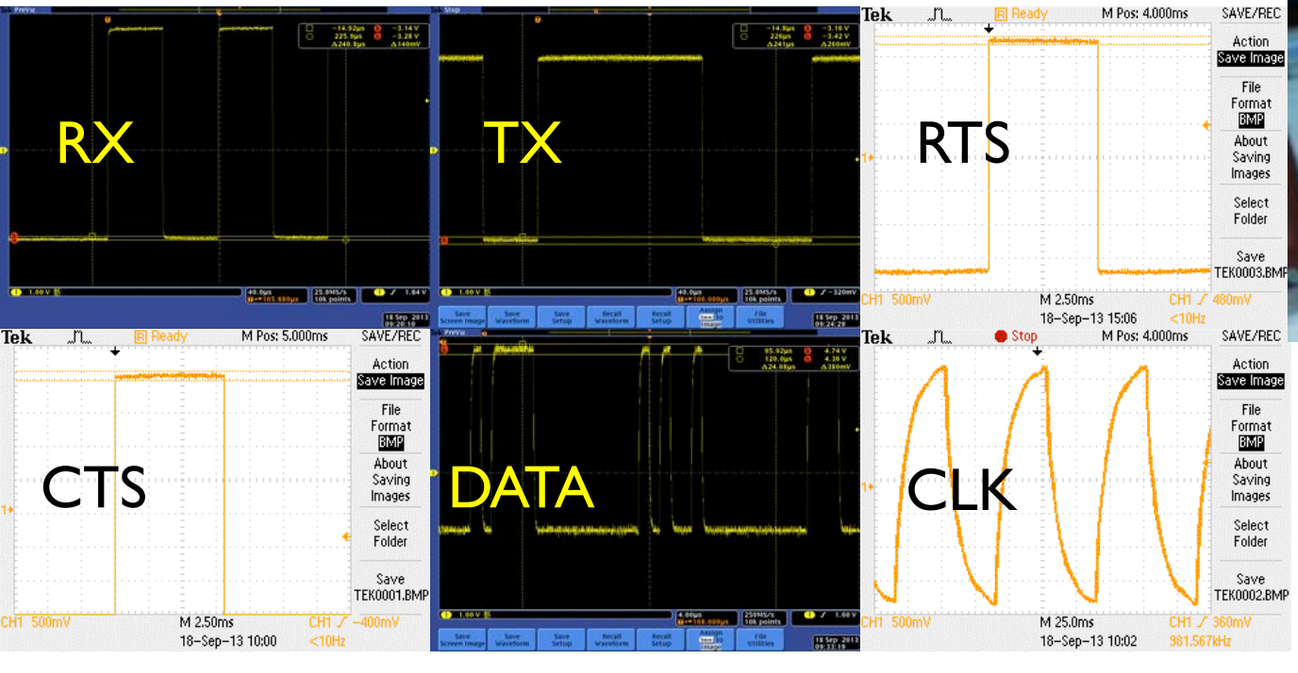

CS on primary power lines - sine wave and spike injection

Primary

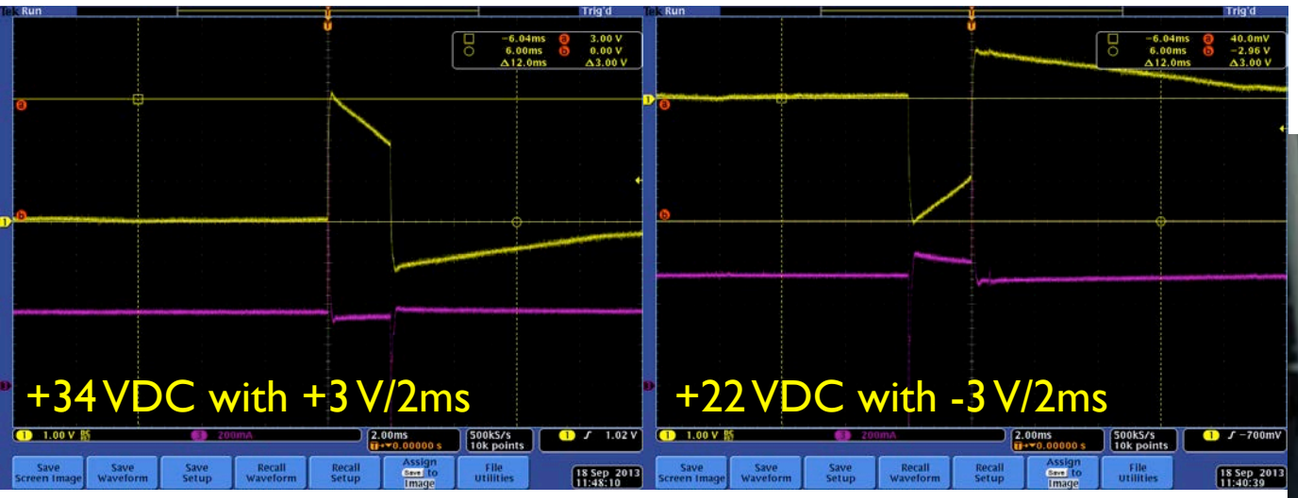

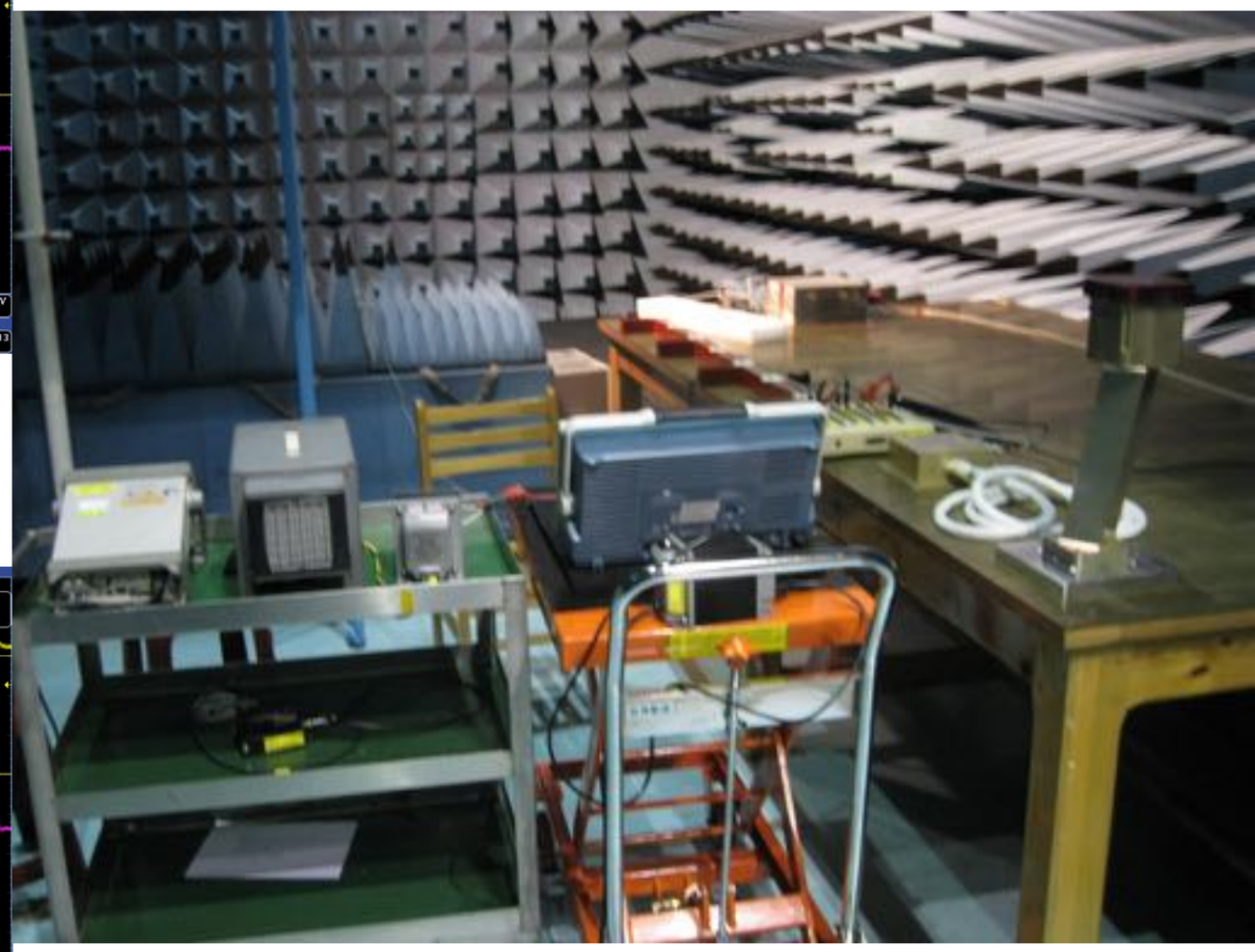

Redundant

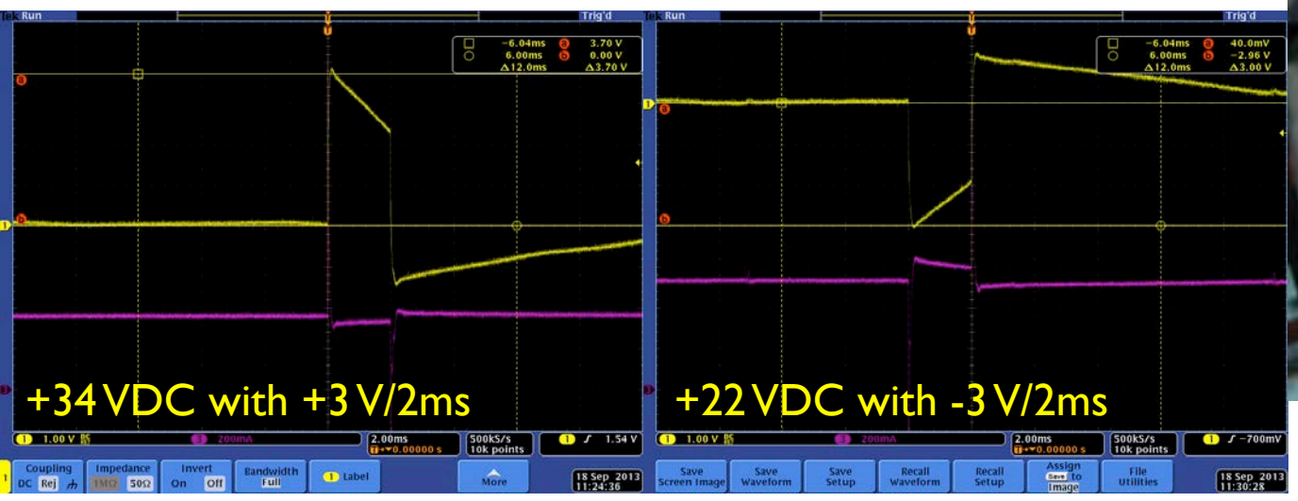

Spike injection

RE (14 KHz to 10 GHz)

Primary

H

14 KHz - 30 MHz

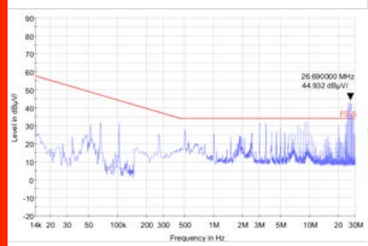

V

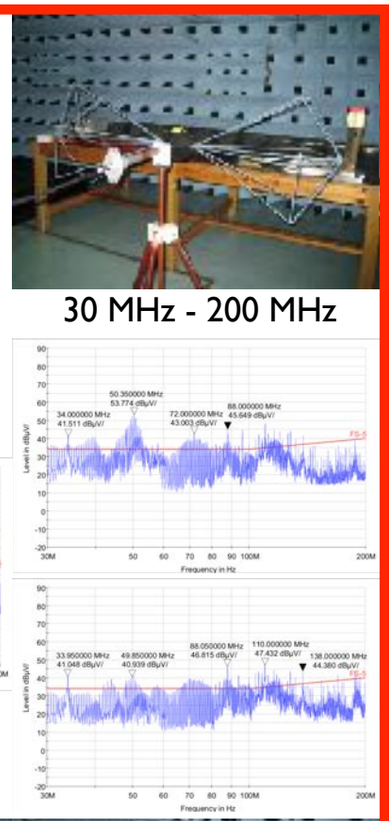

30 MHz - 200 MHz

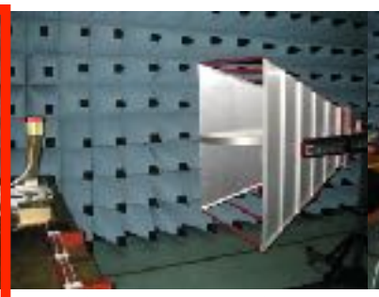

200 MHz - 1 GHz

1 GHz - 10 GHz

1,565 MHz - 1,585 MHz

2,039 MHz - 2,041 MHz

2,025 MHz - 2,110 MHz

30 MHz - 200 MHz

200 MHz - 1 GHz

1 GHz - 10 GHz

1,565 MHz - 1,585 MHz

2,039 MHz - 2,041 MHz

2,025 MHz - 2,110 MHz

Redundant

H

14 KHz - 30 MHz

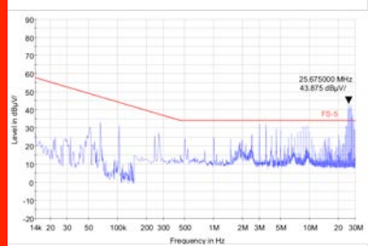

V

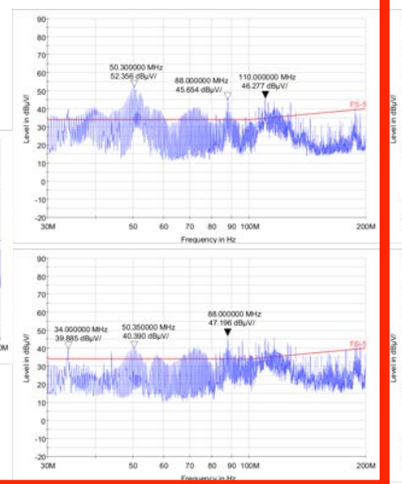

With or without cover on sensor

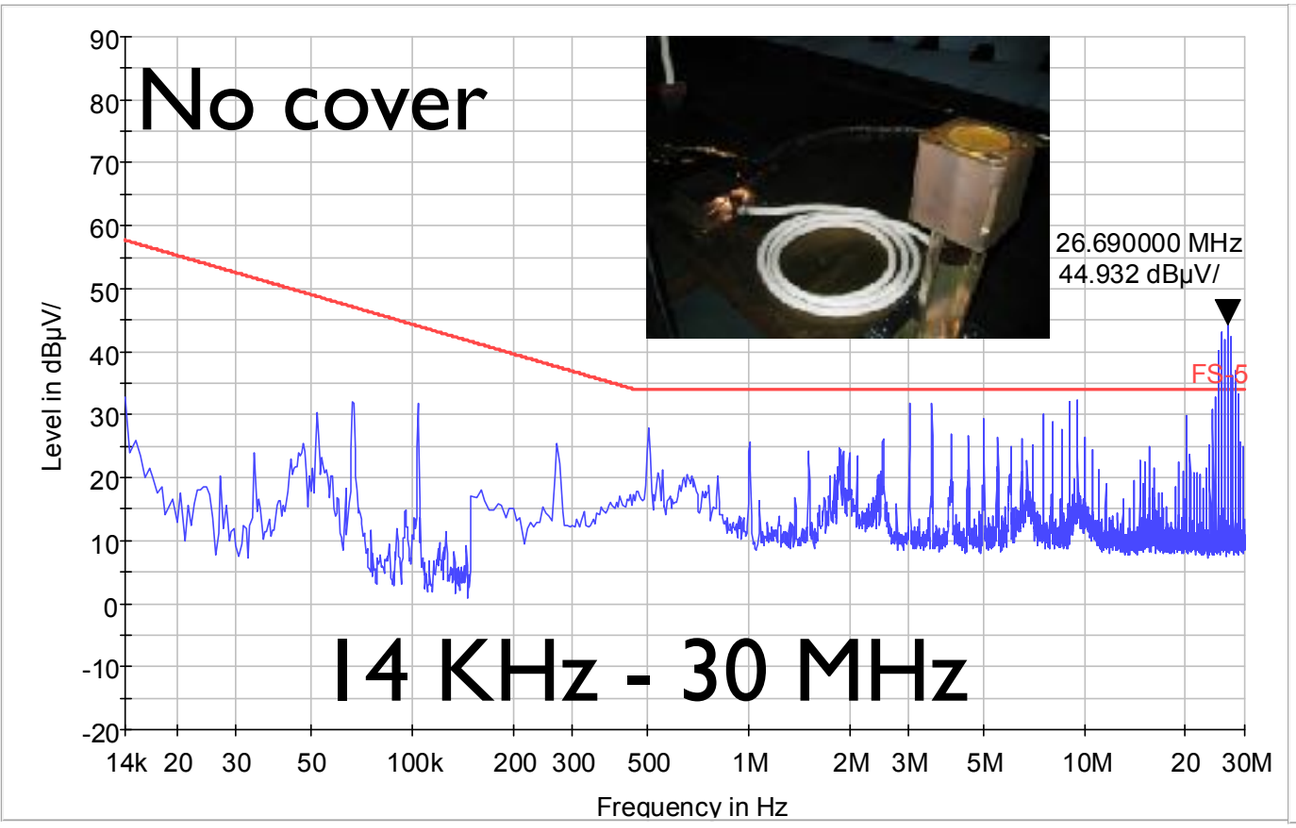

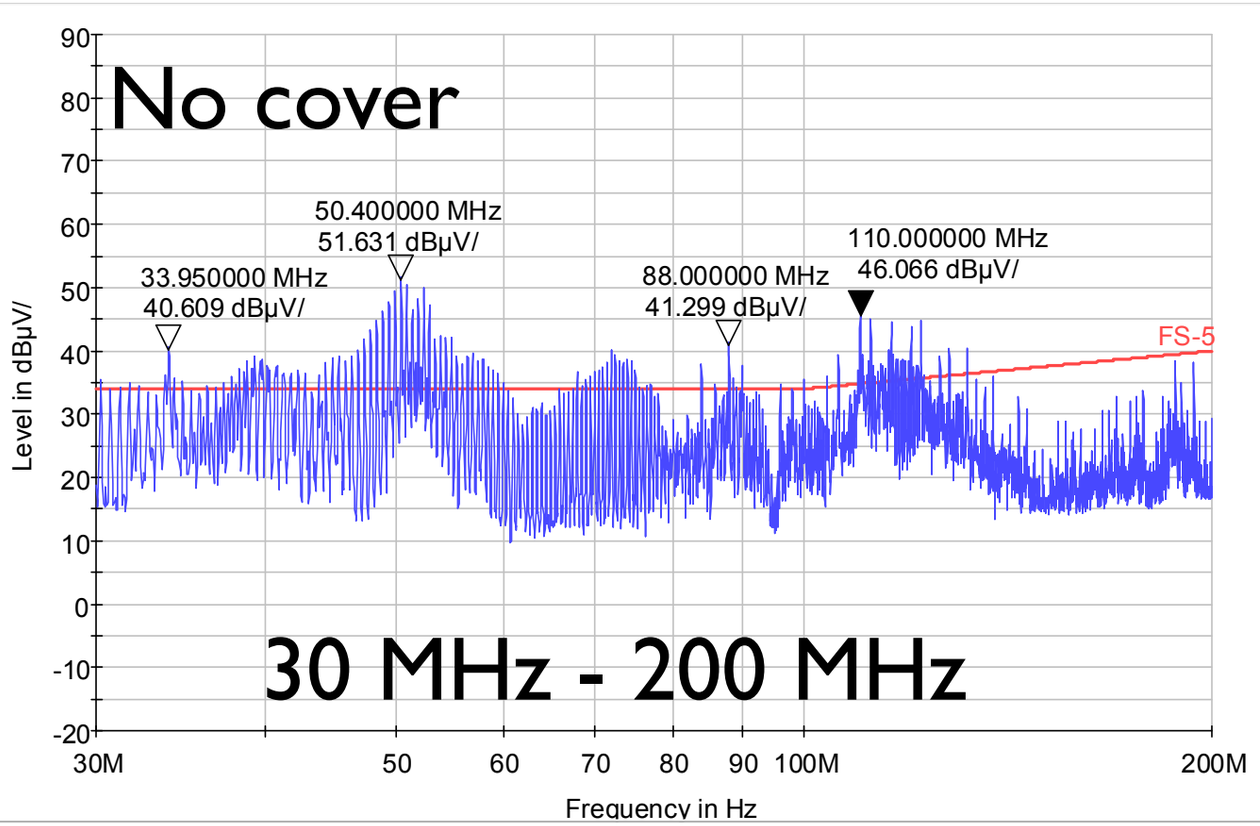

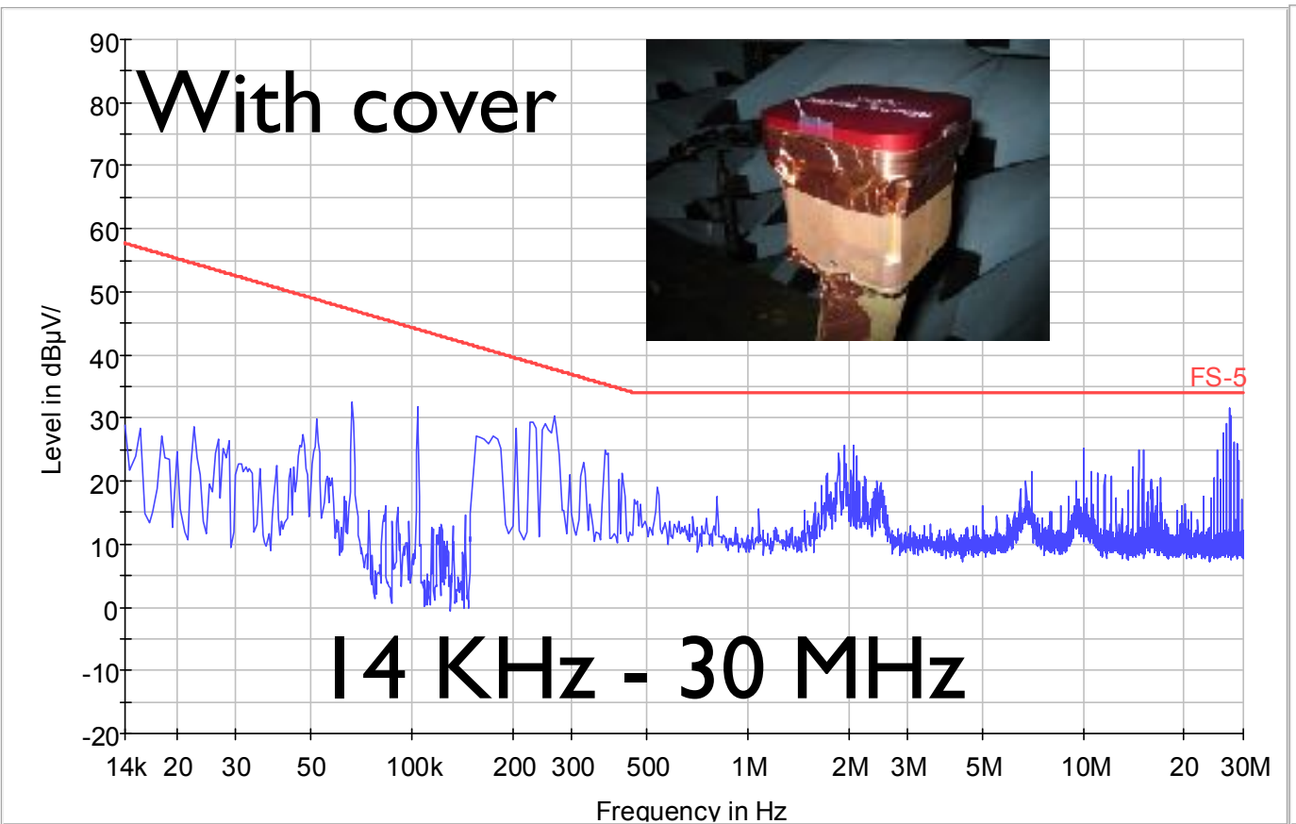

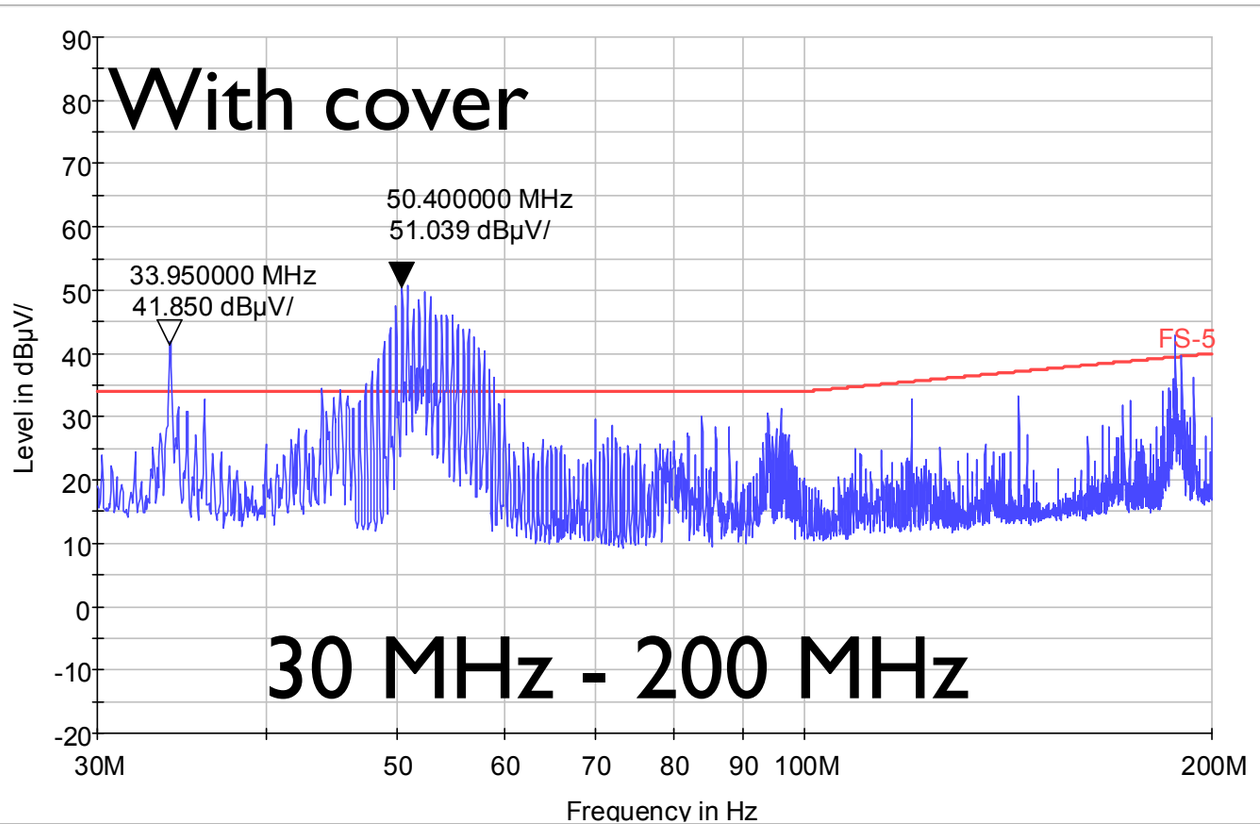

RS (200 MHz to 10 GHz)

200 MHz - 1 GHz

1 GHz - 2 GHz

2 GHz - 10 GHz

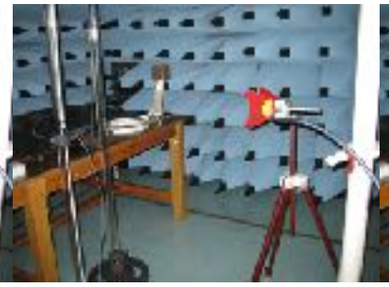

2,214 MHz - 2,216 MHz

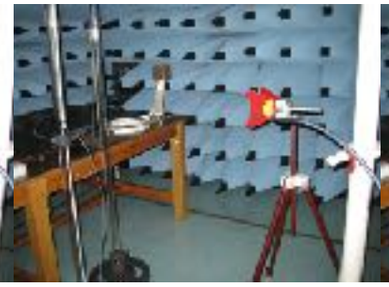

8.0 GHz - 8.4 GHz

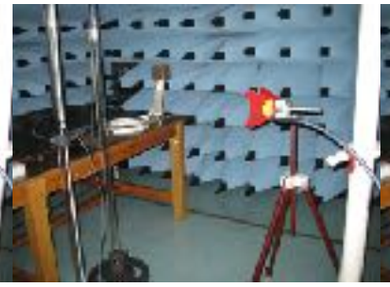

2,200 MHz - 2,300 MHz

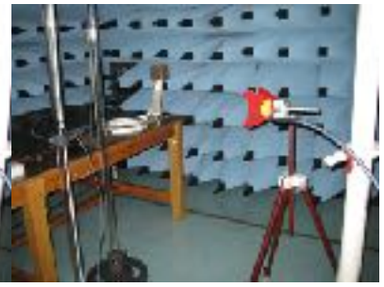

5,400 MHz - 5,900 MHz

H

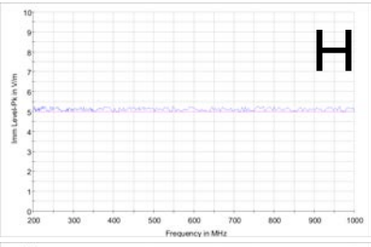

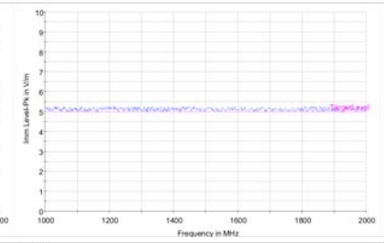

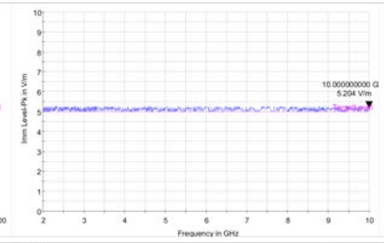

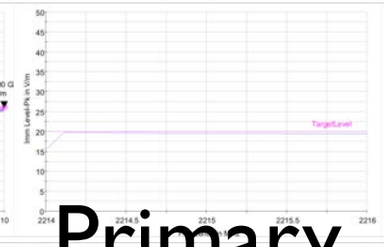

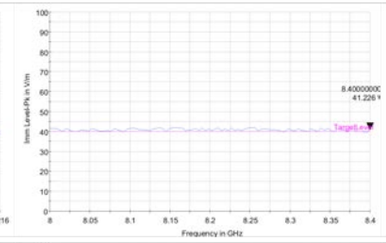

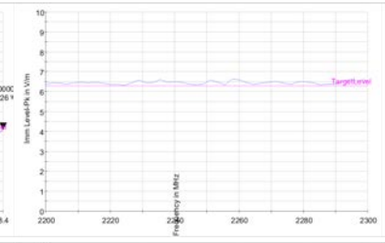

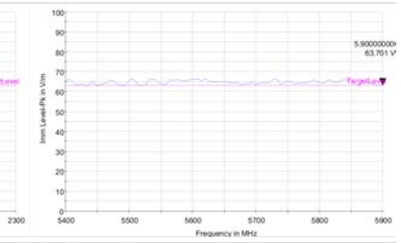

V

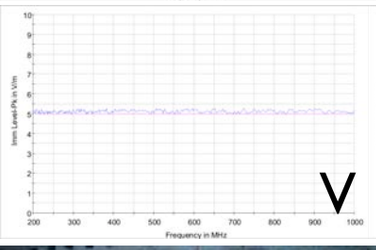

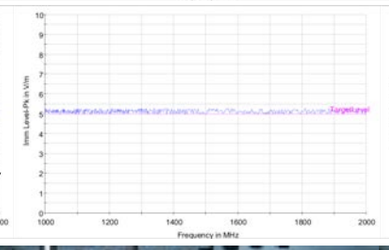

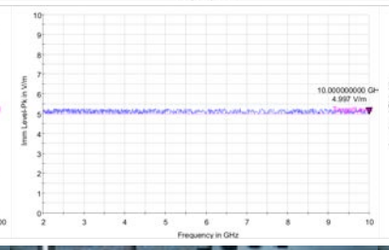

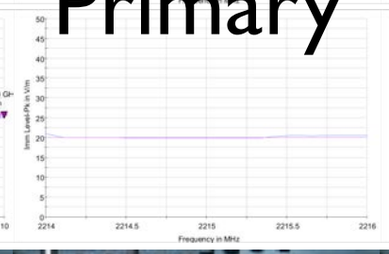

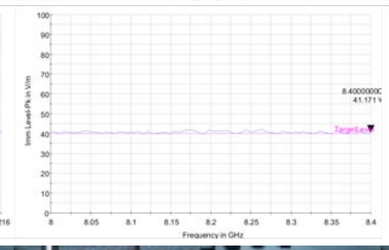

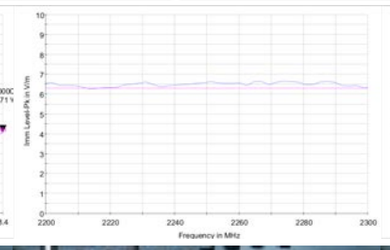

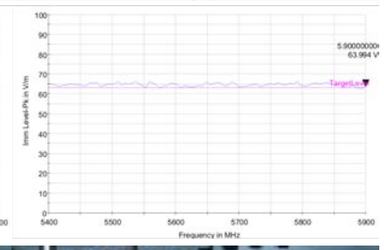

Primary

200 MHz - 1 GHz

1 GHz - 2 GHz

2 GHz - 10 GHz

2,214 MHz - 2,216 MHz

8.0 GHz - 8.4 GHz

2,200 MHz - 2,300 MHz

5,400 MHz - 5,900 MHz

H

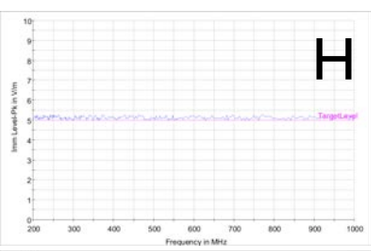

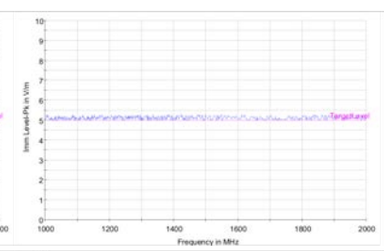

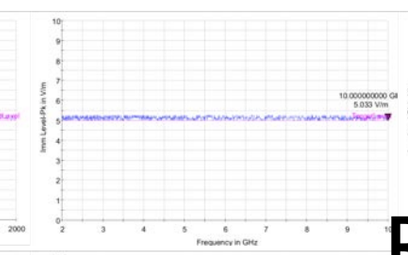

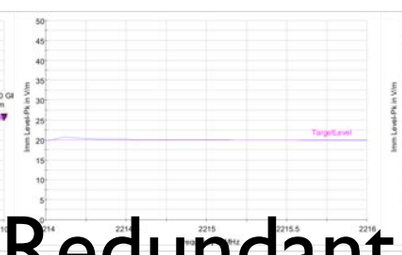

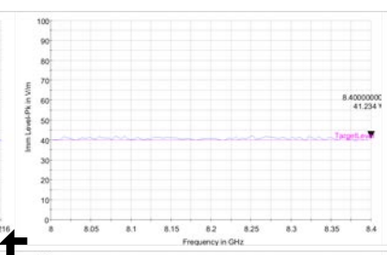

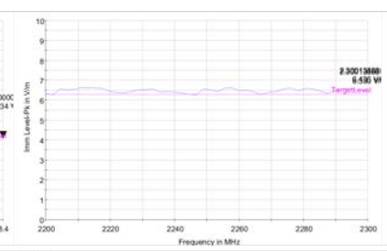

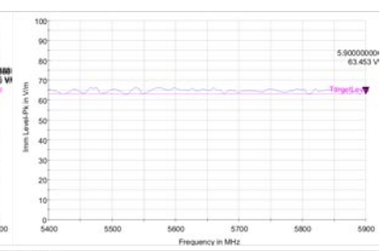

Redundant

V

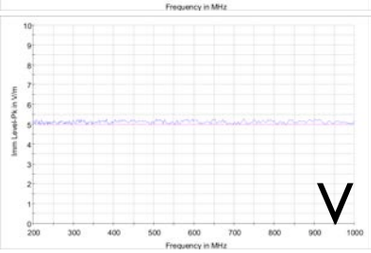

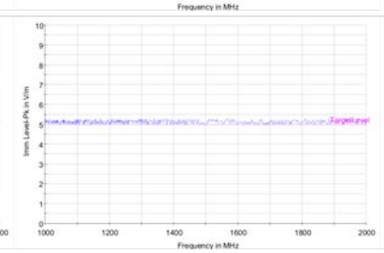

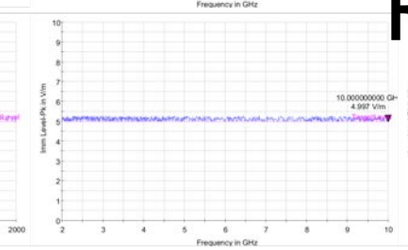

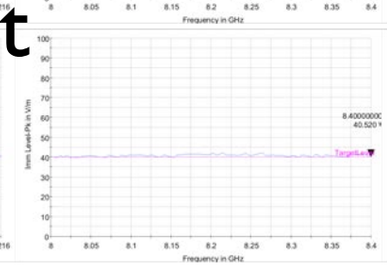

Burn-in test

	Sensor	Primary controller	Redundant controller
Fabrication and programming	40 hours	120 hours	40 hours
Functional tests	11 hours	6 hours	4 hours
Environmental tests	60 hours	26 hours	22 hours
Burn-in test	**200 hours**	**149 hours**	**51 hours**
Summation	**311 (≥ 300) hours**	**301 (≥ 300) hours**	**117 (≥ 100) hours**

SR-IX flight test

- Space Plasma Sensor Package (**SPSP**)
  - Plasma Impedance Analyzer (**PIA**)
  - Plasma sensors (**PS**)
    - Retarding Potential Analyzer (**RPA**) from **AIP**
    - Ion Drift Meter (**IDM**) from **AIP**
    - Planar Langmuir Probe (**PLP**)

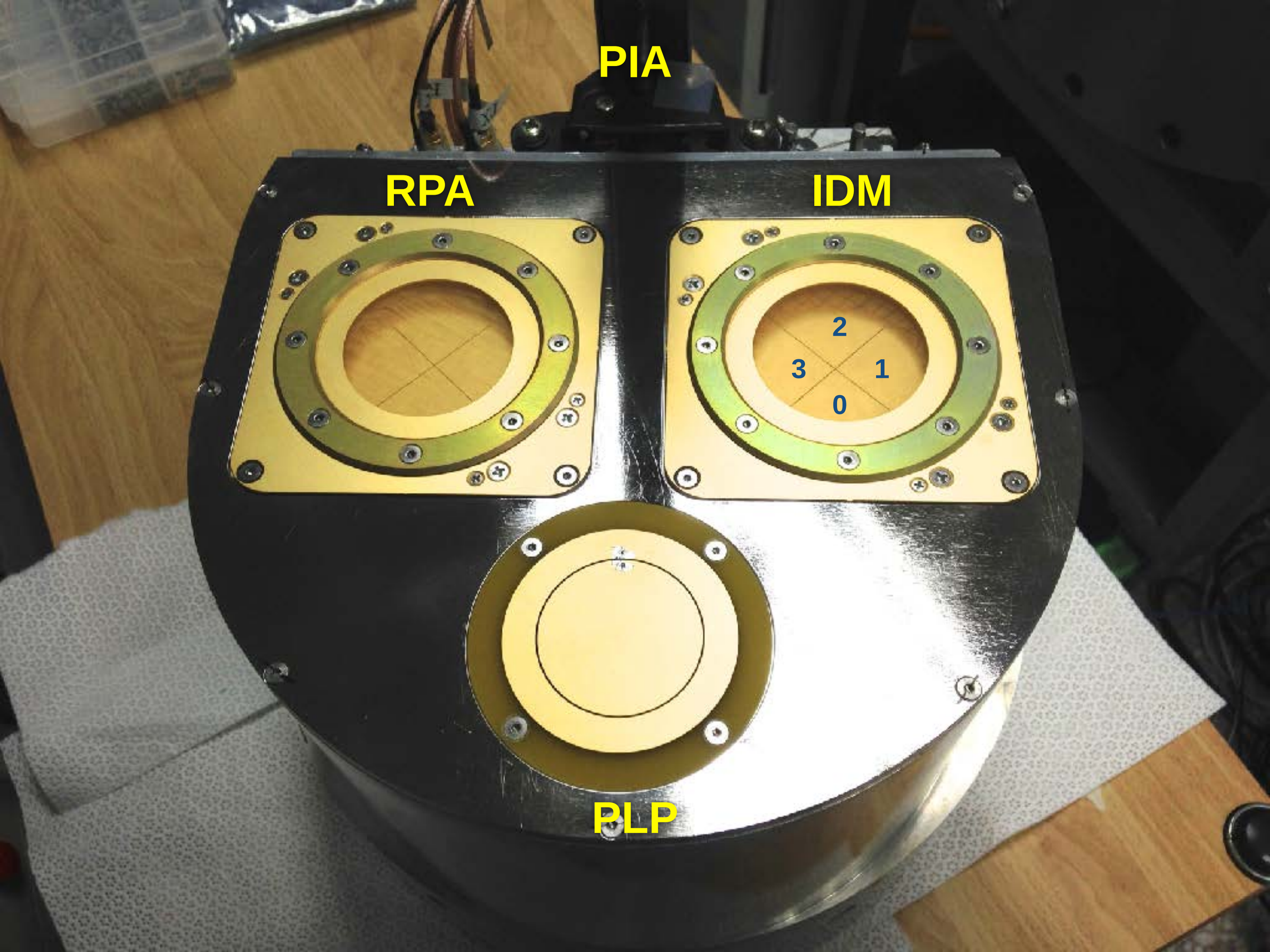
PIA
RPA
IDM
2
3
1
0
PLP

Plasma injection test in lab

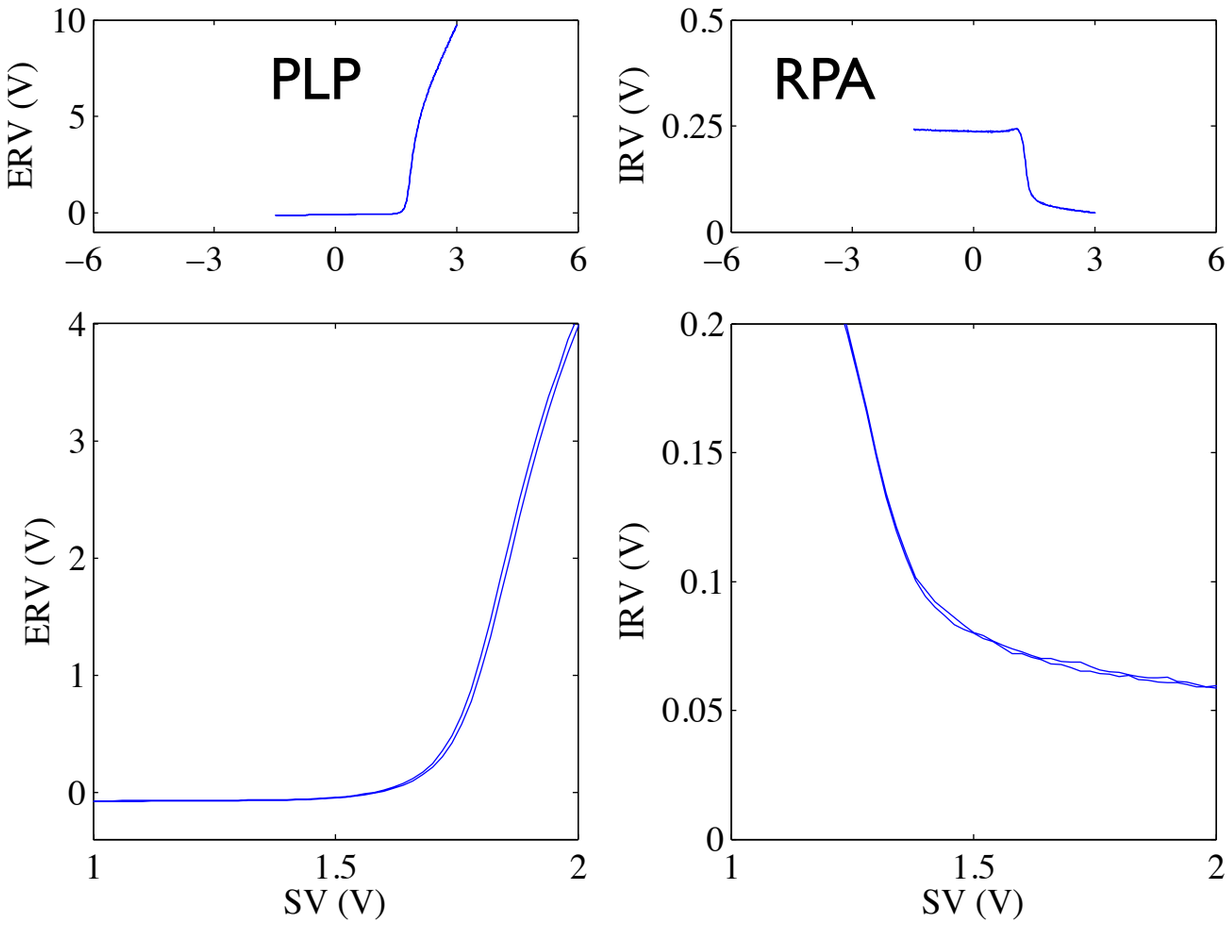

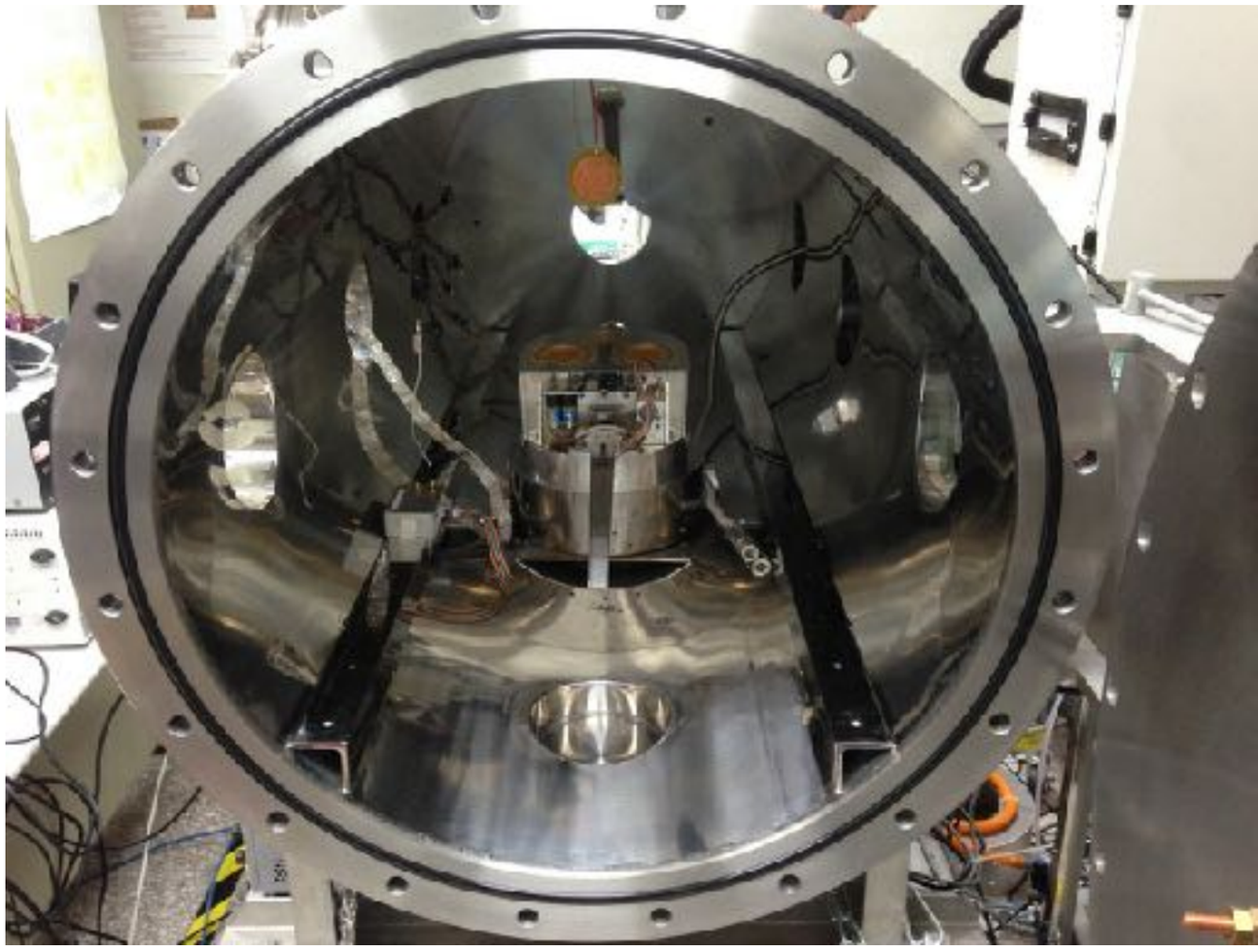

Space Plasma Simulation Chamber

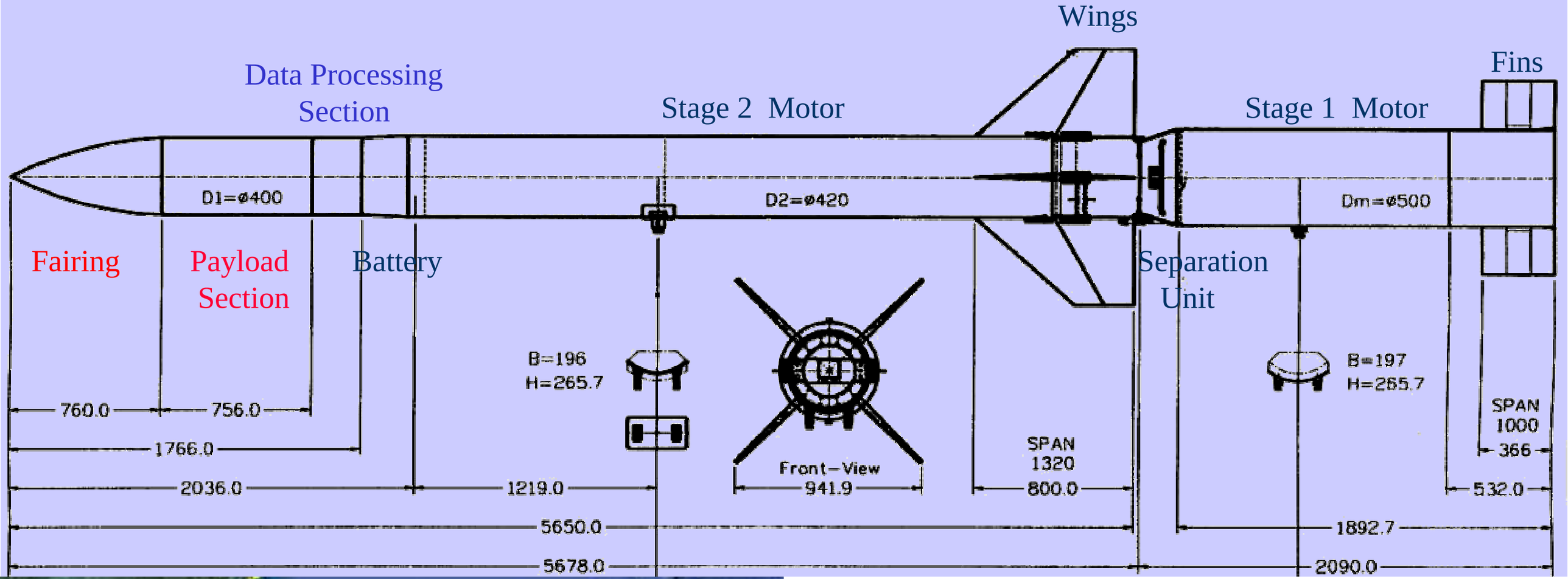
Wings
Data Processing Section
Stage 2 Motor
Stage 1 Motor
Fins
D1=ø400
D2=ø420
Dm=ø500
Fairing
Payload Section
Battery
Separation Unit
B=196
H=265.7
B=197
H=265.7
Front-View
760.0
756.0
1766.0
2036.0
1219.0
941.9
SPAN 1320
800.0
SPAN 1000
366
532.0
5650.0
1892.7
5678.0
2090.0


Taipei
Miyako-jima
Ishigaki-shima
Taiwan
Green island
Launch site
Orchid island

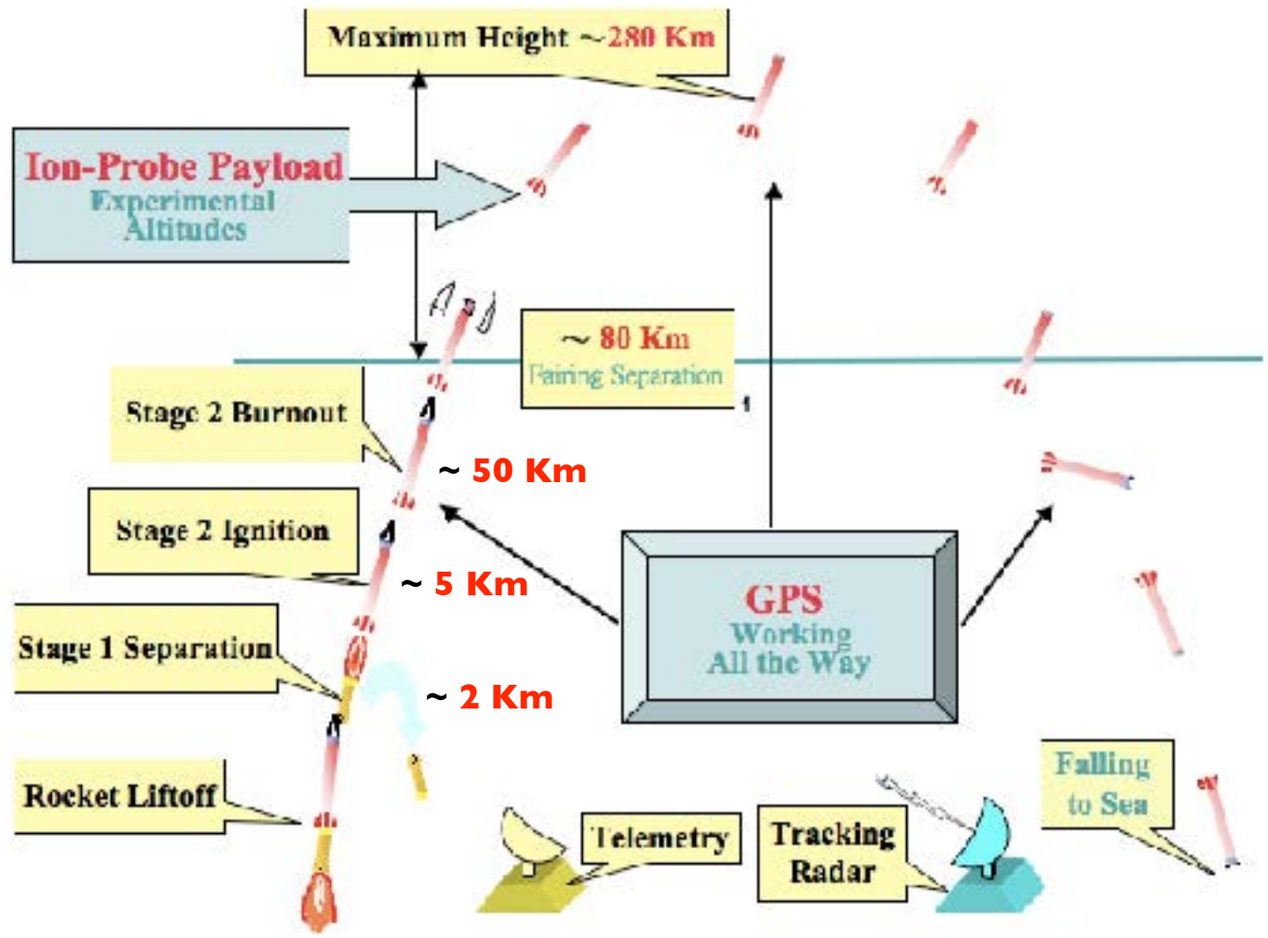
Maximum Height ~280 Km
Ion-Probe Payload
Experimental Altitudes
~ 80 Km
Fairing Separation
Stage 2 Burnout
~ 50 Km
Stage 2 Ignition
~ 5 Km
GPS
Working All the Way
Stage 1 Separation
~ 2 Km
Rocket Liftoff
Telemetry
Tracking Radar
Falling to Sea

Jioupeng radar array

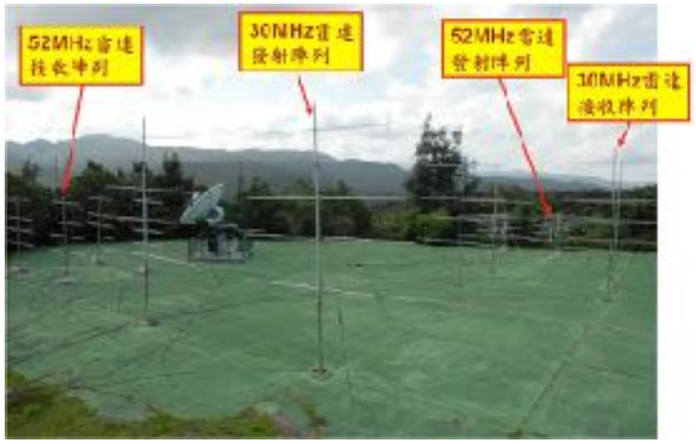

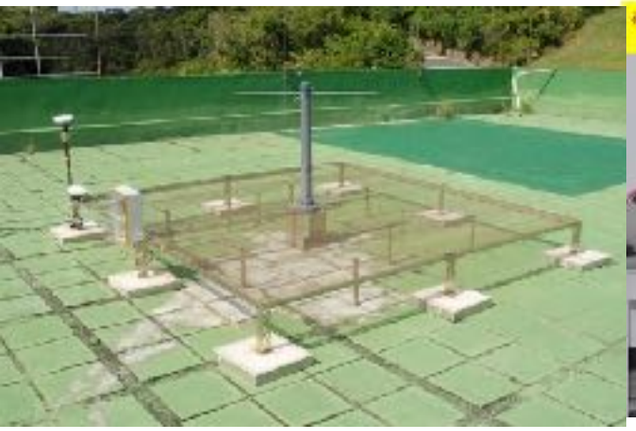

Jioupeng 30 MHz radar

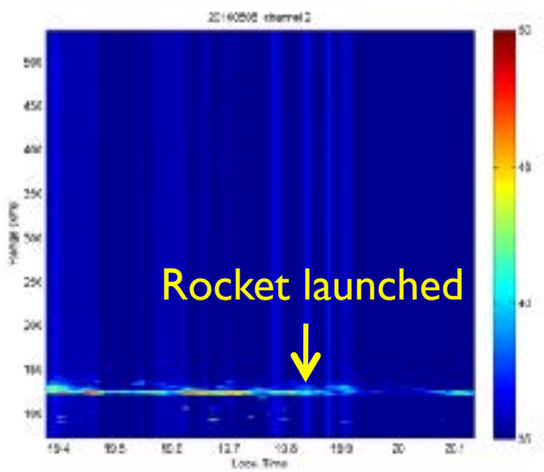

Jioupeng 52 MHz radar

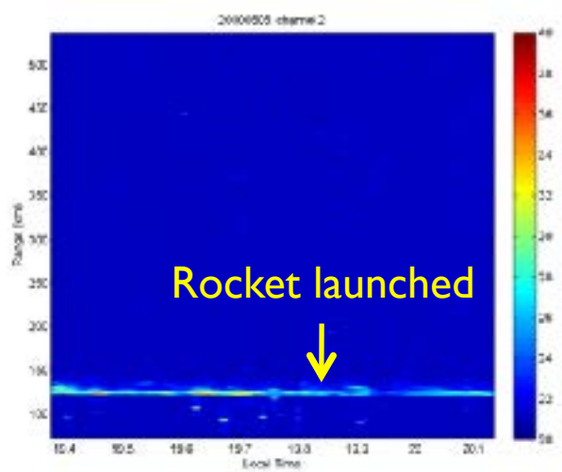

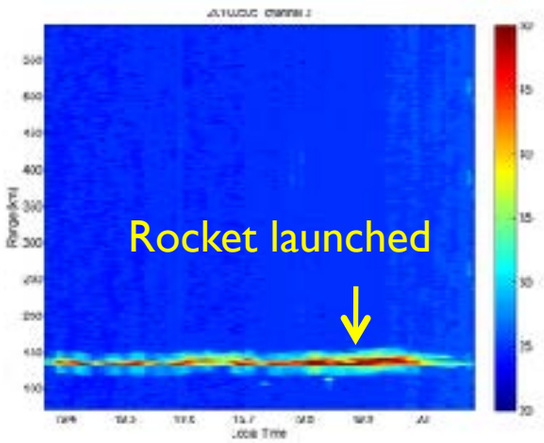

NCU
52 MHz radar

NCU radar array

NCC Ionosonde

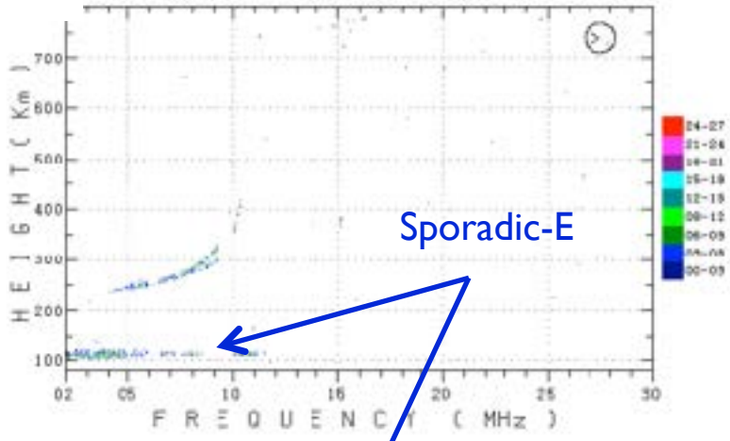

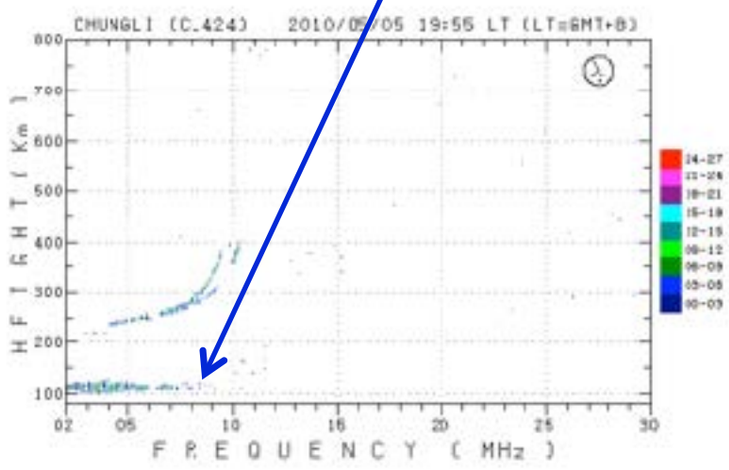

SR-IX flight test (3/26/2014)

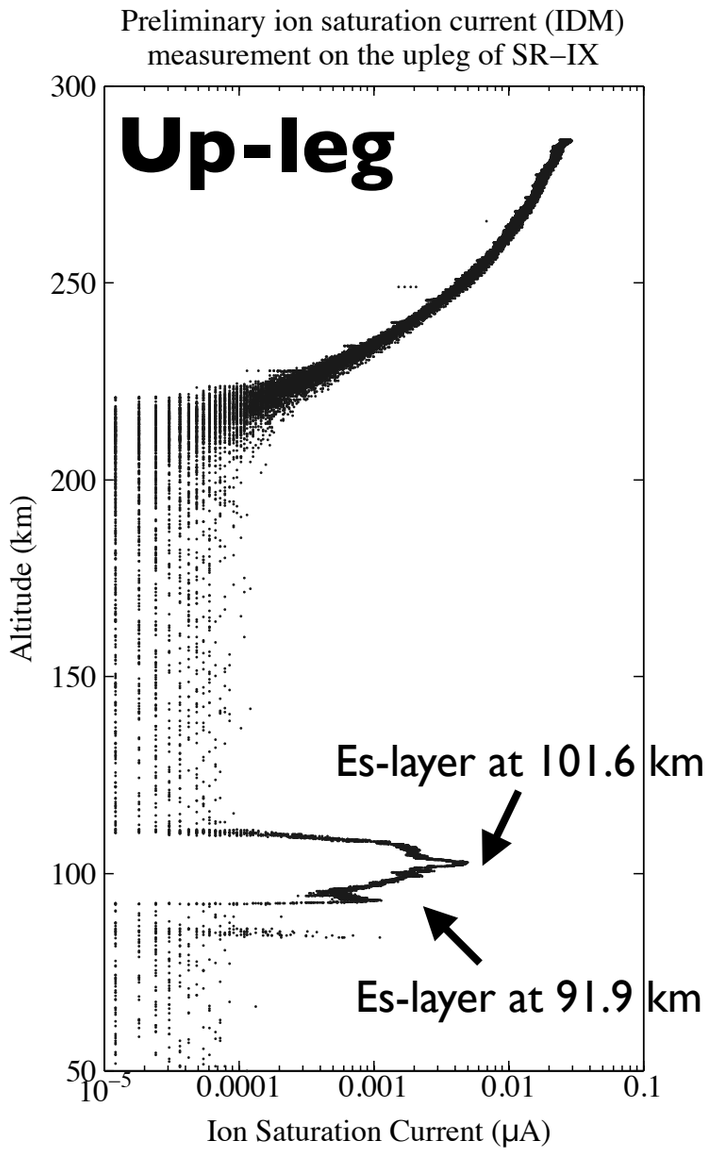

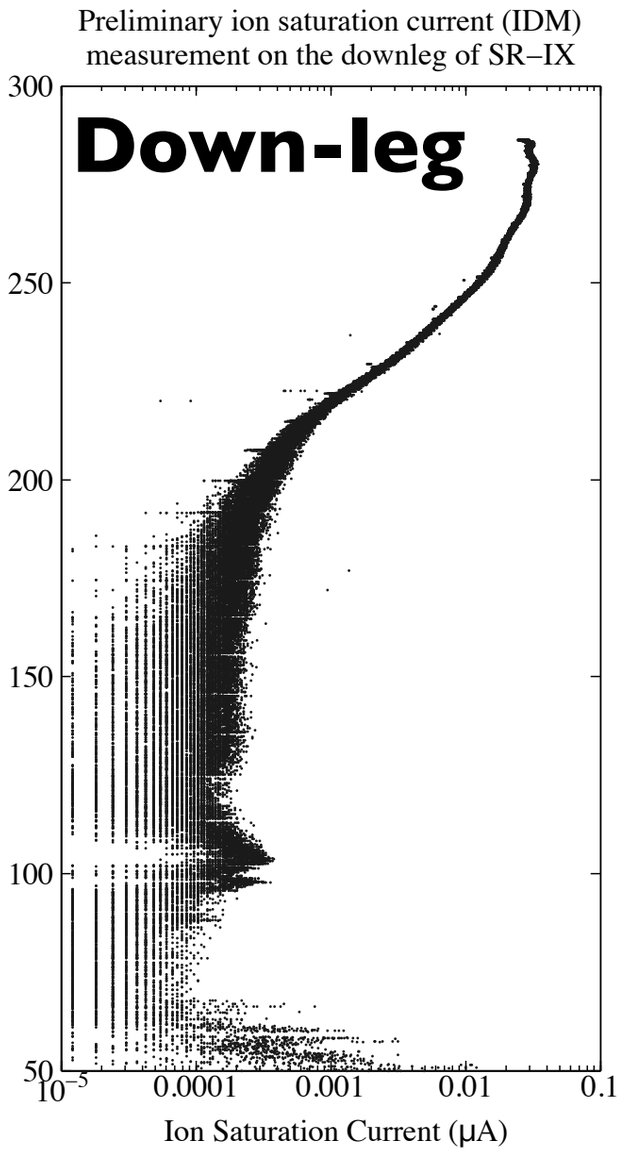

IDM readings at E region

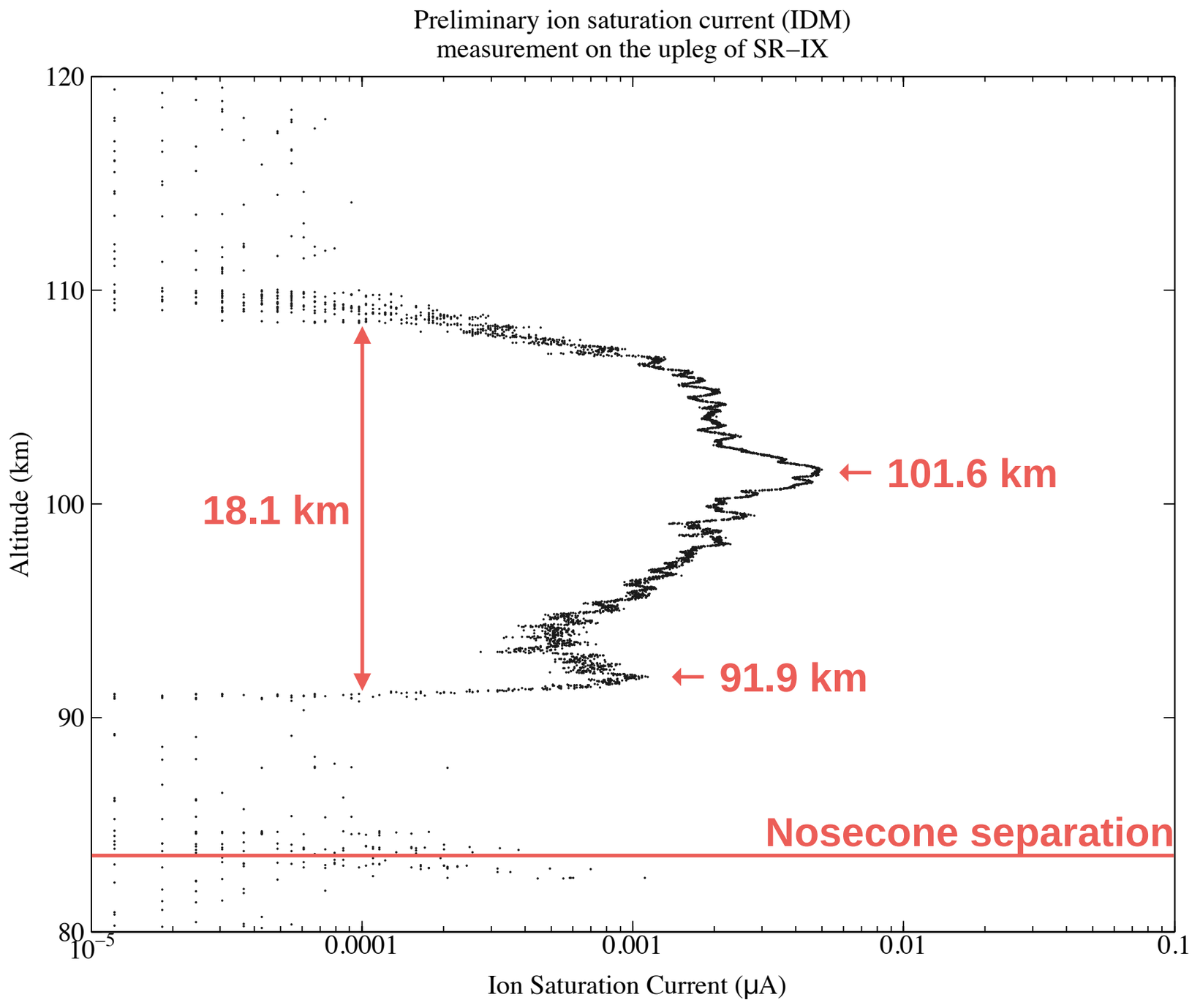

Angles of arrival of ions

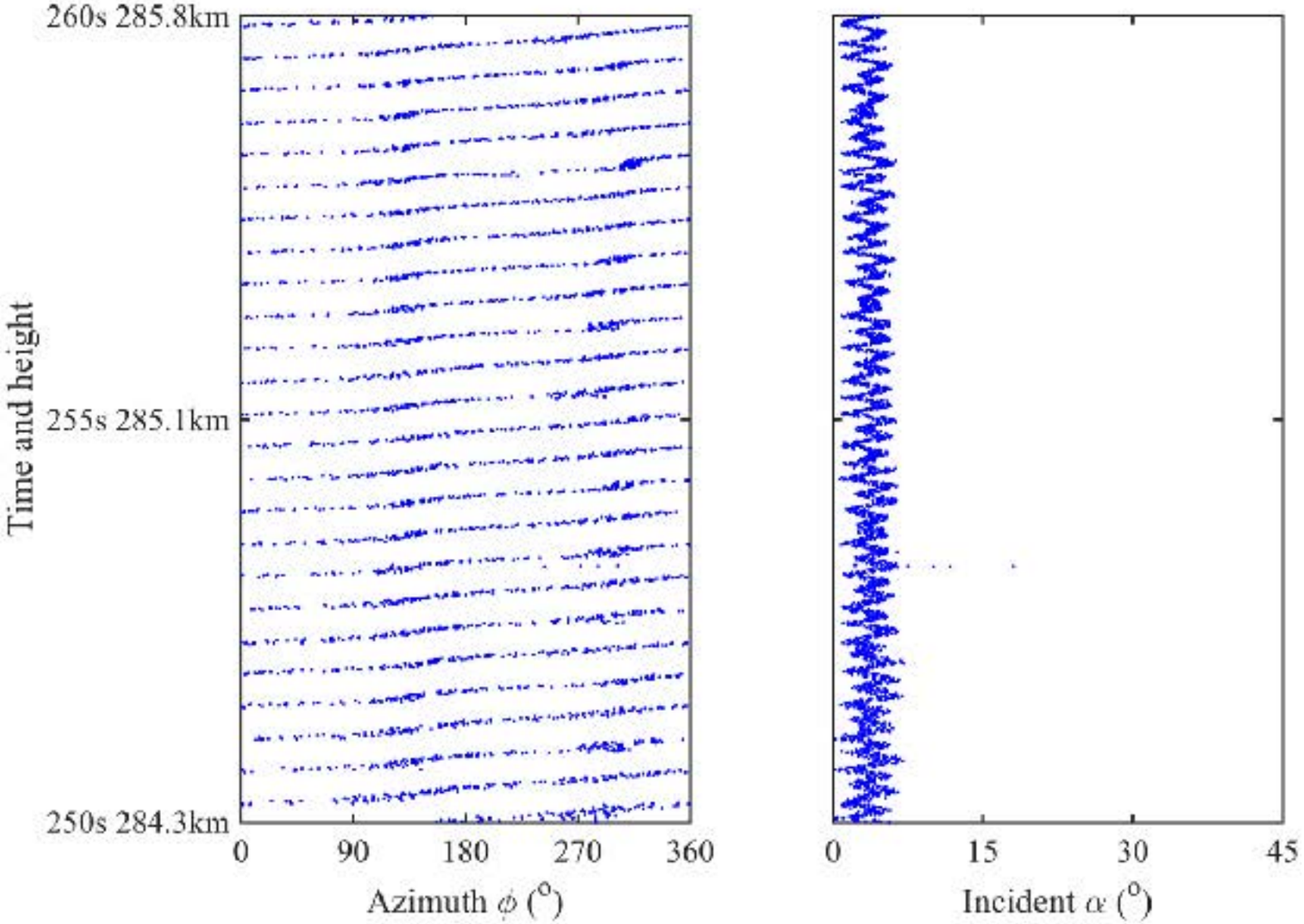

Only significant angles of arrival of ions are available ~ 280 km altitude.

RPA readings, 1,600 S/s

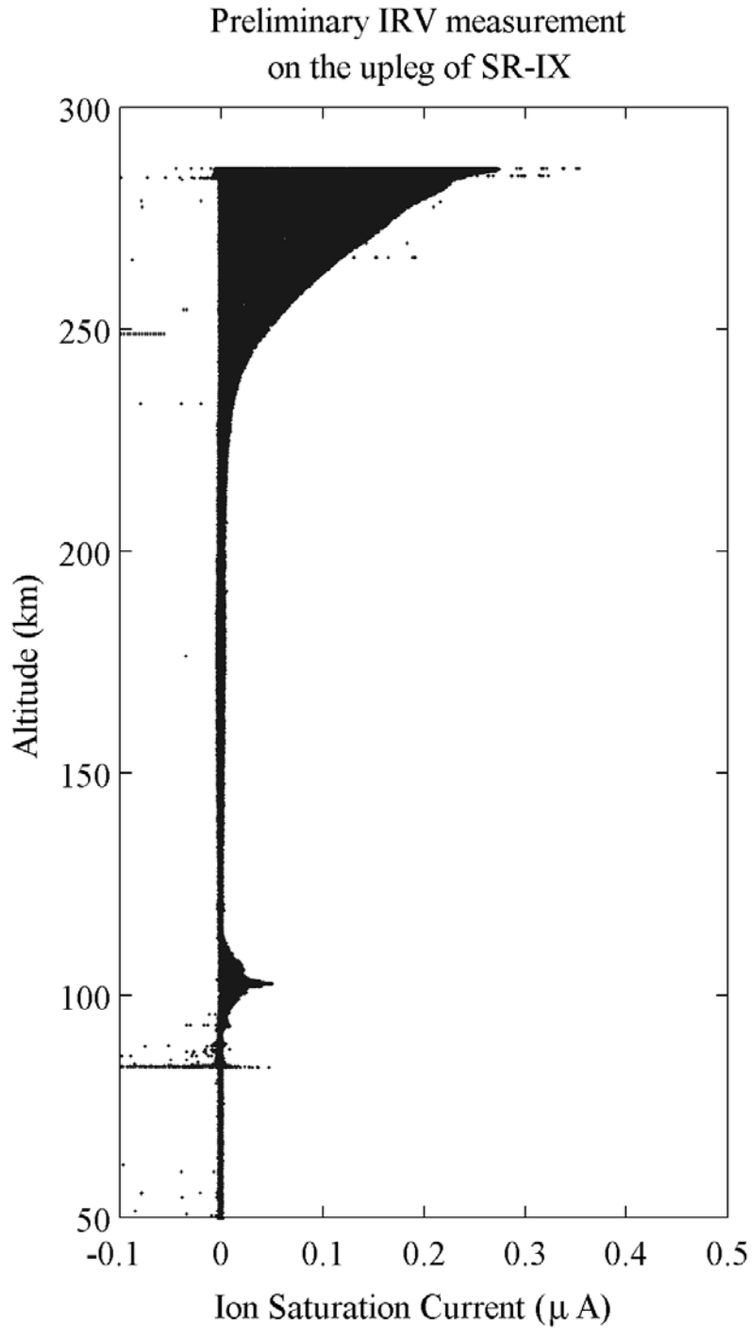

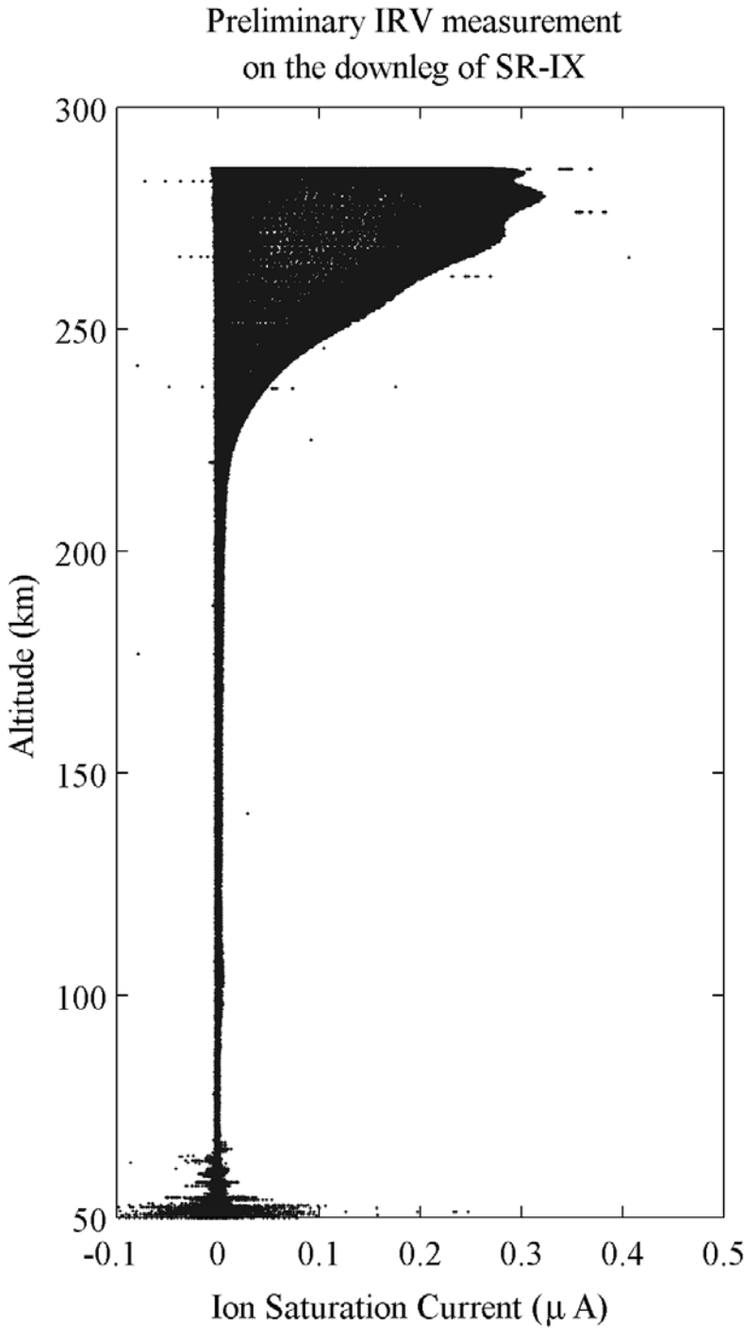

RPA readings at E region

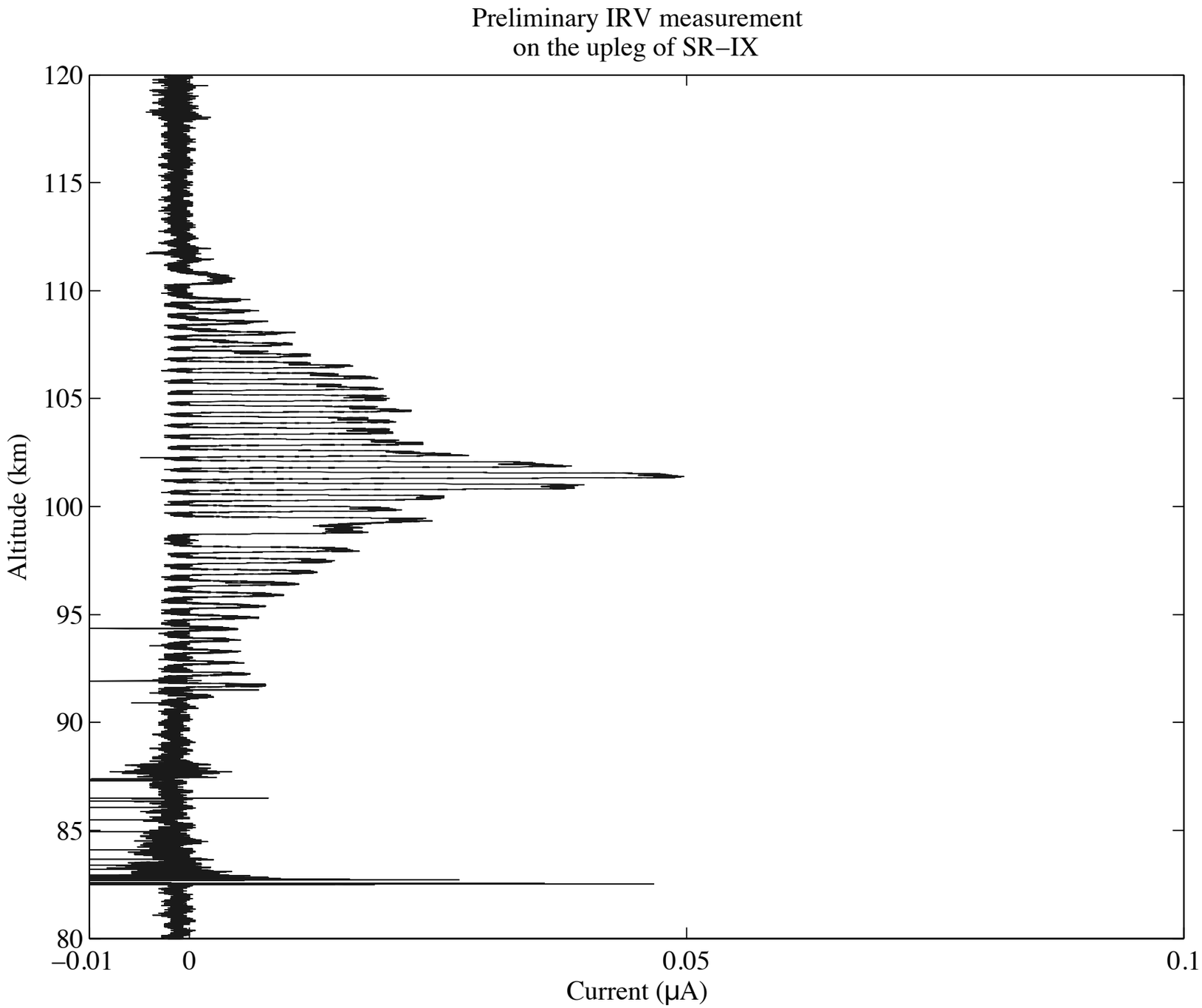

PLP readings, 1,600 S/s

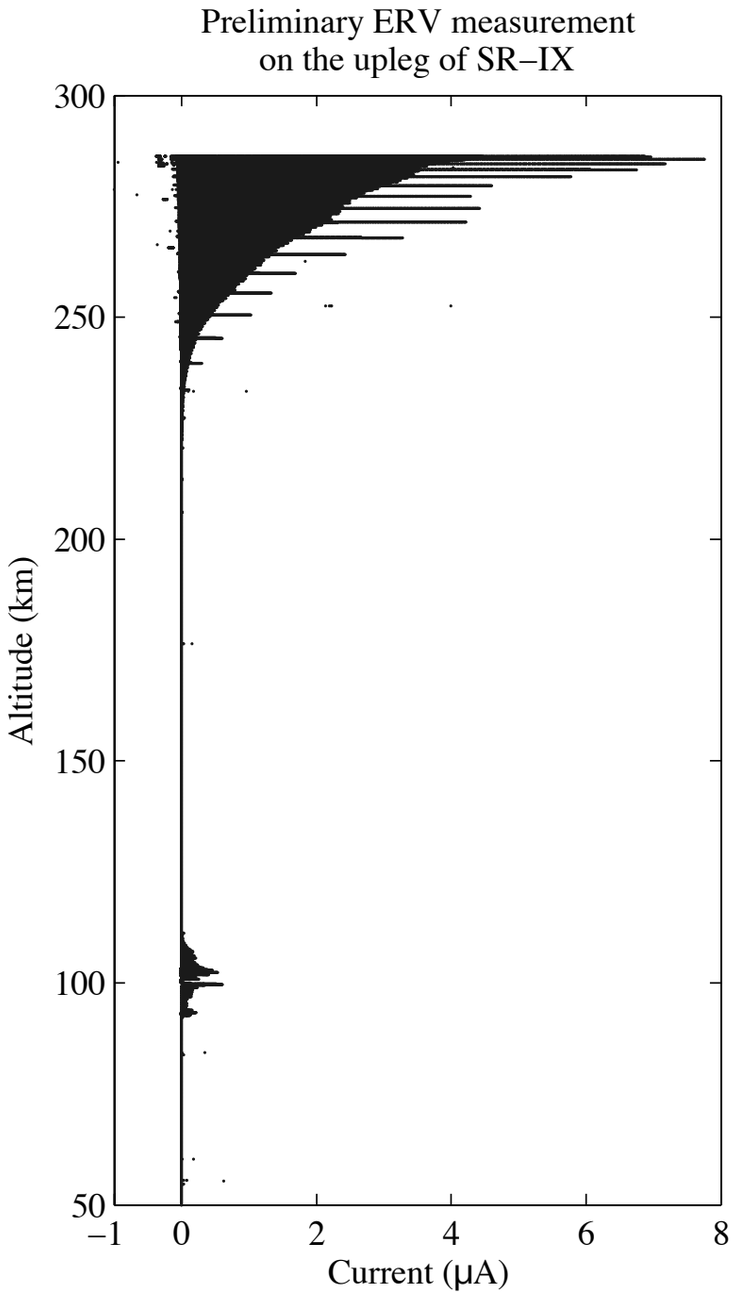

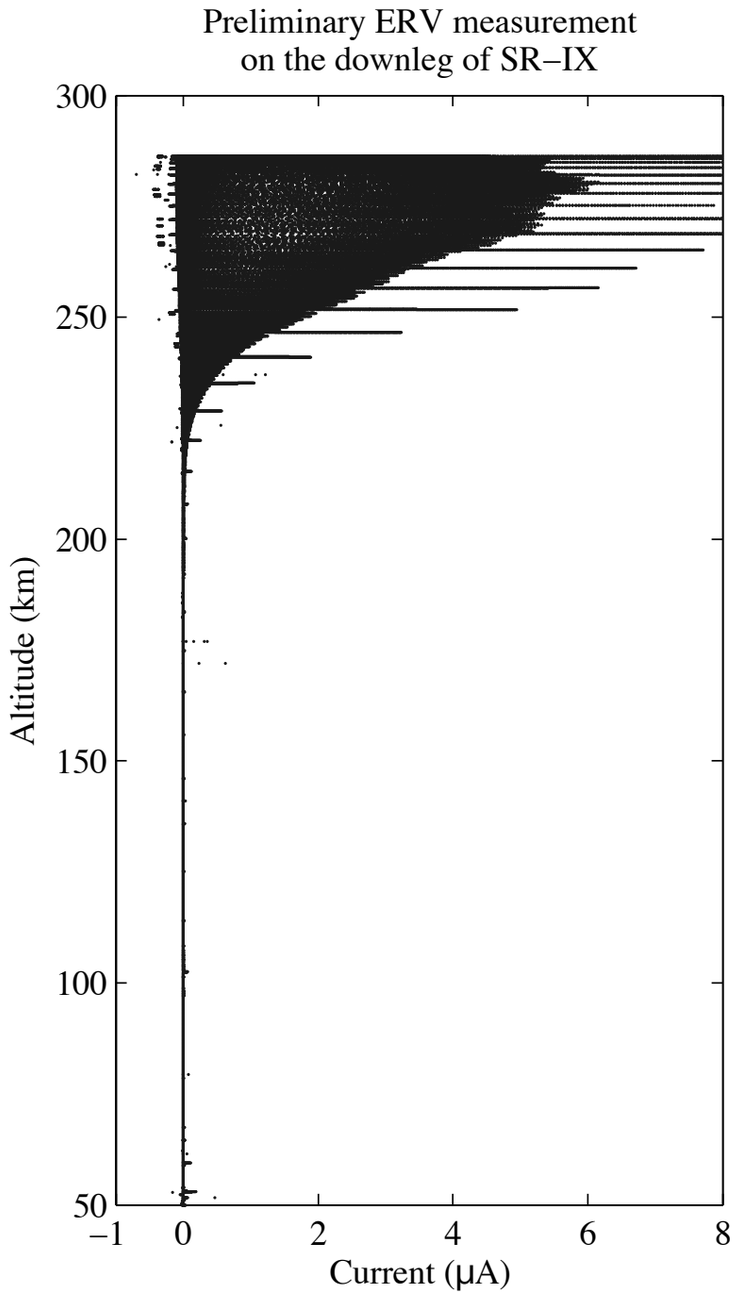

PLP readings at E region

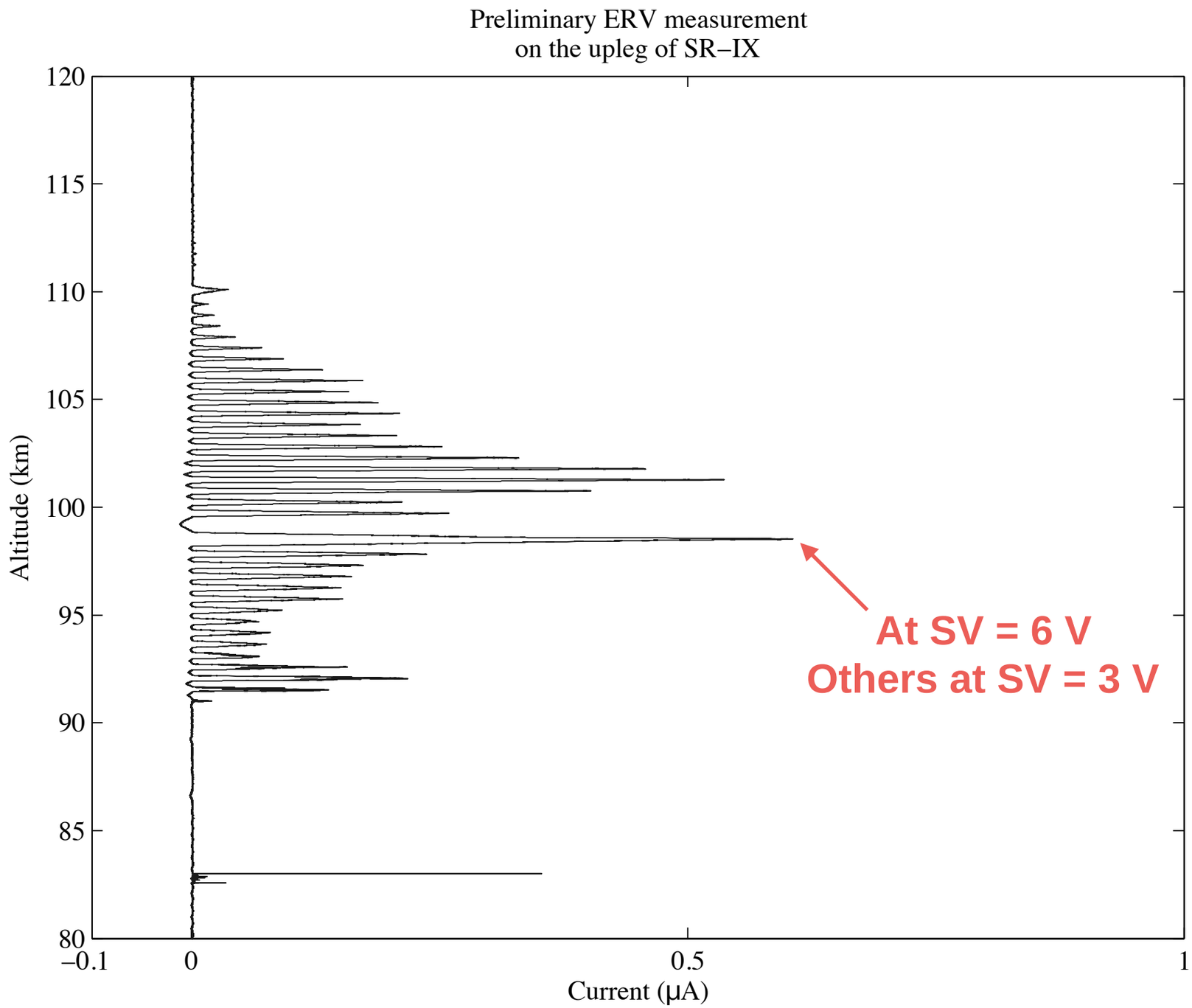

Delivery on Oct. 8, 2013

Installation

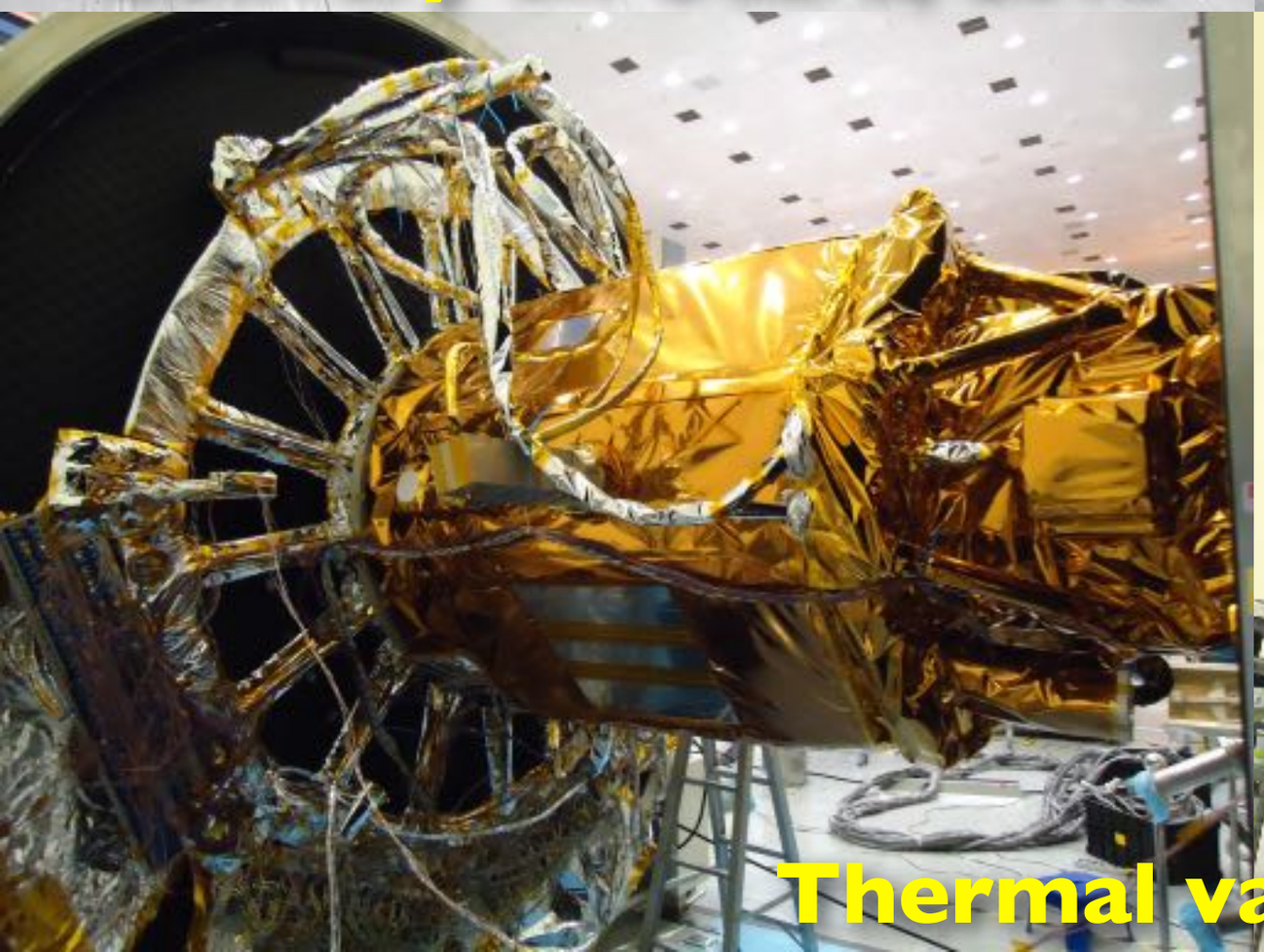

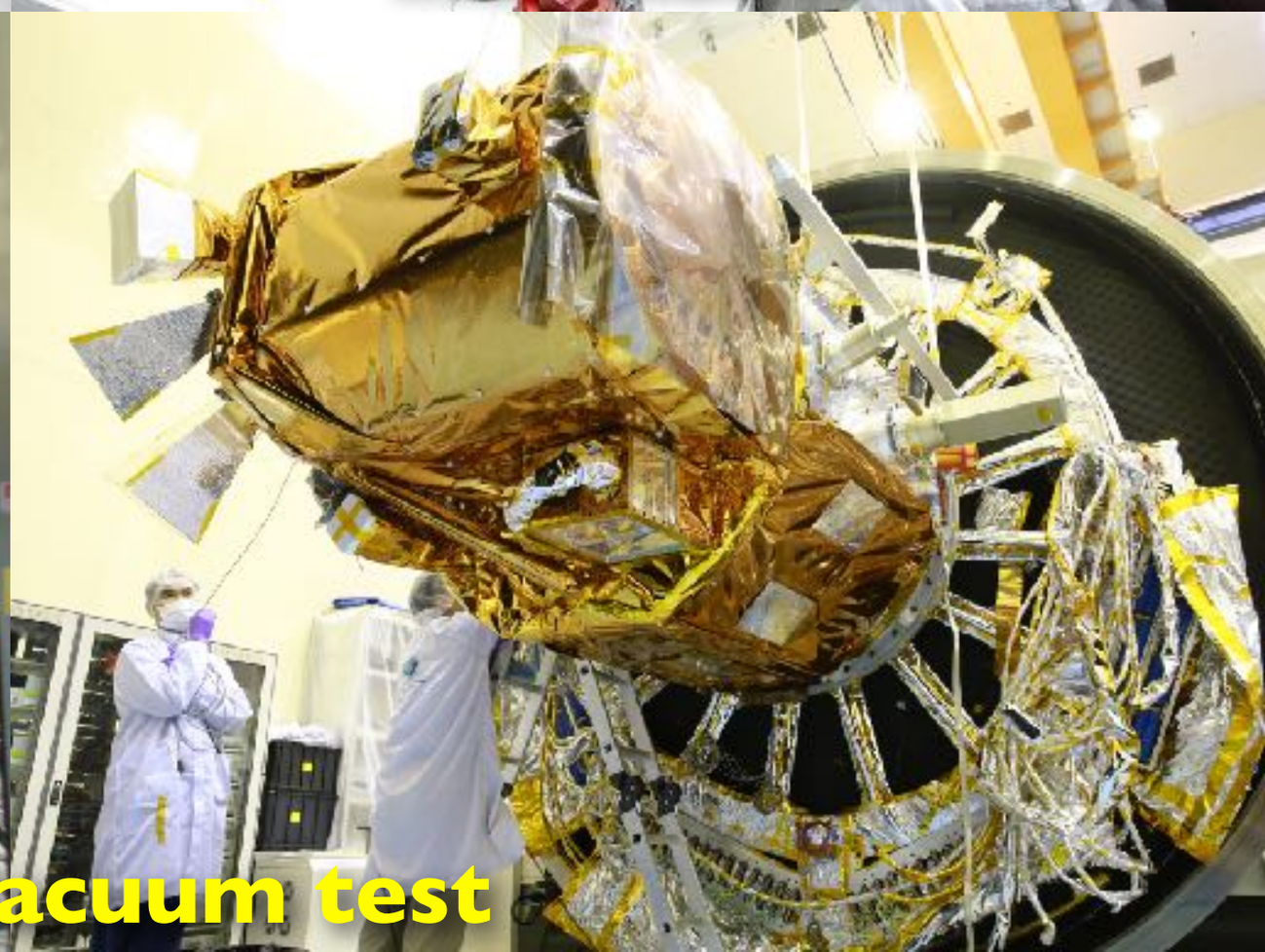

Thermal vacuum test

Dual Ionosphere Probe (DIP)

- Two miniature AIPs (a controller integrated inside the sensor cube) are daisy-chained to mount in ram direction, operate independently, and are mutually redundant for FORMOSAT-7/C2.
- Specifications (TBD)
  - Mass: 4.0-4.5 kg (< 7 kg).
  - Dimension: 100 mm L x 200 mm W x 135 mm H (< 160 mm L x 280 mm W x 135 mm H).
  - Average power: 10 W (< 14 W).
  - Data rate: 225 Mb/day (100% duty cycle) for NORMAL mode.

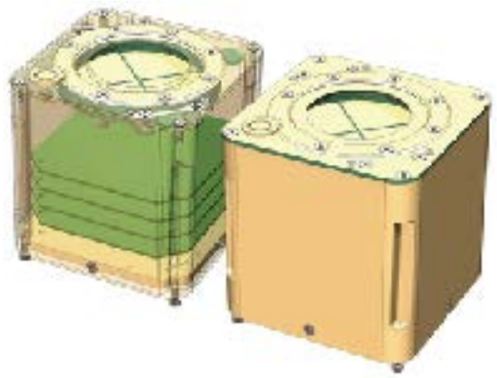

AIP miniaturization

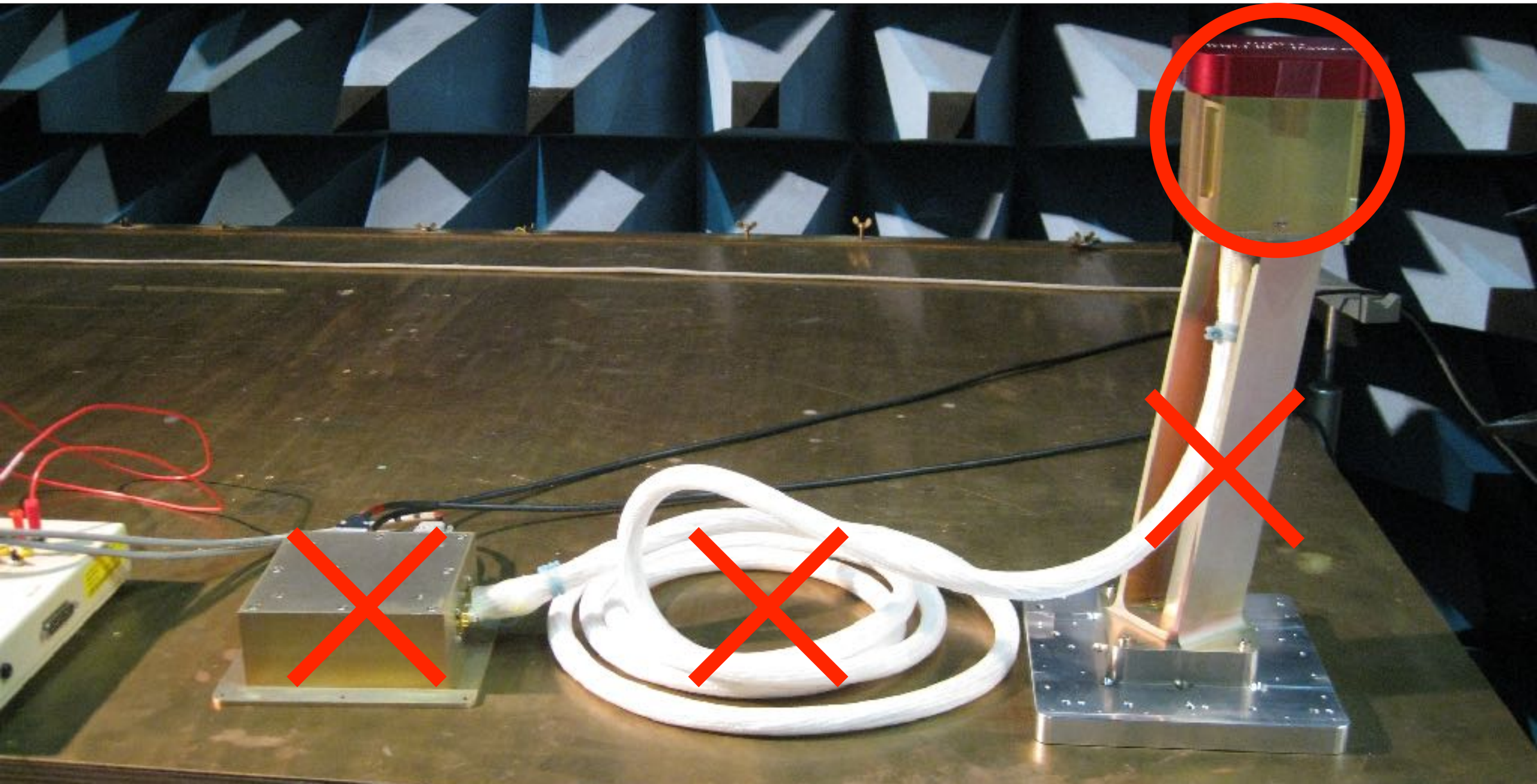

PCBs inside the sensor head

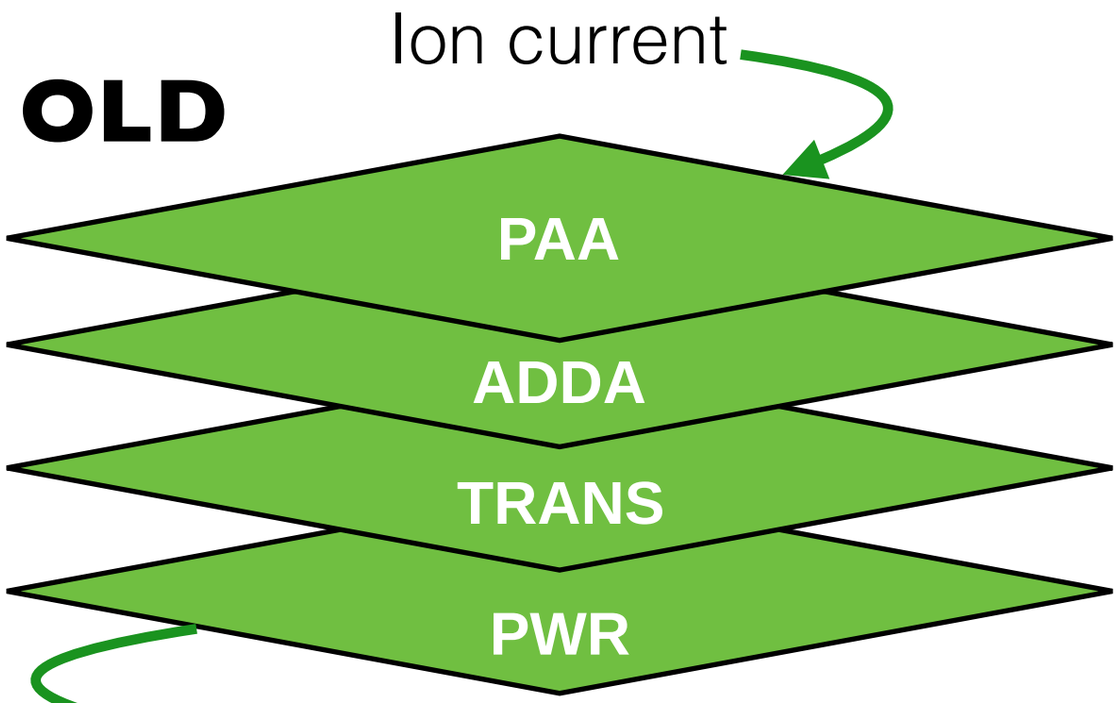

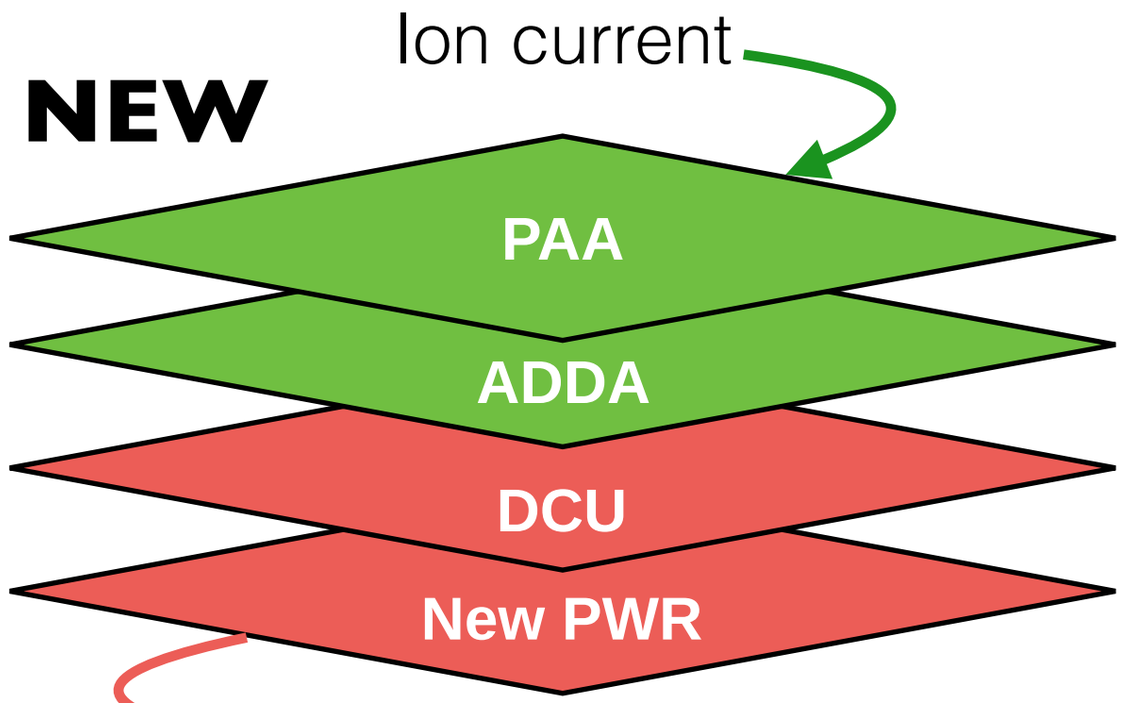

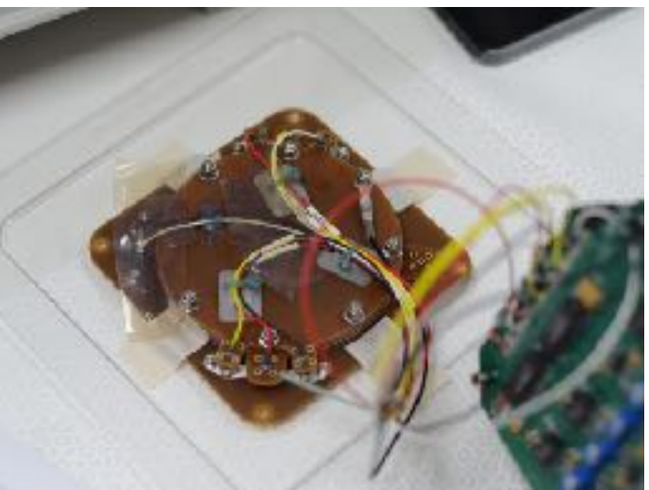

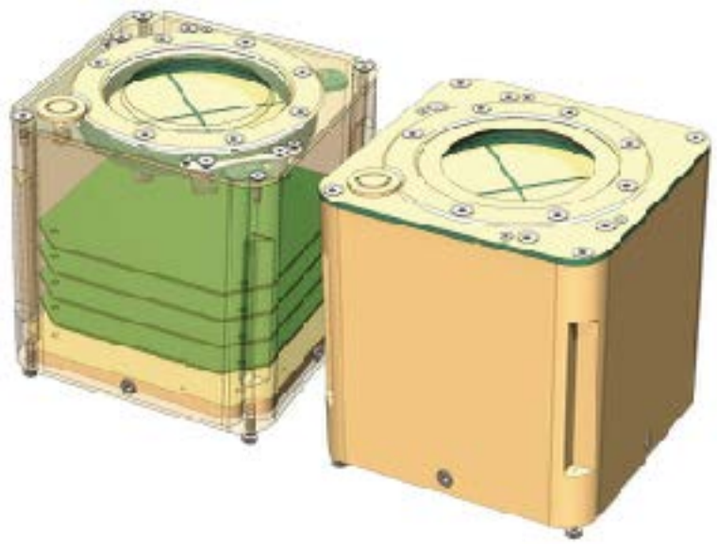

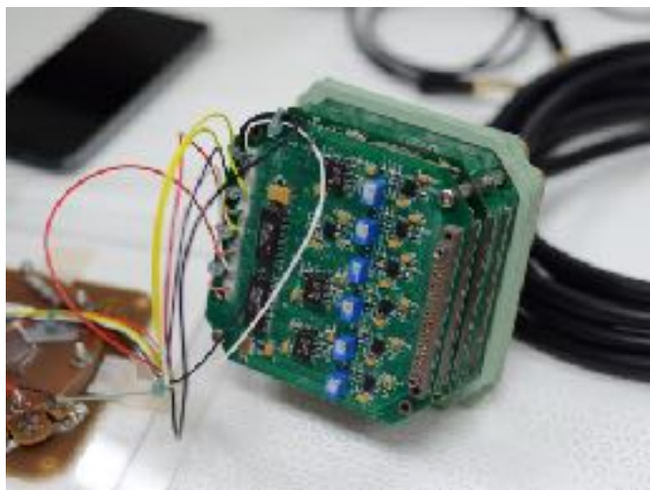

Digital Control Unit (DCU)

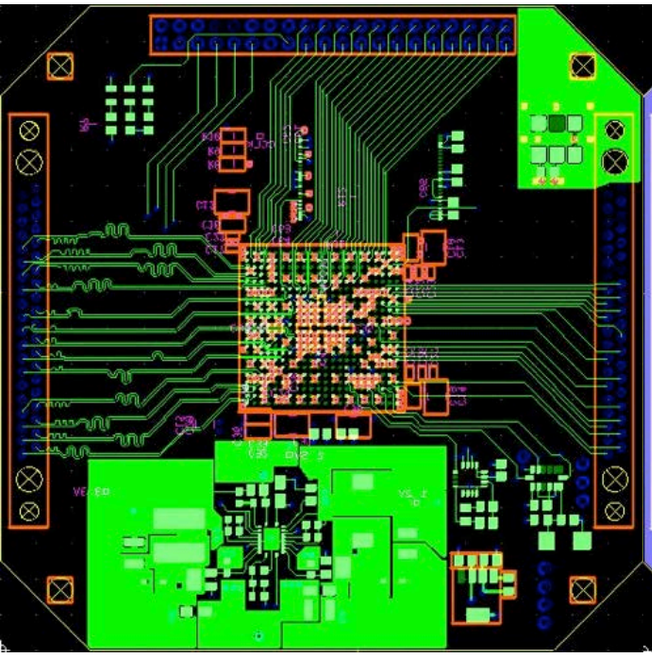

1st layer - signal

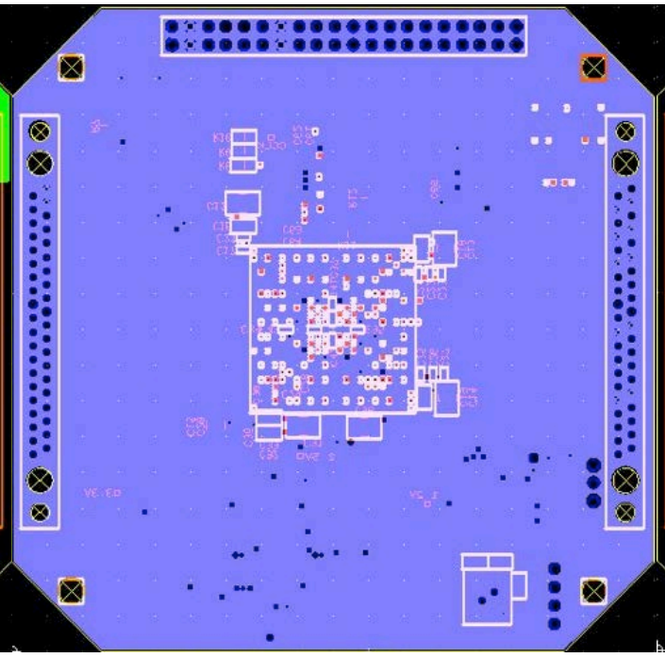

2nd layer - ground

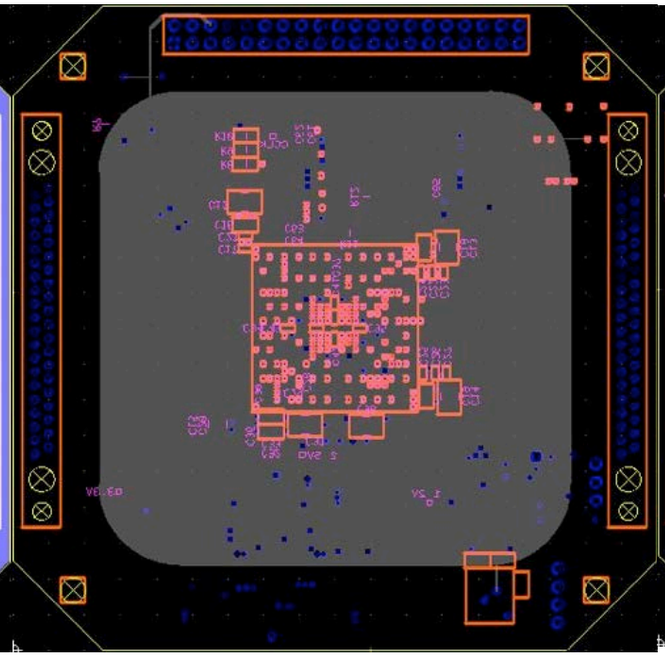

3rd layer - 3.3V power

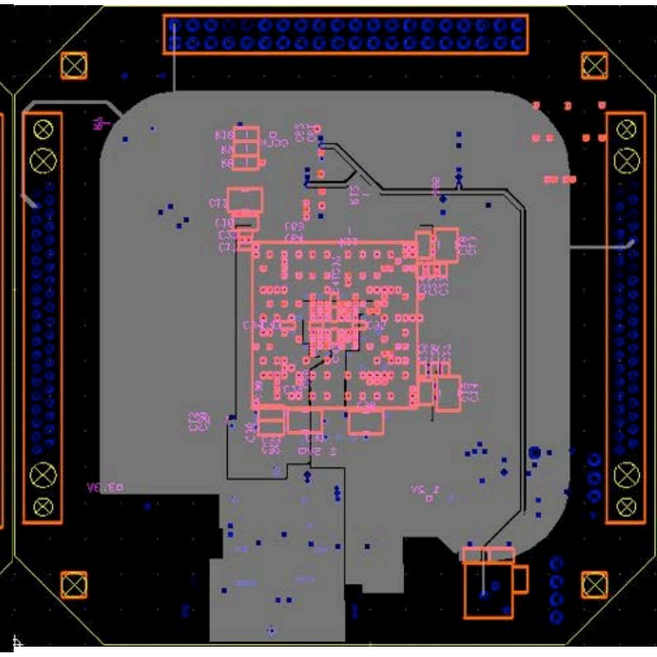

4th layer - 1.2 & 2.5V power

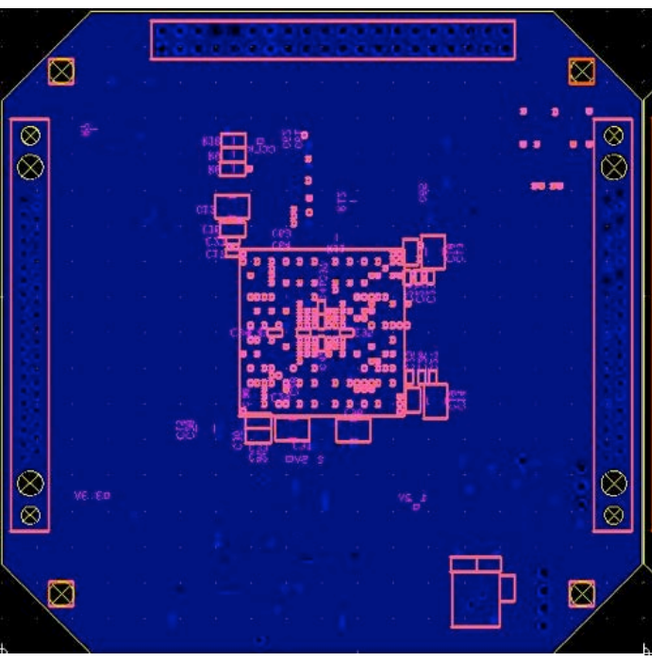

5th layer - ground

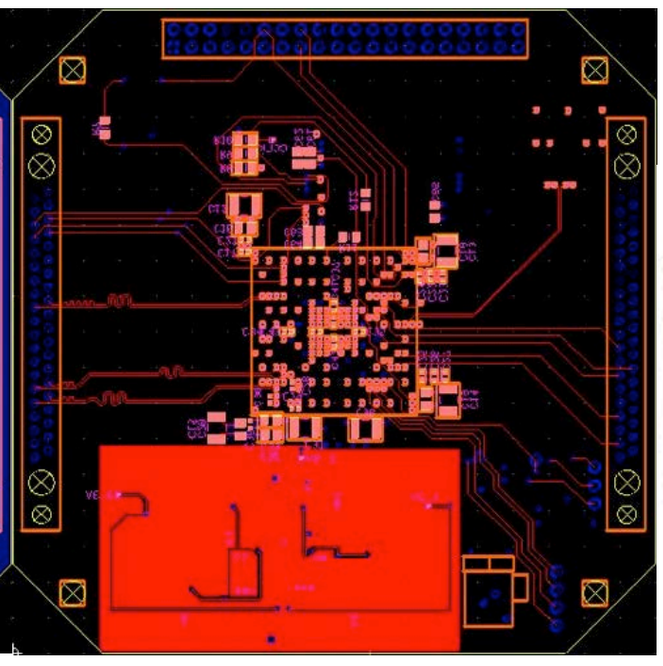

6th layer - signal

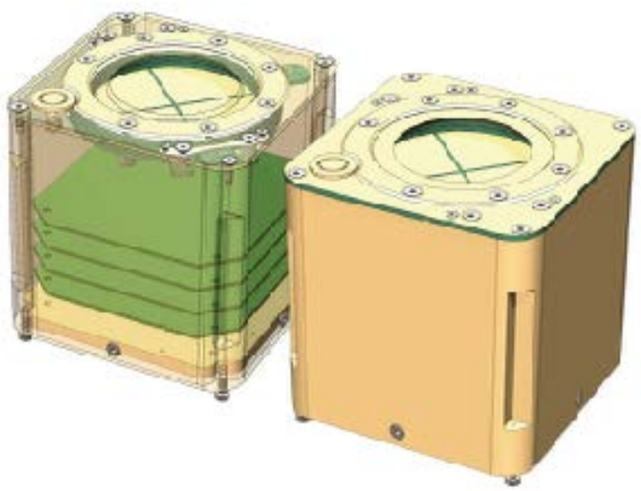

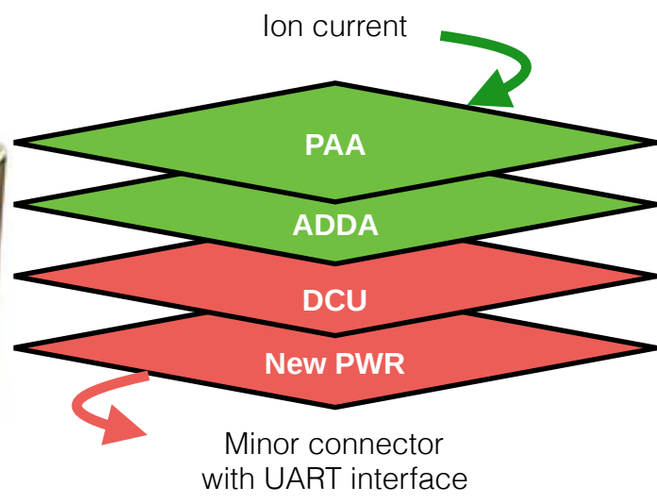

Communication interface

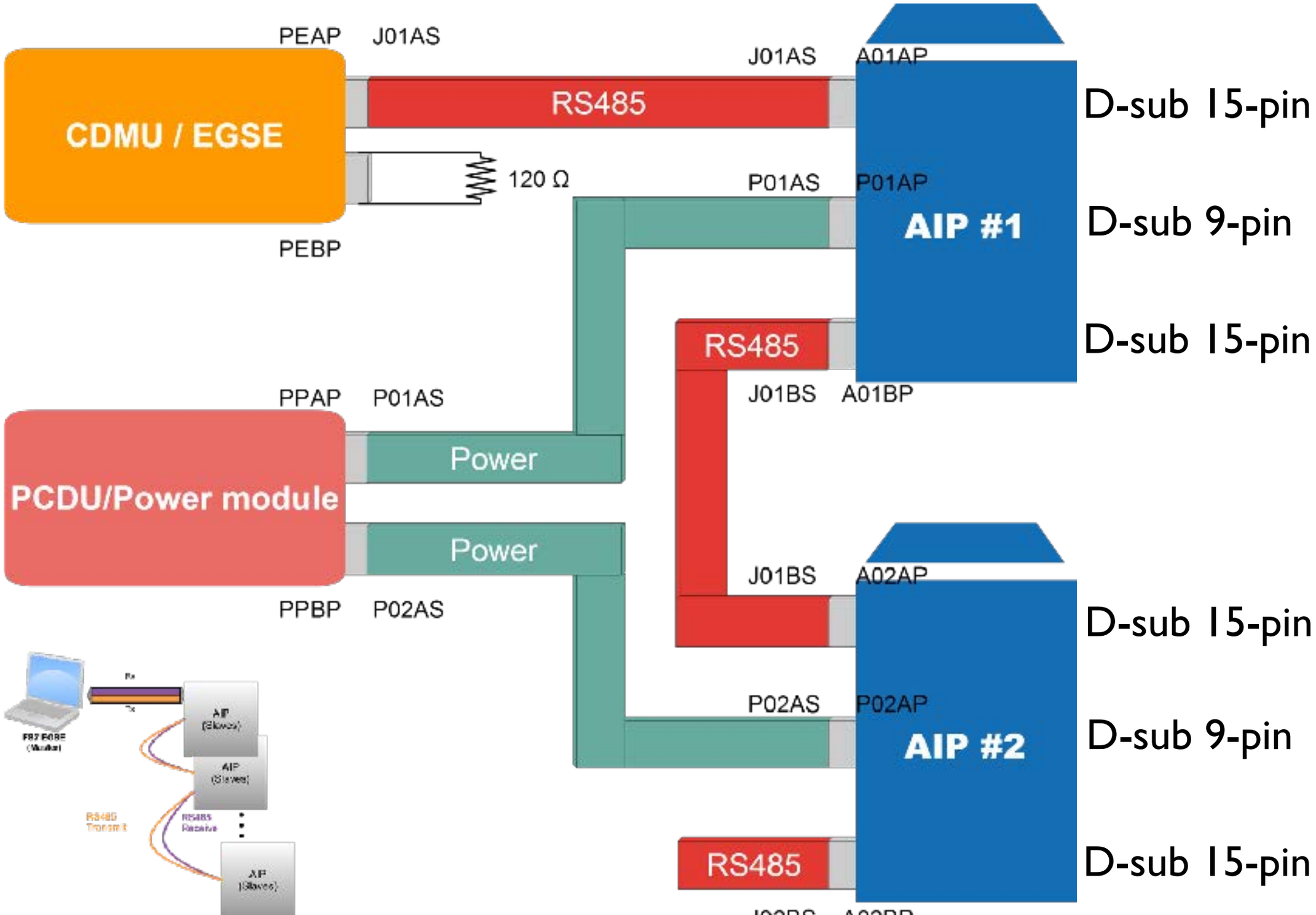

Comparison of FS-7 plasma sensors

S/C & P/L	FS-7C1/IVM	FS-7C2/DAIP
Manufacturers	UTD	NCU
Orbits	520-550 km altitude with 24°-28.5° inclination	720-750 km altitude with 71°-73° inclination
Sensors	2 (RPA/IT + DM)	2 (PLP, RPA, or IDM/IT)
Sampling rates	32 Hz (N_i) 32 Hz ($V_{y,z}$) 1 Hz (others)	128/1,024/8,192 Hz (N_i) 32/256/2,048 Hz ($V_{y,z}$) 1 Hz (others)
Functions	Fixed	Software programmable
Geophysical parameters	N_i, $\boldsymbol{V}$, and T_i	N_i, $\boldsymbol{V}$, T_i, and T_e
Mass	3.3 kg (< 4.2 kg)	4-4.5 kg (< 7 kg)
Dimension (mm)	300 mm L × 400 mm W × 135 mm H	100 mm L × 200 mm W × 135 mm H
Power	3 W (< 4.5 W)	10 W (< 14 W)

Compact Ionosphere Probe (CIP)

- Current missions
  - CIP for a 6U **Ionosphere Trawler**™ by DSI.
  - CIP for a 3U **INSPIRESat-2** by CU and NCU.
  - CIP for a 12U CubeSat by ExoTerra.
- Schedule: PDR in December 2016, CDR and EM in June 2017, and PAR for FM delivery in December 2017.
- Specifications (TBD)
  - Mechanical specification (**1U**): < **1** kg in mass and **90° x 90°** FOV without obstacle in ram direction.
  - Electrical specification: **+12** VDC input voltage, < **5** W in average power, PC/104, URAT, and 225 Mb/day (100% duty cycle) data rate for NORMAL mode.

AIP-C for a 6U Ionosphere Trawler™

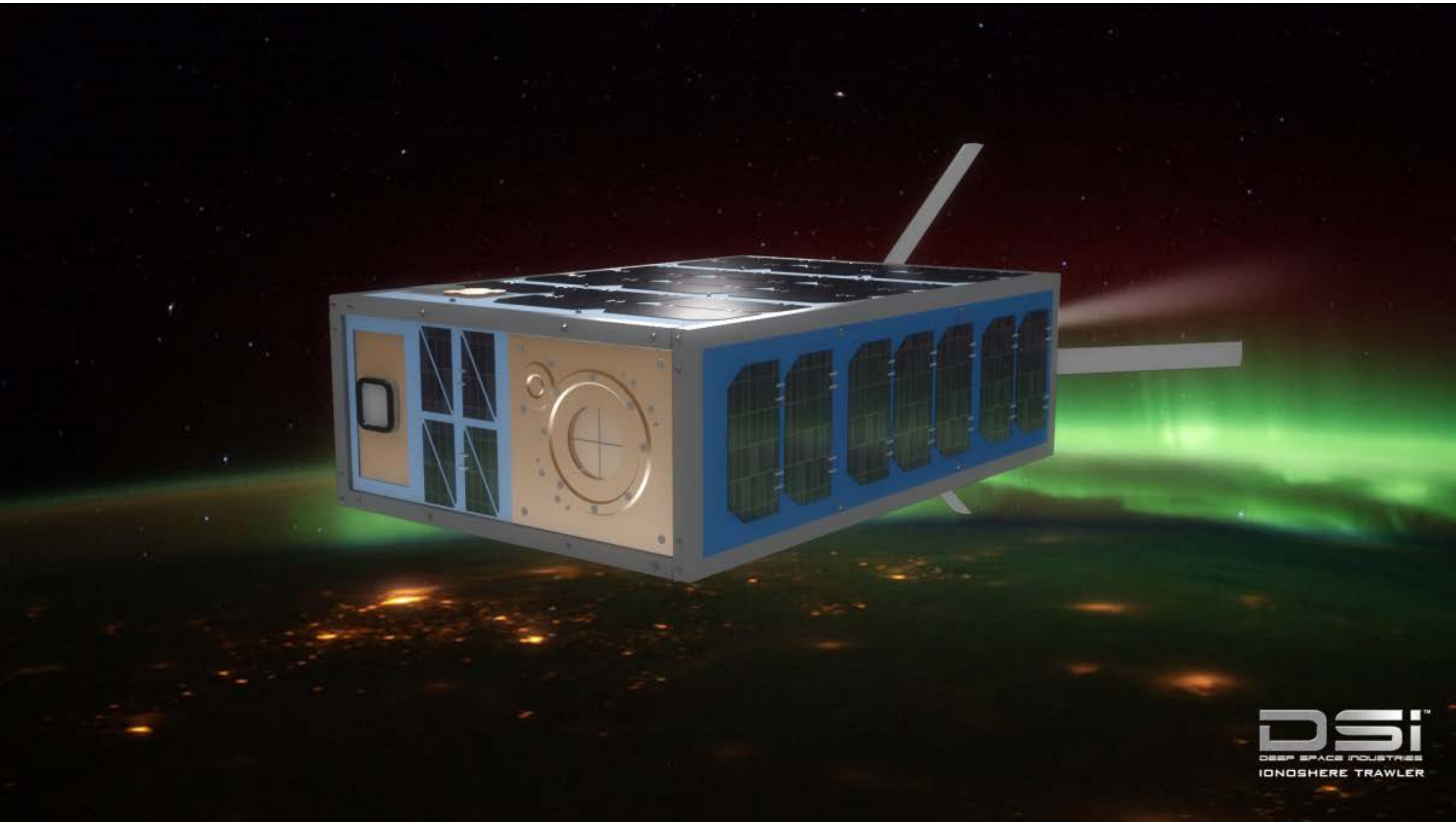

CIP for a 3U INSPIRESat-2